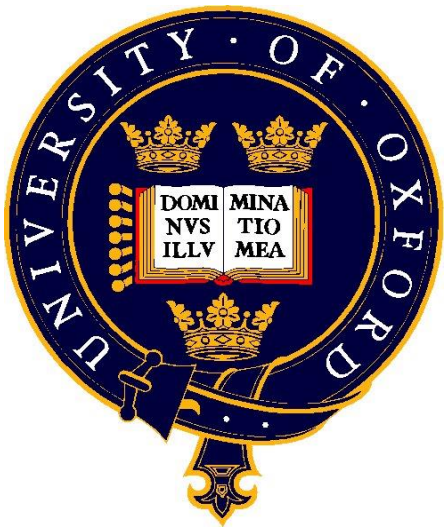

Assessment of Novel Liver-Stage Vaccines using Transgenic Rodent Malaria Parasites

Thesis submitted for the degree of Doctor of Philosophy

Trinity Term 2014

Ahmed M. Salman

St Cross College, University of Oxford

Word count: ~50,000 (excluding Bibliography, Appendix, Tables and Diagrams)

Assessment of Novel Liver-Stage Vaccines using Transgenic Rodent Malaria Parasites

Ahmed M. Salman, St Cross College, University of Oxford

Thesis submitted for the degree of Doctor of Philosophy, Trinity Term 2014

Abstract

Humans develop malaria after being inoculated, via the bite of an infected female mosquito, with the unicellular protozoan parasite, Plasmodium. There were an estimated 207 million cases of malaria and 627 000 deaths in 2012 and it is one of the world's most important global health challenges. At present there is no 100% effective or licensed vaccine against malaria. Plasmodium parasites infect a wide variety of hosts. There are five species associated with human infections, *P. falciparum, P. vivax, P. ovale, P. malariae and P. knowlesi.* Most of the severe pathologies and deaths due to malaria are associated with *P. falciparum* and it is consequently the most studied human malaria parasite. Unfortunately *P. falciparum* does not infect small animals and a number of the candidate vaccine antigens do not contain murine homologs, making pre-clinical efficacy studies unachievable in murine models.

There are two aims of this DPhil. The first aim is to identify several novel *P. falciparum* vaccine candidate antigens, incorporate them into a viral vector vaccine and assess immunogenicity in murine models. Fifteen candidate antigens were chosen: LSA1, LSA3, CelTOS, UIS3, LSAP1, LSAP2, ETRAMP5, Falstatin, CSP, TRAP, HT, RP-L3, SPECT-1, SPECT-2 and B9. Each antigen has either been shown to be well expressed during the liver-stage of infection, is a target of cell-mediated immunity in naturally exposed individuals or those immunised with irradiated sporozoites, or a homolog has been shown to be protective in murine or non-human primate studies. The second aim is to develop novel challenge models to assess the protective efficacy of these new *P. falciparum* pre-erythrocytic vaccine candidates in mice. To accomplish this goal, transgenic *P. berghei* parasites have been generated expressing *P. falciparum* genes of interest thus enabling efficacy assessment *in vivo*. This permits initial screening of the new vaccine candidates and based on their immunogenicity/protective efficacy the most promising candidates can be selected for further clinical evaluation.

P. falciparum liver-stage antigens have been expressed in two viral-vectors, simian adenoviral vector (ChAd63) and Modified Vaccinia Ankara viruses (MVA), and these were used to immunize mice using a prime-boost regimen. In parallel the genes encoding the same *P. falciparum* antigens were cloned into the rodent malaria parasite, *P. berghei*, such that they are expressed in sporozoites and liver stages. These transgenic parasites have been generated by introducing the genes encoding the antigens as an 'additional copy' into a neutral locus of the *P. berghei* genome. In addition, for some of the *P. falciparum* liver-stage antigens, which have homologs in *P. berghei*, we generated chimeric *P. berghei* parasites where the *P. berghei* gene coding sequence is replaced by that of its *P. falciparum* equivalent (i.e. ortholog) such that it is expressed by the endogenous *P. berghei* promoter. These transgenic/chimeric parasites have been used in challenge experiments, where mice immunized with the different *P. falciparum* vaccine candidates were challenged by intravenous injection of the transgenic *P. berghei* sporozoites expressing the cognate *P. falciparum* antigen, in order to determine protective immunity (efficacy) conferred by the different vaccines *in vivo*.

In addition to using chimeric parasites that express a single *P. falciparum* antigen, we have also generated transgenic parasites expressing two *P. falciparum* antigens, in sporozoites and liver-stages. Specifically, two 'double transgenic' parasites have been constructed expressing different combinations of two candidate antigens; the antigens selected were those that had shown the greatest protective efficacy in challenge experiments using the single gene transgenic *P. berghei* parasites. Therefore it has been possible to assess how best to combine multi-antigen vaccines and vaccination combinations using an *in vivo* model, and to generate much better protection than a single-antigen immunization. This work provides the first demonstration that complete protective immunity against malaria can be induced in a rodent animal model using the combination of two viral vector vaccines after only two immunisations.

Acknowledgements

My deepest gratitude and thanks to Allah the most merciful for guiding me through, and giving me the strength to complete this work with the way it is, and peace upon his prophet, Muhammad.

I would never have been able to finish this work without the continued guidance of my supervisors, support from my colleagues, help from friends, and encouragement from my family.

I would like to express my deepest gratitude to my all great supervisors, Professor Adrian Hill, Dr. Chris Janse, Dr. Shahid Khan and Dr. Alex Spencer. Words can't suffice to express my gratitude and thanks for your close supervision, guidance, patience, support, continuous encouragement, valuable help, friendly attitude and kind directions over the past three years. This thesis would not have been possible without your assistance and excellent supervision. It has been an honor and privilege to work under your generous supervision in such an excellent atmosphere for doing research.

I would also like to thank all the members of Hill Group at The Jenner Institute, University of Oxford past and present for their help, in particular:

- Rhea J. Longley for her kind help and providing eight viral vector vaccines which proved crucial for a number of experiments.

- Arturo Reyes, Amar Lall, Eduardo Alves, Karolis Bauza and all the *P. vivax* Malaria group members.

- Julie Furze, Andrew Worth and all members of our Lab Management and Core Facilities.

- Alex Fyfe, Vera Unwin, Sara Zakutansky and Sumi Biswas for the production of mosquitoes.

- Members of the Viral Vector Core facility, with special thanks to Naif Alharbi, Nick Edwards, Jake Matthews, Marzena Wroblewska and Sarah Gilbert.

- Thanks also to Viv Clark, Heather Gray and all staff at the FGF, as Sally Hill, Karla Watson and Magda at the RRI for their continuous cooperation through this work.

- Lisbeth Soederberg, Gary Strickland and all the members of our Finance & HR department.

I would also like to thank all the members of Dr. Chris Janse Group at Leiden Malaria Research Group, LUMC, Leiden University, The Netherlands. Special thank goes to: Takeshi Annoura, Mohammed Sajid, Jingwen Lin, Hans Kroeze, Jai Ramesar, and Blandine Franke-Fayard, Séverine Chevalley and Fiona van Pul. Thank you so much for your teaching, help, friendly support and making my work much easier and enjoyable during my stay at Leiden.

Another special thanks goes to my all friends and colleagues in the malaria group at The Jenner Institute, in particular; Ana Rodríguez, Ben Halbroth, Anita Gola, Lee Li, Sultan Abduljawad, Christos Krastev, Rebecca Hillson, Paulo Bettencourt, Carly Bliss, Georgina Bowyer for your friendship, help and moral support during the laughter and tear, throughout the duration of this thesis. Thanks to all my friends, everywhere, near and far, without your support I would never have made it to the end.

In addition, I would like to thank all the staff, my teachers and my colleagues of the Biochemistry Department, Faculty of Science, Ain Shams University, Cairo, Egypt and everyone who shared in the successfulness of my research career by any means.

Finally, a huge thank you goes out to my family, without which all of this would be impossible: Mum, Dad, Heba, Mohamed, Amany, Hoda, Mostafa and all my amazing nephews. Thanks for your prayers, support, countless love and encouragement that kept me going through life's challenges at all times. Last, but definitely not least, a special thank you go to my sweet angel and lovely fiancee Anna for all her prayers, support and love that gave me the strength and energy to go through hard challenges.

This work has been funded by Prof. Adrian Hill’s Senior Investigator Award from the Wellcome Trust (095540/Z/11/Z), in additional to EVIMalaR's PhD Studentship Programme with funding from the European Community's Seventh Framework Programme (FP7/2007-2013) under grant agreement N° 242095.”

Ahmed M. Salman

CHAPTERS

1 Introduction

2 Materials and Methods

3 Comparison of transgenic *P. berghei* parasites expressing either replacement or additional *P. falciparum* genes as challenge models.

4 The use of a transgenic rodent malaria challenge model for assessment and rank ordering of ten pre-erythrocytic malaria vaccines.

5 Double Chimeric Parasites: design, generation, characterization and their use as challenge models to assess malaria vaccine combinations.

6 Generation of five novel pre-erythrocytic viral vector vaccines and protective efficacy assessment using the Additional Gene (AG) chimeric parasite challenge model

7 Discussion and Future Directions

Contents

ABSTRACT 1

ACKNOWLEDGEMENTS 2

CHAPTERS 4

CONTENTS 5

TABLE OF FIGURES 9

TABLE OF TABLES 11

ABBREVIATIONS 12

PUBLICATION ARISING FROM WORK PRESENTED IN THIS THESIS 17

1 INTRODUCTION 19

1.1 Malaria 19
1.2 Life cycle of malaria parasites 21
1.2.1 Pre-erythrocytic (liver) stage 21
1.2.2 Erythrocytic (blood) stage 22
1.2.3 Mosquito (sexual) stage 22
1.3 Pathogenesis of human Malaria infection 24
1.4 Control Strategies. 25
1.4.1 Vector Control. 26
1.4.2 Medications 27
1.4.3 Vaccines 28
1.5 Naturally Acquired Immunity (NAI) to malaria 30
1.5.1 The innate immune system 30
1.5.2 The adaptive immune system 32
1.6 Malaria vaccine intervention strategies 38
1.6.1 Pre-erythrocytic stage 38
1.6.2 Erythrocytic stage 40
1.6.3 Mosquito stage 40
1.7 The leading pre-erythrocytic stage vaccines 41
1.7.1 Whole sporozoite vaccination strategies 41
1.7.2 Pre-erythrocytic malaria stage subunit vaccines 41
1.8 Heterologous ChAd63-MVA prime-boost vaccination strategy 42
1.9 Identifying further protective pre-erythrocytic antigens 43
1.10 Small-animal models of malaria in vaccine researches 47
1.10.1 Rodent malaria species 47
1.10.2 Transgenic P. berghei malaria parasites 47
1.11 Thesis aims and outlines 51
1.11.1 Aims 51
1.11.2 Outline 52

2 MATERIALS AND METHODS 53

2.1 Materials 53
2.1.1 Reagents 54
2.1.2 Oligonucleotide Primers. 60
2.1.3 Solutions and buffers 64
2.1.4 Basic DNA constructs/plasmids 70
2.1.5 Standard parasites lines used for generation transgenic P. berghei parasites expressing Human Malaria Parasite (P. falciparum) genes. 71
2.1.6 List of all generated chimeric parasites used in this study 73
2.2 Cloning and General Molecular Biology 75
2.2.1 Antigen inserts and constructs design 74
2.2.2 Agarose gel electrophoresis 75
2.2.3 Polymerase chain reaction (PCR) 75

2.2.4 Restriction digestion *76*
2.2.5 DNA ligation *77*
2.2.6 Bacterial transformation *77*
2.2.7 Plasmid DNA preparation *77*
2.2.8 Cloning, generation and preparation of chimeric parasite constructs. *81*
2.2.9 Cloning, generation and preparation of ChAd63 viral vector vaccine constructs using Gateway TM technology *87*
2.2.10 Cloning, generation and preparation of MVA viral vector vaccine constructs *90*
2.2.11 DNA Sequencing reactions *90*
2.3 CHIMERIC PARASITES GENERATION AND TRANSFECTION **91**
2.3.1 Generation chimeric parasites with a P. falciparum gene in a neutral locus: additional gene (AG) mutants *92*
2.3.2 Generation chimeric parasites with a P. falciparum gene: replacement gene (RG) mutants *94*
2.3.3 Generation of double chimeric parasites expressing two different P. falciparum genes *97*
2.4 GENOTYPE ANALYSIS FOR THE CHIMERIC *P. BERGHEI* PARASITE CLONES. **101**
2.4.1 Genomic DNA isolation of blood stages of chimeric P. berghei parasites *101*
2.4.2 Diagnostic integration (confirmation) PCR *101*
2.4.3 Southern analysis of chromosomes separated by pulsed-field gel electrophoresis (PFGE) *102*
2.5 PHENOTYPE ANALYSIS OF THE CHIMERIC *P. BERGHEI* PARASITES. **104**
2.5.1 Confirmation of the expression of the P. falciparum candidates in the chimeric sporozoites using an Immunofluorescence assay test (IFAT) *104*
2.5.2 Chimeric parasite fitness *105*
2.5.3 Fluorescence microscopy *107*
2.5.4 Liver cells culture *107*
2.5.5 In vivo imaging using the IVIS system *108*
2.6 PARASITOLOGY **108**
2.6.1 Sporozoite production of chimeric parasites *108*
2.6.2 Cryopreservation of blood stage parasites *109*
2.6.3 Challenge of immunised mice with chimeric sporozoites *109*
2.6.4 Preparing Thin-blood Smears *109*
2.6.5 Statistical model for parasitaemia prediction *110*
2.7 MOLECULAR VIROLOGY **111**
2.7.1 Viral vector vaccines *111*
2.7.2 Chimpanzee adenovirus (ChAd63) transfection and purification *111*
2.7.3 Recombination of MVA virus, Transfection and Purification *112*
2.8 IMMUNOLOGY **113**
2.8.1 Laboratory animals *113*
2.8.2 Mice vaccination and immunization *114*
2.8.3 Peptides *116*
2.8.4 Splenocyte preparation *117*
2.8.5 Ex-vivo IFN-γ Spleen ELIspot assay *118*
2.8.6 Collection and preparation of peripheral blood mononuclear cells (PBMCs) *118*
2.8.7 PBMC Intracellular Cytokine Staining (ICS) *119*
2.8.8 In vivo CD8+ and CD4+ T-cell depletions *120*
2.9 STATISTICAL ANALYSIS AND SOFTWARE **121**

3 COMPARISON OF TRANSGENIC *P. BERGHEI* PARASITES EXPRESSING EITHER REPLACEMENT OR ADDITIONAL *P. FALCIPARUM* GENES AS CHALLENGE MODELS. **123**

3.1 INTRODUCTION **123**
3.2 RESULTS **125**
3.2.1 Generation of maker-free P. berghei additional gene [AG] chimeric parasites expressing PfCelTOS or PfCSP *125*
3.2.2 Generation of maker-free P. berghei replacement gene [RG] chimeric parasites expressing PfCelTOS or PfCSP *125*
3.2.3 Genotype analysis of Replacement Gene [RG] chimeric parasites and their intermediate GIMO mother-line knock out chimeric parasites. *128*
3.2.4 Phenotype analysis of the Replacement gene [RG] chimeric expressing PfCelTOS or PfCSP by Immunofluorescence assay test (IFAT) *134*

3.2.5 Fitness of chimeric parasites *136*
3.2.6 Assessment of pre-challenge immunogenicity following heterologous prime-boost ChAd63-MVA PfCelTOS and PfCSP viral vector vaccination. *137*
3.2.7 Comparison of vaccine efficacy as determined in the challenge model after challenge with RG and AG chimeric parasites *140*
3.3 Discussion **147**

4 THE USE OF A TRANSGENIC RODENT MALARIA CHALLENGE MODEL FOR ASSESSMENT AND RANK ORDERING OF TEN PRE-ERYTHROCYTIC MALARIA VACCINES. **151**

4.1 Introduction **151**
4.2 Results **153**
4.2.1 Design and generation of the candidate vaccines *153*
4.2.2 Transgenic parasite design and generation *154*
4.2.3 Pbuis4 promoter characterization using mCherry expressing reporter line *156*
4.2.4 Genotype analysis of the Additional Gene chimeric parasites *163*
4.2.5 Phenotype analysis of the additional gene chimeric parasites expressing P. falciparum genes by Immunofluorescence assay test (IFAT) *166*
4.2.6 Transgenic parasite fitness *168*
4.2.7 Protective efficacy of the candidate vaccines in BALB/c mice *168*
4.2.8 Mechanism of protective efficacy in BALB/c inbred mice *172*
4.2.9 In vivo imaging for quantification of chimeric parasite load during the liver-stage using live animal imaging *175*
4.2.10 Protective efficacy of the candidate vaccines in CD-1 outbred mice *178*
4.3 Discussion **183**

5 DOUBLE CHIMERIC PARASITES: DESIGN, GENERATION, CHARACTERIZATION AND THEIR USE AS CHALLENGE MODELS TO ASSESS MALARIA VACCINE COMBINATIONS. **188**

5.1 Introduction **188**
5.2 Results **190**
5.2.1 Generation, fitness and genotype analysis of PbΔs1 (knock-out) GIMO mother-line *190*
5.2.2 Generation of two double transgenic parasites expressing two different P. falciparum genes. *192*
5.2.3 Genotype analysis of the Double Additional Gene chimeric parasites *195*
5.2.4 Phenotype analysis of the additional gene chimeric parasites expressing P. falciparum genes by Immunofluorescence assay test (IFAT) *198*
5.2.5 In vivo imaging for quantification of chimeric parasite load during the liver-stage by imaging *200*
5.2.6 Combined vaccination strategies *201*
5.2.7 Assessment of the pre-challenge cellular immunogenicity in blood following the heterologous prime-boost ChAd63-MVA viral vector vaccination *203*
5.2.8 Protective efficacy of combined vaccination in BALB/c mice *212*
5.3 Discussion **216**

6 GENERATION OF FIVE NOVEL PRE-ERYTHROCYTIC VIRAL VECTOR VACCINES AND PROTECTIVE EFFICACY ASSESSMENT USING THE ADDITIONAL GENE (AG) CHIMERIC PARASITE CHALLENGE MODEL **221**

6.1 Introduction **221**
6.1.1 Sporozoite microneme Proteins Essential for Cell Traversal (PfSPECT-1 and PfSPECT-2) *222*
6.1.2 Hexose Transporter (PfHT) *223*
6.1.3 Ribosomal Protein-L3 (RP-L3) *224*
6.1.4 Plasmodium 6-Cys family-related protein (PfB9). *224*
6.2 Results: **225**
6.2.1 Design and generation of ChAd63 and MVA viral vector vaccines *225*
6.2.2 Design and generation of P. berghei Additional Gene chimeric parasites expressing P. falciparum antigens *225*
6.2.3 Genotype analysis of the Additional Gene chimeric parasites *228*
6.2.4 In vivo imaging for quantification of chimeric parasite load during the liver-stage by imaging *231*
6.2.5 Phenotype analysis of the additional gene chimeric parasites expressing P. falciparum genes by Immunofluorescence assay test (IFAT) *233*
6.2.6 Immunisation and protective efficacy assessment of three P. falciparum vaccines in Balb/c inbred and CD-1 outbred mice in vivo. *234*

6.3 DISCUSSION 238

7 DISCUSSIONS 243

7.1 OVERVIEW 243
7.2 CONCLUSIONS AND FUTURE DIRECTIONS 246
7.2.1 Transgenic P. berghei technology 246
7.2.2 P. falciparum subunit vaccines development technology 248
7.2.3 Comparative assessment of novel pre-erythrocytic malaria subunit vaccines using AG transgenic rodent malaria challenge model. 249
7.2.4 Assessment of subunit malaria vaccine combinations 252
7.2.5 Efficiency of using P. berghei transgenic parasite as a challenge model 254
7.3 FINAL REMARKS 256

REFERENCES 259

APPENDICES 288

Table of Figures

Figure 1.1 Malaria Death Rate	**20**
Figure 1.2 Schematic representation of the life cycle of *Plasmodium* parasites	**23**
Figure 2.1: Cloning and General Molecular Biology steps.	**79**
Figure 2.2: Sequential DNA molecular cloning steps for generating the DNA constructs used for Additional Gene (AG) chimeric parasites generation.	**81**
Figure 2.3 Generation of DNA constructs for generation of Additional Gene (AG) chimeric parasites	**82**
Figure 2.4 Generation of DNA constructs for generation of Replacement Gene (RG) chimeric parasites.	**85**
Figure 2.5 GFP-Luc transgenic parasites are visible at any stage during the life cycle	**86**
Figure 2.6 Cloning steps involved in generation of DNA constructs required for ChAd63 viral vector manufacture	**88**
Figure 2.7 Cloning steps involved in generation of DNA constructs required for MVA viral vector manufacture	**90**
Figure 2.8 Generation of Additional Gene (AG) chimeric parasites	**92**
Figure 2.9 Generation of Replacement Gene (RG) chimeric parasites	**96**
Figure 2.10 Generation of Double Additional Genes Chimeric Parasite (DAG)	**99**
Figure 2.11 Genotyping of AG and RG mutants	**103**
Figure 2.12 Immunisation with *P. falciparum* vaccine and protective efficacy testing	**115**
Figure 2.13 The gating strategy applied for PBMC ICS	**120**
Figure 3.1 Generation of Replacement Gene (RG) chimeric parasite expressing *PfCelTOS* or *PfCSP*	**127**
Figure 3.2 Genotype analysis of Replacement Gene [RG] chimeric parasites	**130**
Figure 3.3 Genotype analysis; Diagnostic PCR	**132**
Figure 3.4 Immunofluorescence analysis demonstrating *P. falciparum* antigen expression in sporozoites of the replacement gene [RG] chimeric *P. berghei* parasites	**135**
Figure 3.5 Fitness assessment of the replacement Gene [RG] chimeric parasites compared to the wilt-type *P. berghei* parasite	**136**
Figure 3.6 Pre-challenge immunogenicity presented as the cytokines responses in the blood following the heterologous prime-boost ChAd63-MVA *P. falciparum* CelTOS viral vector vaccination	**138**
Figure 3.7 Pre-challenge immunogenicity presented as the cytokines responses in the blood following the heterologous prime-boost ChAd63-MVA *P. falciparum* CSP viral vector vaccination	**139**
Figure 3.8 *In vivo* imaging	**141**
Figure 3.9 Protective efficacy after ChAd63-MVA prime boost vaccination	**144**
Figure 3.10 The time to 1% parasitaemia correlates with the bioluminescence of the Replacement Gene (RG) transgenic liver-stage parasites	**146**
Figure 4.1 Schematic representation of the plasmid maps used for generating the Additional Gene [AG] chimeric *P. berghei* parasites expressing mCherry or single *P. falciparum* antigens under *Pbuis4* promoter.	**155**
Figure 4.2 Generation of Additional Gene [AG] chimeric *P. berghei* parasites expressing *P. falciparum* antigens	**157**
Figure 4.3 Generation and analysis of a transgenic $mCherry_{Pbuis4}$ reporter line expressing mCherry under the control of the *Pbuis4* promoter in mosquito stages	**160**
Figure 4.4 Charecterization and analysis of *Pbuis4* promoter in salivary gland sporozoites and liver stages using transgenic $mCherry_{Pbuis4}$ reporter line	**162**
Figure 4.5 Confirmation of correct genotype for the Additional Gene [AG] chimeric *P. berghei* parasite clones expressing *P. falciparum* antigens	**164**
Figure 4.6 Immunofluorescence analysis demonstrating *P. falciparum* antigen expression in sporozoites of chimeric *P. berghei* parasites	**167**
Figure 4.7 Efficacy of the ChAd63-MVA *P. falciparum* vaccines in BALB/c inbred mice	**171**

Figure 4.8 Mechanism of protective efficacy of ChAd63-MVA PfUIS3, PfLSA1 and PfLSAP2 vaccination in BALB/c mice	**174**
Figure 4.9 *In vivo* imaging	**176**
Figure 4.10 Efficacy of the ChAd63-MVA *P. falciparum* vaccines in CD-1 outbred mice	**180**
Figure 4.11 The protective efficacy Rank/order of the eight novel *P. falciparum viral vector vaccine candidates compared to the current two leading malaria vaccines PfCSP and PfTRAP* using the transgenic parasite challenging model	**182**
Figure 5.1 Genotype analysis of *PbΔS1-GIMO (2149 cl1)*	**191**
Figure 5.2 Fitness assessment of sporozoites of PbΔS1-GIMO (2149 cl1)	**192**
Figure 5.3 Generation of Double Additional Genes (DAGs) chimeric parasites	**194**
Figure 5.4 Genotype analysis of the Double Additional Genes (DAGs) chimeric parasites and their intermediate GIMO mother-line knock out chimeric parasites using Southern analysis of chromosomes (chrs) separated by pulsed-field gel electrophoresis (PFGE)	**196**
Figure 5.5 Genotype analysis. Diagnostic PCR of the Double Additional Genes (DAGs) chimeric parasites	**198**
Figure 5.6 Immunofluorescence analysis demonstrating *P. falciparum* antigen expression in sporozoites of chimeric DAGs parasites	**199**
Figure 5.7 Parasite liver loads as determined by *in vivo* imaging	**200**
Figure 5.8 Combined vaccination strategies	**202**
Figure 5.9 Pre-challenge immunogenicity presented as the CD8+ cell cytokine responses in the blood following the heterologous prime-boost ChAd63-MVA *PfLSA1* and *PfLSAP2* viral vector vaccines' combinations	**204**
Figure 5.10 Pre-challenge immunogenicity presented as the CD4+ cell cytokine responses in the blood following the heterologous prime-boost ChAd63-MVA *PfLSA1* and *PfLSAP2* viral vector vaccines' combinations	**206**
Figure 5.11 Pre-challenge immunogenicity presented as the CD8+ cells cytokines responses in the blood following the heterologous prime-boost ChAd63-MVA *PfCSP* and *PfTRAP* viral vector vaccines' combinations	**208**
Figure 5.12 Pre-challenge immunogenicity presented as the CD4+ cells cytokines responses in the blood following the heterologous prime-boost ChAd63-MVA *PfCSP* and *PfTRAP* viral vector vaccines' combinations	**210**
Figure 5.13 Post-challenge protective efficacies after PfLSA1and PfLSAP2 ChAd63-MVA prime boost combined vaccination strategy in BALB/c mice	**214**
Figure 5.14 Post-challenge protective efficacies after PfCSP and PfTRAP ChAd63-MVA prime boost combined vaccination strategy in BALB/c mice	**215**
Figure 6.1 Actual state of proteins identified in sporozoite stages in *Plasmodium falciparum*	**223**
Figure 6.2 First round ID and purity PCR for the five MVA recombinant viral vector vaccines (10 plaques)	**226**
Figure 6.3 Final ID and purity PCR for the purified MVA recombinant viral vector vaccines	**227**
Figure 6.4 Confirmation of correct genotype for the Additional Gene [AG] chimeric *P. berghei* parasite expressing *P. falciparum* antigens; Southern analysis	**229**
Figure 6.5 Confirmation of correct genotype for the Additional Gene (AG) chimeric *P. berghei* parasite expressing *P. falciparum* antigens; Diagnostic PCR	**230**
Figure 6.6 *In vivo* imaging	**232**
Figure 6.7 Immunofluorescence staining analysis of the AG rodent chimeric parasites.	**233**
Figure 6.8 Protective efficacy of the ChAd63-MVA *P. falciparum* vaccination in both inbred BALB/c and outbred CD-1 mice	**236**
Figure 6.9 Overall rank/order showing the protective efficacy of PfSPECT-1 compared to all the assesse *P. falciparum* vaccine candidate in the same challenge model using chimeric parasites	**237**

Table of Tables

Table 1.1 Accession number of all the generated *P. falciparum* pre-erythrocytic vaccines and their *P. berghei* homologs if exist	**44**
Table 1.2 brief descriptions for all the generated *P. falciparum* pre-erythrocytic vaccines and the rationale behind choosing them	**45**
Table 2.1 Details of major commercially available reagents used in this study	**53**
Table 2.2 Primers used for DNA construct generation	**59**
Table 2.3 Primers used for the chimeric parasites confirmation (integration) PCR	**61**
Table 2.4 Primers used for MVA viral vector vaccines ID and confirmation PCR	**63**
Table 2.5 List of all the generated and used chimeric parasites in this thesis	**72**
Table 2.6 Amino acid sequence for the predicted $CD8^+$ epitopes (peptides) used to generate the 14-15mer peptides per protein for the five novel *P. falciparum* antigens; PfHT, PfRP-L3, PfSPECT-1, PfSPECT-2 and PfB9	**117**
Table 4.1 Sterile protection and median delay induced by ChAd63-MVA *P. falciparum* vaccines in BALB/c mice	**170**
Table 4.2 Sterile protection and median delay induced by ChAd63-MVA *P. falciparum* vaccines in CD-1 mice	**179**

Abbreviations

a.a	Amino acid
Ab	Antibody
ACK	Ammonium Chloride Potassium
ACTs	Artemisinin-based Combination Therapy
ADCC	Antibody-Dependent Cellular Cytotoxicity
ADCI	Antibody Dependant Cellular Inhibition
AG	additional gene
AMA-1	Apical Membrane Antigen 1
APC	Antigen Presenting Cells
B Cells	Bone Marrow Derived Lymphocytes
BF	Bright Field
BGH-poly(A)	Bovine Growh Hormone gene poly-(A)
BLS	Bio-Luminescence Signal
bp	base pairs
BSA	Bovine Serum Albumine
CD	Cluster of Differentiation
CDS	Coding Sequence
CEF	Chicken Embryonic Fibroblasts
CelTOS	Cell traversal protein for ookinetes and sporozoites
ChAd63	chimpanzee Adenovirus serotype 63
ChAd-MVA	Adenoviral prime, MVA boost regime (8 weeks interval)
chr	Chromosome
CI	Confidence Interval
CM	Cerebral Malaria
CMC	Carboxymethyl Cellulose Sodium Salt
CMV	Cytomegalovirus
CpG DNA	Central pattern Generator DNA
CR-1	Complement-Receptor 1
CRIR1	Cysteine-Rich Interdomain Region-1
CSA	Chondroitin Sulfate A
CSP	Circumsporozoite Surface Protein
CTLs	Cytotoxic T Lymphocytes
DAG	Double Additional Gene
DAPI	4',6-Diamidino-2-Phenyl Indole
DC	Dendritic cells
DDT	Dichloro-Diphenyl-Trichloroethane
DEET	*N*,*N*-Diethyl-*meta*-Toluamide
DF-1	Checkin Fibroblast cell line
DMSO	Dimethyl Sulfoxide
DNA	Deoxyribonucleic acid
D-PSB	Dulbecco's Phosphate-Buffered Saline

DRG	Double replacement gene
ds	Double-stranded
DXO	Double Crossover
EBA	Erythrocyte binding antigen
EDTA	Ethylenediaminetetraacetic acid
EEF	Exo-Erythrocytic Form
ELISA	Enzyme-linked immunosorbant assay
ELISpot	Enzyme-linked immunosorbent spot assay
EMP-1	Erythrocyte membrane protein 1
ETRAMP5	Early transcribed membrane protein 5
Fab	Fragment antigen-binding
FabB/F	Enzyme of the type II fatty acid biosynthesis (FAS II)
FC	Fluorocytosine
FcR	Fragment Crystallizable Receptor
FP9	Fowlpox strain virus FP9
g	The acceleration due to gravity
GAP	Genetically-attenuated parasites
GFP	Green fluorescent protein
GIA	Growth Inhibitory Activity
GIMO	Gene Insertion-Marker Out
GMEP	Global Malaria Eradication Program
GMP	Guanosine Mono-phosphabe
GPI	Glycosylphosphatidylinositol
GSK	GlaxoSmithKline
h	Hour
HBsAg	Hepatitis B surface antigen
HBV	Hepatitis B virus
hDHFR	Human dihydrofolate reductase
HEPES	4- (2-Hydroxyethyl) -1-Piperazineethanesulfonic acid
HIV	Human immunodeficiency virus
HMP	human malaria protein
hpi	Hours Post Infection
HPV	Human papilloma virus
HT	*Hexose Transporter*
Huh-7	Human Hepatocyte-7
HZ	Haemozoin
i.m.	Intra-muscular
i.p.	Intra-peritoneal
i.v.	Intra-venous
IC	Immune Complex
ICAM-1	Intracellular Adhesion Molecule 1

ICS	Intracellular Cytokine Staining
IE	Infected Erythrocyte
IFAT	immunofluorescence staining
IFN	Interferon
IFNγ	interferon-gamma
ifu	Infectious units
Ig	Immunoglobulin
IL	Interleukin
Int.	Integration
iRBC	Infected red blood cells
ITNs	Insecticide-Treated mosquito Nets
ITR	Inverted Terminl Repeat
IVIS	*In vivo* imaging system
kDa	Kilodalton
KO	Knock-out
LB	Luria Broth
LSA1	Liver-stage antigen 1
LSA3	Liver-stage antigen 3
LSAP1	Liver-Stage Associated Protein 1
LSAP2	Liver-Stage Associated Protein 2
mAb	Monoclonal Antibody
MCS	Multiple Cloning Site
ME	Multi-Epitope string
MEM	Minimum Essentials Medium
MG	Mudgut
MHC	Major Histocompatibility Complex
min	minute
MSP-1	Merozoite surface protein-1
MVA	Modified vaccinia virus Ankara
NAI	Naturally Acquired Immunity
NEB	New England Biolabs
NF-kB	Nuclear Factor-kappa B
NK	Natural Killer Cells
NO	Nitric Oxide
OD	Optical Density
ODN	Oligodeoxynucleotide
ORF	Open Reading Frame
OVA	Ovalbumin
P.	*Plasmodium*
p.i.	Post Infection
p.i.	Post Infection
PABA	4-aminobenzoic Acid

Pb	*Plasmodium berghei*
PBMCs	Peripheral Blood Mononuclear cells
PBS	Phosphate Buffered Saline
PBS/T	0.05% Tween 20 in phosphate buffered saline
PCR	Polymerase chain reaction
Pf	*Plasmodium falciparum*
PFGE	Pulsed-Field Gel Electrophoresis
pfu	Plaque forming units
PHZ	Phenylhydrazine
PKG	GMP-dependent ProteinKinase
pRBC	Parasitized Red Blood Cell
PVM	Parasitophorous Vacuole Membrane
RAP	Rhoptry-associated protein
RAS	Radiation-attenuated sporozoites
RBC	Red blood cell
RESA	Ring-infected erythrocyte surface antigen
RG	*Replacement Gene*
Rh5	Reticulocyte binding protein 5
RNA	Ribonucleic acid
RP-L3	60S Ribosomal protein L3
RPM	Revolutions Per Minute
RT	Room Temperature
RT-PCR	Reverse Transcriptase - Polymerase Chain Reaction
RTS,S	CSP based malaria vaccine based on a HBsAg fusion polypeptide from GSK
s.c.	Subcutaneous
SAP1	Sporozoite asparagine-rich protein 1
SCID	Severe Combined Immunodeficient Mice
SDS	Sodyl Dodecyl Sulfate
SFU	Spot forming unit
SG	Salivary Glands
SM	Selectable Marker
SNA	Sporozoite Neutralization Assay
SPECT	Sporozoite Protein Essential for Cell Traversal
Spz	Sporozoite
ss	Single-Stranded
SSC	Saline Sodium Citreate
T Cells	Thymus Derived Lymphocytes
TAE	Tris-Acetate EDTA
TB	Tuberculosis
TCR	T-cell Receptor

TE	Tris- EDTA
TE	Tris- EDTA buffer
Tg	Transgenic
Th	T helper cells
TK	Thymidine Kinase Locus
TLRs	toll-like receptors
TM	Transmembrane
TNFα	Tumour necrosis factor alpha
tPA	Tissue plasminogen activator
TRAP	Thrombospondin-related adhesion protein
TRs	targeting regions
UIS	Upregulated in infectious sporozoites
UIS3	Upregulated in infective sporozoites gene 3
UIS4	Upregulated in infective sporozoites gene 4
UTR	Untranslated region
WHO	World Health Organization
WT	Wild-type
y*fcu*	Yeast cytosine deaminase and uridyl phosphoribosyl transferase

Publication arising from work presented in this thesis

Title: Comparative assessment of vaccine vectors encoding ten pre-erythrocytic malaria antigens in mice identifies two highly protective liver-stage antigens, PfLSA1 and PfLSAP2

Authors: **Ahmed M. Salman1,2*,** Rhea J. Longley[1*], Matthew G. Cottingham[1], Katie Ewer[1], Chris J. Janse[2], Shahid M. Khan[2], Alexandra J. Spencer[1], Adrian V. S. Hill[1].

[1]The Jenner Institute; University of Oxford; Oxford, OX3 7DQ; United Kingdom.

[2]Leiden University Medical Centre; Leiden University; Leiden, 2333 ZA; The Netherlands.

***Co-first author.**

Submitted to PLOS Pathogens Journal

Title: Generation of transgenic rodent malaria parasites expressing human-malaria parasite proteins

Authors: **Ahmed M. Salman[1,2],** Catherin Marin Mogollon[1], Jing-wen Lin[1,3], Fiona J.A. van Pul[1], Chris J. Janse[1], Shahid M. Khan[1]

[1]The Jenner Institute; University of Oxford; Oxford, OX3 7DQ; United Kingdom.

[2]Leiden University Medical Centre; Leiden University; Leiden, 2333 ZA; The Netherlands.

Submitted as a method chapter to book entitled 'Malaria Vaccines' (Humana Press; Edited by Ashley Vaughan).

Chapter 1

Introduction

1 Introduction

1.1 Malaria

Malaria remains one of the most problematic global infectious diseases and a leading cause of morbidity and mortality in tropical regions. Nearly half of the world's population is living at risk of malaria infection (an estimated 3.4 billion people). In 2013, 104 countries and territories were affected, including countries in sub-Saharan Africa, Asia, Latin America and parts of the Middle East and Europe. The World Health Organization (WHO) estimated 207 million cases of malaria and 627,000 deaths (uncertainty interval 473.000- 789.000) in 2012. Of the estimated deaths, most occured in sub-Saharan Africa (90%) and in children under 5 years of age (77%) **(Figure 1.1)** [2].

Malaria is caused by protozoan parasites of the genus *Plasmodium* that are transmitted via bites of infected female *Anopheles spp.* mosquitoes [3]. The disease is characterized by symptoms including high fever, headache, vomiting and chills that appear between 10-15 days after infection [2]. In severe cases neurological complications such as brain injury or coma can be caused often leading to death [3]. There are five main *Plasmodium* species that cause human malaria, namely *P. falciparum*, *P. vivax*, *P. malariae*, *P. ovale* and *P. knowlesi*, whereby *P. falciparum* and *P. vivax* are the most prevalent causative agents. *P. falciparum* is the leading cause of most death, predominantly in Africa with nearly 98 percent of malaria infections in sub-Saharan Africa caused by *P. falciparum* [4].

In addition to being a significant health risk, malaria also contributes to the loss of productivity and economic prosperity in endemic nations [5] and there is a strong negative correlation between country's long-term economic growth prospects and the disease burden [6]. Despite malaria's huge health and economic burden, there are some indications that the disease incidence in the endemic regions is decreasing. This is thought mainly to be due to the recent increase in access to anti-malarial interventions, such as artemisinin-based

combination drugs due to increasing resistance of parasites to essentially all anti-malarial drugs given alone [7-9], beside the use of long-lasting insecticide-treated bed nets and indoor residual spraying [10]. However, the deployment of efficacious vaccine(s) would probably have the greatest impact on the disease burden [11, 12], and therefore, the malaria vaccine field remains an active area of biomedical research.

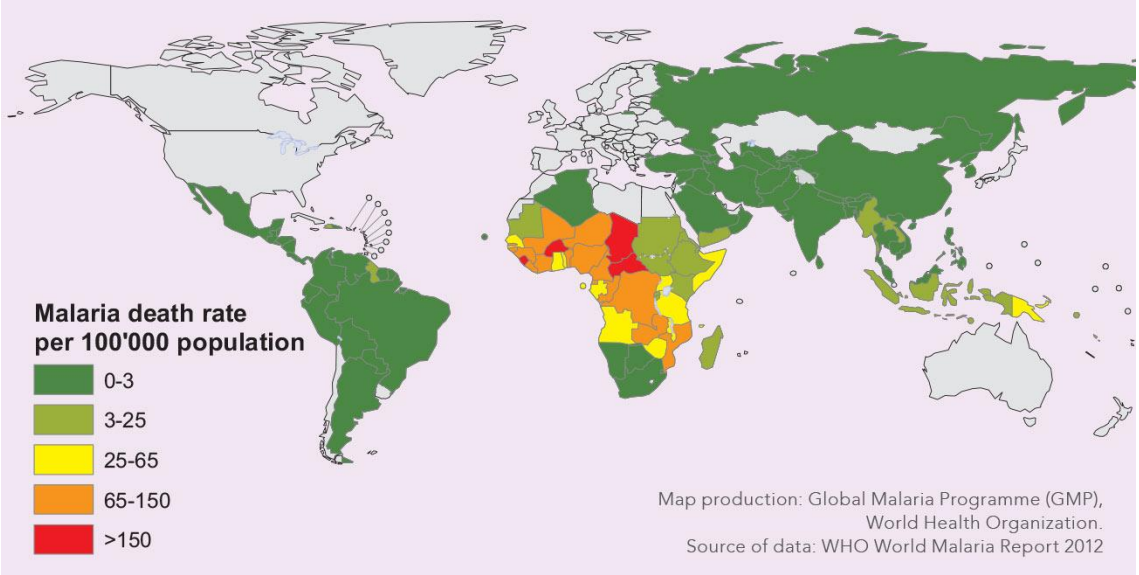

Figure 1.1 Malaria Death Rate. According to the World Health Organization (WHO), there were an estimated 207 million cases of malaria in 2012, the last year such data was available. Those infections resulted in an estimated 627,000 deaths. 90% of all malaria deaths occur in sub-Saharan Africa, and 77% occur in children under five.

1.2 Life cycle of malaria parasites

Malaria parasites have a complex life cycle with stages in the invertebrate host, the *Anopheles spp.* mosquito, and the vertebrate host, such as humans **(Figure 1.2)**. The parasites undergo a characteristic change of generations with alternating sexual and asexual proliferation cycles [13]. The life cycle can be divided into three main stages:

1.2.1 Pre-erythrocytic (liver) stage

Plasmodium parasites are transmitted to humans in the motile infective form of sporozoites that are injected by bites of infected female *Anopheles spp.* mosquitoes. Only female mosquitoes are able to transmit the disease, because they need mammalian blood to provide optimal prerequisites for the development of their eggs. While taking the blood meal, several hundred sporozoites are injected into the skin or directly into the circulatory system [3]. The sporozoites migrate within minutes by the systemic circulation to the liver and infect target hepatocytes by forming a parasitophorous vacuolar membrane (PVM) [14]. The liver stage development for most human malaria species lasts for 5-9 days including *P. falciparum*, whereas a much shorter period of 2-3 days is enough for rodent malaria species, including *P. berghei*. It is in this stage that some *P. vivax* and *P. ovale* are able to establish the dormant hypnozoite forms responsible for relapses of infection a few months or even years later [1, 15]. This stage of the life cycle is difficult to study in human, because neither species can infect small animals and there is no simple way to culture parasites of this phase *in vitro.* Within the PVM, sporozoites undergo asexual replication into pre-erythrocytic schizonts, where up to 30,000 merozoites can be developed from a single sporozoite by forming a schizont. After degradation of the matured schizonts and dying of the host cells, the merozoites are released tied into vesicles and gradually enter the bloodstream, initiating the blood stage infection [16]. The pre-erythrocytic stage of the lifecycle is asymptomatic.

1.2.2 Erythrocytic (blood) stage

In the blood, the merozoites invade red blood cells (RBCs) and a series of asexual multiplication cycles (erythrocytic schizogony) takes place. The merozoites mature into trophozoites which then mature into schizonts. Depending on *Plasmodium*-type, the schizont produces 8 to 32 new infective merozoites per RBC, resulting in burst of erythrocytes and distribution in blood plasma where they can infect more RBCs [3]. The *P. falciparum* asexual blood cycle takes 44–48 hours to complete, while in *P. berghei* takes 22–24 hours. *P. falciparum* can invade both mature and immature RBCs, whereas *P. berghei* parasites have, like the human parasite *P. vivax*, a strong preference for invading and growing in immature RBCs (reticulocytes). Malaria signs and symptoms are typically linked to the erythrocytic stage of the lifecycle. Some merozoites that invade RBC do not proceed with asexual multiplication but differentiate into male or female gametocytes, the sexual precursor cells of gametes. These gametocytes are responsible for malaria transmission between the vertebrate host and mosquito.

1.2.3 Mosquito (sexual) stage

Mature male and female gametocytes can be taken up by mosquitoes during a blood meal [1]. After the ingestion of gametocytes, they differentiate into female macrogametes and male microgametes that fuse to form a diploid zygote in the mosquito midgut [3]. After meiosis, the zygotes develop into motile ookinetes that migrate through the midgut wall to form oocysts. In the oocyst, an asexual proliferation takes place (sporogony) producing thousands of new sporozoites that migrate to the salivary glands of the mosquito and are ready to infect a new vertebrate host [1, 3].

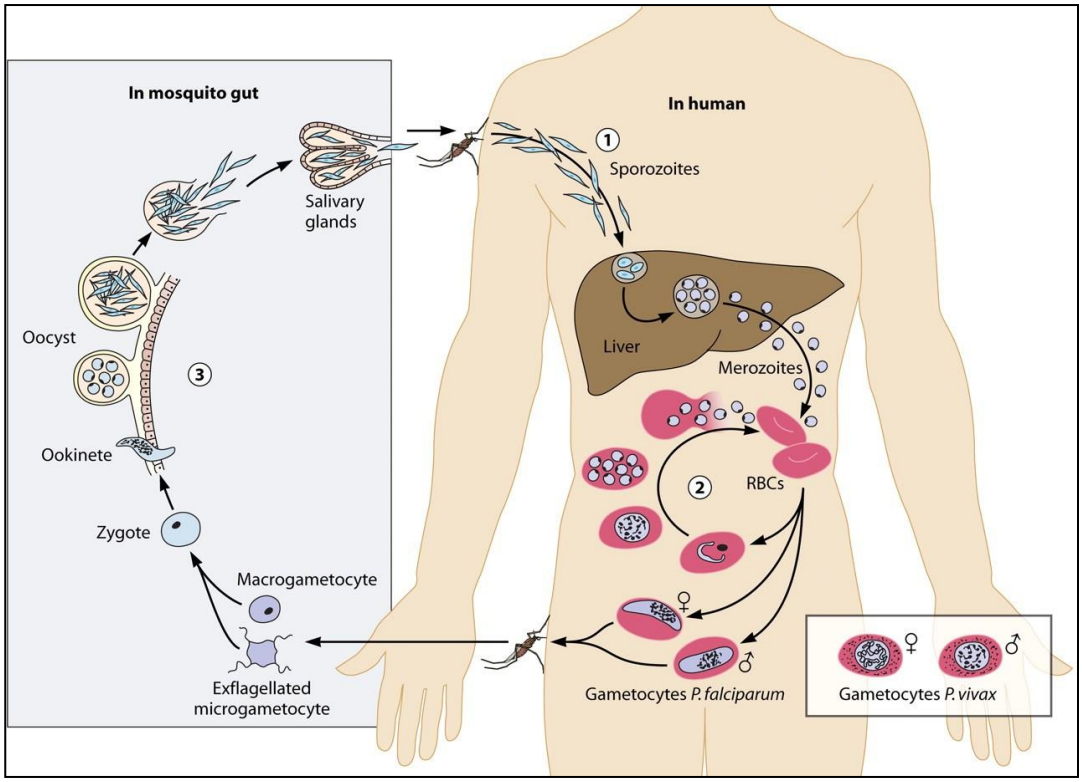

Figure 1.2 Schematic representation of the life cycle of *Plasmodium* parasites showing: (1) the pre-erythrocytic stage, (2) erythrocytic (blood) stage, and (3) Mosquito / sexual stage [1].

1.3 Pathogenesis of human Malaria infection

Human malaria pre-erythrocytic stage development is clinically silent. The subsequent blood-stage of the disease leads to a rapid onset of symptoms due to the increase in parasite numbers, the repeated lysis and invasion of RBCs, and the associated release of cell fragments induce excessive immune responses which cause the typical symptoms of malaria such fever, joint pain, severe headaches and anemia [17, 18]. Infection with *P. malariae* and *P. ovale* is an infrequent cause of mild-moderate clinical malaria, whilst *P. vivax* is a major cause of clinical malaria, but is rarely fatal. *P. vivax* and *P. ovale* also both form dormant hepatic hypnozoites, which can lead to relapse many years after apparent cure.

P. falciparum and *P. vivax* are the major cause of clinical malaria. The global distribution of *P. vivax* is wider because they can develop in mosquitoes at a lower temperature. However, the geographical range of *P. vivax* has been restricted in areas such as West Africa and Papua New Guinea by the evolutionary emergence of the Duffy antigen negative blood group, constituting a loss of an essential receptor for *P. vivax* erythrocytic invasion [19, 20]. *P. falciparum* infections lead to severe symptoms and death if untreated; the most common clinical features of severe malaria are high fever, respiratory distress, vascular obstructions, metabolic acidosis, multi-organ derangement, severe anaemia and neurological syndrome known as cerebral malaria (CM) [21]. CM is believed to be associated with iRBC sequestration in brain microvasculature and is thought to be enhanced by the proinflammatory status of the host and virulence characteristics of the infecting parasites [22, 23]. Sequestration also protects the parasite from being rapidly cleared away by the spleen [24].

The *P. falciparum* specific *P. falciparum* erythrocyte membrane protein 1 (PfEMP1) molecules are thought to be responsible for the aggregation and adhesion of *P. falciparum* infected RBCs. This PfEMP1 molecule is encoded by polymorphic *var* genes, whose transcriptional changes lead to antigenic variation [25]. This single molecule mediates parasite binding to a diverse range

of host receptors expressed in various organs like the heart, lung, brain, liver, kidney, endothelium and placenta, which is associated with respiratory distress, cerebral malaria and pregnancy malaria [26-28].

The cytokines of the proinflammatory cascade, such as TNFα, interleukins, and nitric oxide, are linked to the pathogenesis of malaria [29]. Pro-inflammatory cytokines are initially triggered by the innate immune system provided by the pattern-recognition receptors, such as toll-like receptors (TLRs). TNFα levels have been shown to increase as much as tenfold in patients with cerebral malaria [30]. *In vitro* studies showed the upregulation effect of TNFα on the expression of ICAM1 in the brain endothelial cells, leading to the increase of *infected erythrocyte* sequestration [31]. Also, in cerebral malaria vessels in the brain exhibit increased expression of ICAM1 [32]. It has been suggested that the glycosylphosphatidylinositol (GPI) anchor on the merozoite surface proteins, can activate macrophages through the recognition of a TLR2/TLR1 receptor complex [33]. Similarly, it has been found that the product of parasite-mediated intraerythrocytic digestion of hemoglobin, hemozoin (HZ), through the contaminating plasmodial DNA can activate TLR9 [34, 35]. The development of cerebral malaria in the absence of individual TLR receptors has however been observed in mice [36], therefore it is unclear which (if any) of these TLRs are on the severe malaria causal pathway. A causal and consistent association between immunopathology in severe malaria and these cytokines is not clear, and data from humans is still lacking.

1.4 Control Strategies.

As *Plasmodium falciparum* is the deadliest of the five human malaria species, and is responsible for most of the morbidity and mortality associated with malaria, this thesis focuses on *P. falciparum*. At present, the strategies used to prevent malaria include medications, mosquito elimination and the prevention of bites. There is no vaccine available that provides an effective long-term

protection against *P. falciparum* disease, but theoretically, a vaccine remains a feasible prevention strategy that could enable complete eradication of malaria, if it could be cheaply and efficiently manufactured and delivered throughout endemic areas.

1.4.1 Vector Control.

Vector control refers to methods to decrease malaria transmission by mosquitoes. Enhanced vector control efforts with bed nets and insecticide spraying and better combination drug treatments have led to substantial reductions in malaria cases in the last few years [37]. However, in many other locations there has been no detectable change in disease burden [38]. It is likely that current advances in control will be time-limited unless new interventions are developed and deployed. For individual protection, the most effective insect repellents are based on DEET or picaridin [39]. Insecticide-treated mosquito nets (ITNs) and indoor residual spraying (IRS) have been shown to be highly effective in preventing malaria among children in areas where malaria is common [40, 41]. Encouraged by the early success of using dichloro-diphenyl-trichloroethane (DDT) against malaria, the World Health Organization (WHO) embarked on the Global Malaria Eradication Program (GMEP) in 1955. DDT effectively cleared some endemic areas of malaria. By 1969 the campaign was discontinued when it was recognised that eradication was not achievable in many areas, although the long-term goal remained unchanged [42]. Although a number of wealthier countries, with more temperate climates, succeeded in the eradication of malaria, a steady resurgence occurred in the less-developed countries of tropical latitude in Africa and many parts of Asia [43]. The major cause of this deterioration in malaria control has been the emergence of insecticide-resistant vector and drug-resistant parasites [5], although it was also exacerbated by climate change, civil unrest, travel and increasing levels of HIV infection. Trials of insecticide-treated nets consistently demonstrate efficacy in

terms of reduced child mortality, episodes of clinical disease in both children and pregnant women, and extension of protection to homes without ITNs in the same area [40]. Despite the proven benefits, efforts remain hampered by cost, widespread provision, compliance, and the sustained re-treatment of bed-nets with durable insecticide, coupled with the inevitable emergence of mosquito resistance to modern pyrethroid insecticides (the only class of insecticide approved for use in ITN) are also increasing [44-47]. Although vector control is a simple and highly effective strategy, without sustained and major commitment from international donors and the development of long-lasting bed-nets and new insecticides, this approach can only contribute to malaria control, and consequently further interventions are essential.

1.4.2 Medications

Malaria treatment with antimalarial medications formed the mainstay of malaria prophylaxis for many years and it is the most cost effective means of malaria control available to date [48]. Chloroquine has been the main prophylaxis for malaria but the failure of chloroquine globally elicited the need for new replacement drugs, but the parasite has also successfully gained resistance to few of these drugs. The discovery of artemisinin and the development of artemisinin-based combination therapy (ACTs) have provided some hope [7, 49]. ACTs provide mutual protection against resistance and also reduce transmission, but there is limited implementation due to the high cost associated with them [5, 49]. Intermittent preventive therapy is another intervention that has been used to control malaria in pregnant women and infants [50], and in preschool children where transmission is seasonal [51]. There are several success stories to show that the expansion of prevention programs and improved access to effective anti-malarial drugs can reduce malaria cases and deaths associated with the disease, but in general achieving this remains a major public health challenge.

Enhanced vector control efforts with bed nets and insecticide spraying and better combination drug treatment have led to substantial reductions in malaria cases in the last few years [37]. After the introduction of ACTs and vector control in South Africa the number of cases and deaths fell by 80%. However, in many other locations there has been no detectable change in disease burden [38]. It is likely that current advances in control will be time-limited unless new interventions are developed and deployed.

History suggests that this is unlikely to retain the current levels of efficacy with only using the same traditional vector control and medication strategies. There are precedents for mosquitoes becoming resistant to insecticides [52] and changing their feeding habits to diminish the impact of the bednets [53]. *P. falciparum* malaria parasites have developed resistance to antimalarial drugs like chloroquine in the past [54], and Artemisinin resistance in *Plasmodium falciparum* has emerged in Southeast Asia [55, 56]. *New* and improved *tools* are needed to control and eliminate *malaria*, highlighting the need for an effective malaria vaccine.

1.4.3 Vaccines

Vaccines have saved more lives than any other class of biomedical intervention [57]. The global eradication of smallpox in the 1970s was entirely dependent upon the deployment of a highly efficacious vaccine [58, 59]. Thus, an efficient vaccine can be an extremely powerful public-health tool. A malaria vaccine is urgently needed global health priority, especially with the increasing reports of resistance to anti-malarial drugs and insecticides [60]. An efficient malaria vaccine would be a cost effective tool and could potentially allow complete eradication of malaria, if it could be cheaply and efficiently manufactured and delivered throughout endemic areas. The complex *Plasmodium* life cycle would appear to hamper the development of a vaccine against malaria. Specifically as for most of its development the malaria parasite is intracellular, developing

either inside hepatocytes or erythrocytes and thereby limiting its recognition and removal by the immune system. Moreover it exists as many morphologically and antigenically different forms, and parasite molecules most readily detected by the host immune response exhibit high levels of antigenic diversity (highly diverse allelic polymorphisms) and several of these critical parasite proteins are immunologically variant, where the genome encodes multiple copies of antigenically diverse but functionally related proteins [61-63]. At present there is no completely efficient or licensed vaccine against malaria or any parasitic diseases for use in humans [64]. For protection of individuals, studies of experimental and naturally acquired immunity provide a solid rationale for the feasibility of a malaria vaccine that can target either pre-erythrocytic (sporozoite and liver) stage or asexual erythrocytic blood stages of the parasite, or both. Additionally, protection against malaria in humans was first demonstrated in the 1970s through vaccination with irradiated parasites delivered by mosquito bite [26, 65, 66]. Ideally, a malaria vaccine would be cheap, safe, and easy to manufacture and administer, and confer life-long immunity. The challenges faced by malaria vaccine developers are clearly daunting, even before any effective vaccine is commercially available. Huge political and financial efforts are also likely to be required to persuade the governments of poor and developing countries of the economic cost-benefit ratio of deploying an effective, but expensive, vaccine.

1.5 Naturally Acquired Immunity (NAI) to malaria

Epidemiological evidence showed individuals living in malaria endemic areas do not develop severe malaria despite chronic parasitaemia in their blood. This state of protection against malaria is referred to as naturally-acquired immunity (NAI), and is slow to develop requiring 10-15 years of continuous exposure and is imperfect [21, 67]. Sterilizing immunity against infection is never fully achieved, and an asymptomatic carrier status is the rule among adults. This

phenomenon of a high degree of immune responsiveness together with the nearly permanent presence of relatively low densities of parasites was originally described by Koch in 1900 [68]. NAI provides solid protection against severe morbidity and mortality. Even mild disease is relatively uncommon. The final degree of immunity, termed sterilising immunity, confers the ability to completely clear parasites from the blood-although this class of immunity is by definition impossible to fully distinguish from asymptomic because there may always be a subpatent (i.e. non-microscopically detectable) blood-stage infection. Immunity against the pre-erythrocytic stages of the life cycle probably has only a minor role in protection [69]. Malaria parasites can be targeted by the immune system at any point during their developmental cycle in mammalian host. However, naturally acquired immunity is directed at the erythrocytic stage, with little evidence of naturally acquired immunity to the pre-erythrocytic stage [69, 70]. The direct injection of blood-stage parasites into naturally immune individuals bypassing the pre-erythrocytic stage, have showed that these adults were able to control parasite multiplication rates in the blood and avoid the disease symptoms [71]. Research suggests this could be because parasite numbers are too low prior to multiplication in the liver to induce a high level of immunogenicity, and possibly because natural immune ligands are hidden from pattern recognition receptors (PRRs), leading to a minimal innate response [72]. Alternatively, it could be because the liver is programmed to minimize inflammation (and hence the innate system is not activated) [73]. It could be important to understand naturally acquired immunity in order to better inform our vaccine efforts.

1.5.1 The innate immune system

The innate immune system is the first line of immune defence. In malaria, the innate immune response has two functions: first, acting to control infections with a degree of direct parasite killing; and second, the detection of an infection

in order to stimulate an adaptive immune response [74]. Innate immune recognition is mediated by PRRs, such as toll-like receptors (TLRs), and each receptor has broad specificities for general microorganism characteristics [75, 76]. The innate system includes the complement system (with roles such as opsonization, triggering inflammation and induction of antibodies), innate immune cells, such as natural killer (NK) cells, phagocytic cells (e.g. neutrophils, macrophages and dendritic cells) and B cells which can process and present antigens to T cells [76]. Strictly speaking B cells are part of the adaptive immune system as their B cell receptors are antigen specific. Although they do present antigen to T cells, it is more for increased self-activation

After a mosquito bite, sporozoites enter the bloodstream and are transported to the liver where they infect and then replicate inside hepatocytes. Blood-stage Plasmodium infections have been shown to induce innate immune responses, but whether the liver stage of malaria infection activates the innate immune system is less clear. A study by Kappe and colleagues used RNA sequencing techniques to analyse gene expression data from mouse livers after infection with attenuated *Plasmodium yoelii*, which only develop into liver-stage forms. They found that the parasites induced an innate immune response in the liver that was mediated by type I interferons (IFNs) and IFNγ, and mice that lacked IFNγ, the type I IFN receptor or IFN-regulatory factor 3, could not suppress liver-stage infection. Thus, in mice, innate immune responses are induced during malaria liver-stage infection, and this response can limit parasite development prior to the infection of red blood cells [77]. Additionally, there are data to suggest a weak response is induced which the parasite is able to evade. The evidence supporting an interaction between the innate immune system and sporozoites is two-fold: first, DCs are able to capture sporozoites that remain in the lymphatic system [78]; second, there is evidence in murine models of an innate cellular infiltrate in the liver surrounding infected hepatocytes [79-81]. This infiltrate is not seen when heat-killed sporozoites are injected [82], and a greater infiltrate is seen in BALB/c mice than C57BL/6 mice (which are more

susceptible to malaria) [83]. Furthermore, the difference in virulence between *P. yoelii* (17X non-lethal) and *P. berghei* has been correlated with the innate cell infiltrating the liver [84].

Whilst the blood-stage of the parasite life-cycle has been well studied, our knowledge of the role of the innate immune system in recognizing Plasmodium blood-stage infections is still limited. Natural killer (NK) cells mediate cytotoxicity and IFN production are essential for blood stage immunity [85]. Research has demonstrated that the innate system responds quickly to blood-stage infection by inducing a high amount of pro-inflammatory cytokines [86, 87], which contributes not only to the first line of defence but also to immunopathology. It is likely that many molecular host-parasite interactions instigate this response, however, the relevance of each is not yet known. Both the glycosylphosphatidylinositol (GPI) anchors on the parasite and the by-product haemozoin have been suggested as targets of recognition by innate cells, through PRRs such as TLR2, 4 and 9 [33, 88, 89]. Consequently, TLR ligands have more recently been exploited as adjuvants or targets for blood-stage vaccines (e.g. GPI [90], CpG DNA [91] and haemozoin [92]). Adjuvants help activate the immune system, allowing the antigens in vaccines to stimulate a response that leads to long-term protection.

1.5.2 The adaptive immune system

The innate immune system tells the adaptive immune system when it's time to help mount a defence. The adaptive system delivers specific, long-lasting immunity and memory and is the target of vaccination strategies. There are two broad classes of such responses, cell-mediated immune responses and humoral (antibody) responses, and they are carried out by different classes of lymphocytes, called T cells and B cells, respectively. In general the cell-mediated immune responses are comprised of activated T cells that react directly against a foreign antigen presented to them on the surface of a host cell. The T cell

could kill an infected host cell with intracellular pathogen that has immunogenic antigens presented on its surface major histocompatibility molecules (MHC), thereby eliminating the infected cell before the pathogen has had a chance to replicate. In other cases, the T cell produces signal molecules that activate macrophages to destroy the invading microbes that they have phagocytosed. In humoral responses, the second class of adaptive immune response, B cells are activated to secrete antibodies, which are proteins called immunoglobulins.

1.5.2.1 Cellular immunity: CD4+ and CD8+ T cells

T lymphocytes are defined by the surface expression of the markers $CD4^+$ and $CD8^+$, and the co-receptor $CD3^+$ into $CD4^+$ T helper cells and cytotoxic $CD8^+$ T cells. $CD4^+$ T cells are divided into a number of subsets, including Th1, Th2, Th17 and T regulatory cells, which primarily act through the recruitment and activation of other cell types through the release of cytokines after recognising antigen presented by MHC Class II molecules only on the surface of professional antigen presenting cells. $CD8^+$ T cells have the capacity to sample the peptide-MHC class I complexes expressed on the surface of infected cells, thus indirectly sampling the repertoire of proteins found inside those cells. In response to recognition of a peptide MHC class I complex and giving appropriate conditions, effector $CD8^+$ T cells are able to kill their target cells. This can occur through a number of mechanisms, including exposing the target cell to the FasL death ligand, thus inducing apoptosis, and through the release of perforin and granzyme proteins, which have direct killing activity.

Pre-erythrocytic immunity appears to play only a minor role in naturally acquired immunity against malaria in humans, despite the ability of infected hepatocytes to present antigen on MHC class I complexes. RBCs do not express MHC class I on their surface in humans, meaning that $CD8^+$ T cells cannot play a direct role in clearance of blood stage parasites. The role of CD4 T cells in NAI is also not clear [93, 94]. A few studies have shown associations between cellular

immune responses and liver-stage malaria. These include: cytokine responses and cytotoxic cells directed against the protein liver-stage antigen 1 (LSA1) [95, 96]; memory responses against the thrombospondin-related adhesion protein (TRAP) [97]; and $CD4^+$ T cells response directed against the CSP [98]. Also, it has been shown that $CD4^+$ and $CD8^+$ T cells from non-exposed individuals are able to inhibit *P. falciparum* growth *in vitro* [99]. Immunity after experimental infection with parasitized RBCs was characterized by an absence of detectable antibodies, but the presence of a proliferative T cell response [100]. However, naturally acquired immunity directed towards the blood-stage has more often been associated with antibody-mediated protection.

The importance of T cells in protection against blood-stage infection in murine models has been clearly demonstrated [101-103]. Vaccine-induced protection from *P. chabauidi adami* in mice can be reversed by depletion of $CD4^+$ cells, and granted to naïve mice by passive transfer of $CD4^+$ T cells from vaccinated mice [104]. Thus, $CD4^+$ T cells can have a protective role in some species of rodent malaria. However, the evidence for a similar role against *P. falciparum* disease is less well established. This does not rule out the indirect role played by $CD4^+$ helper T cells in the development of the humoral immune response [105]. Severe combined immunodeficient mice (SCID) reconstituted with T cells from immune donors suppress the growth of *P. chabaudi* parasites suggesting that T cells contribute to immunity [106].

The *in vitro* lymphocyte proliferation and interferon-gamma (IFN-γ) production in a response to MSP1 antigen increase with age and strongly correlate (together with Ab responses) with the resistance to episodes of malaria-associated fever as shown in partially immune children in West Africa [107]. Also, an association between the number of malaria episodes and the frequency of anti-MSP1 T cell responses in the exposed donors following *in vitro* stimulation was observed in Brazil [108], suggesting that the induction of blood-stage cellular immunity may heavily rely on the number of malaria episodes.

However, cell-mediated immunity has been consistently demonstrated as a major factor in vaccine-induced protection in both humans and animal models [109, 110]. Pre-erythrocytic stage of infection is an excellent target for a T-cell dependent vaccine, because of the extremely low numbers of parasites and infected cells. Whilst T cell mechanistic studies are technically challenging on human samples, murine research has shown that T cells can recognize parasite-derived peptides on the surface of hepatocytes [66, 111, 112]. These T cells could either be primed in the liver [113, 114], or primed in draining lymph nodes and the spleen, followed by homing to the liver [115].

1.5.2.2 Humoral immunity: B cells and Antibodies

B cells producing antibodies generate humoral immunity. The functions of antibodies include neutralization, opsonization and activation of complement, as well as antibody-dependent cellular cytotoxicity (through NK cells). In malaria, antibodies can inhibit the migration, invasion and traversal activity of sporozoites, as well as inhibiting invasion of merozoites into RBCs and the subsequent intracellular growth. Antibody-mediated immunity has a crucial contribution to naturally acquired immunity at the blood-stage and, to a lesser extent, to the pre-erythrocytic stage. In 1961, a pivotal study demonstrated that transferring serum from malaria immune adults to children could protect against malarial infection [116, 117].

The most widely studied sporozoite antigen, CSP, can induce high antibody levels which were associated with a decreased risk of malaria infection in Kenya [118, 119]. Antibodies directed against surface proteins of merozoites either block RBC invasion or make them susceptible to phagocytosis via Antibody-dependant cellular inhibition (ADCI). These antibodies bind to phagocytes via their Fc receptors which lead to the inhibition of parasite growth [120-123]. Antibodies also initiate parasite clearance by opsonization or complement-mediated damage [124]. The levels of antibody in humans against merozoite

surface proteins or those critical for erythrocyte invasion, such as MSP-1 and apical membrane antigen-1 (AMA-1), have been associated with protection against clinical disease and/or high parasitaemia in field studies [107, 125].

Naturally acquired immunity is largely dependent on the acquisition of specific and protective antibodies against *P. falciparum* erythrocyte membrane protein 1 (PfEMP1) [126]. These antigens expressed on the surface of infected erythrocytes are relatively polymorphic and the protection associated with them seems to be strain-specific [127] [128]. Nonetheless, it has recently been suggested that the anti-PfEMP1 Ab response is the key determinant of the infection outcome in the naturally immune individuals [129]. The sequestration of pRBCs is mediated by the expression of *P. falciparum* erythrocyte membrane protein 1 (PfEMP1) on the surface of the infected cell, thus preventing their rapid clearance upon circulation through the spleen [130]. PfEMP1 is encoded by ~60 copies of the *var* multigene family per parasite genome. PfEMP1 divided into three families A, B and C, based on their conserved upstream regions, and can undergo clonal antigenic switching in response to immune pressure [131-133]. This differential expression is central to host-parasite interactions and pathogenesis [134], and certain variants are recognised as major virulence factors [135]. For example, group A variants do not bind CD36, and have been implicated in mediating RBC rosetting [136, 137] [138], a process whereby iRBC adhere to the complement-receptor 1 (CR1) located on the surface of uninfected erythrocytes causing RBC clustering [139]. On the other hand, group B and C variants can bind to the protein receptor CD36 (also a co-receptor for toll-like receptor 2) expressed on the endothelial cells of microvasculature leading to IE sequestration, and activate $CD4^+$ T cells [140] and/or modulate the development of dendritic cells (DCs) [141]. The cysteine-rich interdomain region-1 (CRIR1), one of the PfEMP1 cytoadhesion modules interacts with CD36 receptor and participates in the adhesion of infected erythrocytes to the endothelial microvascular cells. CRIR1 is highly conserved and can induce anti-

sequestration Abs that prevents cytoadhesion of infected erythrocytes [142]. Also, parasites causing placental malaria, the form of severe malaria in pregnant women, uniformly express a particular PfEMP1 protein (VAR2CSA) that mediates binding to chondroitin sulfate A (CSA) in the intervillous space [143]. Furthermore, histological studies performed on patients who died from cerebral malaria have shown that IEs and intercellular adhesion molecule-1 (ICAM-1) colocalise on microvascular endothelial cells [144] [145], suggesting that cytoadhesion through ICAM-1 may contribute to the IE sequestration in severe malaria.

The predominance of different immunoglobulin G (IgG) isotopes has been linked to protection or susceptibility to malaria. It has been shown that the dominance of immunoglobulin IgG1 and IgG3, two cytophilic isotypes, correlated strongly with protection. The non-cytophilic IgG2 predominated in nonprotected subjects [146], whereas IgG4 enhanced the risk of malaria infection [121] Non-cytophilic IgG4 may compete with the cytophilic isotypes for antigen recognition, thus blocking cytotoxicity mediated by cellular responses; possibly similar in principle to that documented for non-protective blocking and protective inhibitory antibody epitopes within *P. falciparum* MSP-119 [147, 148]. In conclusion, the mechanisms which are involved in the Ab-mediated natural protection include binding of the merozoites and the prevention of RBC invasion, antibody-dependent cellular cytotoxicity (ADCC) mediated by cytophilic Abs, and binding of antibodies to the parasite-specific molecules translocated to the surface of infected RBCs that way preventing parasitized RBC sequestration and, possibly, leading to greater clearance of infected RBCs by spleen.

Despite the importance of antibody responses in naturally acquired immunity and their role in blood-stage parasite inhibition, an antibody-mediated vaccine against blood-stage malaria has not reached the same level of efficacy as demonstrated for pre-erythrocytic vaccines [149, 150]. This is likely due in part

to the limited understanding of the targets and the exact effector mechanism of the antibodies, the very high numbers of parasitized RBCs, the short transit time for merozoites between RBCs and because naturally acquired immunity is never sterilizing. The pre-erythrocytic leading vaccine, RTS,S is primarily protective through inhibition of sporozoite invasion into the liver, by inducing antibodies against CSP [151]. However, there is only a short amount of time available for sporozoites and the immune system to interact, which may account for the sub-optimal efficacy induced by RTS,S. Nevertheless, both antibody and cell-mediated approaches for pre-erythrocytic vaccines are being actively linked.

1.6 Malaria vaccine intervention strategies

Development of any new vaccine is a difficult task, and the malaria parasite is even more challenging because of its complex life cycle and antigenic complexity. *P. falciparum* can only undergo sexual reproduction in *Anopheles* mosquitoes, its definitive host. The human is the intermediate host where parasites only reproduce asexually in both the liver and the blood [152]. However the life cycle provides a number of opportunities to disrupt transmission of the parasite, and to clear infection once it has established itself. Most vaccine development initiatives target one or more of the following three stages of parasite development:

1.6.1 Pre-erythrocytic stage

Pre-erythrocytic vaccines target the sporozoites and/or liver stages and aim to generate antibody responses against sporozoites to prevent hepatocyte invasion and/or T-cell responses to kill infected hepatocytes [153]. Most researchers agree that a future malaria vaccine will certainly contain a central component that targets the pre-erythrocytic stage of malaria as the first line of defense [154]. Vaccines based on the pre-erythrocytic stages usually aim to prevent infection completely before the development of any clinical symptoms.

However, vaccines acting at the pre-erythrocytic stage may also reduce the severity of the subsequent blood infection. This could occur by reduction in the number of parasites emerging from the liver into the blood or by delaying the initiation of the blood-stage infection thereby allowing the immune system additional time to mount effective immune responses.

1.6.2 Erythrocytic stage

Erythrocytic vaccines target merozoites or iRBC and aim to generate antibody responses that target either merozoite antigens or parasite antigens expressed on the surface of infected RBC (iRBC), therefore blocking parasite entry into a RBC or opsonising parasite/iRBC for phagocytic destruction [155]. Blood-stage vaccines aim to reduce (and perhaps eventually eliminate) the parasite load once a person has been infected, thus alleviating the clinical symptoms.

1.6.3 Mosquito stage

Transmission blocking vaccines target sexual and/or ookinete stages within the mosquito midgut and aim to reduce transmission. Such vaccines do not provide protection against a malaria infection for the immunized individual but are aimed at reducing infections within the community. Consequently, they are likely to be deployed as part of multi-stage vaccine strategy thereby limiting disease in the host and transmission to the population [156].

In this study, we have focused in the development of some novel pre-erythrocytic malaria vaccines (blood stage and transmission blocking vaccines are also in development in our lab, but will not be discussed here).

1.7 The leading pre-erythrocytic stage vaccines

Developing an effective vaccine against malaria remains a global priority. Vaccination is the most cost effective method to control the disease, and ultimately eradication, especially with the increasing reports of resistance to anti-malarial drugs and insecticides [47, 157-159]. Pre-erythrocytic stage malaria vaccines have made substantially more progress than those targeting any other stage of the parasite's life-cycle [160, 161]. There are currently two major types of vaccines for the pre-erythrocytic stage of malaria that are under active clinical development.

1.7.1 Whole sporozoite vaccination strategies

The earliest and first approach is based on the administration of whole irradiated sporozoite using irradiated infected mosquitoes to deliver the irradiated sporozoite to vaccinees and thereby provided pre-erythrocytic immunity that has been shown to last many months, although many thousands of bites were necessary [24, 26, 28, 65, 66]. Recently, the biotech company Sanaria [162] has developed a vaccination method with needle injection of irradiated cryopreserved sporozoites purified from the glands of irradiated mosquitoes. Despite the encouraging developments, this method of vaccination still appears unsuitable for large-scale deployment [77]. Irradiated sporozoites are capable of invading hepatocytes but their development is arrested, providing a repertoire of antigens for the immune system to respond against whilst not producing a blood-stage (or symptomatic) infection [32].

1.7.2 Pre-erythrocytic malaria stage subunit vaccines

Alternative approaches to malaria vaccines have been developed sub-unit vaccines targeting a particular antigen expressed at one or more stages of the parasite's life-cycle. There are two subunit malaria vaccines in advanced clinical trials. The first most advanced sub-unit vaccine, RTS,S administered in adjuvant AS01 [163]. The vaccine includes a hybrid protein RTS, a genetic fusion of the

surface antigen of hepatitis B to the central repeat and C terminus of the *P. falciparum* circumsporozoite protein [164], which targets the circumsporozoite protein (CSP) at the pre-erythrocytic stage. RTS,S may be licensed in the near future but still lacks high levels of durable efficacy [165-167]. RTS,S primarily provides protection through antibodies, with perhaps some contribution from CD4+ T cells [151, 168].

The second approach to malaria vaccine development is another sub-unit vaccination strategy; the use of viral vectored vaccines expressing a chosen antigens in a heterologous prime-boost regimen, mainly targeting the liver-stage parasite through cellular immunity but more recently also to provide blood-stage immunity [169, 170]. Vectored vaccines are a relatively new technology compared to protein/adjuvant or attenuated pathogen vaccines. They have the advantage of being able to reliably express most sequences, with insert sizes of up to 6Kb even in adenoviruses, being able to induce an exceptional high T cell response and have excellent thermostability properties in trehalose-based formulations [171, 172]. The leading viral vector vaccine combination is vaccination with a chimpanzee Adenovirus serotype 63 (ChAd63) followed by a boost with a Modified Vaccinia Ankara virus (MVA) encoding the antigen ME-TRAP, the pre-erythrocytic thrombospondin-related adhesion protein (TRAP) fused to a multi-epitope string (ME) [173]. Whilst this vaccine displays only moderate levels of efficacy in naïve-adults [109], it induces exceptionally high $CD8^+$ T cells [173], a key feature of this viral vectored prime-boost approach **(see 1.8)** [174-176]. There is a strong rationale for the development of a $CD8^+$ T cell-inducing liver-stage vaccine given the mode of action of irradiated sporozoite vaccines, and the general advantages of pre-erythrocytic vaccines.

1.8 Heterologous ChAd63-MVA prime-boost vaccination strategy

Protection by irradiated sporozoites in mice and non-human primates is dependent upon $CD8^+$ T cells targeting the liver-stage [26, 66, 177, 178]. Abundant evidence has indicated that $CD8^+$ T cells can provide protective immunity at the liver-stage of rodent malarial infections, but converting this understanding into a deployable liver-stage subunit vaccine in human has proved difficult due to the limited ability to induce $CD8^+$ T cells in humans using available vaccine technologies [179, 180]. An effective *P. falciparum* pre-erythrocytic vaccine should ideally induce high antibody (Ab) titres to target sporozoites and high frequencies of T cells capable of eliminating infected hepatocytes to arrest the parasite's cycle during its development in the parasitophorous vacuole membrane (PVM).

Many combinations have existed, but a ChAd63 prime followed by a MVA boost has shown to be the most potent at producing $CD8^+$ T cells [109, 173] and protective efficacy in the field [181]. Interestingly, both the order and length of interval have been crucially important in inducing a good response [182-185]; MVA is not good a priming vector, but is excellent at boosting and an extended eight-week interval has shown the best results in our group so far. Whilst $CD8^+$ T cell responses are required for an effect at the liver-stage, and hence crucial for a pre-erythrocytic vaccine, antibodies are needed for a blood-stage effect. Whilst viral vectors can induce high levels of antibodies, prime-boost regimens incorporating a protein vaccine have also demonstrated potent antibody production [186-188]. This may prove vital in a combination vaccine, targeting both the liver and blood or sporozoite stages, where both a high level of $CD8^+$ T cells and antibodies will be required to exert the anticipated effect. Heterologous prime-boost regimens have been extensively evaluated with liver- and blood-stage malaria antigens and consistently induced strong immune responses in murine [171, 183], rabbit [189], rhesus monkey [190] and human models [173, 176, 191]. ChAd63 and MVA have been used as recombinant vectored vaccines to induce strong and protective antibody and T cell responses

against the encoded *P. falciparum* TRAP (PfTRAP) both in pre-clinical studies and clinical trials [173, 182, 192-194]. In this study we have applied the heterologous prime-boost vaccinations utilizing this clinically relevant recombinant ChAd63 and MVA viral vectors expressing novel *P. falciparum* transgenes. Furthermore, the vaccine efficacy was measured using a novel 'marker-free' transgenic (tg) *P. berghei* parasite expressing *P. falciparum* genes of interest **(see 1.10.2).**

1.9 Identifying further protective pre-erythrocytic antigens

The availability of a full genome sequence of *P. falciparum* and subsequent transcriptomic and proteomic work on it [195, 196] and rodent parasites [197] has opened new avenues for research and identified several genes expressed at the sporozoite and liver-stage of *P. falciparum* that are potential targets for a liver-stage subunit vaccine. Sub-unit vaccines are easier and less expensive to manufacture and deploy, number of approaches are being assessed in order to increase their efficacy. These include the use of new adjuvants, different sub-unit vaccination platforms and the use or addition of new antigens. There is increasing evidence that antigens other than CSP or TRAP may contribute to a protective immune response [195, 198-200] and it is likely that multiple antigens will be needed to reach the high levels of efficacy achievable with large doses of irradiated sporozoites. We have selected fifteen candidate pre-erythrocytic *P. falciparum* antigens identified from the literature and through database mining and bioinformatic analysis (**see Table 1**). Each antigen has either been shown to be well expressed in the sporozoite or during the liver-stage of infection, is a target of cell-mediated immunity in naturally exposed individuals or those immunised with irradiated sporozoites, or a homolog has been shown to be protective in murine or non-human primate studies (**see Table 2**).

Table 1.1: Accession number of all the generated *P. falciparum* pre-erythrocytic vaccines and their *P. berghei* homologs if exist.

Pf Gene	Gene ID	Gene Size (bp)	OFR Size (bp)	Total SNPs	Non-Syn SNPs	Syn SNPs	Non-Syn/Syn Ratio	*Pb* Genes ortholog	Gene ID
PfLSA-1	*PF3D7_1036400*	3489	3489	312	155	157	0.99	*NA*	*NA*
PfLSA-3	*PF3D7_0220000*	4835	4677	380	270	110	2.45	*NA*	*NA*
PfCelTOS	*PF3D7_1216600*	549	549	37	36	1	36	*PbCelTOS*	*PBANKA_143230*
PfUIS3	*PF3D7_1302200*	690	690	7	5	2	2.5	*PfUIS3*	*PBANKA_140080*
PfLSAP1	*PF3D7_1201300*	321	321	5	4	1	4	*NA*	*NA*
PfLSAP2	*PF3D7_0202100*	1017	909	27	22	5	4.4	*NA*	*NA*
PfETRAMP5	*PF3D7_0532100*	546	546	18	13	5	2.6	*NA*	*NA*
PfFalstatin	*PF3D7_0911900*	1652	1242	49	13	36	0.36	*Inhibitor of cysteine proteases*	*PBANKA_081300*
PfCSP	*PF3D7_0304600*	1194	1194	93	44	49	0.9	*PbCSP*	*PBANKA_040320*
PfTRAP	*PF3D7_1335900*	1725	1725	110	105	5	21	*PbTRAP*	*PBANKA_134980*
PfHT	*PF3D7_0204700*	1515	1515	13	5	8	0.63	*PbHT*	*PBANKA_030250*
PfRP-L3	*PF3D7_1027800*	1161	1161	4	0	4	0	*PbRP-L3*	*PBANKA_051190*
PfSPECT-1	*PF3D7_1342500*	1263	738	57	11	46	0.24	*PbSPECT-1*	*PBANKA_135560*
PfSPECT-2	*PF3D7_0408700*	3453	2529	170	38	132	0.29	*PbSPECT-2*	*PBANKA_100630*
PfB9	*PF3D7_0317100*	3201	2910	101	39	62	0.63	*PbB9*	*PBANKA_080810*

Table 1.2 brief descriptions for all the generated *P. falciparum* pre-erythrocytic vaccines and the rationale behind choosing them:

Pf Gene	***Reason for inclusion***	***Reference***
PfLSA-1	*Target of T cells in naturally exposed individuals and volunteers immunized with irradiated sporozoites; liver-stage specific; conserved.*	[201-203]
PfLSA-3	*Target of T cells in naturally exposed individuals and volunteers immunized with irradiated sporozoites; protection in mice, chimpanzees and monkeys; highly conserved.*	[204-208]
PfCelTOS	*Target of T cells in volunteers immunized with irradiated sporozoites; cross species protection in inbred and out bred mice; highly conserved; expressed in mosquito-stage parasites so potential for transmission blocking effect.*	[195, 209, 210]
PfUIS3	*Protection in mice in combination with Pf*Falstatin*; P. yoelii UIS3 GAP sporozoite immunization gives sterile protection; transcript level is reduced by 53% in irradiated sporozoites.*	[211-213]
PfLSAP1	*Up regulated during liver infection in P. falciparum; liver-stage specific.*	[214]
PfLSAP2	*Up regulated during liver infection in P. falciparum.*	[214]
PfETRAMP5	*Interaction with apolipoprotein alleles which are associated with increased risk of malaria.*	[211, 215]
PfFalstatin	*Protection in mice in combination with PfUIS3; P. berghei homolog (falstatin) inhibits parasite growth.*	[211]
PfCSP	*CSP is the antigen of the only vaccine candidate, RTS,S/AS01, that has advanced to Phase III clinical trials. CSP is involved in the sporozoite motility and invasion of hepatocytes. It is a target of both cellular immunity and antibodies and probably contributesd to protection induced by irradiated sporozoite vaccination.*	[216-222]
PfTRAP	*TRAP is a type-1 transmembrane protein. It is essential for attachment, invasion of both salivary gland and the liver, and is also important for the sporozoite's gliding motility. TRAP, like CSP, was found to be an*	[223-227]

	immunogenic target in volunteers vaccinated with irradiated sporozoites. P. yoelii TRAP homolog was shown to induce CD8+ T cell dependent protection in mice. PfTRAP is included in the leading vaccine ChAd63-MVA ME-TRAP (ME is a multi-epitope from various pre-erythrocytic antigens) which was designed to induce maximal cellular immunity, particularly of CD8+ T cells.	
PfHT	*PfHT is a facilitative hexose transporter in the Major Facilitator Superfamily of integral membrane proteins that mediates the uptake of glucose and fructose by the parasite. PfHT is a single copy gene in the P. falciparum genome with no close paralogues. It is one of the identified surface-exposed proteins in the Malaria Parasite Salivary Gland Sporozoites which bears 12 predicted transmembrane domains.*	[228, 229]
PfRP-L3	*Unlike the well-studied CSP antigen that coats the infectious sporozoite, the Ribosomal Protein-L3 (RP-L3) is not highly expressed until later in the liver and RBC stages. According to a study that has been done by Murphy, S. C.et. al., the RP-L3 response was mediated by CD8+ T cells because anti-CD8 but not anti-CD4 antibodies blocked the response. RP-L3 is conserved in Plasmodium berghei ANKA (PBANKA_051190), Plasmodium falciparum (PF10_0272), and Plasmodium vivax (PVX_111330).*	[230]
PfSPECT-1	*The sporozoite microneme proteins essential for cell traversal, SPECT-1 and SPECT-2, are considered attractive pre-erythrocytic immune targets due to the key role they play in crossing of the malaria parasite across the dermis and the liver sinusoidal wall, prior to invasion of hepatocytes.*	[231]
PfSPECT-2		
PfB9	*PfB9 is one of the '6-cysteine protein family' in the Plasmodium parasite, a family which includes proteins that possess two or more structurally conserved domains, each of which comprise a core of 6 interspaced cysteine amino acid residues and all members contain a signal sequence. Several of these proteins have a critical function in fertilization or in infection of hepatocytes. Reverse genetic analysis of B9 protein shows that it plays an important role in development of the pre-erythrocytic parasite forms.*	[21]

1.10 Small-animal models of malaria in vaccine researches

1.10.1 Rodent malaria species

There are four rodent malaria species, namely *P. berghei*, *P. yoelii*, *P. chabaudi*, and *P. vinckei*. These models are used to study drug action and to identify targets for protective immune responses. Although a high level of homology exists between the genes of *Plasmodium* species that infect rodents and humans [232, 233], critical differences often exist in the sequence and structure between the encoded proteins. In addition, *P. falciparum* malaria parasites express genes that are absent from rodent parasite genomes, for example the original liver-stage specific antigen LSA-1 has no rodent homologue. These genetic differences complicate the analysis of drugs/inhibitors or immune factors in rodent models and the effective translation of findings to human malaria. Moreover, it has been suggested that immune-effector functions of $CD8^+$ T cells against liver stage antigens may be Plasmodium species specific [196, 234, 235]. Despite their intrinsic differences rodent malaria parasites have provided invaluable insights into malaria vaccine design and continue to be the major *in vivo* proof-of-concept models.

1.10.2 Transgenic *P. berghei* malaria parasites

Development of malaria vaccines, including *P. falciparum* has been impaired by numerous factors. Amongst them, none of the human malaria sporozoites infect mice and therefore the easily accessible rodent models cannot be used to test the protective efficacy of a new vaccine. For this reason, the assessment of vaccine efficacy has relied on the use of mouse and primate models, which are infected by other malaria parasites that can differ in the sequence or presence of genes and proteins that are tested as vaccine candidates. We propose here approaches to circumventing this limitation to enable the assessment of vaccine efficacy in a pre-clinical model; we constructed transgenic *P. berghei* parasites expressing *P. falciparum* antigens that showed normal infectivity in mice. We

used these parasites in a challenge model where mice immunized with viral vectored vaccines were challenged with transgenic parasites expressing *P. falciparum* antigens. Protective efficacy in these mice was determined by liver load and/or prepatent period. In addition, this strategy could further help to define the correlates for protection, such as the quality or quantity of antibodies and T cells required to protect against sporozoite challenge. This approach permits an easier validation of new vaccine candidate antigens and may reduce the need for parasite challenge studies in non-human primates.

Falciparumized rodent parasites have been used to assess the efficacy of candidate vaccines against the *P. vivax* TRAP protein [236], the *P. falciparum* and *P. vivax* CS proteins [237, 238], the *P. falciparum* and *P. vivax* P25 proteins [239, 240] and the *P. falciparum* MSP1 gene [241, 242]. In addition, humanized *Pb* parasites expressing *P. falciparum* cyclic GMP-dependent protein kinase (PKG) and *P. falciparum* hexose transporter 1 have been generated, permitting *in vivo* screening of inhibitors interfering with PKG and antimalarial sugar anologues respectively [243, 244].

Our strategy of generating these transgenic parasites minimized the risk of introducing exogenous sequences in these parasites that may affect sporozoite fitness of the transgenic parasites. We applied the novel 'gene insertion/marker out' (GIMO) system for transfection of the rodent malaria parasites, *P. berghei* [245]. Reference mother lines were created that contain the hdhfr::yfcu selection marker stably integrated into a silent genomic locus, either Pb230p locus in chromosome-3 or Pbs1 locus in chromosome-12. Transfecting these mother lines with DNA constructs that target the modified loci, followed by negative selection of transformed parasites with 5-FC is a simple and fast method to generate mutants that stably express heterologous proteins and are free of drug-selectable markers **(**see **Figure 2.8).** The GIMO transfection technology is a useful tool to generate a wide range of mutants expressing reporter and/or other heterologous proteins (under the control of different

promoters) without restricting subsequent modification of the genome of these parasites. In addition, GIMO-transfection is a simple and fast method to genetically complement, restoring the wild-type genotype of parasite mutants with a gene deletion or gene mutation. Importantly, GIMO transfection can be easily partnered for use with a recently developed 'recombineering' system for high-throughput, genome wide and highly efficient generation of gene targeting constructs [245, 246]

In this thesis, heterologous prime-boost vaccinations using the clinically relevant recombinant adenovirus ChAd63 and MVA viral vectors expressing the *P. falciparum* transgenes were assessed for immunogenicity and protective efficacy using a full infectious transgenic *P. berghei* parasite expressing a *P. falciparum* gene of interest. Inclusion of the GFP-luciferase cassette in the generated transgenic parasites allows for a novel method of measuring vaccine efficacy *in vivo* useing transgenic *P. berghei* parasites expressing the luciferase gene [247]. Bioluminescence emitted at 44 hours after challenge with sporozoites is used to determine parasite liver load and can be used to directly quantify exo-erythrocytic development in live mice. This allows measuring both liver load and subsequent the prepatent period by measuring blood stage parasitaemia in the same animals.

1.11 Thesis aims and outlines

1.11.1 Aims

There are three aims of this DPhil.

- To generate novel transgenic rodent parasites that express *Plasmodium falciparum* pre-erythrocytic vaccine antigens not previously expressed in transgenic parasites.
- To use these transgenic parasites to assess the efficacy of the *Plasmodium falciparum* pre-erythrocytic vaccine candidates in a 'Transgenic Rodent Malaria Challenge Model'.
- To maximize the protective efficacy of the most promising pre-erythrocytic antigens by assessing vaccine combinations using double transgenic parasites.

1.11.2 Outline

- **Chapter 2** describes the material and methods used throughout this thesis.
- **Chapter 3** Demonstrates a comparison between the use of transgenic *P. berghei* parasites expressing either replacement or additional *P. falciparum* genes and their validity as challenge models.
- **Chapter 4** describes the use of a Transgenic Rodent Malaria Challenge Model for assessment and rank/order of ten pre-erythrocytic malaria vaccines.
- **Chapter 5** describes the design, generation, characterization of two double transgenic parasites; and their use as challenge models to assess two malaria vaccine combinations.
- **Chapter 6** describes the generation of five novel pre-erythrocytic viral vector vaccines and their protective efficacy assessment using the additional copy transgenic parasite challenge model
- **Chapter 7** summarises and discusses the results of this thesis and indicates the future directions of this project.

Chapter 2

Materials and Methods

2 Materials and Methods

2.1 Materials

2.1.1 Reagents

Table 2.1 Details of major commercially available reagents used in this study.

Material	Supplier	Catalogue Number
0.2µm bottle top filter (Nalgene)	Fisher	TKV-240-015F
0.2µm syringe filter	Sartorius	16534
15ml centrifuge tubes	Fisher, Inc.	FB55950
24-well tissue culture plates	Fisher, Inc.	TKV123011R
2ml syringes	Nu-Care Products	M0185
2-β Mercaptoethanol [50µm]	Gibco	31350-010
50ml centrifuge tubes	Greiner	227261
5-Fluorocytosine	Invivogen	2022-85-7
60mm petri dishes	Corning	430166
6-well tissue culture plates	Fisher, Inc.	TKT-520-030T
8-well microscope slides	VWR International	631-0451
96-well U bottom plates	VWR International	734-0027
96-well V bottom plates	Fisher Scientific	DIS-210-150L
Agar	Sigma Aldrich	A6686
Agarose	Sigma Aldrich	A9539
Alexa Fluor® 488 Goat Anti-Mouse IgG	Life Technologies	A-11001
Ammonium chloride (NH4Cl) [0.15M]	Sigma Aldrich	A4514
Ampicillin	Sigma Aldrich	A5354
Anti-mouse CD107a PE (Clone: eBio1D48)	eBioscience	12-1071-82
Anti-mouse CD16/CD32 (Fc Blocker, Clone: 93)	eBioscience	14-0161-86
Anti-mouse CD3ε-APC on day	eBioscience	11-0452
Anti-mouse CD4 eFluor450 (Clone: RM4-5)	eBioscience	48-0042-82

Anti-mouse CD4 Clone GK1.5 (rat IgG2a)	eBioscience	12-0031
Anti-mouse CD4-FITC clone RM4-4	eBioscience	11-4031
Anti-mouse CD8 Clone 2.43 (rat IgG2a)	eBioscience	14-4321
Anti-mouse CD8α PreCp-Cy5-5 (Clone: 53-6.7)	eBioscience	45-0081-82
Anti-mouse IFN-γ APC (Clone: XMG 1.2)	eBioscience	17-7311-82
Anti-mouse interleukin-2 (IL-2) PE-Cy7 (Clone: JES6-5H4)	eBioscience	25-7021-82
Anti-mouse TNFα Alexa Fluor 488 (Clone: MP6-XT22)	eBioscience	53-7321-82
Anti-*Pb*CSP (3D11) monoclonal antibody	MR4	3D11, MRA-100
Anti-*Pf*CSP (210A) monoclonal antibodies	MR4	2A10, MRA-183
Benzonase® Nuclease	Novagen	70664-3
Betaine	Sigma Aldrich	61962
Bovine Serum Albumin (BSA)	PAA Laboratories	K41-001
Caesium Chloride	Sigma Aldrich	203025
Carbonate-bicarbonate buffer	Sigma Aldrich	C3041
Carboxymethylcellulose sodium salt High viscosity (CMC)	VWR BDH Prolabo	279294T
Cell lifter	Fisher	FB55160
Cell Scraper, sterile, 32cm	Nalge Nunc International Corp	179707
Cell strainer (70µm)	Falcon	352350
Chicken Embryo Fibroblasts (CEF) primary cells	Institute for Animal Health, Compton, UK	
Cluster tubes	Corning	4401
Corning conical tubes, 250 ml PP Centrifuge tube, plug seal cap	Fisher	CFT-900-021Y
DAPI (4',6-diamidino-2-phenylindole)	Sigma Aldrich	101101353
DH5α maximum efficiency cells	Invitrogen	12297-016
Diethanolamine buffer	Pierce	34064

Dimethyl sulphoxide (DMSO)	Sigma Aldrich	D2650
Disposable Counting Slides	Immune Systems Ltd	BVS100
D-Luciferin potassium salt	PerkinElmer	122796
DMEM Medium	Sigma Aldrich	D6546
DNAreleasy™ Kit	Anachem Ltd	LS02
Domitor™	Oxford University Veterinary Services	N/A
Doug Foster strain-1 Fibroblast (DF-1)	ATCC®	CRL-12203
Dried skimmed milk powder	Waitrose	N/A
Dulbecco's Modified Eagle's Medium (DMEM)	Sigma Aldrich	D6546
Dulbecco's PBS (D-PBS)	Sigma Aldrich	D8537
Effectene Transfection Reagent Kit	Qiagen	301425
ELIspot colour development kit	BioRad	170-6432
Endotoxin Free water	Sigma Aldrich	W3500
Ethanol	Sigma Aldrich	32221
Ethidium bromide solution	Sigma Aldrich	E1510
Ethylenediaminetetraacetic acid (EDTA)	Sigma Aldrich	E7889
Fetal Calf Serum (FCS)	Sigma Aldrich	F-2442
Fluorescence Mounting Medium	Dako	S3023
Fructose	Sigma Aldrich	F0127
Gateway® LR Clonase® II enzyme mix	Invitrogen	11791-020
Giemsa	Sigma Aldrich	GS1L
Glutamine	Sigma Aldrich	G7513
Glycerol	Sigma Aldrich	G5516-1L
Goat anti-mouse whole IgG alkaline phosphatase conjugate	Sigma Aldrich	A-3562
GolgiPlug	Becton Dickinson Ltd.	555028
Heparin	Sigma Aldrich	H3149

Hoechst-33342	Cell Signaling Technology	4082S
Human hepatocyte carcinoma cell line Huh7	JCRB Cell Bank, JP	JCRB0403
Human IFNγ ELISpot kit	Mabtech	3420-2A
Hydrochloric Acid (HCl) [1M]	Sigma Aldrich	S-7653
Immersion Oil	Sigma-Aldrich	10890
Isofluorane	Oxford University Veterinary Services	N/A
Kanamycin	Sigma Aldrich	K0254
Ketaset™ (ketamine)	Oxford University Veterinary Services	N/A
KHCO3 [1mM]	Sigma Aldrich	P-9144
Klenow DNA Polymerase	Fermentas	EP0421
LB agar tablet	Sigma Aldrich	L7025-500TAB
LB broth tablet	Sigma Aldrich	L7275-500TAB
L-glutamine [4mM]	Sigma Aldrich	G-7513
Lipofectamine™	Invitrogen	11668-019
Magnesium chloride (MgCl2)	Sigma Aldrich	M2393
MAIP ELIspot Plates	Millipore	MAIPS4510
MEM α-modification	Sigma Aldrich	M-4526
Methanol	Sigma Aldrich	32213
Microcentrifuge tubes	Fisher Scientific	FB74031
Micro-fine Insulin Syringe with needle 0.5ml 29g x 12.7mm	Nu-Care Products	M4892
Micro-fine Insulin Syringe with needle 1mL 29g x 12.7mm	Nu-care products	M4891
Microlance needle 26g x 5/8 inch	Nu-care products	M4300
Microscope slides	Fisher Scientific	MNJ-200-010H
Microvette tubes	Sarstedt	CB300K2E
MinElute gel extraction kit	QIAgen	28606

Minimum Essential Medium Eagle (MEM) α-modification	Sigma Aldrich	M4526
Mouse IFN-γ ELISPOT kit (ALP)	Mabtech	3321-2A
Mowiol® 20-98	Sigma-Aldrich	11773
Mr. Frosty cryocontainer	Fisher Scientific	CRY-120-010T
Neomycin sulfate, USP grade	Invitrogen	21810-031
Neutral buffered formalin	Sigma-Aldrich	HT501128
NH4Cl [0.15M]	Sigma Aldrich	A-4514
Nucleofector solution 88A6	Amaxa, GmbH	88A6
Nycodenz density-gradient solution	Lucron Bioproducts	1002424
PCR primers	Sigma Aldrich	N/A
Pen/strep [100U penicillin / 100μg strep]	Sigma Aldrich	P-0781
Percoll	Sigma Aldrich	P1644
Permeabilization Buffer (10X)™	eBioscience	00-8333
Phosphate Buffered Saline (PBS)	Sigma Aldrich	D-8537
Phusion® High-Fidelity DNA Polymerase	NEB	M0530L
Plastipak syringe 1mL Luer slip	Nu-care products	M0013
Propan-2-ol	Fisher Scientific	P/7490/17
Protein G agarose	Pierce	22852
Proteinase K	Sigma Aldrich	P2308
Purified Mouse IgG1	Sigma Aldrich	M5284
Purified Rat IgG	Sigma Aldrich	I4131
Pyrimethamine	Sigma Aldrich	P-7771
QIAamp DNA mini kit	Qiagen	51304
Qiagen plasmid midi kit	Qiagen	12143
QIAprep spin miniprep kit	Qiagen	27106
Quick Ligation™ Kit	NEB	M2200L
Restriction and Ligation Enzymes	NEB	Various

Ribonuclease A	Sigma Aldrich	R6513
Rompun® (Xylazine)	Oxford University Veterinary Services	N/A
RPMI-1640 Medium	Sigma Aldrich	R0883
S.O.C. Medium	Invitrogen	15544-034
Smart Ladder DNA marker	EurogenTec	MW-1700-02
Sodium Azide	Sigma Aldrich	S2002
Sodium bicarbonate solution 7.5%	Life Technologies	1423629
Sodium dodecyl sulfate (SDS)	Sigma Aldrich	L4390
Sucrose	Fluka	84097
SYBR Safe in DMSO	Invitrogen	S33102
T175 Cell culture Flask Corning	Fisher, Inc.	TKV123061C
T25 Cell culture Flask Corning	Fisher, Inc.	TKV123011R
T75 Cell culture Flask Corning	Fisher, Inc.	TKV123031L
Terrific Broth	Sigma Aldrich	T0918
Tetracycline hydrochloride	Sigma Aldrich	T7660-5G
Transfer pipettes	Fisher Scientific	FB55348
T-REx™ 293 cells	Life Technologies	R710-07
Tris-acetate-EDTA (TAE)	Fisher Scientific	BP1332-1
Triton™ X-100	Sigma Aldrich	X100
Trizma pH 9.0 solution (1M)	Sigma Aldrich	T2819
Trizma® HCL buffer solution (pH8)	Sigma Aldrich	T2694
Trypan Blue	Sigma Aldrich	T8154
TrypLE™ Express Enzyme (1X)	Life Technologies	12605-010
Ultra-centrifuge polycarbonate 1.6 ml tubes	Beckman Coulter	362305
WR99210 solution	Jacobus Pharmaceutical Company	

2.1.2 Oligonucleotide Primers.

2.1.2.1 Primers used for DNA construct generation

Table 2.2 Primers used for DNA construct generation

DNA-Construct	Primer No.	Primer sequences *	Restriction sites	PCR Size (bp)	Descirption
pL2005	7169	tatcctgcaggGTGATAGTGTAGATTTTTTTGTTTGAC	SbfI	1519	*Pbuis4* 5'-UTR Promoter sequence, F
	7170	ataagaatgcggccgcAGACGTAATAATTATGTGCTGAAAGG	NotI		*Pbuis4* 5'-UTR Promoter sequence, R
	7171	cggatatcTATAATTCATTATGAGTAGTGTAATTCAG	EcoRV	1025	*Pbuis4 3'*-UTR sequence, F
	7172	ggccggtaccTTTCGCTTTAATGCTTGTCATC	KpnI		*Pbuis4 3'*-UTR sequence, R
pL1937	7287	ataagaatgcggccgcATGGTGAGCAAGGGCGAGGAG	NotI	739	*mCherry, F*
	7288	ggggatatcAGATTACTTGTACAGCTCGTCCATGCC	EcoRV		*mCherry, R*
pL1963	7323	ataagaatgcggccgcATGAAGCACATCCTGTACATC	NotI	1411	*PfLSA-1, F*
	7324	ggggatatcTCACAGCTTCATGAAGTACTTGG	EcoRV		*PfLSA-1, R*
pL1987	7355	ataagaatgcggccgcATGAACCCCATCAAGAAATGCC	NotI	4165	*PfLSA-3, F*
	7326	CGCTCATTTGCTTTTCTGTGTCCG			*PfLSA-3, R*
pL1964	7191	ataagaatgcggccgcATGAATGCCTTAAGAAGATTACCAG	NotI	587	*PfCelTOS, F*
	7192	gtgtcaccggcgCGTGTGATTTTTAATCGAAAAAATCATCTG	SgrAI		*PfCelTOS, R*
pL1966	7195	ataagaatgcggccgcAATGAAGGTCTCTAAATTAGTCTTG	NotI	716	*Pfuis3, F*
	7196	ggggatatcTTAGTTCTCTTCTTGAGATAAATAATTAGCATAAAC	EcoRV		*Pfuis3, R*
pL1967	7197	ataagaatgcggccgcCAAAATGAAAACCATAATAATAGTAACCCTTTTC	NotI	372	*PfLSAP-1, F*
	7198	ggggatatcGATATTGTCTATTTATTTGGTTTTATTCTACC	EcoRV		*PfLSAP-1, R*
pL1968	7199	ataagaatgcggccgcATGTGGTTATGCAAAAGGGGACTG	NotI	1048	*PfLSAP-2, F*
	7200	ggggatatcATATATTTAATTTGTAACATTTCTCATGTTATTTTCTAAAG	EcoRV		*PfLSAP-2, R*
pL1969	7201	ataagaatgcggccgcATGAGATTCTCCAAAGTATTTTCTTTTTTCG	NotI	571	*PfETRAMP-5, F*
	7202	ggggatatcTTATTGTTCTTTTTTGGGTTCTTCGG	EcoRV		*PfETRAMP-5, R*
pL1991	7353	atacagtagcggccgcATGAACCTCTTGGTCTTCTTCTG	NotI	1271	*PfFalstatin, F*
	7230	ggggatatcCATATTATTGCACGTTTAACTCTACAATTCTTG	EcoRV		*PfFalstatin, R*
pL1970	7244	ataagaatgcggccgcCAATTCATGATGAGAAAATTAGC	NotI	1243	*PfCSP, F*
	7240	gtgtcaccggcgAGATGTGTTCTTTATCTAATTAAGG	SgrAI		*PfCSP, R*
pL1992	7379	ataagaatgcggccgcgttaacATGAATCATCTTGGGAATGTTAAATATTTAGTC	NotI +HpaI	1764	*PfTRAP, F*

	7380	gggatatcggatccATTTAATTCCACTCGTTTTCTTCAGG	EcoRV +BamHI		*PfTRAP, R*
pL1960	7221	tatcctgcaggCTGTAGCATATGTCTATACTAAGC	SbfI	1583	*PbCelTOS* 5'-UTR Promoter sequence, F
	7222	ataagaatgcggccgcGTATATTTTAATTATAAATGACAGTTTGAATGATG	NotI		*PbCelTOS* 5'-UTR Promoter sequence, R
	7223	gtgtcaccggcgCATTTAATATCAATGATAATAATAATAATAATGTAAAC	SgrAI	1003	*PbCelTOS* *3'*-UTR sequence, F
	7224	cggatccGTATTTTGCACATATCTAATCCGTAAG	BamHI		*PbCelTOS* *3'*-UTR sequence, R
pL1971	7191	ataagaatgcggccgcATGAATGCCTTAAGAAGATTACCAG	NotI	587	PfCelTOS, F
	7192	gtgtcaccggcgCGTGTGATTTTTAATCGAAAAAATCATCTG	SgrAI		PfCelTOS, R
pL1972	7329	atggatccgcggccgctgcagCTTTAATTAAATAAACATTACGCATG	BamHI+NotI+PstI	944	*PbCSP* 3'-UTR sequence, F
	7330	gcgcgagctcATAATATATATTAGGAGAATTAACCAATGCTG	SacI		*PbCSP* 3'-UTR sequence, R
	7244	ataagaatgcggccgcCAATTCATGATGAGAAAATTAGC	NotI	1243	*PfCSP, F*
	7240	gtgtcaccggcgAGATGTGTTCTTTATCTAATTAAGG	SgrAI		*PfCSP, R*
pL1928	1003	catgggcccACCATGCTTTGTCTGAGAGTG	ApaI	788	*Pbs1* 5'TR sequence, F
	1004	aaggcctggtaccATACTGTTCTTCCCAATGGATC	StuI+KpnI		*Pbs1* 5'TR sequence, R
	1005	ataagaatgcggccgcctgcagCATTCAAATGCTTGAAGGCGATG	NotI+PstI	851	*Pbs1* 3'TR sequence, F
	1006	acatggcgccaagcttATGGCACATGGATCGAACAG	KasI+HindIII		*Pbs1* 3'TR sequence, R
pL2047	1063	GCATGACCAAGAGCAGCAAGGAC		1515	*PfHT, F*
	1064	CACCACGGACTTGGTCATGTG			*PfHT, R*
pL2048	1065	GCATGAGCCACCGGAAGTTCG		1161	*PfRP-L3, F*
	1066	GGCCTTCAGGTCCTTCTTCAG			*PfRP-L3, R*
pL2049	1067	GCATGAAGATGAAGATCCCTATCTGCTTCC		753	*PfSPECT-1, F*
	1068	GCTCAGGGCCATGTTCAGG			*PfSPECT-1, R*
pL2053	1069	GCATGAAGCTGAGAATCCTGAAGAAAC		2548	*PfSPECT-2, F*
	1071	CTTGTTGTTTTTGCACAGCATGTAG			*PfSPECT-2, R*
pL2041	7225	cggatccGAGGGATGAATAGGGGATGGC		3201	*PfB9, F*
	7226	gtgtcaccggcgCACTTCAACATTACTAGAAGAATGTGATAC			*PfB9, R*

* Red, Blue and Green: Restriction sites

2.1.2.2 Primers used for the chimeric parasites confirmation (integration) PCR

Table 2.3 Primers used for the chimeric parasites confirmation (integration) PCR

Primer No.	Descirption	Primer sequences *
1011	PfCSP F	cccg**ctcgag**CGCCAATTCATGATGAGAAAATTAGC
1012	PfCSP R	ataagaat**gcggccgc**CTTTATCTAATTAAGGAACAAGAAGGA TAATACC
1042	$PfCS_{PbCS}$ 5'Int. F	AGAGACAAACCAACCTTAGGAAC
1043	$PfCS_{PbCS}$ 5'Int. R	CTTCCATAGCACTGGTATTCCTG
1044	$PfCS_{PbCS}$ 3'Int. F	AGTTAGAATAAAGCCTGGCTCTG
1045	$PfCS_{PbCS}$ 3'Int. R	TTACTATTCGTGCCCATTACGAC
1048	hDHFR-yFCU (+/-SM) F	ATCATGCAAGACTTTGAAAGTGAC
1049	hDHFR-yFCU (+/-SM) R	CATCGATTCACCAGCTCTGAC
1051	Luciferase F	GTCGCCAGTCAAGTAACAAC
1052	GFP R	ACAAGAATTGGGACAACTCCAG
1054	PbCSP F	CCAAAGGAACTTAAACGAGCTATG
1055	PbCSP R	CTTATACCAGAACCACATGTTACG
1080	Pb5'230p Int. F	ACTGTTATATTTGGTGATGGAATGG
1081	Pb5'230p Int. R	TATACATCCACGGATGCATAGAAG
1082	Pb3'230p Int F	TCTGCATTAACCTTAAATATGAAAAACAC
1083	Pb3'230p Int R	TTCAGTGAAATCGCAAACATAAGTATC
1084	mCherry Int. F	ATGGTGAGCAAGGGCGAGGAG
1085	mCherry Int. R	AGATTACTTGTACAGCTCGTCCATGCC
1086	PfLSA-1 ox** Int. F	ATGAAGCACATCCTGTACATC
1087	PfLSA-1 ox** Int. R	TCACAGCTTCATGAAGTACTTGG
1090	PfLSA-3 ox** Int. F	AAGAAGTCATCGACGTCATAGAAG
1091	PfLSA-3 ox** Int. R	TTCTTTCAGCTCGTGCACTTC
1092	PfCelTOS Integration F	ATGAATGCCTTAAGAAGATTACCAG
1093	PfCelTOS Integration R	CGTGTGATTTTTAATCGAAAAAATCATCTG
1096	PfUIS3 Int. F	AATGAAGGTCTCTAAATTAGTCTTG
1097	PfUIS3 Int. R	TTAGTTCTCTTCTTGAGATAAATAATTAGCATAAAC
1098	PfLSAP1 Int. F	CAAAATGAAAACCATAATAATAGTAACCCTTTTC
1099	PfLSAP1 Int. R	GATATTGTCTATTTATTTGGTTTTATTCTACC
1100	PfLSAP2 Int. F	ATGTGGTTATGCAAAAGGGGACTG
1101	PfLSAP2 Int. R	ATATATTTAATTTGTAACATTTCTCATGTTATTTTCTAAAG
1102	PfETRAMP-5 Int. F	ATGAGATTCTCCAAAGTATTTTCTTTTTTCG
1103	PfETRAMP-5 Int. R	TTATTGTTCTTTTTTGGGTTCTTCGG
1104	PfFalstatin Int. F	ATGAACCTCTTGGTCTTCTTCTG

1105	PfFalstatin Int. R	CATATTATTGCACGTTTAACTCTACAATTCTTG
1106	PfTRAP Int. F	ATGAATCATCTTGGGAATGTTAAATATTTAGTC
1107	PfTRAP Int. R	ATTTAATTCCACTCGTTTTCTTCAGG
1108	$PfCelTOS_{PbCelTOS}$ 5'Int. F	TTAATTTTATCGAATTTGCGCATAACAC
1109	$PfCelTOS_{PbCelTOS}$ 5'Int. R	CTAAGAAAGAGCAAATAACTGGTAATCTTC
1110	$PfCelTOS_{PbCelTOS}$ 3'Int. F	TCTCAGAAAGTGAAGAAAGTTTATCAG
1111	$PfCelTOS_{PbCelTOS}$ 3'Int. R	GATAGCCCTAATGAAAATAATTGCCTC
1112	PbCelTOS F	ACAAAATTGTCAGTTATATCATCTGTCTTTG
1113	PbCelTOS R	ATCATTATCGAAGTTGTCTTCTTCAGTTTC
1127	Pb3'S1 Int. R	TGTACTACTTTCACATCAAATTCAGTAACC
1128	Pb5'S1 Int. F	TAAAGGTTAGCATTCAATCTGTCTG
1141	Pbs1 inside F	AATGAATGCGTCTATTGAAATAAAGCATC
1142	Pbs1 inside R	ATCTTTACTGCTACAATTCGTACTTCC
1143	Pb3'dhfr/ts F	TTCCTTCAATTTCGGGTACCCTC
1144	Pb5'eef1a R	TAATTACGACTAGTTAATAAAGGGCAC

* Red, Blue and Green: Restriction sites

** Human optimized DNA sequence.

2.1.2.3 Primers used for MVA viral vector vaccines ID and confirmation PCR

Table 2.4 Primers used for MVA viral vector vaccines ID and confirmation PCR

Primer No.	Descirption	Primer sequences
J1205	MVA P7.5 promoter F	CCATCGAGTGCGGCTACTAT
J492F	GFP inside F	TCGCCGACCACTACCAGCAGAACACCC
J491R	MVA TKL Flank R	CCGATTATCAACTGAATATGTCCGCCGTTC
VVCF21	PfB9 Int. R	ACAACTCCAACAAGAACGGC
VVCF22	PfHT Int. R	ATCAAGGAAACAAAGGGCGG
VVCF23	PfRP-L3 Int. R	CCCTGAAGTTCATCGACACC
VVCF24	PfSPECT-1 Int. R	ACCCTGAAGAACGAGGAAGG
VVCF25	PfSPECT-2 Int. R	TGGAATTTCACACCAGCAGC
1029	p856 MVA seq F	ATTCTAATTTATTGCACGGTAAGGAAG
1030	p856 MVA seq R	TTACGTTGAAATGTCCCATCGAG

2.1.3 Solutions and buffers

• γ-32P dATP (10 μCi/μl, Amersham Pharmacia Biotech).

• 0.5% BSA/PBS: 2.5g BSA and 250μl sodium azide (0.05%) were added to 500ml D-PBS.

• 10mM Tris pH9.0 for MVA production: 10 ml 1M Trizma pH 9.0 diluted in 1000 ml using Milli-Q water and filter sterilised through a 0.2 um bottle top filter unit (Nalgene).

• 5-Fluorocytosine (5-FC) (Sigma). Stock solution: 20 mg/ml in PBS.

• ACK Lysis Buffer: 8.29g NH_4Cl (0.15M), 1g $KHCO_3$ (1mM), 37.2mg Na_2EDTA in 800ml dH_2O. pH adjusted to 7.2-7.4 with HCl (1M) before making a final solution up to 1L with dH_2O.

• Buffer A: 50mM Tris, 100mM NaCl, 5mM $MgCl_2$ and 1% Triton X-100 in dH_2O.

• Buffered medium for preparation of the density-gradient solution 5 mM Tris/HCl, 3 mM KCl, 0.3 mM $CaNa_2EDTA$; pH 7.5. Store at −4 °C.

• Cells Freezing Medium. For Huh-7 hepatocyte; 50% RPMI + 40% FBS + 10% DMS. For DF-1 cell line; 90% FBS + 10% DMSO.

• Cesium Chloride solution: CsCl solutions at density 1.25g/ml or 1.35g/ml were prepared in 10mM Tris pH7.8 buffer with filter sterilized deionized H_2O.

• CMC solution (1.6% w/v). Stock solution (3x): 6.4 g high viscosity CMC dissolved in approximately 300 ml Milli-Q water to a 1000 ml Duran bottle with continuous shaking then the total volume completed up to 400 ml prior to autoclaving and preparation of 15 ml aliquots. For a working CMC solution (1x), the stock solution (3x) is diluted with two volumes of 2% FCS DMEM culture medium.

• Coating Buffer: 15mM sodium carbonate and 35mM sodium bicarbonate capsules were dissolved in dH_2O and autoclaved.

• Complete DMEM culture medium for CEF cells: 500 ml DMEM was supplemented with 5ml L-glutamine (1%), 5ml pen/strep (100U penicillin, 100µg streptomycin) and of heat inactivated FCS; 50ml for (10%) or 10ml for (2%).

• Complete DMEM culture medium for DF-1 cells: 500 ml DMEM was supplemented with 5ml L-glutamine (1%), 5ml pen/strep (100U penicillin, 100µg streptomycin), 10ml sodium carbonate solution 7.5% and of heat inactivated FCS; 50ml for (10%) or 10ml for (2%).

• Complete α-MEM Medium: 500ml MEM α-modification was supplemented with 5ml L-glutamine (2mM), 5ml pen/strep (100U penicillin, 100µg streptomycin), 500µl 2-mercaptoethanol (50µm) and 50ml of heat inactivated FCS (10%).

• Denhardt's solution (100 X): 2% (w/v) ficoll, 2% (w/v) polyvinylpyrrolidone, 2% (w/v) BSA, dissolve it in demineralised water and store at –20°C.

• DNA constructs (5–10 µg) in 10 µl TE buffer or distilled water used for transfection (stored at −20 °C).

• Ex-flagellation Medium: RPMI-1640 was supplemented with 25mM HEPES, 20% FCS, 10mM sodium bicarbonate and 50µm xanthurenic acid. pH was adjusted to 7.6.

• FACS Buffer: 1% FCS and 0.1% Sodium Azide in PBS.

• Fructose/PABA Solution: 80g fructose and 0.5g PABA were added to 1L of dH_2O. The solution was autoclaved prior to use.

• Giemsa staining solution: 5% Giemsa in dH2O.

• Heparin (*Stock solution: 200 I.U. /ml):* One Heparin ampoule (0.2 ml = 5000 I.U.) in 25ml RPMI1640 culture medium (pH 7.2) without fetal calf serum.

• Hoechst (Bisbenzimide H) 33342. Stock solution; Hoechst 33342 dissolved in Milli-Q water to a final concentration of 500 µM. Store at -20°C. For working solution the stock is diluted 100 times in PBS or medium.

• Hybridisation buffer: For 100ml, take 50 ml of demineralised water and add 30 ml of 20 X SSC, 5 ml of 100 X Denhardt's solution, 5 ml of a 10% (w/v) SDS solution, 1 ml of a 10% (w/v) disodium pyrophosphate solution, and 150 µl of a 10 mg/ml tRNA solution. Add demineralised water up to 100 ml. Before use, place at 60°C.

• LB Agar/Broth: Tablets were dissolved in dH_2O (1 tablet per 50ml). Antibiotics were added at the following working concentrations: ampicillin 100µg/ml, kanamycin 25µg/ml.

• Micro Bio-Spin P-30 Tris Chromatography Columns (Biorad).

• Mowiol: 6g glycerol and 2.4g polyvinyl alcohol 4-88 were dissolved in 6ml dH_2O for two hours at 50°C with agitation. 12ml Tris pH 8.5 (0.2M) was added and the solution was dissolved for a further three hours at 50°C with agitation. The solution was centrifuged at 5000xg for five minutes to remove any undissolved solids. DAPI was then added at a final concentration of 0.1µg/ml.

• Neomycin sulfate stock solution: a stock solution of 10 mg/ml neomycin sulfate was prepared by dissolving in distilled water.

• Nucleofector solution 88A6 (Amaxa, GmbH). Store at 4 °C. The kit includes 2.5 ml of the 88A6 solution with supplement solution (for 25 transfections), 25 cuvettes and 25 plastic pipettes. http://www.amaxa.com.

• Nycodenz density-gradient solution (Lucron Bioproducts). Stock solution: 138 g Nycodenz powder is dissolved in 500 ml Buffered Medium (density of 1.15 g/ml at 20 °C) and sterilized by autoclaving for 20 min at 120 °C. Store at 4 °C.

• PBS (0.1M): 0.138M NaCl, 0.0027M KCl, pH 7.4; made by dissolving tablets in dH_2O according to the manufacturer's instructions.

• Perm/Wash: 10x Perm/Wash buffer was diluted in dH_2O prior to use.

• *Plasmodium berghei* Freezing Medium: glycerol/PBS solution (30% glycerol; v/v), containing 0.1 ml of Heparin stock-solution (*200 I.U./ml*). Or: 11ml FCS, 4.2ml 5% $NaHCO_3$ and 5.5mg neomycin were added to 96ml RPMI-1640.

• Pyrimethamine solution (Sigma). Pyrimethamine powder (5-4-Chlorophenyl-6-ethyl 2,4-pyrimidinediamine) dissolved in DMSO to a final concentration of 7 mg/ml (stirring on a vortex) and diluted 100 times with normal tap water with an adjusted pH of 3.5–5.0 (with 1 M HCl). Stored at 4 °C and the solution used for the drinking water of mice for a maximum of 7 days.

• RPMI-1640 Complete Medium: 500ml RPMI-1640 was supplemented with 5ml L-glutamine (2mM), 5ml pen/strep (100U penicillin, 100µg streptomycin), 500µl 2-mercaptoethanol (50µm) and 50ml of heat inactivated FCS or FBS (10%).

• Sörensen staining buffer: For a working solution, dissolve 2.541 g KH2PO4 and 8.55 g $Na_2HPO_4.2H_2O$ in 5 L of distilled water; adjust the pH to 7.2 and store at room temperature.

• SSC stock solution (20 X): 174 g of NaCl and 88.2 g of sodium citrate.$2H_2O$ dissolved in demineralized water, to a final volume of 1L, then sterilise at 120°C during 15 min.

• Sucrose solution 36% w/v (in 10mM Tris pH9): Filter sterilised. It is important that this material is low in endotoxins.

• TAE Buffer: Made from 50x concentrate diluted in Milli-Q dH_2O.

• TE buffer: 10 mM Tris, pH 8.0; 1 mM Na_2EDTA, and store at room temperature.

• TNE buffer: 10 mM Tris pH 8.0, 5 mM EDTA pH 8.0, 100 mM NaCl in dH_2O.

• Tris Borate EDTA Buffer (TBE) 5X stock solution (1L): dissolve 54 g of Tris and 27.5 g boric acid in 300ml of demineralized water, add 20ml of EDTA (pH 8.0) and adjust the volume up to 1L. For Working solution 1 X (1L): take 200ml form the 5X stock solution and dissolve it until 1L with demineralized water.

• Triton X-100 in PBS (0.2%): 100ul Triton X-100 dissolved in 50ml sterile PBS. Cut of end of pipette tip to dispense this viscous detergent.

• WR99210 solution (Jacobus Pharmaceutical Company). Working solution; add 16 mg WR99210 powder to 2 ml ethanol (98%) and 0.15 ml benzyl alcohol. Mix by stirring on a vortex to dissolve WR99210. Add up to 5 ml with 2.85 ml distilled water. Store at room temperature and use the solution for a maximum of 7 days.

2.1.4 Basic DNA constructs/plasmids

1. Plasmid pL0043 [245]. This is a basic construct that is used to rapidly introduce transgenes into the *230p* locus (PBANKA_030600) of the PbANKA-*230p* gene in marker out (GIMO) mother line. This construct integrates by double cross-over recombination and replaces the positive-negative selection marker (SM) (h*dhfr*::y*fcu)* cassette with the transgene-expression cassette.

2. Plasmid pL2023. This is a basic construct that can be used to rapidly introduce transgenes into the *Pb s1* locus (PBANKA_120680) of the PbANKA-*s1* GIMO mother line. This construct integrates by double cross-over recombination and replaces the positive-negative (h*dhfr*::y*fcu*) SM.

3. Plasmid pL0034. This construct contains the positive-negative (h*dhfr*::y*fcu)* SM cassette. It can be used to clone any specific 5' and 3' gene targeting region (TR) to generate a targeted gene-deletion mutant in the *Pb* genome by double cross-over homologous recombination; replacing the *Pb* target gene with the h*dhfr*::y*fcu* SM, thereby generating a gene-specific GIMO locus (selected by positive selection using pyrimethamine). The generated gene-specific GIMO line can then be used, in a subsequent transfection to introduce the orthologous *P. falciparum* gene into this GIMO locus. Specifically, by using a modified DNA construct that contains the *Pb* gene 5' and 3'TRs (these TR must include the complete *Pb* gene promoter and transcription terminator sequences), replacing the SM with a *P. falciparum* gene CDS, thereby creating a *P. falciparum* expression cassette. The GIMO protocol can then be employed to insert the *P. falciparum* expression cassette (gene insertion) and replacing the introduced h*dhfr*::y*fcu* SM cassette (marker out), using negative selection. This results in generation of a double step replacement (DsR) chimeric parasite without SM.

2.1.5 Standard parasites lines used for generation transgenic *P. berghei* parasites expressing Human Malaria Parasite (*P. falciparum*) genes.

1. Wild type (WT) lines of *P. berghei* ANKA or NK65; the most frequently used is the reference ANKA line, cl15cy1 [248].

2. The reporter *Pb*ANKA parasite line *Pb*GFP-Luc_{con} (676m1cl1) expresses a fusion protein of GFP (mutant3) and firefly luciferase (LUC-IAV) under the constitutive *Pbeef1a* promoter and is SM free [249]. The reporter-cassette is integrated into the neutral *230p* locus (PBANKA_030600).

3. The standard PbANKA-*230p* GIMO mother line ($GIMO_{PbANKA}$ 1596cl1). The line contains a positive-negative SM cassette, a fusion gene of h*dhfr (*human dihydrofolate reductase; positive SM) and y*fcu* (yeast cytosine deaminase and uridyl phosphoribosyl transferase; negative SM) under control of the constitutive *Pbeef1a* promoter, stably integrated into the neutral *230p* locus (PBANKA_030600) through double cross-over recombination [245]. The GIMO mother line is used for introduction of transgenes into the modified *230p* locus through transfection with constructs that target the *230p* locus. These constructs insert into the *230p* locus ('gene insertion'), thereby removing the h*dhfr::*y*fcu* SM ('marker out') from the genome of the mother line. Transgenic parasites that are SM free are subsequently selected by applying negative drug selection using 5-Fluorocytosine (5-FC). This selection procedure is performed *in vivo* in mice.

4. The standard PbANKA-*s1* GIMO mother line (2149cl1). The line contains a positive-negative h*dhfr*::y*fcu* selection marker (SM) cassette, under control of the constitutive *eef1a* promoter stably integrated into the neutral *s1* gene-locus (PBANKA_120680) through double cross-over recombination [250]. In addition, it contains GFP under the constitutive *Pbeef1a* promoter integrated into the neutral 230p locus (PBANKA_030600). The GIMO mother line is used for introduction of transgenes into the modified s1 locus through transfection with

constructs that target the s1 locus in a similar process as described above. The PbANKA-s1 GIMO mother line contains a GFP-luciferase fusion expression cassette in the 230p locus and therefore transgenic parasites made in this line express both GFP and luciferase under the constitutive *Pbeef1a* promoter. In contrast, transgenic parasites made in the PbANKA-230p GIMO do not express a reporter protein.

2.1.6 List of all generated chimeric parasites used in this study:

Table 2.5 List of all the generated and used chimeric parasites in this thesis

No	Product/Mutant Name	Tested Clones	Transgene	Gene ID	Transgene Name
Reporter lines (Fluorescent) parasites					
1	*mCherry*$_{Pbuis4}$	2204 cl1	*mCherry*	NA	*mCherry*
Single additional copy parasites					
2	*Pf*LSA1$_{Pbuis4}$ GFP::Luc$_{Pbeef1a}$	2230 cl1	*PfLSA-1*	PF3D7_1036400	Liver-stage antigen 1
3	*Pf*LSA3$_{Pbuis4}$ GFP::Luc$_{Pbeef1a}$	2263 cl2	*PfLSA-3*	PF3D7_0220000	Liver-stage antigen 3
4	*Pf*CelTOS$_{Pbuis4}$ GFP::Luc$_{Pbeef1a}$	2231 cl1	*PfCelTOS*	PF3D7_1216600	Cell traversal protein for ookinetes and sporozoites
5	*Pf*UIS3$_{Pbuis4}$ GFP::Luc$_{Pbeef1a}$	2236 cl1	*PfUIS3*	PF3D7_1302200	Upregulated in infective sporozoites gene 3
6	*Pf*LSAP1$_{Pbuis4}$ GFP::Luc$_{Pbeef1a}$	2237 cl1	*PfLSAP1*	PF3D7_1201300	Liver-Stage Associated Protein 1
7	*Pf*LSAP2$_{Pbuis4}$ GFP::Luc$_{Pbeef1a}$	2239 cl1	*PfLSAP2*	PF3D7_0202100	Liver-Stage Associated Protein 2
8	*Pf*ETRAMP5$_{Pbuis4}$ GFP::Luc$_{Pbeef1a}$	2241 cl1	*PfETRAMP5*	PF3D7_0532100	Early transcribed membrane protein 5
9	*Pf*Falstatin$_{Pbuis4}$ GFP::Luc$_{Pbeef1a}$	2280 cl1	*PfFalstatin*	PF3D7_0911900	Falstatin
10	*Pf*CSP$_{Pbuis4}$ GFP::Luc$_{Pbeef1a}$	2243 cl3	*PfCSP*	PF3D7_0304600	Circumsporozoite protein
11	*Pf*TRAP$_{Pbuis4}$ GFP::Luc$_{Pbeef1a}$	2281 cl1	*PfTRAP*	PF3D7_1335900	Thrombospondin Related Adhesion Protein
12	*PfHT*$_{Pbuis4}$ *GFP::Luc*$_{Pbeef1a}$	2409 cl4	*PfHT*	PF3D7_0204700	Hexose Transporter
13	*PfRP-L3*$_{Pbuis4}$ *GFP::Luc*$_{Pbeef1a}$	2411 cl1	*PfRP-L3*	PF3D7_1027800	60S Ribosomal protein L3
14	*Pf*SPECT-1$_{Pbuis4}$ GFP::Luc$_{Pbeef1a}$	2414 cl1	*PfSPECT-1*	PF3D7_1342500	Sporozoite Protein Essential for Cell Traversal
15	*Pf*SPECT-2$_{Pbuis4}$ *GFP::Luc*$_{Pbeef1a}$*	2431 cl1	*PfSPECT-2*	PF3D7_0408700	Perforin like protein 1
16	*PfB9*$_{Pbuis4}$ *GFP::Luc*$_{Pbeef1a}$*	2392 cl1	*PfB9*	PF3D7_0317100	Member of 6-cysteine family of Plasmodium proteins
Knock out/GIMO mother-line parasites					
17	*PbANKA-ΔCelTOS GFP::Luc*$_{Pbeef1a}$ *GIMO line*	2217 cl1	NA	NA	NA
18	*PbANKA-ΔCSP GFP::Luc*$_{Pbeef1a}$ *GIMO line***	2151 cl1	NA	NA	NA
19	*PbANKA-ΔS1 GFP::Luc*$_{Pbeef1a}$ *GIMO line*	2149 cl1	NA	NA	NA
20	*PbANKA-Pf*TRAP$_{Pbuis4_230p}$ *ΔS1* GFP::Luc$_{Pbeef1a}$ *GIMO line*	2253 cl2	*PfTRAP*	PF3D7_1335900	Thrombospondin Related Adhesion Protein

21	*PbANKA-Pf*LSA1$_{Pbuis4_230p}$ *ΔS1* GFP::Luc$_{Pbeef1a}$ *GIMO line*	*2374 cl1*	*PfLSA-1*	*PF3D7_1036400*	*Liver-stage antigen 1*
Single replacement copy parasites					
22	*PbANKA-PfCelTOS(r)*$_{PbCelTOS}$ *GFP::Luc*$_{Pbeef1a}$	*2258 cl2*	*PfCelTOS*	*PF3D7_1216600*	*Cell traversal protein for ookinetes and sporozoites*
23	*PbANKA-PfCSP(r)*$_{PbCSP}$ *GFP::Luc*$_{Pbeef1a}$	*2257 cl2*	*PfCSP*	*PF3D7_0304600*	*Circumsporozoite protein*
24	*PbANKA-PfB9(r)*$_{PbB9}$ *GFP::Luc*$_{Pbeef1a}$*	*2355 cl1*	*PfB9*	*PF3D7_0317100*	*Member of 6-cysteine family of Plasmodium proteins*
Double transgenic parasites					
25	*PbANKA-Pf*TRAP$_{Pbuis4_230p}$ *PfCSP*$_{Pbuis4\_S1}$ GFP::Luc$_{Pbeef1a}$	*2369 cl4*	*PfCSP / PfTRAP*	*PF3D7_0304600 PF3D7_1335900*	*Circumsporozoite protein / Thrombospondin Related Adhesion Protein*
26	*PbANKA-Pf*LSA1$_{Pbuis4_230p}$ *PfLSAP2*$_{Pbuis4\_S1}$ GFP::Luc$_{Pbeef1a}$	*2403 cl1*	*PfLSA-1/ PfLSAP2*	*PF3D7_1036400 PF3D7_0202100*	*Liver-stage antigen 1 / Liver-Stage Associated Protein 2*

*Chimeric parasites generate non-Infectious sporozoites.

**Knock out GIMO mother-line parasite generated previously by LMRG at LUMC.

2.2 Cloning and General Molecular Biology

2.2.1 Antigen inserts and constructs design

P. berghei ANKA and *P. falciparum* 3D7 gene sequence for both the transgenic parasites and the viral vector vaccine candidates was first identified using PlasmoDB website (http://plasmodb.org/plasmo/) and NCBI GenBank website (http://www.ncbi.nlm.nih.gov/genbank/). The 3D7 strain was chosen as the genome is sequenced (Sanger Institute, Cambridge UK) and hence a sequence was available for each candidate antigen. Furthermore, the strain used in the Jenner Institute clinical trials is 3D7, and if one of the antigens proceeded to clinical trial it would be a homologous with the challenge strain. The sequences were then imported into Clone Manager 9 (Professional Edition) for annotation.

In order to determine whether any modifications were required for the new viral vector vaccine candidates design, the predicted structures were analysed through the following websites:

- SignalP 3.0 server (www.cbs.dtu.dk/services/SignalP/): predicts whether the antigen is secreted.

- TMHMM Server v2.0 (www.cbs.dtu.dk/services/TMHMM/): predicts whether the antigen has transmembrane domains, glycosylation sites and other features.

- DotPlot 1.0 (www.changbioscience.com/res/resd.html): by aligning the sequence against itself, you can identify areas of repeats.

Each gene sequence was ordered from GeneArt (Life Technologies, New York USA); modifications requested were the deletion of repetitive regions of sequence, the addition of the KpnI restriction enzyme site and the Kozak sequence and the human tPA leader sequence (GenBank Accession K03021) - respectively- upstream to the *P. falciparum* protein coding sequence at the 5' DNA appendix. The antigen sequence, or tissue plasminogen activator (tPA)

leader sequence, was preceded by the Kozak sequence to aid translation in mammalian cells. His-tag sequence, a STOP codon and NotI restriction enzyme site added respectively at the 3' DNA appendix and codon usage was optimized for human expression [251, 252]. Any internal Pac1, Pme1, Kpn1 and Not1 sites were modified by GeneArt, and no internal TTTTTNT sequences were permitted.

2.2.2 Agarose gel electrophoresis

DNA reaction products were separated by 1-1.25% agarose gel electrophoresis (95V, 50-70min) in 1x Tris-acetate-EDTA (TAE) buffer, stained using ethidium bromide (FINAl conc SIGMA) or SYBR Safe. Visualization of the DNA was accomplished by the use of transilluminator. The size of bands was estimated by comparison to the DNA marker smart ladder.

2.2.3 Polymerase chain reaction (PCR)

Standard PCR reactions was employed to amplify specific sequence, modify the relevant DNA constructs or perform diagnostic analysis of obtained DNA or parasite clones or recombinant viral vaccine. For the modification of DNA sequences high-fidelity Phusion PCR kit from New England Biolabs (NEB) was used following manufacturer's recommended conditions. Optimizations were applied to either mastermix or the PCR program when that was required.

• Mastermix in general was prepared as following:

25µl Phusion High-Fidelity ready master mix (2x)

0.5µl Primer 1 (100µM)

0.5µl Primer 2 (100µM)

50ng sample template

10ul of 5M Betaine

To 50µl with Milli-Q H_20

- **General PCR program setting:**

Primary denaturation	95 °C	10:00 min	
Denaturation	98 °C	00:30 min	x 30-40 cycles
Anneal	57 °C	00:05 min	
	62 °C	00:15 min	
	68 °C	00:20 min	
Elongation	72 °C	10 sec/1Kb	
Final elongation	72 °C	07:00 min	
End	4-12 °C	Overnight	

2.2.4 Restriction digestion

Most of the digestions were performed using NEB restriction endonuclease enzymes. PCR DNA product or plasmids were digested in 20-100 µL reaction mixtures and incubated ranged between 2-16 hours based on the required concentration of the digested DNA material at 37 °C, unless the suggested incubation temperature for enzymes differed. Alkaline Phosphatase (AP) was included in the Reaction mixtures to minimize the vector re-ligation if any complementary 'blunt' or 'sticky' ends were generated from the digestion reaction.

2 µL	5 µL	Total NEB Restriction Enzyme(s) (10,000U/mL)*
2 µL	5 µL	NEB restriction buffer (10x)
1 µL	2 µL	Alkaline Phosphatase (AP)
> 1µg	> 1µg	Plasmid DNA or PCR product
To 20 µL	To 50 µL	Sterile Milli-Q H_2O

*If double-digest performed using two enzymes, the volume of each enzyme was halved.

2.2.5 DNA ligation

Digested DNA fragments (vectors and inserts) were purified using QIAgen MinElute gel extraction kit and eluted into Milli-Q H_2O. Ligation was then performed for 1-2 h at 25 °C using Quick Ligation™ Kit and the outlined below. After ligation; the reaction mixture was used for bacterial transformations.

Reagent	**Ligation Reaction**
Milli-Q H_2O	5 µL
10x ligation buffer	2 µL
Plasmid DNA	1 µL
Insert DNA	1 µL
Quick T4 DNA ligase	1 µL

2.2.6 Bacterial transformation

Chemically competent sub-cloning efficiency DH5-alpha *E. coli* cells (Invitrogen) were transformed with the ligation products. The competent bacteria were thawed on ice then gently mixed with the ligation product and incubated on ice for 30 minutes. Cells were subsequently heat-shocked at 42°C for 40 seconds then placed on ice for 2-5 minutes. 200µL of SOC media was added, and then the whole mixture was incubated at 37°C in the shaking incubator for 30-60 min before seeding the cells onto LB agar plates containing the relevant antibiotic for the resistant gene in the transformed plasmid **(Figure 2.1).**

2.2.7 Plasmid DNA preparation

Individual 5-10 colonies from LB Agar plates supplemented with relevant antibiotic were picked using clean 10µl pipette tips and cultured overnight at 37°C in 2-4mL LB broth plus the same relevant antibiotic. Next day Plasmid DNA was extracted by Qiagen QIAprep spin miniprep kits according to the manufacturer's instructions. Extracted DNA plasmid was quantified using a Nanodrop spectrophotometer and correct cloning was confirmed using

restriction enzyme digestion analysis as described in section 2.2.4. Bacteria containing a correct version of each construct were amplified by incubation overnight in 100-200mL LB medium with the selection antibiotics. Next day glycerol stock was generated by mixing 1 ml of the culture with 1ml of 50% glycerol in Luria Broth (LB) medium with the relevant selection antibiotic and stored at -80°C for long-term use, while the plasmid DNA was extracted from the remaining culture using Qiagen plasmid midi-prep or maxi-prep kits, quantified using a Nanodrop spectrophotometer, and then stored at -20°C till further use **(Figure 2.1).**

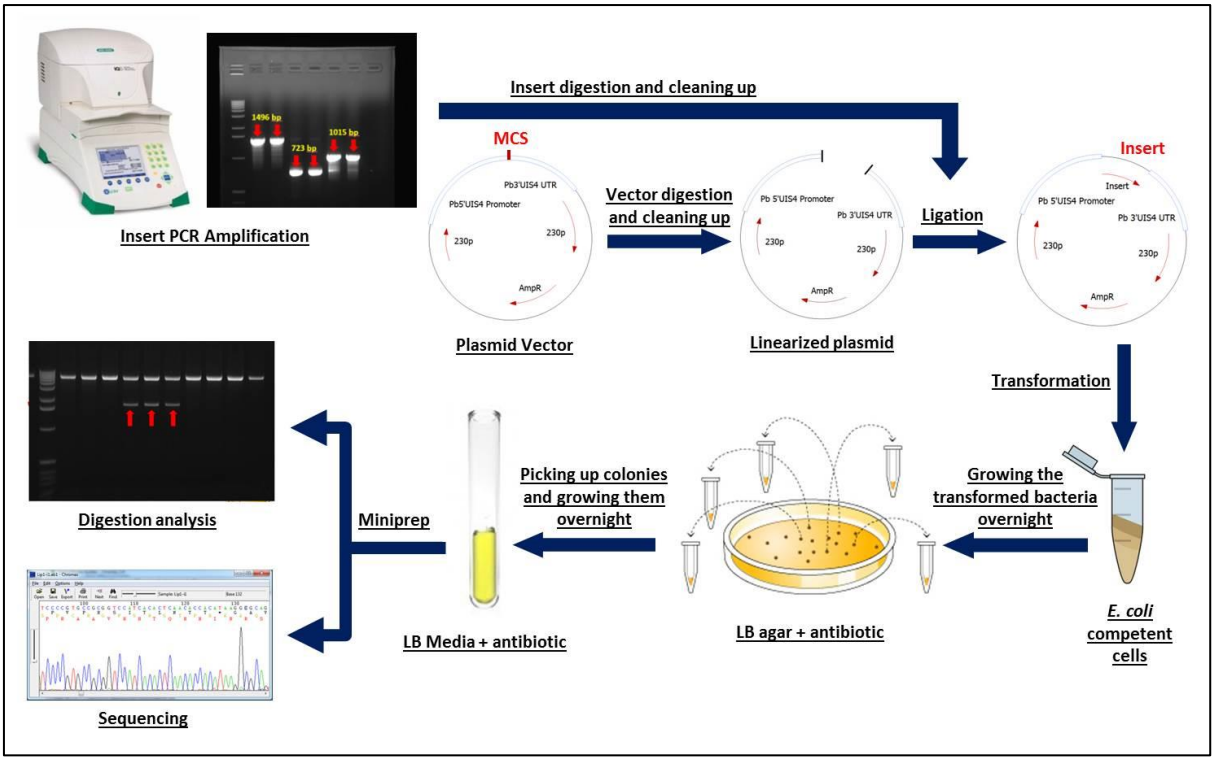

Figure 2.1: Cloning and General Molecular Biology steps.
Standard PCR reactions was employed to amplify a specific insert sequence with including unique restriction sites flanking the insert sequence that exist within the plasmid vector MCS sequence. Both vector and insert were digested with the same restriction enzymes, then purified using DNA QIAgen MinElute gel extraction kit and the DNA eluted into Milli-Q H_2O. Ligation was then performed for 1-2 h at 25 °C using Quick Ligation™ Kit. After ligation; the reaction mixture containing the ligated plasmid vector and insert was transformed into an *E. coli* competent cell following the bacterial transformation protocol in section 2.2.6. Transformed *E. coli* competent cells were seeded onto a LB agar plate containing relevant antibiotic for the resistant gene in the transformed plasmid and grew overnight at 37°C. Next day, individual 5-10 colonies from LB Agar plates supplemented with relevant antibiotic were picked and cultured overnight at 37°C in 2-4mL LB broth plus the same relevant antibiotic. Next day, the DNA plasmid was extracted by Qiagen QIAprep spin miniprep kits according to the manufacturer's instructions. Extracted DNA plasmid was quantified using a Nanodrop spectrophotometer and correct cloning was confirmed using multiple unique restriction enzymes digestion analysis and DNA sequencing reactions.

2.2.8 Cloning, generation and preparation of chimeric parasite constructs.

2.2.8.1 Constructs to generate additional gene (AG) chimeric parasites.

Two basic constructs were used to rapidly introduce transgenes into neutral *Pb* loci by GIMO transfection; specifically pL0043 to introduce transgenes into the 230p locus (for transfection into the PbANKA-230p GIMO mother line; 1596cl1) **(Figure 2.2)** and pL2023 for the s1 locus (for transfection into the PbANKA-s1 GIMO mother line; 2149cl1) **(Figure 2.3 A).** These basic constructs contain 5' and 3'TRs for these loci as well as a multiple-cloning site. This multi-cloning site is used to introduce the *P. falciparum* coding sequences (CDs), which were PCR-amplified from *P. falciparum* genomic DNA (gDNA) or cDNA. The *P. falciparum* CDS is flanked upstream by the 5'UTR (containing the gene promoter region) and downstream by 3'UTR (containing the transcription terminator sequence) regions of a chosen *Pbuis4* gene, both of which were PCR-amplified from Pb genomic DNA (gDNA) **(Figure 2.3 B).** The selection of the Pb promoter region was dependent on the timing and strength of *P. falciparum* gene expression required **(see Chapter 4).** The regions critical for the *P. falciparum* genes expression (i.e. the promoter and *P. falciparum* CDS) of the final construct were sequenced to ensure that the *P. falciparum* genes are correctly expressed in the additional gene (AG) chimeric parasite. In addition, an expression cassette containing a reporter gene was also introduced into this construct. The GFP::luciferase expression cassette was PCR-amplified from construct pL1063 **(Figure 2.3 C)** [249]. In case of using PbANKA-s1 (2149cl1) GIMO mother line there was no need to include the GFP-Luciferase cassette into the s1 targeting construct, since this line already contains the GFP-Luciferase cassette integrated into the neutral 230p locus. The final construct 1 is linearized using appropriate restriction enzymes outside of the 5'and 3' targeting regions (TRs). Inclusion of the GFP-Luc cassette makes the chimeric parasite is visible at any stage during the life cycle **(Figure 2.5).**

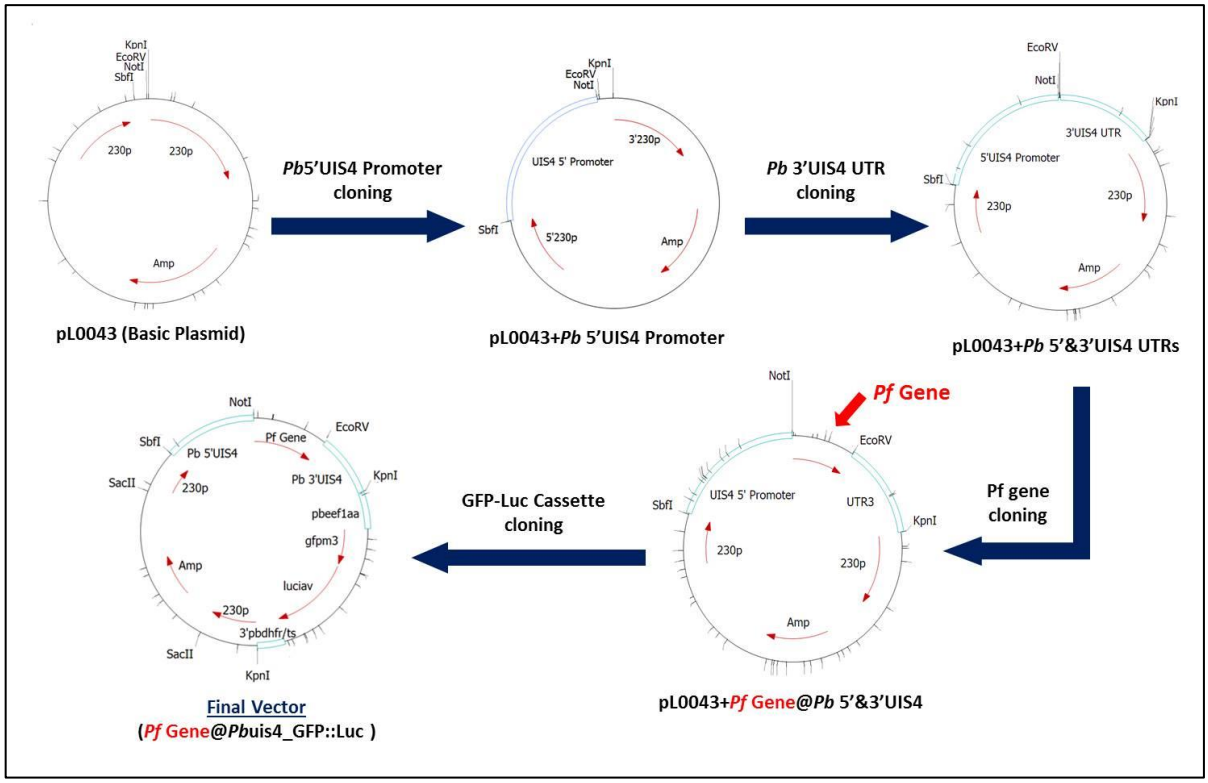

Figure 2.2: Sequential DNA molecular cloning steps for generating the DNA constructs used for Additional Gene (AG) chimeric parasites generation.

Schematic representation shows the followed molecular cloning steps to generate the DNA plasmid constructs used for generating the AG chimeric parasites expressing single *P. falciparum* antigen under the control of *Pbuis4* promoter. This figure shows the unique restriction enzymes used to clone each DNA fragment and thier positions in the plasmids. This Figure also shows the cloning order for each DNA fragmnet in the basic GIMO plasmid pL0043 till the generation of the final plasmid/construct that targets the *Pb230p* locus in chr-3 containg all the required DNA elements fro generating each AG chimeric parasites.

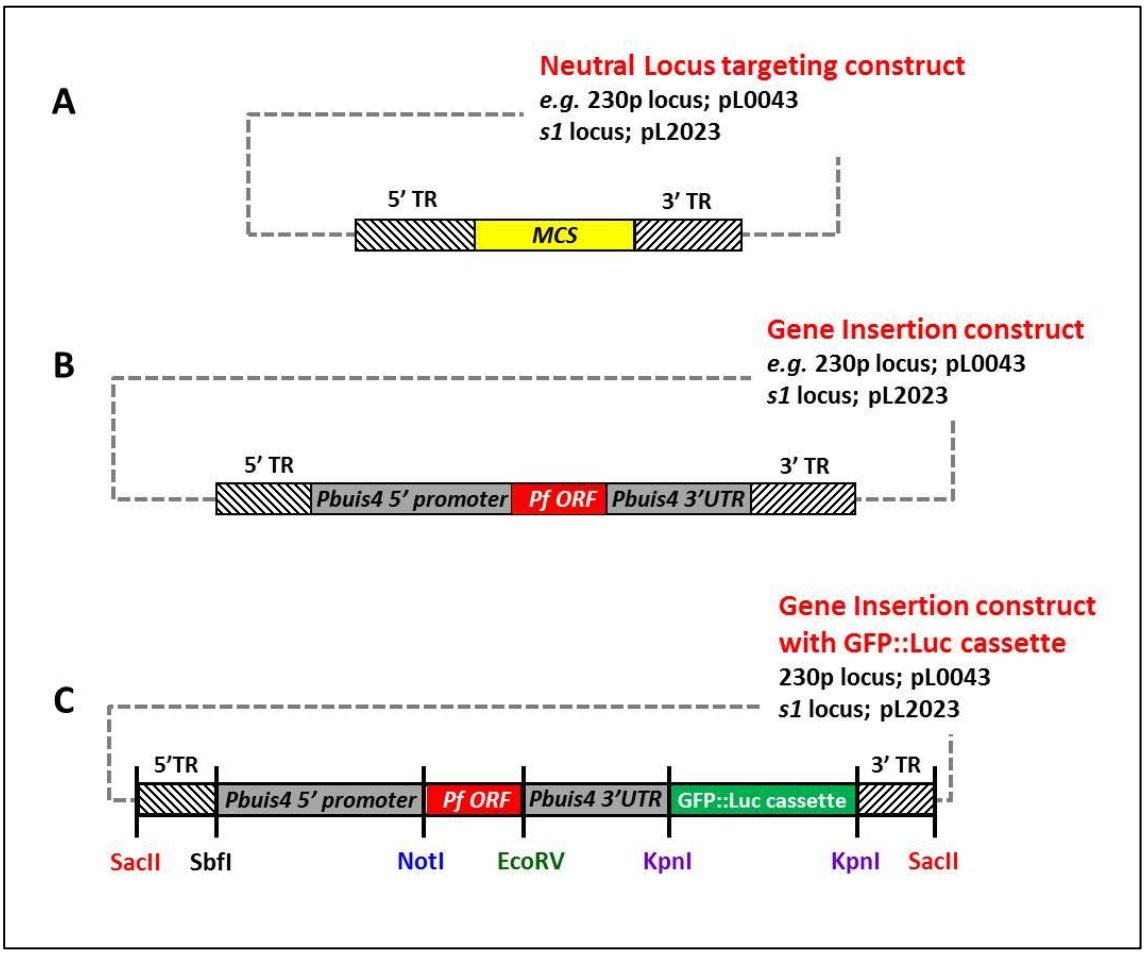

Figure 2.3 Generation of DNA constructs for generation of Additional Gene (AG) chimeric parasites.

A. Two basic constructs can be used to rapidly introduce transgenes into neutral *P. berghei* loci by GIMO transfection; specifically pL0043 to introduce transgenes into the *230p* locus (for transfection into the *PbANKA-230p* GIMO mother line; 1596cl1) and pL2023 for the *s1* locus (for transfection into the *PbANKA-s1* GIMO mother line; 2149cl1). These basic constructs contain 5' and 3' TRs for these loci as well as a multiple-cloning site.

B. The final Gene Insertion construct contains the *P. falciparum* CDS is flanked upstream by the *Pbuis4* 5'UTR (containing the gene promoter region) and downstream by *Pbuis4* 3'UTR (containing the transcription terminator sequence) regions, both of which were PCR-amplified from *Pb* gDNA. The selection of the *Pb* promoter region was dependent on the timing and strength of *P. falciparum* gene expression required. The *P. falciparum* CDS was PCR-amplified from *Pf* gDNA.

C. GFP::Luc fused transgenes expressed under the control of a constitutive promoter which is active for the whole parasite life cycle (*Pb*eef1α) was cloned to the Additional Gene constructs to be used to determine the number of parasites in the liver (i.e. liver loads) in live animals over time, using *in vivo* imaging methodologies or detect the GFP green signal all over the life cycle. The unique restriction enzymes used to clone each DNA fragment and thier positions in the construct are shown in the schematic represenation. Constructs were linearized by SacII restriction enzyme before transfection.

2.2.8.2 Constructs to generate replacement gene (RG) chimeric parasites.

Construct 1 (GIMO Deletion construct): This construct was generated by cloning 5' and 3'TRs of the *Pb* gene (these regions were included the complete *Pb* gene promoter and transcriptional terminator sequences) into the cloning sites of the basic construct pL0034 **(Figure 2.4 A),** upstream and downstream of the h*dhfr*::y*fcu* SM, respectively. Both TRs were PCR amplified from *Pb* gDNA. The targeting regions were chosen usually to be outside of the *Pb* CDS sequence and preferably > 0.6 kb in size **(Figure 2.4 B).** The generated construct was linearized using appropriate restriction enzymes outside of the 5' and 3'TRs. The first transfection with **construct 1** was aiming to replace the *Pb* CDS with the h*dhfr::*y*fcu* SM cassette. Construct 1 was transfected into a standard reporter parasite line *Pb*GFP-Luc_{con} (676m1cl1) to generate a specific *Pb* gene deletion GIMO mother line that also encodes the GFP-Luciferase expression cassette to make the chimeric parasite is visible at any stage during the life cycle **(Figure 2.5).**

Construct 2 (GIMO Insertion construct): This construct was generated based on Construct 1, replacing the h*dfhr*::y*fcu* SM cassette in Construct 1 with the orthologous *P. falciparum* gene CDS sequence, which was PCR amplified from *P. falciparum* gDNA or cDNA, resulting a *P. falciparum* gene expression construct under the control of the 5' and 3' regulatory elements of the *Pb* ortholog. Construct 1 was constructed with unique restriction sites just before and after the h*dhfr*::y*fcu* SM cassette; therefore digestion with these enzymes released the h*dhfr*::y*fcu* SM cassette from the plasmid resulting in a linear DNA construct containing only both 5' and 3'TRs of the target *Pb gene*. This linear construct was used as a vector to clone/insert the orthologous *P. falciparum* CDS into it to generate **Construct 2** which contains the *P. falciparum* CDS flanked upstream by the orthologous *Pb* 5'UTR (containing the gene promoter region) and downstream by Pb 3'UTR (containing the transcription terminator sequence) **(Figure 2.4 C).**

The generated **construct 2** was linearized using appropriate restriction enzymes outside of the 5' and 3'TRs. A second transfection was performed in the gene-deletion GIMO mother line with **construct 2** resulting in a replacement of the h*dhfr::*y*fcu* SM cassette with the orthologous human malaria protein (HMP) gene. This method creates parasites that express a *P. falciparum* gene under the control of its *Pb* ortholog regulatory sequences; these mutants are also SM free, facilitating easier additional genetic modifications.

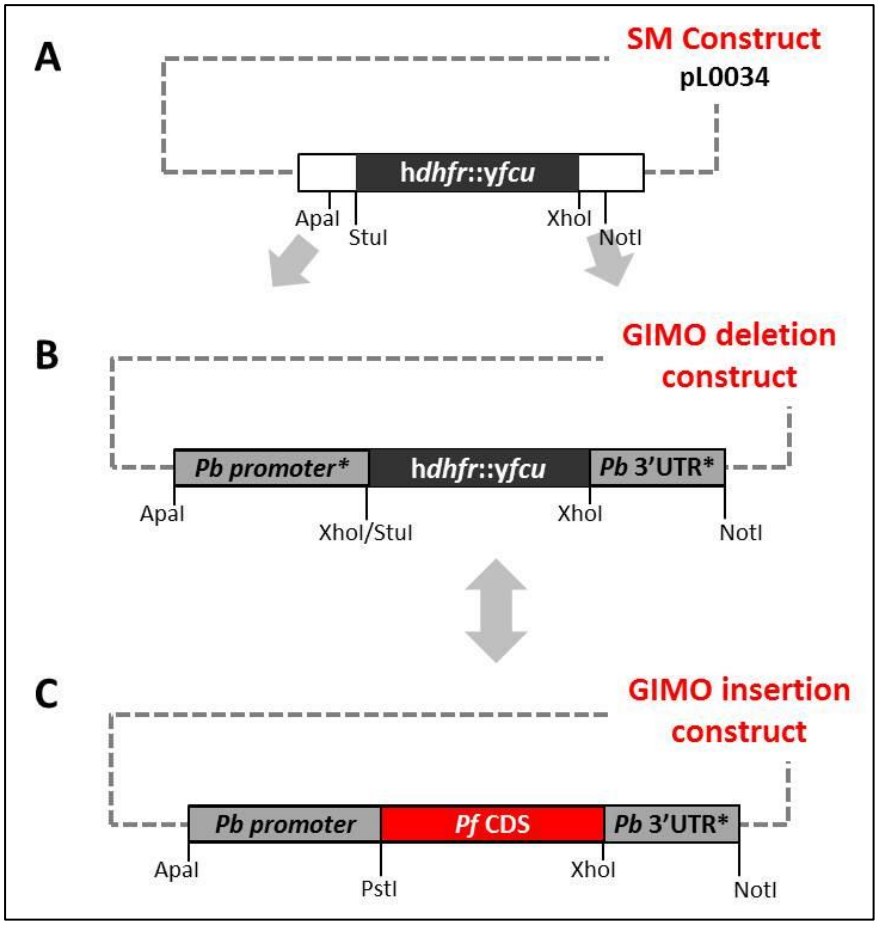

Figure 2.4 Generation of DNA constructs for generation of Replacement Gene (RG) chimeric parasites.

A. Schematic representation of pL0034 basic construct contains the positive-negative (h*dhfr*::y*fcu)* SM cassette with MCS flanking it.

B. Schematic representation describing the generation of **Construct 1** (**GIMO Deletion construct**) by cloning 5-' and 3'-TRs of the *Pb* gene (these regions need to include the complete *Pb* gene promoter and transcriptional terminator sequences) into the cloning sites of the basic construct pL0034, upstream and downstream of the h*dhfr*::y*fcu* SM, respectively. Note: the h*dhfr*::y*fcu* SM cassette (shown in the schematic as h*dhfr*::y*fcu*) is the complete expression cassette; flanked by the constitutive *Pb eef1α* promoter and the *Pb dhfr/ts* transcription terminator sequences. TRs were amplified by PCR from *Pb* gDNA. Introducing additional restriction sites in the used primers for amplifying the *Pb* 5'- and 3'-TRs were considered to facilitate the subsequent release of the SM in order to generate **Construct 2.**

C. Schematic representation describing **Construct 2 (GIMO Insertion construct)**. This schematic shows as an example the 5'-TR created with an *Xho*I restriction site at the 5' end and a *Pst*I/*Xho*I double restriction sites at the 3' end. Similarly the 3'-TR has been generated with an *Xho*I restriction site at the 5' end and *Not*I restriction sites at the 3' end. Therefore Construct 1 has been constructed with a unique restriction site (*XhoI*) both just before and after the h*dhfr*::y*fcu* SM cassette, and digestion with this enzyme releases the h*dhfr*::y*fcu* SM cassette from the plasmid resulting in a linear DNA construct containing both 5' and 3' TRs with complementary ends. Self-ligation can then be performed to generate a 'marker-free' construct with only the 5'-and 3'-TRs and a multiple-cloning site in-between these TR which can in turn be used to insert the orthologous *P. falciparum* gene and thereby create **Construct 2** (GIMO Insertion construct). The *P. falciparum* CDS being flanked upstream by the orthologous *Pb* 5' UTR (containing the gene promoter region) and downstream by Pb 3' UTR (containing the transcription terminator sequence).

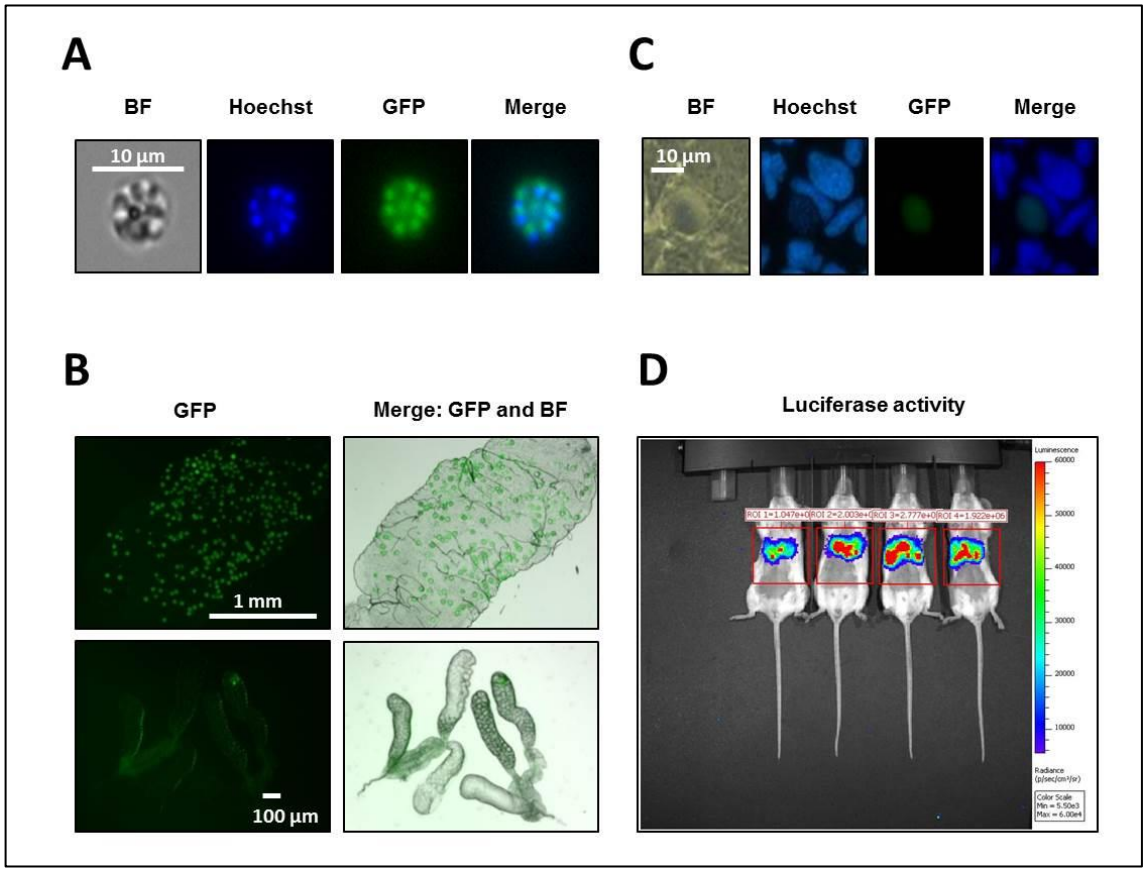

Figure 2.5 GFP-Luc transgenic parasites are visible at any stage during the life cycle. Including the GFP-Luciferase cassette make it possible to visualize the transgenic parasites during any stage of the life cycle [A] Blood stage, [B] Mosquito stage (midgut oocysts and salivary gland sporozoites) and also [C] Liver stage through the expression of GFP and Luciferase under the constitutively active *Pbeef1α* promoter. [D] Liver loads in immunized mice that are challenged with transgenic chimeric sporozoites are quantified by measuring luminescence levels at 44 hours after infection (i.e.: reduction in liver load corresponds to protective immunity).

2.2.9 Cloning, generation and preparation of ChAd63 viral vector vaccine constructs using Gateway TM technology

All DNA constructs required for ChAd63 viral vector vaccine manufacture were generated using the two step cloning strategy as described in **(Figure 2.6).** In the first step of cloning, a unique predesigned synthetic transgene insert (provided by GeneArt) with KpnI and NotI was cloned into the ChAd63 entry vector pENTR™4-Mono (p2022), which contains the human CMV immediate-early promoter used to drive transcription and the bovine growth hormone (BGH) poly (A) transcription termination sequence and under the control of a non-splicing CMV promoter without intron A to avoid deletion risk during production. The entry plasmid also contained attachment L (attL) sequences, which were required for site-specific recombination with attachment R (attR) sites located on the destination vector using a LR Clonase™ II mediated site-specific recombination. Correct cloning was confirmed by analytical restriction enzyme digest using PsiI restriction enzyme (RE) or other suitable set of restriction enzymes.

In the second step of cloning, *in vitro* Gateway reaction was performed using LR Clonase II system (Invitrogen). This Gateway® technology was used to integrate the entry vector containing transgene together with its transcription and translation regulation elements into the ChAd63 destination plasmid vector (p1916) by site-specific recombinase through attL-attR interaction. Following confirmation of the correct sequence of the insert; the transgene containing destination vector was linearized with Pme1 as per J004, and stored at -20°C till transfection and purification.

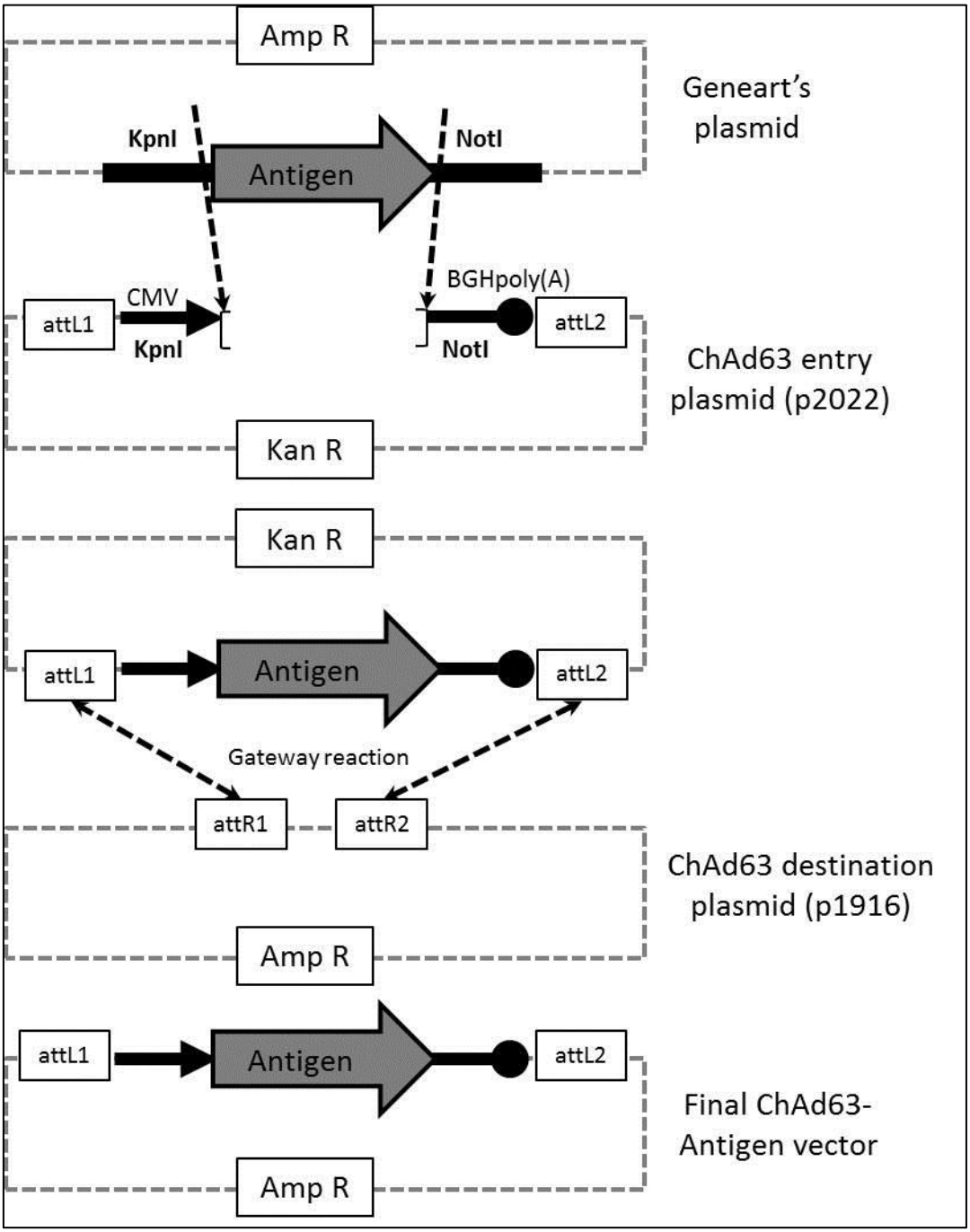

Figure 2.6 Cloning steps involved in generation of DNA constructs required for ChAd63 viral vector manufacture.

Malarial antigens were synthesized by GeneArt and cloned into plasmids at the pre-designed unique restriction sites; KpnI and NotI sites located at the 5' and 3' ends of the transgene, respectively, were used for inserting synthetic malarial antigen into the ChAd63 entry plasmid (p2022) between CMV promoter and BGH poly(A) regions. In the second step of cloning, site-specific recombination between attL and attR sequences was performed in the ChAd63 destination vector (p1916) resulting in transgene incorporation into the adenovirus destination vector.

2.2.10 Cloning, generation and preparation of MVA viral vector vaccine constructs

To generate recombinant MVAs the antigen of interest was cloned into MVA-mCherry vector (p3753) with KpnI/ NotI site using the same cloning strategy **(Figure 2.7).** The gene insertion site is at the thymidine kinase (TK) locus with the antigen under control of the p7.5 promoter, whereas the mCherry gene expressed under the control of FP4b promoter. The transgene sequences were extracted from the plasmids provided by GeneArt by digestion with KpnI and NotI restriction enzymes. MVA-mCherry vector (p*3753*) was also digested with the same restriction enzymes and alkaline phosphatase as described earlier in **2.2.4**. The antigen insert was then ligated into the MVA-mCherry vector and then transformed into *E. coli* bacteria. Plasmid DNA preparation and diagnostic digestion analysis were performed to confirm the correct cloning. The MVA-mCherry-[transgene] vectors were stored at -20°C till transfection and purification.

2.2.11 DNA Sequencing reactions

The regions critical for transgene expression (i.e. the promoter and *P. falciparum* CDS) of the final constructs for the chimeric parasites or the viral vector vaccines were sequenced to ensure that the transgenes are correctly expressed in both chimeric parasite and the viral vector vaccines.

100ng/µl plasmid DNA in total volume 15µL water and 10µL of 3.3µM/µL in total volume 10µL were provided separately per independent sequencing reaction to Source Bioscience Sequencing (Cambridge, UK).

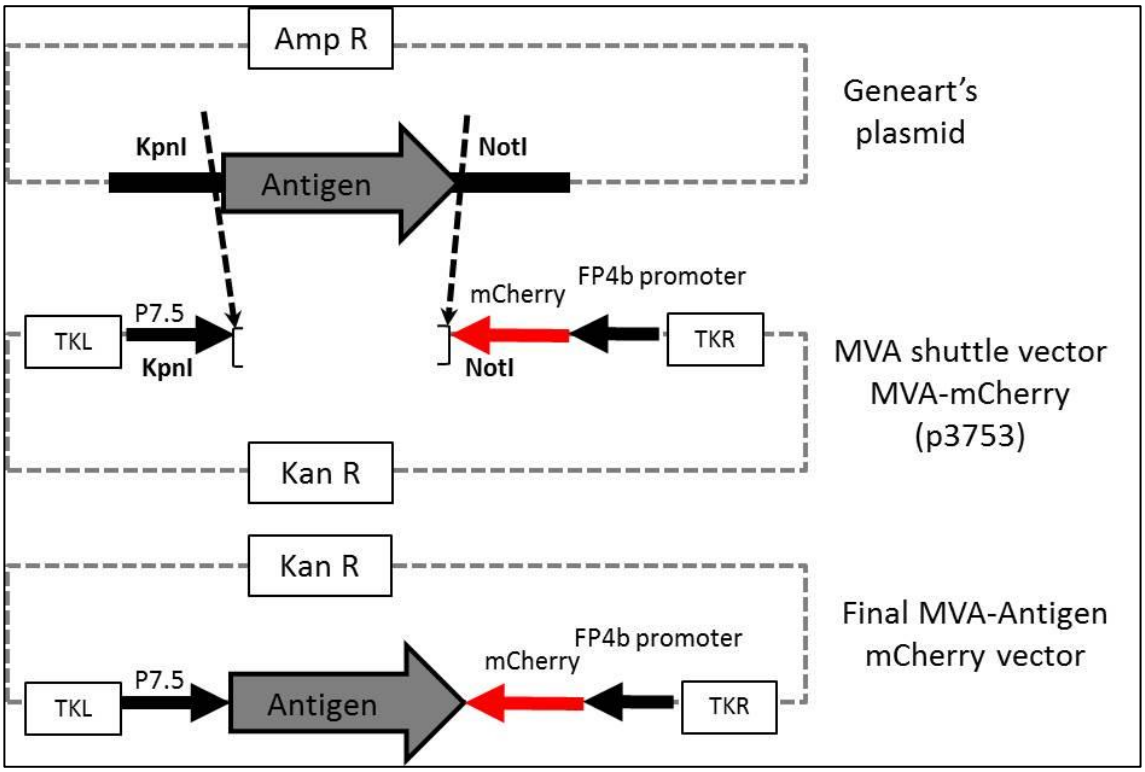

Figure 2.7 Cloning steps involved in generation of DNA constructs required for MVA viral vector manufacture.
Malarial antigens were synthesized by GeneArt and cloned into plasmids at the pre-designed unique restriction sites; KpnI and NotI sites located at the 5' and 3' ends of the transgene, respectively, were used for inserting synthetic malarial antigen into the MVA shuttle vector, termed MVA-mCherry (p3753) in a single step cloning, which was subsequently used for the production of recombinant MVA.

2.3 Chimeric parasites generation and transfection

In this thesis two methods were described for the rapid generation of chimeric rodent *P. berghei p*arasites that express *P. falciparum* proteins, using the recently developed efficient GIMO-based transfection methodology (Gene Insertion-Marker Out; [245] that greatly simplifies and speeds up the generation of transgenic parasites expressing heterologous proteins, free of drug-selection marker genes. Two different genetic modifications are described here resulting in two types of chimeric parasites that express *P. falciparum* proteins. The different types of chimeric parasites were used to evaluate vaccine-efficacy *in vivo* using mice immunised with their corresponding novel *P. falciparum*-vaccines.

2.3.1 Generation chimeric parasites with a *P. falciparum* gene in a neutral locus: additional gene (AG) mutants

When a functional orthologue of a *P. falciparum* gene is absent in the *Pb* genome, the *P. falciparum* gene can be introduced into a neutral/silent locus of the Pb genome. Moreover, this approach can be used when the stage specificity and/or level of HMP expression needs to be altered. In these mutants the *P. falciparum* gene is introduced as an 'additional gene' into a silent/neutral locus of the Pb genome under the control of either a constitutive or stage specific Pb promoter. This method uses the GIMO-transfection protocol and AG mutants are generated by replacing the positive-negative selection marker (SM) hdhfr::yfcu cassette in a neutral locus of a standard GIMO mother line with the *P. falciparum* gene expression cassette, resulting in SM free transgenic parasites

2.3.1.1 Generation of GIMO mother lines in *P. berghei* ANKA

The standard GIMO mother lines PbANKA-230p (GIMOPbANKA 1596cl1) and PbANKA-s1 GIMO mother line (2149cl1) contain a positive-negative selection marker (SM) cassette, a fusion gene of hdhfr and yfcu SM under control of the constitutive eef1a promoter [249], stably integrated into the neutral 230p locus (PBANKA_030600) by using a specific PbANKA-230p targeting deletion construct (pL1063) [245] or the neutral s1 gene-locus (PBANKA_120680) by using a specific PbANKA-s1 targeting deletion construct (pL1928), respectively through double cross-over recombination. The neutral s1 locus has also been used in *P. yoelii* to introduce reporter proteins [250]. In addition, it contains GFP under the constitutive eef1a promoter integrated into the neutral 230p locus (PBANKA_030600). *PbANKA* GIMO mother-lines with SM were subsequently selected by applying positive drug selection using pyrimethamine, and cloned using the standard procedures described for transfection of *P. berghei* [248] (**Figure 2.8, step 1**).

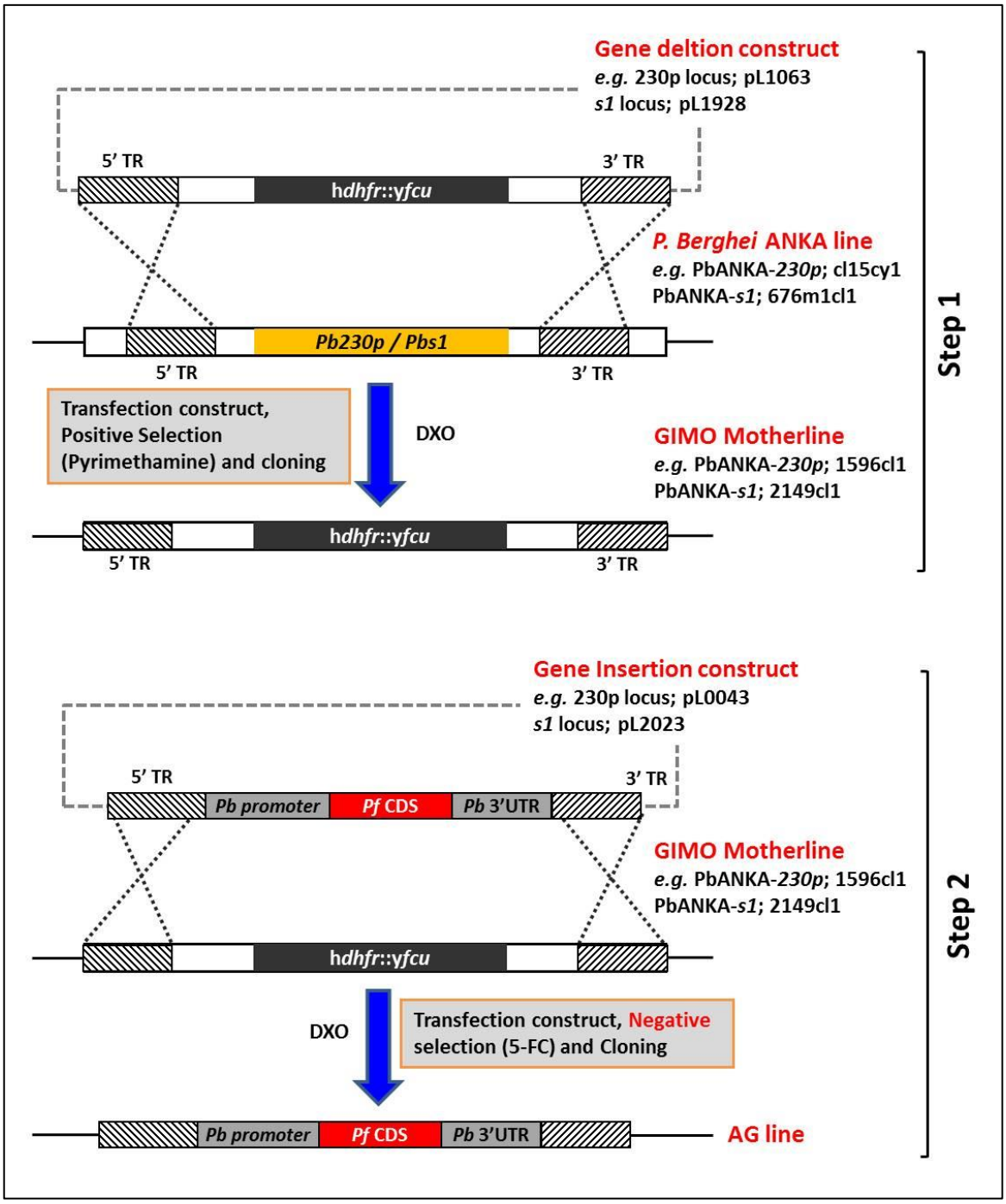

Figure 2.8 Generation of Additional Gene (AG) chimeric parasites.
Step 1: Schematic representation of the constructs used to introduce the positive-negative selectable maker cassette into the *P. berghei ANKA* neutral loci (230p locus; pL1063, or s1 locus; pL1928) to generate the GIMO mother-lines which were selected by positive selection using pyrimethamine drug.

Step 2: Additional Gene (AG) mutants have a human malaria parasite *P. falciparum* gene introduced into a neutral locus (*230p* or *s1* locus) of *P. berghei* GIMO mother lines genome by a second independent GIMO-transfection. Schematic representation of the construct to introduce the *P. falciparum* malaria parasite gene into the *230p* or *s1* locus of GIMO mother-lines, resulting in the generation of the AG mutant after negative selection with 5-FC. Two basic constructs can be used to rapidly introduce transgenes into neutral *Pb* loci by GIMO transfection; specifically pL0043 to introduce transgenes into the *230p* locus (for transfection into the *PbANKA-230p* GIMO mother line; 1596cl1) and pL2023 for the *s1* locus (for transfection into the *PbANKA-s1* GIMO mother line; 2149cl1) (see **Figure 1**). The construct is targeting the *230p* or *s1* target regions (hatched boxes) by double cross-over homologous recombination (DXO), resulting in replacement of the h*dhfr*/*yfcu* selectable marker cassette that is present in the GIMO parasites with the *P. falciparum* gene expression cassette.

2.3.1.2 Transfection of parasites and injection into mice

5-10 µg of linearized DNA construct was prepared in 5-10 µL water or TE buffer. This construct is based on a standard GIMO construct and contains the 5' and 3' TRs of the 230p or s1 targeting regions of the GIMO mother line and a *P. falciparum* gene expression cassette (i.e. the *P. falciparum* gene CDS flanked by 5'UTR (promoter) and 3' UTR of a chosen *Pbuis4* gene (**Figure 2.8, step 2**). Cultured (*in vitro* matured) *P. berghei* schizonts of a standard PbANKA-230p or PbANKA-s1 GIMO mother lines were collected and transfected with the DNA construct using a Nucleofector device [248] prior to intravenous injection into mice.

2.3.1.3 Negative selection of parasites (5-FC) and cloning

Transfected parasites were selected by negative selection with 5-FC which was provided to the mouse in the drinking water one day after infection, for a period of 8–11 days when transfected and selected parasites were collected from the mice by cardiac puncture prior to cryopreservation in glycerol-PBS solution. In successful transfection experiments, the parasitemia typically increased to 2–5% between days 8 and 11. Some blood (0.4-0.8 ml) was reserved to genotype the transfected parasite population by Southern analysis of separated

chromosomes (**Figure 2.11**) or digested genomic DNA or by diagnostic PCR as described in [248]. On confirmation of the correct deletion of the h*dhfr::*y*fcu* SM cassette, parasites were cloned by the method of *in vivo* limiting dilution [253]. Blood stocks of cloned parasite lines were collected around 8 to 9 days post infection (1-3% parasitaemia) and cryopreserved as above with some blood set-aside for genotype analysis (**Figure 2.11**). The cloned AG parasites with a correct genotype were used for phenotype analysis to (i) determine (normal) development throughout the life cycle and (ii) to confirm correct *P. falciparum* expression **(see phenotype analysis in subheading 2.5).**

2.3.2 Generation chimeric parasites with a *P. falciparum* gene: replacement gene (RG) mutants

In these mutants, the coding sequence of the Pb gene is replaced with the CDS of the *P. falciparum* ortholog in the standard two-step GIMO-transfection procedure whereby there is first replacement of a specific Pb CDS with the hdhfr::yfcu SM, prior to insertion of the *P. falciparum* orthologue.

2.3.2.1 Transfection of parasites and injection into mice: transfection step 1.

5-10 µg of linearized DNA construct was prepared in 5-10 µL water or TE buffer. This construct (construct 1) is a gene-deletion construct containing the hdhfr::yfcu SM cassette flanked by the 5' and 3' TRs of the *Pb* gene and is based on standard construct pL0034 **(Figure 2.9, Step 1).** Cultured (*in vitro* matured) *P. berghei* schizonts of wild-type were collected and transfected with the DNA construct using a Nucleofector device [248] prior to intravenous injection into mice.

2.3.2.2 Positive selection of parasites (pyrimethamine) and cloning: transfection step 1

Transfected parasites were selected by positive selection with pyrimethamine: provided which was provided to the mouse in the drinking water one day after infection, for a period of 8–11 days up to the collection of infected blood. Transfected and selected parasites were collected from the mice by cardiac puncture prior to cryopreservation in glycerol-PBS solution. In successful transfection experiments, the parasitemia typically increased to 2–5% between days 8 and 11. Some blood (0.4-0.8 ml) was reserved to genotype the transfected parasite population by Southern analysis of separated chromosomes (**Figure 2.11**) or digested genomic DNA or by diagnostic PCR as described in [248]. On confirmation of the correct deletion of the Pb-CDS and its replacement with the h*dhfr::*y*fcu* SM cassette, parasites were cloned by the method of *in vivo* limiting dilution [253]. Blood stocks of cloned parasite lines were collected around 8 to 9 days post infection (1-3% parasitaemia) and cryopreserved as above with some blood set-aside for genotype analysis (**Figure 2.11**). The cloned *Pb* gene deletion GIMO mother-line parasites with a correct genotype were used for phenotype analysis to (i) determine (normal) development throughout the life cycle and (ii) to confirm correct *P. falciparum* expression **(see phenotype analysis in subheading 2.5).**

2.3.2.3 Transfection of parasites and injection into mice: transfection step 2

5-10 µg of linearized DNA construct was prepared in 5-10 µL water or TE buffer. This construct (construct 2) is a *P. falciparum* gene insertion construct containing the *P. falciparum*-CDS flanked by the same *Pb* 5' UTR and 3' UTR sequences present in **construct 1 (Figure 2.9, Step 2).** Cultured (*in vitro* matured) *P. berghei* schizonts of the GIMO mother-line parasite were collected and transfected with the DNA construct using a Nucleofector device [248] prior to intravenous injection into mice.

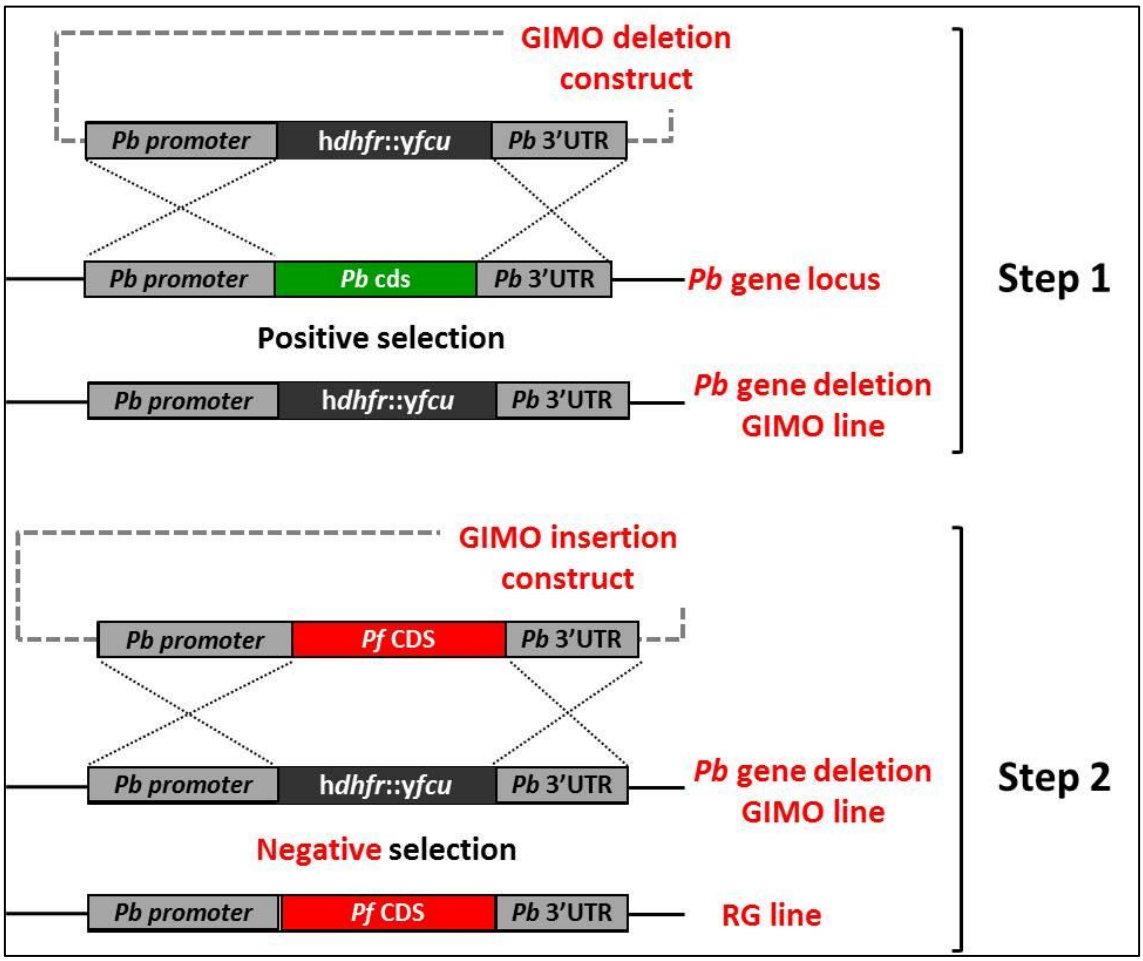

Figure 2.9 Generation of Replacement Gene (RG) chimeric parasites where the *Pb* target gene (TG) is replaced with the orthologous gene of a human malaria *P. falciparum* parasite.

Step 1: The **GIMO Deletion construct** (**Construct 1**) was used to replace the *P. berghei* gene with the positive/negative selectable maker (h*dhfr::*y*fcu*) cassette, resulting in the generation of the chimeric GIMO mother-line after positive selection with pyrimethamine. **Construct 1** targets the chimeric parasite at the target regions (gray boxes) by double cross-over homologous recombination. After genotyping and confirming the correct construct integration, this line was cloned.

Step 2: The **GIMO insertion construct** (**Construct 2**) was used to replace the SM in the GIMO line with the *P. falciparum* CDS, under negative (5-FC) selection, resulting in RG chimeric parasite. **Construct 2** integrates by double cross-over homologous recombination using the same TRs employed in construct 1, resulting in the introduction of the *P. falciparum* gene under the control of the *Pb* target gene promoter and transcriptional terminator sequences.

2.3.2.4 Negative selection of parasites (5-FC) and cloning: transfection step 2

Transfected parasites were selected by negative selection with 5-FC which was provided to the mouse in the drinking water one day after infection, for a period of 8–11 days when transfected and selected parasites were collected from the mice by cardiac puncture prior to cryopreservation in glycerol-PBS solution. In successful transfection experiments, the parasitemia typically increased to 2–5% between days 8 and 11. Some blood (0.4-0.8 ml) was reserved to genotype the transfected parasite population by Southern analysis of separated chromosomes (**Figure 2.11**) or digested genomic DNA or by diagnostic PCR as described in [248]. On confirmation of the correct deletion of the h*dhfr::*y*fcu* SM cassette, parasites were cloned by the method of *in vivo* limiting dilution [253]. Blood stocks of cloned parasite lines were collected around 8 to 9 days post infection (1-3% parasitaemia) and cryopreserved as above with some blood set-aside for genotype analysis (**Figure 2.11**). The cloned RG parasites with a correct genotype were used for phenotype analysis to (i) determine (normal) development throughout the life cycle and (ii) to confirm correct *P. falciparum* expression **(see phenotype analysis in subheading 2.5).**

2.3.3 Generation of double chimeric parasites expressing two different *P. falciparum* genes:

Due to the huge antigenic polymorphism in *P. falciparum* parasite, it was highly likely that more protective malaria vaccine might rely on the induction of immune responses against multiple antigens. We therefore aimed to generate transgenic chimeric parasites that express two *P. falciparum* antigens in different combinations of the promising vaccine candidates. We have followed the previous two transfection approaches to generate either additional gene or replacement gene double transgenic parasites.

It is still a valid approach to apply the previous two approaches in one chimeric parasite since the chimeric parasites are SM free in case of they show a normal fitness. This novel approach will open the door to generate triple or multiple chimeric parasite(s) to allow testing the combination of more than two vaccine candidates.

2.3.3.1 Generation of chimeric parasites by introducing two genes in two neutral loci of the genome: double additional gene (DAG) mutants

The standard GIMO transfection method to generate additional gene mutants (AG) was applied here but in this case two independent transfections were performed in both neutral loci PbANKA-230p (PBANKA_030600) (Chr-3) and PbANKA-s1 (PBANKA_120680) (Chr-12) in one chimeric parasite but in a sequential order. The standard GIMO basic constructs (pL0043, pL2023, pL1063 and pL1928) were used to generate the targeting constructs as described earlier in subheading **2.3.1 (Figure 2.10)**

2.3.3.2 Generation of chimeric parasites by replacement of two *P. berghei* genes by their *P. falciparum* orthologs: double replacement gene (DRG) mutants.

The standard GIMO transfection method to generate replacement gene mutants (RG) was applied here but in this case two independent transfections were performed and in each transfection we targeted a specific *P. falciparum* orthologous gene in one chimeric *P. berghei* parasite but in a sequential order. The standard GIMO basic construct (pL0034) was used to generate the targeting constructs as described earlier in subheading **2.3.2 (Figure 2.9)**

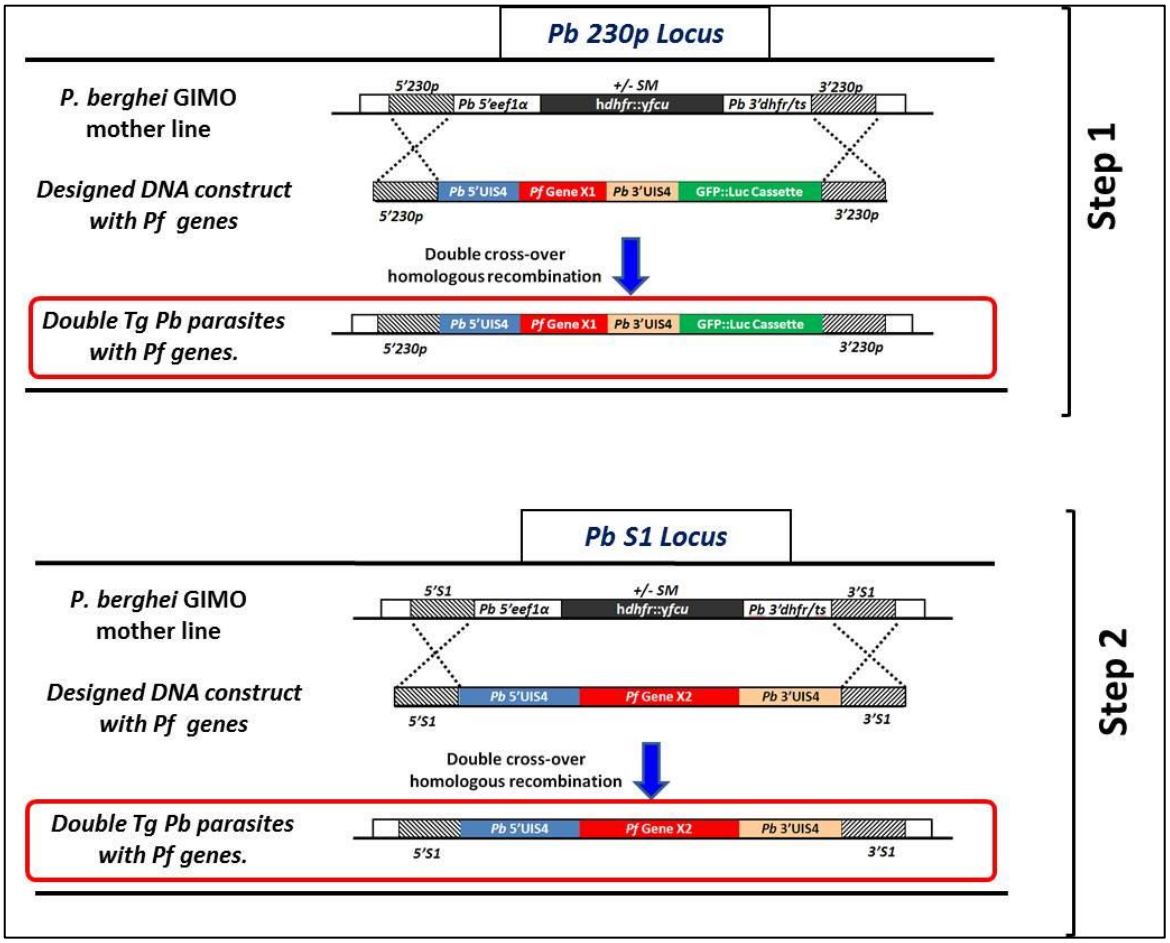

Figure 2.10 Generation of Double Additional Genes Chimeric Parasite (DAG).
Schematic representation of the constructs and the steps used to generate the double *P. berghei* transgenic parasites which could express two different *P. falciparum* antigens. The standard GIMO transfection strategy has been followed to generate these *P. berghei GIMO* mother line(s) and the transgenic *P. berghei* parasites to express two different *P. falciparum* antigens, by targeting two different neutral loci in the *P. berghei* parasite; the first is the 230p locus in chromosome-3, and the second is the S1 locus in chromosome-12 in two independent additional transfections. Two different *P. falciparum* gene expression cassettes were constructed to express different combinations of *P. falciparum* proteins. The double additional genes (DAG) chimeric parasites enabled the test of different vaccine combinations which was a major step that permitted the assessment of the potential of multi-antigen vaccines to develop an optimal combination vaccine to afford better protection than single antigen vaccination.

2.4 Genotype analysis for the chimeric *P. berghei* parasite clones.

2.4.1 Genomic DNA isolation of blood stages of chimeric *P. berghei* parasites

The parasite pellet was re-suspended in 2ml Eppendorf tube with 700 µl TNE buffer and the following supplements were added: 200 µg RNase (20 µl of a 10 mg/ml solution) and 1% (v/v) SDS (100 µl of a 10% solution), and then volume completed by Milli-Q water up to 1 ml**.** The tube was incubated for 10 minutes at 37°C. After incubation, 200 µg Proteinase K (20 µl of a 10 mg/ml solution) was added with gentle mixing by pipetting and incubated for 1 hour at 37°C. Buffered phenol was added up to 1.5 ml with inverting the tube several times followed by centrifugation for 5 minutes at maximum speed at 4°C. Then, the aqueous upper phase was transferred to a new tube and buffered Phenol:Chloroform:Isoamylalcohol (25:24:1) was added up to 1.5 ml with inverting the tube several times followed by centrifugation for 5 minutes at maximum speed at 4°C. The aqueous upper phase was transferred to a new tube and Chloroform:Isoamylalcohol (24:1) was added up to 1.5 ml with inverting the tube several times followed by centrifugation for 5 minutes at maximum speed. The aqueous upper phase was transferred to a new tube and the following supplements were added: 0.1 volume of 3 M NaAc, pH 5.2, and 2 volumes of 96% ethanol were added with inverting the tube several times, and then tube was incubated at –20°C to let the DNA to precipitate for a couple of hours to overnight. After the incubation, the tube was centrifuged for 10 minutes at maximum speed at 4°C and the DNA pellet was washed by adding 500 µl 70% ethanol, and then centrifuged for 5 minutes at maximum speed at 4°C. The supernatant was discarded and the DNA pellet left to air-dry. The DNA pellet was re-suspended in 300 µl of Milli-Q water when started with a big parasite pellet and in 50 µl when started with a small parasite pellet.

2.4.2 Diagnostic integration (confirmation) PCR

Different primers were designed for the diagnostic PCR analysis of chimeric parasite lines to confirm correct integration of the *P. falciparum* antigen expression cassettes. Correct integration in all lines was confirmed by the absence of the *hdhfr::yfcu* SM, the presence of the *P. falciparum* gene coding sequence and the correct integration of the construct into the genome at both the 5'and 3'regions (5' int and 3' int).

2.4.3 Southern analysis of chromosomes separated by pulsed-field gel electrophoresis (PFGE)

Correct integration of the *P. falciparum* antigen expression cassettes was also confirmed by Southern analyses of chromosomes separated by pulse-field gel electrophoresis hybridized with specific probes for the transfected *P. falciparum* expression cassette or the selectable maker. This work has been done by Jai Ramesar from Dr. Chris Janse's group at LUMC, Leiden, The Netherlands.

2.4.3.1 Additional Gene (AG) chimeric parasite.

The Southern analysis of the separated chromosomes was performed by pulsed-field gel electrophoresis (PFGE) to confirm the correct integration of the DNA construct in the GIMO locus by showing the absence of the h*dhfr::*y*fcu* SM cassette both in the uncloned (parent) and cloned parasites. Separated chromosomes were hybridized with a mixture of two probes: one recognizing h*dhfr* (recognizing the SM in chr-3 and chr-12 for the *230p* and *s1* mother lines respectively) and a control probe used (frequently, *pb25* gene probe is used that recognizes *Pb* chromosome 5). As an additional control (ctrl) parasite line was used with the h*dhfr::*y*fcu* SM integrated into a known Pb chromosome (frequently line 2117cl1 was used as it has the SM in chr-3) (**Figure 2.11 A)**.

2.4.3.2 Replacement Gene (RG) chimeric parasite.

Southern analysis of PFGE-separated chromosomes was performed to confirm the correct integration of the DNA construct in the target *Pb* gene both in uncloned (parent 1) and cloned parasites selected with positive selection in step 1. The chromosomes were hybridized using a probe recognizing the *Pbdhfr/ts* 3'UTR of the SM of the integrated construct which also hybridizes to the endogenous *Pbdhfr/ts* gene on chromosome 7. The ratio between the hybridization signal of the target chromosome and of chromosome 7 is informative for both the success of vector integration, the contamination with wild-type parasites and the possible presence of plasmids that usually migrate at the height of chromosome 9-11. For genotyping of selected parasites in step 2 (uncloned/parent 2 and cloned) Southern analysis of PFGE-separated chromosomes was performed to confirm the correct integration of the orthologous *P. falciparum* gene in the GIMO locus by showing the absence of the h*dhfr::*y*fcu* SM cassette. Separated chromosomes were hybridized with a mixture of two probes: one recognizing h*dhfr* and a control probe (for example recognizing chr-5; *pb25*) as described under **(2.4.3.2)** for the AG mutants (**Figure 2.11 B)**.

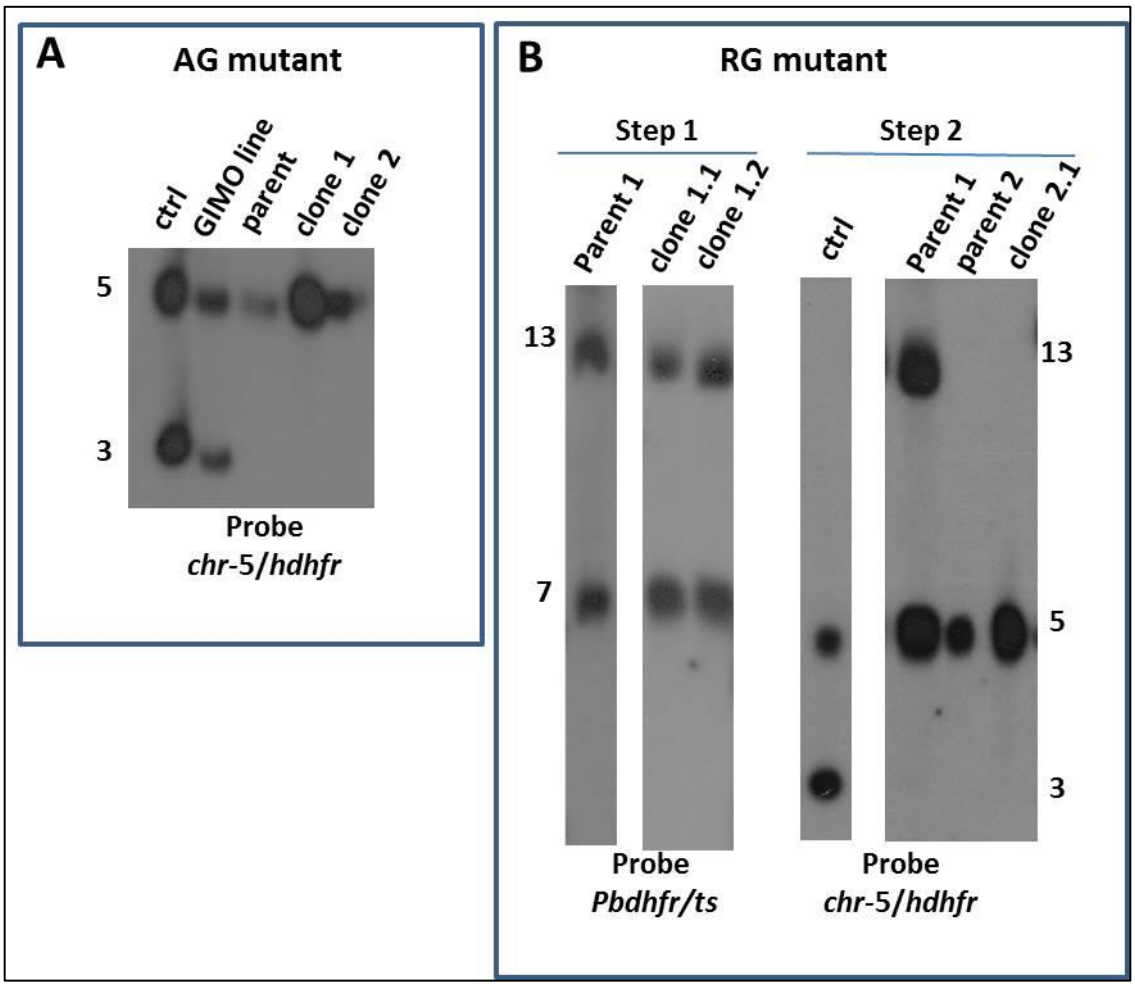

Figure 2.11 Genotyping of AG and RG mutants.

A. <u>AG mutants</u>: Southern analysis of chromosomes (chrs) separated by pulsed-field gel electrophoresis (PFGE) to confirm integration of the DNA construct in the GIMO locus by showing the removal of the h*dhfr::*y*fcu* SM cassette both in uncloned (parent) and cloned parasites. The southern blot is hybridized with a mixture of two probes: one recognizing h*dhfr* and a control probe recognizing chr-5. As an additional control (ctrl), parasite line 2117cl1 is used with the h*dhfr::*y*fcu* SM integrated into chr-3.

B. <u>RG mutants</u>: Southern analysis of PFGE-separated chrs to confirm integration of the DNA construct into the target *Pb* gene both in uncloned (parent 1) and cloned parasites selected in step 1 of the DsR transfection protocol. The chrs are hybridized using a probe recognizing the 3'UTR *Pbdhfr/ts* of the SM of the integrated construct which also hybridizes to the endogenous *Pbdhfr/ts* on chr-7. For genotyping of selected parasites in step 2 of the DsR protocol (i.e. the uncloned parent 2 and cloned parasites): Southern analysis of PFGE-separated chrs to confirm integration of the orthologous HMP gene in the GIMO locus by showing the absence of the h*dhfr::*y*fcu* SM cassette. Separated chrs are hybridized with a mixture of two probes: one recognizing h*dhfr* and a control pb25 probe recognizing chromosome 5 as described above for the AG mutants.

2.5 Phenotype analysis of the chimeric *P. berghei* parasites.

2.5.1 Confirmation of the expression of the *P. falciparum* candidates in the chimeric sporozoites using an Immunofluorescence assay test (IFAT)

2.5.1.1 IFAT Slide Preparation:

8-well microscope slides were coated with 20 µl of 0.01% poly-Lysine in Milli-Q water (10X dilution from stock) and left to dry over-night. Samples (20,000 sporozoites in RPMI per well) were added in wells and left to settle down for 20 min on ice, at which point excess liquid was removed by careful pipetting. Fixation was performed by adding 50-60 µL of 4% PFA in PBS for 20min prior to washing slides at least 2 times with PBS and storage in 50mL falcon tubes containing sterile PBS for 6 months or longer at 4°C until staining.

2.5.1.2 IFAT Slides immunofluorescence- staining

Expression of *P. falciparum* antigens in sporozoites of the chimeric parasites was analysed by immunofluorescence- staining assay (IFA), using anti-*P. falciparum* antigen monoclonal antibodies or serum-antibodies from mice immunized with the viral vector expressing the specific *P. falciparum* antigen. Fixed sporozoites were washed three times with PBS and blocked with 20µl 10% FCS+1% BSA in PBS for 30 min at room temperature. The blocking medium was removed, followed by the addition of 20-25µL primary monoclonal antibody (diluted 1000 times) or mouse serum (from vaccinated mice) (diluted 50-200 times) in 10% FCS+1% BSA in PBS and incubate for 1-2 hours at room temperature or overnight at 4 °*C*. Antibody was removed and the slides washed three times with PBS, followed by the staining with the secondary antibody (Alexa Fluor® 488 Goat Anti-Mouse IgG) diluted 800 times in 10% FCS+1% BSA in PBS (blocking medium) for 1 hour at room temperature. After washing three times with PBS, nuclei were stained with 2% Hoechst-33342 in PBS for 10 minutes at room temperature, washed twice with PBS and left to air-dry, followed by addition of Fluorescence Mounting Medium (Dako). Cover

slips were mounted onto the slides, and the slides were sealed with nail polish and left to dry overnight in the dark. The parasites were visualised in both blue and green channels using a DMI-300B Leica fluorescence microscope and images analysed using ImageJ software

2.5.2 Chimeric parasite fitness

2.5.2.1 Phenotype analysis of transgenic parasites expressing *P. falciparum* genes

Before using transgenic *Pb* parasites expressing *P. falciparum* genes in assays, the phenotype was analysed to i) determine whether *P. falciparum* gene expression affects normal development and ii) to confirm correct timing and level of *P. falciparum* gene expression. Several assays were performed to confirm the normal and wild-type fitness of the chimeric parasites before using them in any assay.

2.5.2.2 Blood stage development of chimeric parasites

Blood stage growth was calculated from the multiplication rate of asexual blood stages *in vivo* during the cloning procedure of mutants [254] and was calculated as follows: the percentage of infected erythrocytes in Swiss OF1 mice injected with a single parasite was quantified at days 8–11 by examination of Giemsa-stained blood films. The mean asexual multiplication rate per 24 h was then calculated assuming a total of 1.2×10^{10} erythrocytes per mouse (2 ml of blood). The percentage of infected erythrocytes in mice infected with a single parasite of a *Pb* ANKA reference lines ranges between 0.5 and 2% at day 8 after infection, resulting in a mean multiplication rate of 10 per 24 h [254].

A second frequently used method to determine asexual growth rate was by examining the course of parasitemia after infecting mice with a standard dose of infected red blood cells (irbc, i.e. 10^3-10^4 irbc). The course of parasitemia can be determined by counting irbc in Giemsa stained blood films or by standard FACS [255] or simple bioluminescence assays [256] when parasites express GFP or Luciferase. Determination of *P. falciparum* expression was also performed using standard Northern analysis of transcription, Western and or immunofluorescence analysis of protein expression methods.

2.5.2.3 Mosquito development of chimeric parasites

Gametocyte production was typically determined by counting mature gametocytes in mice that have either synchronized or non-synchronized blood stage infections [257]. Ookinete production was usually determined in standard *in vitro* cultures of ookinetes [258] and defined as the percentage of female gametocytes/gametes that develop into mature ookinetes. The ratio of unfertilized female gametocytes/gametes to ookinetes was determined in Giemsa stained slides of samples taken from the ookinete cultures at 16-24 hour [259]. Oocyst and sporozoite production was determined in *A. stephensi* mosquitoes that were fed on infected mice by microscopic analysis of dissected midguts and salivary glands [260]. Determination of *P. falciparum* expression was performed using standard Northern analysis of transcription, Western and or immunofluorescence analysis of protein expression methods.

2.5.2.4 Liver stage development of chimeric parasites

Sporozoite infectivity and liver stage development were determined in cultures of hepatocytes (e.g. HepG2, Huh7) or in mice infected with sporozoites, either by mosquito bite or by intravenous injection of sporozoites [261]. Sporozoites were obtained by standard methods of dissection of salivary glands of infected

mosquitoes. Sporozoite infectivity and liver parasite loads were quantified by bioluminescence assays (both *in vitro* and *in vivo* imaging) [261] when parasites express Luciferase, by measuring the prepatent period (time taken, in days, to achieve a parasitemia in the blood of 0.5-2% after infection of mice with defined numbers of sporozoites; [262], Also, it could be quantified by qPCR [263]. Determination of *P. falciparum* expression was performed using standard Northern analysis of transcription, Western and or immunofluorescence analysis of protein expression methods.

2.5.3 Fluorescence microscopy

Leica DMR or DMI-300B Leica fluorescent microscopes with standard GFP and Texas Red filters were used to analyze of GFP- or mCherry- expression in blood, liver or mosquito stages of transgenic parasites. Parasite nuclei were labelled by staining with Hoechst-33342 (**Figure 2.5)**.

2.5.4 Liver cell culture

Huh-7 cells, a human hepatoma cell line, were used in *in vitro* analysis of sporozoite infectivity. Huh-7 cells were cultured in 'complete' RPMI 1640 medium supplemented with 10% (v/v) fetal bovine serum (FBS), 1% (v/v) penicillin-streptomycin, 1% (v/v) GultaMAX (Invitrogen), and maintained at 37°C with 5% CO2. Briefly, Huh-7 cells were suspended in 'complete' medium and were seeded in 24 well plates (10^5 cells/ml). After the Huh7 monolayers were >80% confluent, 10^5 sporozoites were added. Huh-7 cells (5×10^4 cells per well) were seeded onto coverslips in 24-well plates and on the following day, cells were infected with 5×10^4 sporozoites, plates were centrifuged at 600 g for 4 minutes. Three hours after adding the sporozoites, culture medium was removed and replaced with fresh medium. At different time-points after addition of sporozoites, culture medium was removed and nuclei stained with

Hoechst-33342 for 10 minutes prior to washing once with PBS and fixation of cells with 4% paraformaldehyde for 20 min. The parasites in both blue and red channels were analyzed using a DM-IRBE Flu Leica fluorescence microscope and processed using ImageJ software.

2.5.5 *In vivo* imaging using the IVIS system

All the transgenic parasite lines were generated to express the fusion protein GFP-Luciferase under the control of the constitutive *eef1α* promoter. The *gfp-luc* expression cassette is stably integrated into the *Pb230p* locus without introduction of a drug-selectable marker [248, 254]. *In vivo* imaging of mice was performed using the IVIS 200 imaging system to determined parasite loads in livers of infected mice 44 hours post-infection [264]. Mice were firstly shaved over the area of the liver, then anaesthetized and subcutaneously (s.c.) injected with 50µl of 50mg/ml D-luciferin substrate. Eight minutes after the injection of luciferin, mice were imaged for two minutes. Quantification of the bioluminescence signal was performed using the Living Image 4.2 image analysis software program. The readings were expressed as the total flux of photons emitted per second of exposure time.

2.6 Parasitology

2.6.1 Sporozoite production of chimeric parasites

Frozen *P. berghei* pRBC were thawed and 100-300 µl injected intra-peritoneal (i.p.) into a naive TO mouse. Five to six days later the parasitaemia and gametocytaemia were determined by analysing Geimsa stained thin blood films and addition of a drop of blood to exflagellation media enabled the analysis of exflagellation. Anaesthetized mice were placed onto pots of starved 4-7 day old female *Anopheles stephensi* mosquitoes for approximately 10-15 minutes. Mosquitoes infected with the chimeric *P. berghei* parasite were maintained at

19-23°C in a humidified incubator and fed on fructose solution. At approximately 21-23 days post-feed mosquito salivary glands were dissected to obtain infectious sporozoites in the appropriate cell culture media and homogenized on ice. Sporozoite numbers were counted using a haemocytometer under phase contrast.

2.6.2 Cryopreservation of blood stage parasites

Blood stocks of the different chimeric parasite lines/clones were cryopreserved and stored in liquid nitrogen. These blood stocks were obtained from infected mice by collecting 0.8-1 ml of blood by cardiac-puncture from a mouse with a parasitaemia of 5-10% and mixing with 1 ml of a glycerol/PBS solution (30% glycerol; v/v), containing 0.1 ml of Heparin stock-solution (200 I.U./ml), prior to aliquoting into cryotubes (Nunc) and snap freezing with liquid nitrogen.

2.6.3 Challenge of immunised mice with chimeric sporozoites

To test the efficacy of the liver-stage vaccines, vaccinated and naïve control mice groups were injected with 1000 sporozoites intra-venous (i.v.) into the lateral tail vein approximately eight days post-MVA boost. Mice were monitored from day five post-injection via thin blood films. Once parasite positive blood films had been confirmed on three consecutive days, mice were sacrificed. The parasitemia level from three blood smears allowed calculation of time to 1% parasitemia via linear regression. If thin blood films were negative fourteen days post-infection mice were classes as “protected” and were sacrificed.

2.6.4 Preparing Thin-blood Smears

Thin-blood smears were prepared on glass slides from a drop of blood obtained from the tail snip. The blood smear was allowed to air-dry, then fixed with methanol, and stained for 0.5-1 h with 5% Giemsa diluted in Milli-QH_2O. Slides

were then removed and allowed to air-dry at room temperature. The slide was viewed on a light microscope at 100x under oil immersion.

2.6.5 Statistical model for parasitaemia prediction

To predict the time to 1% blood-stage infection a linear regression modelling was used as described previously [182]. The logarithm to base 10 of the calculated percentage of parasitaemia was plotted against the time post-challenge and GraphPad Prism 5 statistical analysis software used for generating linear regression model on the linear part of the blood-stage growth curve. This approach has been previously used; because time to blood-stage parasitaemia reflects number of parasites erupting from the liver, provided there is no blood stage immunity [265].

2.7 Molecular Virology

2.7.1 Viral vector vaccines

• *P. falciparum* CSP (PfCSP) ChAd63 and MVA viral vector vaccines

The CSP sequence (PlasmoDB PF3D7_0304600) was synthesized by GeneArt and cloned into ChAd63 and MVA vectors by Dr. Sue Morris, Dr. Matthew Cottingham and Nick Edwards [266]. The sequence had two modifications, the addition of the tPA leader sequence and removal of 26 of the NANP repeats from the central region.

• *P. falciparum* TRAP (*Pf*TRIP) ChAd63 and MVA viral vector vaccines

The TRIP construct is based on *P. falciparum* 3D7 TRAP (PlasmoDB PF3D7_1335900). It was codon optimized for expression in human cells, contains the Kozak sequence and also had the same fifteen amino acids deleted as for ME-TRAP [267]. The predicted transmembrane helix and cytoplasmic

domains were also deleted. Dr. Matthew Cottingham designed the construct and cloned it into ChAd63 and MVA vectors.

• In this thesis, eight viral vector vaccines were kindly provided by a former DPhil student Rhea J. Longley. Rhea performed the cloning and the Viral Vector Core Facility at the Jenner Institute performed the transfection and purification of recombinant viruses. ChAd63 and MVA viral vector vaccines were generated for the following eight *P. falciparum* antigens: PfLSA1, PfLSA3, PfCelTOS, PfUIS3, PfLSAP1, PfLSAP2, PfETRAMP-5, PfFalstatin. While Rhea performed detailed immunological assessment as part of her thesis, challenge studies using these eight viral vector vaccines were a collaborative project and hence presented in this thesis.

• In this thesis, five new MVA viral vector vaccines were designed, cloned, transfected, and purified. While for the generation of the corresponding five ChAd63 viral vector vaccines; Ahmed M. Salman performed all the cloning and the constructs' preparations and the Viral Vector Core Facility at the Jenner Institute performed the transfection and purification of the recombinant ChAd63 viruses. The five novel viral vector vaccines were generated for the following *P. falciparum* antigens: PfHT, PfRP-L3, PfSPECT-1, PfSPECT-2 and PfB9.

2.7.2 Chimpanzee adenovirus (ChAd63) transfection and purification

Adenovirus vector preparation and transfection was carried out as described in J004a and J004b, respectively. Briefly, to expose the left and right viral ITRs to allow proper viral replication and packaging plasmid encoding adenovirus was linearized with PmeI restriction enzyme. 85µl linearised recombinant adenoviral plasmid was mixed with 215µl Opti-MEM®. 300µl of 1:10 lipofectamine in Opti-MEM® was then prepared and mixed with the 300µl of linearized plasmid,

followed by incubation of the resulting mixture for at least twenty minutes at room temperature. The DNA/lipid complexes mixture was then loaded onto flasks of pre-prepared T-REx™ 293 cells. The 293TREx cells are permissive for the synthesis of replication-incompetent adenoviruses as the cell line provides E1 transcripts *in trans*. Cells were incubated at 37°C, 5% CO2 in a humidified incubator and starting at 48 hours post-transfection their viability and cytophilic effect was monitored using microscope. Cells showing cytophilic effect were detached from the flask by gentle tapping. Recombinant adenovirus was purified using caesium chloride (CsCl) gradient as described in J005. Virus titre was quantified using plaque forming unit assay (pfu) as suggested in J006 and immunostaining of infected cell monolayers as described in J259. Full protocols are given in the Appendix section.

2.7.3 Recombination of MVA virus, Transfection and Purification

P. falciparum antigens were cloned into the MVA-mCherry plasmid (p3753) where the mCherry gene is present inside the TK locus. Approximately 80-90% confluency DF-1 cells or Chicken Embryo Fibroblasts (CEFs) (obtained from the Pirbright Institute, Compton, UK) were infected with parental MVA virus expressing GFP (Stock #1378), as outlined in J176. These cells were then transfected with the MVA-mCherry-[antigen] plasmid 90 minutes later, which enables homologous recombination to occur between the MVA virus and the plasmid. As the plasmid is circular, a single crossover event occurs resulting in a large unstable intermediate product containing the entire plasmid and MVA parental genome. This unstable product then resolves into either the recombinant MVA-mCherry-[antigen] or the parental MVA containing GFP. After 2-days incubation of the plasmid with the virus in DF-1 or CEFs, cells were sorted using a MoFlo cell sorter operated by Andrew Worth at the Jenner Institute Flow Sorting Facility, as described in J131. The unstable intermediate products expressing only mCherry were collected and the lysate used to infect

CEFs again. Successful recombinant MVAs containing the antigen were selected by repeated rounds of plaque picking assays as in J018, initially selecting mChery positive cells followed by repeating the plaque picking assay, followed by extraction and preparation of template recombinant MVA viral DNA using DNAReleasy kit (Anachem Ltd) as in J173 and then ID and purity PCR for analysis were performed as described in J079 to confirm the correct MVA viral vector vaccine recombination and the absence of the MVA-GFP parental virus contamination. The virus was then bulked up and purified as per J019, J208, J209 and J332 protocols. Titration (pfu) was performed as per J083.

2.8 Immunology

2.8.1 Laboratory animals

For experiments undertaken at Oxford University, female BALB/c, C57BL/6 and CD-1 mice, of at least six weeks of age, were purchased from Harlan, UK. All animal work was conducted in accordance with the UK Animals (Scientific Procedures) Act 1986 and approved by the University of Oxford Animal Care and Ethical Review Committee for use under Project License PPL 30/2889. For the generation of chimeric parasites performed at the Leiden University Medical Centre, female Swiss OF1 mice of six weeks of age were purchased from Charles River Laboratories. All animal work was approved by the Animal Experiments Committee of the Leiden University Medical Centre (DEC 12042). The Dutch Experiments on Animals Act was established under European guidelines (EU directive number 86/609/EEC regarding the Protection of Animals used for Experimental and Other Scientific Purposes).

2.8.2 Mice vaccination and immunization

Standard heterologous prime-boost immunization was applied in all the vaccination experiments unless otherwise mentioned in female BALB/c, CD1 or C57BL/6 mice. ChAd63-[antigen] prime vaccination was given intramuscularly (i.m.) in a single injection site in a total volume of 50µl. Approximately eight weeks later MVA-[antigen] boost vaccination was given i.m. in a single injection site in a total volume of 50µl. Adenovirus vectored vaccines were given at a dose of $1x10^8$ infectious units (ifu), whilst MVA vectored vaccines were given at $1x10^7$ plaque forming units (pfu) (**Figure 2.12)**.

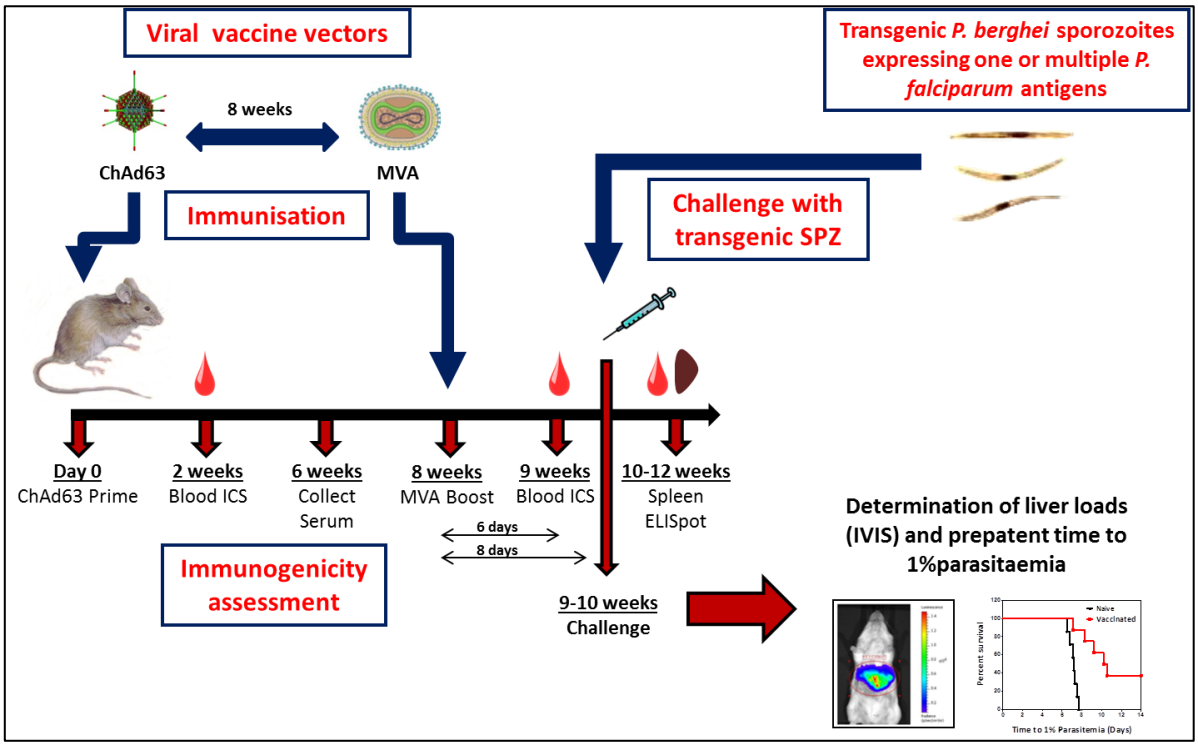

Figure 2.12 Immunisation with *P. falciparum* vaccine and protective efficacy testing.
The novel *P. falciparum* vaccine candidate antigens have been incorporated into a virally vectored sub-unit *P. falciparum* malaria vaccines (both ChAd63 and MVA) targeting the liver-stage of infection. In parallel the same *P. falciparum* antigens have been expressed in *P. berghei* by generating a corresponding *P. berghei* transgenic parasite to be used in a novel challenge model to assess the efficacy of these new *P. falciparum* pre-erythrocytic vaccine candidates in mice. This had permitted an initial screening of several vaccine candidates and considering the selection of the most promising ones to be taken to further clinical trials. To set up the challenge model, for each vaccine candidate, mice were vaccinated i.m. with 10^8 ifu of ChAd63-Pf candidate as prime followed eight weeks later by 10^7 pfu of MVA *P. falciparum* candidate as boost vaccinations. Blood was taken two weeks after the prime and again one-week after the MVA-boost vaccination to assess the immunogenicity and both CD8+ and CD4+ cytokine responses by intra-cellular staining (ICS), after stimulation for six hours with a pool of overlapping peptides from the appropriate antigen. Eight days after the MVA boost each vaccinated and control group has been challenged with its corresponding transgenic *P. berghei* sporozoites expressing the cognate *P. falciparum* antigen. Mice were monitored daily from day five post challenge to enable calculation of the time to 1% parasitaemia. Mice that were slide negative till day 14 post-challenge were considered sterilely protected, which in turn measures the protective efficacy for each vaccine after the ChAd63-MVA vaccination strategy.

2.8.3 Peptides

Mixtures of overlapping peptides representing the different antigens were used in the Intra-cellular Staining assays (ICS) at final concentration of 5µg/ml. In the *ex-vivo* IFN-γ ELISpot assay; a final individual peptide concentration of 10µg/ml was used for the immunodominant peptides screening. Individual peptide stock was reconstituted in DMSO at a concentration of 5-100mg/ml depending on the solubility. Peptides were subsequently combined into a total pool for use in the cellular assays.

Crude 20mer peptides overlapping by ten amino acids for nine *P. falciparum* 3D7 proteins were kindly provided by a former PhD student at the Jenner Institute Rhea J Longley. These nine proteins were synthesized for the entire protein sequence; PfLSA1, PfLSA3, PfUIS3, PfLSAP1, PfLSAP2, PfETRAMP-5, PfFalstatin, PfCSP, and PfTRAP. While crude 15mer peptides overlapping by ten amino acids for the entire sequence of *P. falciparum* 3D7 CelTOS are kindly provided by Dr. Simon Draper.

Two or three crude 14-15mer peptides per protein of predicted CD8 epitopes containing peptides for five different new *P. falciparum* antigens were synthesized to be used in the cellular assays to assess the immunogenicity of these novel *P. falciparum* vaccine candidates *in vitro* **(Table 2.6).** These peptides were reconstituted as stated above. CD8 epitopes were predicted for five *P. falciparum* 3D7 antigens; PfHT, PfRP-L3, PfSPECT-1, PfSPECT-2 and PfB9 using the servers MIMOTOPES: (http://www.mimotopes.com/peptideLibraries.asp), IEDB [268] (http://tools.immuneepitope.org/main/html/tcell_tools.html) and SYPEITHI [269] (http://www.syfpeithi.de/index.html). These individual peptides were synthesized and ordered separately from Mimotopes.

Table 2.6 Amino acid sequence for the predicted $CD8^+$ epitopes (peptides) used to generate the 14-15mer peptides per protein for the five novel *P. falciparum* antigens; PfHT, PfRP-L3, PfSPECT-1, PfSPECT-2 and PfB9

Peptide Name	*Amino Acid Sequence*	*FractionMass*	*PurityMS*
PfB9-1	PSYDFNDLLHEKKN	1.8	67.6
PfB9-4	KNGNNHNDNNNNNQN	1.3	58.3
PfHT-2	EWCKGEKDRLNCSN	1.4	53.2
PfHT-4	KDICSENEGKKNGKS	1.7	49.3
PfRPL3-1	VGYRETPKGLRILS	1.3	51.4
PfRPL3-2	LRILSTVWANHVSD	1.5	40.3
PfSPECT1-1	KDDVEDDSKNEIVD	1.3	43
PfSPECT1-3	DDFKNNLSNYETEQN	1.3	78.1
PfSPECT1-4	LNNDLSKNNNFSLNT	1.3	55.7
PfSPECT2-1	LSTLQPVNGWIRKE	1.7	44.8
PfSPECT2-2	KRLNFNGDQKDEDN	1.7	70.4
PfSPECT2-4	SSNDNNDEENEEQDD	1.3	37.9

2.8.4 Splenocyte preparation

Mice were sacrificed by cervical dislocation and spleens were dissected and collected in sterile D-PBS. Individual spleens were subsequently crushed in 5ml PBS using the flat end of a 5ml syringe plunger. Single cell suspensions were prepared by passaging splenocytes through a 70µm cell strainer (Falcon 352350) into a 50ml tube and the volume was completed to 15ml with PBS prior to centrifugation at 500 g for 5 minutes. To remove erythrocytes, supernatants were discarded and cell pellets resuspended in 5ml ACK (Ammonium Chloride Potassium) lysis buffer with gentle shaking for 3-5 minutes at room temperature before addition of 25ml PBS to stop the reaction. Splenocytes were centrifuged again and the resulting cell pellets re-suspended in 5ml complete α-MEM medium and the ghost (clump of cell debris) was removed. Total number of splenocytes was determined by CASY counter (Schärfe Systems, Germany) and adjusted to $1x10^7$ cells per ml of complete medium for the use in *ex-vivo* IFN-γ ELISPOT assay.

2.8.5 Ex-vivo IFN-γ Spleen ELIspot assay

All ELISpot reagents were supplied in a mouse IFNγ ELISpot kit from Mabtech. MAIP plates were coated with anti-mouse-IFN-γ mAb AN18 diluted to 5µg/ml in carbonate-bicarbonate buffer and incubated overnight at 4°C. Splenocytes were prepared as described in **(section 2.8.4)** and plates were blocked with 100µl complete α-MEM medium for ≥ 1 h at 37°C. Splenocytes were diluted to a standard concentration of $1x10^7$ cells per ml, and then 50µL splenocytes (containing $0.5x10^6$ cells) were plated in duplicate and serially diluted two-fold down the blocked plates. 50µL of peptide diluted in complete α-MEM medium to 10µg/ml final concentration were added to stimulated wells and complete medium alone added to control wells. Plates were incubated for 18-20 hours at 37°C 5% CO_2 in a humidified incubator. Plates were washed 6 times with PBS and incubated with 50µl per well of for 2 hours at room temperature with biotinylated rat anti-mouse-IFN-γ mAb R46A2 diluted to 1µg/ml (1/1000) in PBS; followed by washing 6 times with PBS and incubation for 1 hours at room temperature with 50µl per well of streptavidin alkaline phosphatase polymer diluted to 1µg/ml (1/1000) in PBS. Plates were washed 6 times with PBS, and then spots developed by adding 50µl of BioRad AP conjugate development buffer, and counted using an ELISPOT reader (Autoimmun Diagnostika (AID), Strassberg, Germany). Results are expressed as spot forming units (SFU) per million of PBMCs. Background responses in media-only wells were subtracted from those measured in peptide-stimulated wells.

2.8.6 Collection and preparation of peripheral blood mononuclear cells (PBMCs)

Six drops of blood were collected from lateral tail vein into 200 µl 10mM EDTA in PBS. Approximately 1 ml of ACK lysis buffer was added to the blood, followed immediately by thorough vortexing and centrifugation at 1500 g for 4 minutes. The cell pellets were re-suspended in 1 ml ACK lysis buffer and again centrifuged

at 4000 rpm for 4 minutes prior to resuspending the pellets in 320 µl complete α-MEM media.

2.8.7 PBMC Intracellular Cytokine Staining (ICS)

After PBMC processing with ACK lysis buffer and resuspension in complete α-MEM, 150 µl of PBMC cells were incubated with 50µl of stimulatory or un-stimulatory mixtures in a 96 well U bottom plate. The stimulatory mixture contained a peptide pool specific to the antigen vaccinated with (final concentration of 5µg/ml) plus 1µl/ml Golgi Plug (BD Biosciences). The unstimulatory mixture contained media with the same concentration of Golgi Plug, but no peptide. Plates were incubated for 6 hours at 37°C then stored at 4°C until the following day. When staining cells for CD107a expression, this antibody was added at the same time as the peptide at a concentration of the following plates were washed with PBS-BSA (0.5% BSA and 0.05% sodium azide, Sigma) and then stained with 50µl 1/50 Fc Block (CD16/CD32), 1/100 CD4 ef450 and 1/200 CD8 PerCPCy5.5 for 30 minutes at 4°C. Cells were washed followed by fixation with 4% paraformaldehyde (10% Neutral Buffered Formalin, Sigma) for five minutes at 4°C followed by washing twice with buffer containing saponin (Perm/Wash – BD Biosciences) and by staining with 50µl 1/100 TNFα FITC, 1/100 IL-2 PE and 1/100 IFNγ APC for 30 minutes at 4°C. Cells were then washed three times with Perm/Wash followed by two washes with PBS-BSA and finally re-suspended in 100µl PBS-BSA for acquisition on the flow cytometer. A typical gating strategy is shown in (**Figure 2.13)**; subsequent analysis simply subtracts the un-stimulated wells from the stimulated wells.

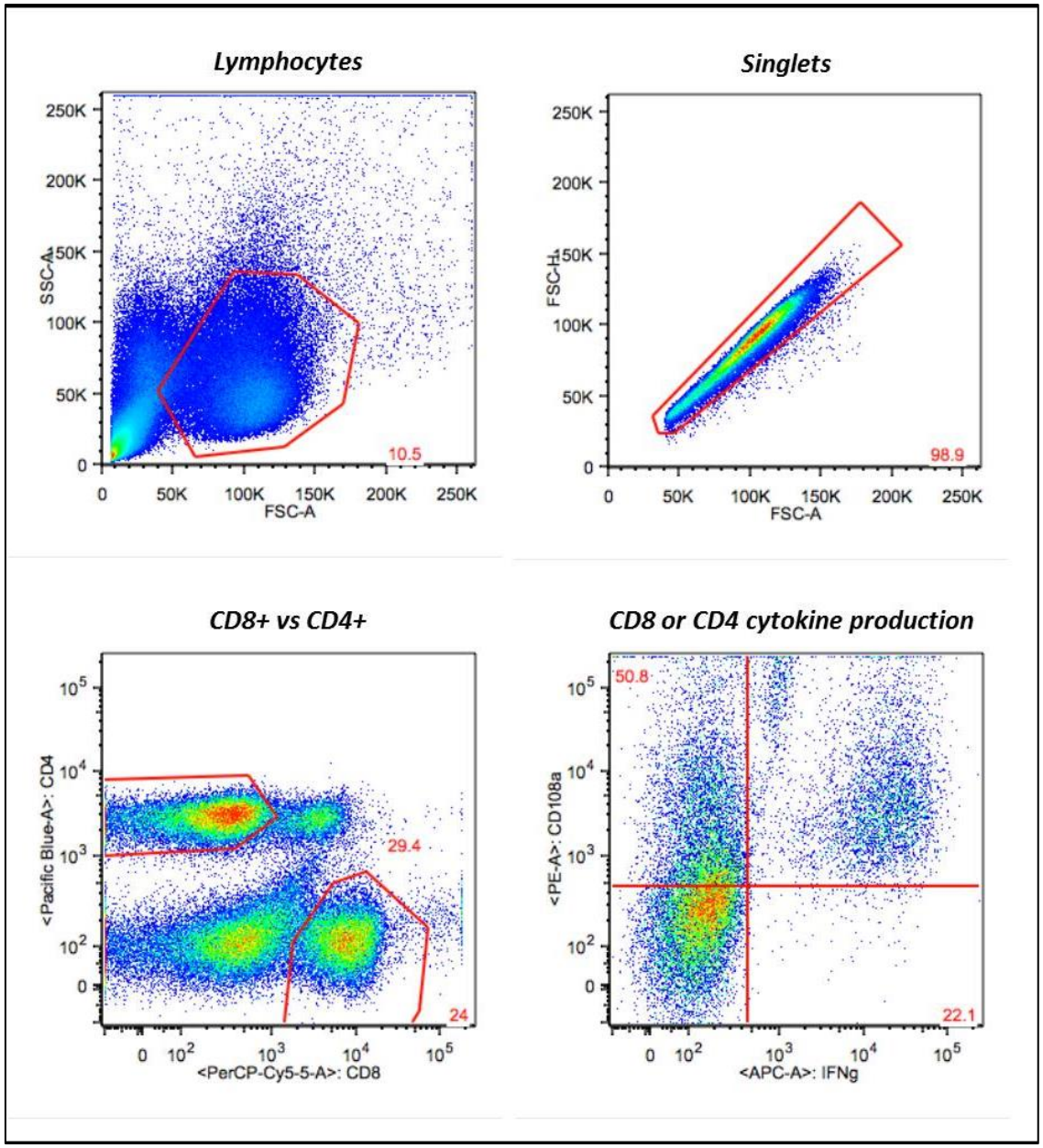

Figure 2.13 The gating strategy applied for PBMC ICS. First the lymphocytes are selected, followed by only single cells. Those cells are then split into CD8+ or CD4+. Within these subsets, then cytokines IFNγ, TNFα, IL-2 and the cell sub-set CD107a can be analysed.

2.8.8 In vivo CD8+ and CD4+ T-cell depletions

The T-cell depletions were performed *in vivo* to show the contribution of both T cells subsets in protection from malaria. T cells were depleted using monoclonal antibodies (mAbs) which were purified by protein G affinity chromatography columns from hybridoma culture supernatants. Anti-CD4 GK1.5 (rat IgG2a) and anti-CD8 2.43 (rat IgG2a) were sterile filtered and diluted in sterile PBS. Normal

rat IgG (nRatIgG) was purchased from Sigma and purified by the same method. Purifications were kindly performed by Julie Furze. For depletion of $CD4^+$ or $CD8^+$ T cells, mice were injected i.p. with 100µg of the relevant mAb on days −2 and −1 before and on the day of challenge. Control mice were treated in the same way. *In vivo* T cell depletion for both $CD4^+$ and $CD8^+$ T cells were confirmed by flow cytometry of surface-stained PBMCs from depleted and control mice on day +4 after challenge using 1/100 anti-CD4-FITC clone RM4-4, 1/200 anti-CD8-PerCPCy5.5 clone 53-6.7 and 1/50 anti-CD3ε-APC.

2.9 Statistical Analysis and Software

Statistical analysis was performed using GraphPad Prism version 5 (Graphpad, USA) unless indicated otherwise. Prior to statistical analysis to compare two or more populations, the Kolmogorov-Smirnov test for normality was used to determine whether the values followed a Gaussian distribution. An unpaired t-test was employed to compare two normally distributed groups, whereas Mann-Whitney rank test was used for comparing two non-parametric groups. Correlations were tested using Spearman's rank correlation on nonparametric. A two-way ANOVA with Bonferroni post-test for multiple comparisons was used to explore the effect of two variables. Survival and protective efficacy to in challenge experiments was presented using Kaplan-Meier curves and significance tested using the Log-Rank (Mantel-Cox) Test. The value of $p<0.05$ was considered statistically significant (*$p<0.05$, **$p<0.01$, **$p<0.001$, and ***$p<0.001$). Flow cytometry experiments gating and data analysis were performed by FlowJo™ Software (Version 8.8.7). For the *in vivo* imaging experiments the quantification of the bioluminescence signal was performed using the Living Image 4.2 image analysis software program. For image processing and microscopic image analysis ImageJ Software was used.

Chapter 3

Comparison of transgenic *P. berghei* parasites expressing either replacement or additional *P. falciparum* genes as challenge models.

3 Comparison of transgenic *P. berghei* parasites expressing either replacement or additional *P. falciparum* genes as challenge models.

3.1 Introduction

Development of a vaccine against *P. falciparum* malaria has been impaired by the lack of a suitable pre-clinical challenge models. Rodent malaria parasites are used as models for human malaria and in particular to aid drug-discovery and vaccine development. These models are used to study drug action and to identify targets for protective immune responses, *in vivo*. Although a high level of orthology exists between the genes of *Plasmodium* species that infect rodents and humans [232, 233] critical differences often exist in the sequence and structure between the encoded proteins. In addition, human malaria parasites (HMP; e.g. *P. falciparum* and *P. vivax*) express genes that are absent from rodent parasite genomes. These genetic differences complicate the analysis of drugs/inhibitors or immune factors in rodent models and the effective translation of findings in model systems to human malaria. 'Humanizing' rodent parasites by introducing HMP genes into rodent malaria parasite can help to circumvent problems of interpreting data arising from structural differences between functional HMP and rodent malaria parasite orthologs. In addition, it increases the possibilities of analyzing HMP-specific proteins, *in vivo* [270].

Here I describe methods to generate 'humanised' rodent malaria parasites in the *P. berghei (Pb)* model. Efficient methods exist for *P. berghei* genetic modification including a recently described method for GIMO-transfection (Gene Insertion-Marker Out; [245] that greatly simplifies and speeds up the generation of transgenic parasites expressing heterologous proteins, free of drug-selection marker genes. Two different genetic modifications are described here resulting in two types of transgenic parasites that express *P. falciparum* proteins, namely Replacement Gene and Additional Gene.

In Replacement Gene (RG) mutants the coding sequence of a *P. berghei* gene is replaced with the CDS of the orthologous *P. falciparum* gene, in a two-step GIMO transfection. First, the *P. berghei* gene is deleted by double cross-over homologous recombination with a construct having the *hdhfr::yfcu* SM flanked by 5' untranslated region (UTR; containing the gene promoter) and 3' UTR (containing the transcriptional terminator sequences) of the *P. berghei* gene as gene targeting regions (TRs), thereby creating an 'GIMO locus'. Next, this GIMO locus is replaced by *the P. falciparum* gene expression cassette with the *P. falciparum* homolog flanked by the same 5' UTR and 3' UTR regions of the orthologous *P. berghei* gene. This method creates transgenic parasites expressing a *P. falciparum* gene free of selectable marker (SM).

In Additional Gene (AG) chimeric parasites mutants the *P. faciparum* gene is introduced as into a silent/neutral locus of the Pb genome under the control of *Pbuis4* promoter (PBANKA_050120) which is a strong and specific sporozoite and liver-stage promoter. This method has the advantage over the replacement method when a functional ortholog of the *P. falciparum* gene is absent in *P. berghei* parasite genome or when the *P. berghei* gene is essential and its orthologous *P. falciparum* gene can't complement its function. The absence of SM in the RG and AG chimeric parasites facilitates rapid additional genetic modifications in these lines, for example the introduction of additional HMP genes or reporter genes encoding fluorescent or luminescent proteins.

This Chapter describes the generation of RG and AG transgenic *P. berghei* parasites for two different *P. falciparum* antigens that have homologs in *P. berghei*; *PfCelTOS* and *PfCSP.* Specifically, RG transgenic parasites were generated by replacing the *P. berghei CelTOS* or *CSP* gene coding sequences with those from the corresponding *P. falciparum* genes; consequently these coding sequence of these *P. falciparum* genes are expressed by the *P. berghei* transcriptional control elements (i.e. promoter and transcriptional terminator) of *PbCelTOS* and *PbCSP* respectively. In parallel, two AG chimeric parasites were

generated to express the Pf*CelTOS* and Pf*CSP* gene coding sequences under the control of Pb*uis4* promoter (5' UTR) and transcriptional terminator (3'UTR). The availability of these parasites enabled us to compare AG and RG chimeric parasites as challenge models, in immunization-challenge studies. All four chimeric parasite versions were used to challenge naïve and (PfCelTOS or PfCSP) vaccinated mice with to determine whether the different method of expressing the *P. falciparum* antigen (either in RG and AG parasite) affected the challenge models ability to establish vaccine efficacy.

3.2 Results

3.2.1 Generation of maker-free *P. berghei* additional gene [AG] chimeric parasites expressing *PfCelTOS* or *PfCSP*

AG chimeric parasites generation, genotyping, phenotyping and fitness analysis including these two AG parasites expressing PfCelTOS or PfCSP genes will be described in detail in **chapter-4**.

3.2.2 Generation of maker-free *P. berghei* replacement gene [RG] chimeric parasites expressing PfCelTOS or *PfCSP*

To generate RG chimeric parasites, GIMO Deletion construct (construct 1) was generated **(see section 2.3.2)** by cloning 5' and 3' targeting regions (TRs) of the *PbCelTOS* or *PbCSP* genes (these regions include the *Pb* gene promoter and transcriptional terminator sequences) into the cloning sites of the basic construct pL0034, upstream and downstream of the *hdhfr::yfcu* SM, respectively. The generated construct was linearized using appropriate restriction enzymes outside of the 5' and 3' TRs. The first transfection with **construct 1** (**GIMO deletion Construct**) aimed to replace the endogenous *P. berghei* gene with the selectable marker. Construct 1 was transfected into a standard reporter parasite line *Pb*GFP-Luccon (676m1cl1) to generate a specific *Pb* gene deletion GIMO mother line that also encodes the GFP-Luciferase

expression cassette. Transfection and selection with pyrimethamine resulted in selection of parasites in which the Pb CDS was replaced with the *hdhfr::yfcu* SM cassette. Cloning resulted in generation of *Pb*ANKA- *ΔCelTOS GIMO mother-line (*2217 cl1) and *Pb*ANKA- *ΔCSP GIMO* mother-line *(*2151 cl1) (for genotyping see **section 3.2.3**). Subsequently these parasites were transfected with **construct 2 (GIMO Insertion construct).** This construct was generated based on Construct 1, replacing the hdfhr::yfcu SM cassette in Construct 1 with the orthologous *P. falciparum CelTOS* or *CSP* CDS sequence, which was PCR amplified from *P. falciparum* gDNA, resulting a *P. falciparum* gene expression construct under the control of the 5' and 3' regulatory elements of the Pb ortholog. The generated construct 2 was linearized using appropriate restriction enzymes outside of the 5' and 3' TRs and a second transfection was performed in the gene-deletion GIMO mother line with construct 2 resulting in a replacement of the *hdhfr::yfcu* SM cassette with the orthologous P. falciparum CelTOS or CSP gene (**see Figure 3.1).** Cloning resulted in the parasite lines *PbANKA-PfCelTOS(r)*$_{PbCelTOS}$ *(*2258cl2) and *PfCSP(r)*$_{PbCSP}$ *(*2257cl2) (for genotyping see **section 3.2.3**).

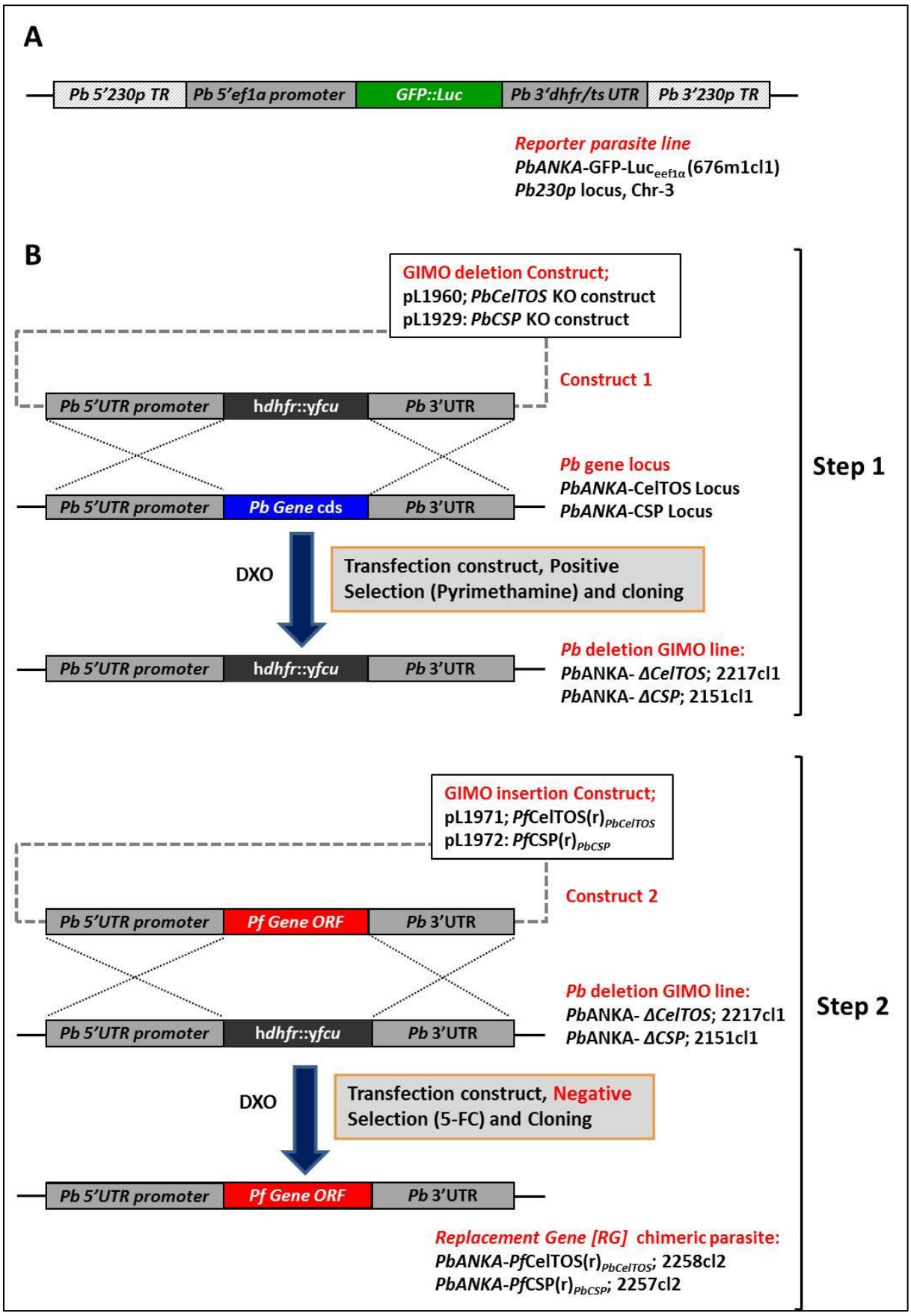
A
Pb 5'230p TR
Pb 5'ef1a promoter
GFP::Luc
Pb 3'dhfr/ts UTR
Pb 3'230p TR
Reporter parasite line
PbANKA-GFP-Luc$_{eef1\alpha}$(676m1cl1)
Pb230p locus, Chr-3
B
GIMO deletion Construct;
pL1960; PbCelTOS KO construct
pL1929: PbCSP KO construct
Construct 1
Pb 5'UTR promoter
hdhfr::yfcu
Pb 3'UTR
Pb gene locus
PbANKA-CelTOS Locus
PbANKA-CSP Locus
Pb 5'UTR promoter
Pb Gene cds
Pb 3'UTR
DXO
Transfection construct, Positive Selection (Pyrimethamine) and cloning
Pb deletion GIMO line:
PbANKA- ΔCelTOS; 2217cl1
PbANKA- ΔCSP; 2151cl1
Step 1
GIMO insertion Construct;
pL1971; PfCelTOS(r)$_{PbCelTOS}$
pL1972: PfCSP(r)$_{PbCSP}$
Construct 2
Pb 5'UTR promoter
Pf Gene ORF
Pb 3'UTR
Pb deletion GIMO line:
PbANKA- ΔCelTOS; 2217cl1
PbANKA- ΔCSP; 2151cl1
DXO
Transfection construct, Negative Selection (5-FC) and Cloning
Replacement Gene [RG] chimeric parasite:
PbANKA-PfCelTOS(r)$_{PbCelTOS}$; 2258cl2
PbANKA-PfCSP(r)$_{PbCSP}$; 2257cl2
Step 2

Figure 3.1 Generation of Replacement Gene (RG) chimeric parasite expressing *PfCelTOS* or *PfCSP*.

A. Schematic representation of the reporter *Pb*ANKA parasite line *PbGFP-Luc*$_{eef1\alpha}$ (676m1cl1) which used to generate the replacement gene [RG] chimeric parasites. *It* expresses a fusion protein of GFP and firefly luciferase (LUC-IAV) under the constitutive *Pbeef1a* promoter and is selectable marker (SM) free. The reporter-cassette is integrated into the neutral *230p* locus in chromosome-3.

B. Schematic representation describing the transfections and the generation steps of replacement gene [RG] chimeric parasites; where the *PbCelTOS or PbCSP* target gene (TG) is replaced with its orthologous *PfCelTOS* or *PfCSP* gene of the human malaria parasite. 1st step: The **GIMO Deletion construct** (**Construct 1; pL1960 or Pl1929**) is used to replace the *PbCelTOS or PbCSP* gene with the positive/negative selectable maker (h*dhfr::*y*fcu*) cassette, resulting in the generation of the GIMO line (***Pb*ANKA-*ΔCelTOS*; 2217cl1, or *Pb*ANKA- *ΔCSP*; 2151cl1, respectively**) after positive selection with pyrimethamine. **Construct 1** targets the *P. berghei* gene by double cross-over homologous recombination. After genotyping and confirming the correct construct integration, these lines are cloned. 2nd step: The **GIMO insertion construct** (**Construct 2; pL1971; *Pf*CelTOS(r)$_{PbCelTOS}$, or pL1972: *Pf*CSP(r)$_{PbCSP}$, respectively**) is used to replace the selectable maker (SM) in the GIMO line with *PfCelTOS or PfCSP* CDS, under negative (5-FC) selection, resulting in ***PbANKA-Pf*CelTOS(r)$_{PbCelTOS}$; 2258cl2, or *PbANKA-Pf*CSP(r)$_{PbCSP}$; 2257cl2, respectively. Construct 2** integrates by double cross-over homologous recombination using the same targeting regions (TRs) employed in construct 1, resulting in the introduction of *P. falciparum* gene under the control of its orthologous *P. berghei* gene promoter and transcriptional terminator sequences.

3.2.3 Genotype analysis of Replacement Gene [RG] chimeric parasites and their intermediate GIMO mother-line knock out chimeric parasites.

3.2.3.1 Southern analysis of chromosomes (chrs) separated by pulsed-field gel electrophoresis (PFGE)

To confirm the correct integration of the DNA construct in the chimeric *P. berghei* parasite Southern analysis was performed **(2.4.3 section)** using two different sets of probes to recognize the absence or the presence of the selectable marker or the transgene in the chimeric parasites. The first probe mixture consists of a mixture of two probes: one recognizing h*dhfr* in the SM and a control probe recognizing chr-5. The second probe mixture recognizes the

3'UTR *Pbdhfr/ts* of the SM of the integrated construct which also hybridizes to the endogenous *Pbdhfr/ts* on chr-7.

Southern analysis of *Pb*ANKA- *ΔCelTOS GIMO mother-line (*2217 cl1) showed correct integration of the DNA construct into the target *P. berghei CelTOS (PBANKA_143230)* gene locus in Chr-14. Chromosomes are hybridized using a probe recognizing the 3'UTR *Pbdhfr/ts* of the SM of the integrated construct which hybridized to Chr-3 because of the presence of the GFP-Luc cassette with *3'UTR Pbdhfr/ts* to hybridized Chr-14, confirming the correct integration of the SM cassette into the right locus and replacing *PbCelTOS* gene with the SM and also hybridizes to the endogenous *Pbdhfr/ts* on Chr. 7 (**Figure 3.2 A**).

The correct integration of the *PfCelTOS* expressing construct into the GIMO locus was confirmed by showing the removal of the h*dhfr::*y*fcu* SM cassette in the cloned RG chimeric parasite line *PbANKA-PfCelTOS(r)*$_{PbCelTOS}$ *(*2258cl2) when the Southern blot was hybridized with a mixture of two probes: one recognizing h*dhfr* which showed no signal and a control probe recognizing chr. 5 which showed a positive signal (**Figure 3.2 B**).

In *Pb*ANKA- *ΔCSP GIMO* mother-line *(*2151 cl1); the correct integration of the *SM* in the right locus in Chr-4 and replacing the endogenous *PbCSP* gene (PBANKA_040320) was confirmed by using the 3'UTR *Pbdhfr/ts* probe which hybridized to the GFP-Luc cassette on Chr-3 *(see* **Figure 3.2 C***) and* hybridized to Chr-4 confirming the correct integration of the SM cassette into the right locus and replacing *PbCSP* gene with the SM and also hybridizes to the endogenous *Pbdhfr/ts* on Chr. 7. The correct integration of the *SM* also confirmed by using a mixture of two probes ***hdhfr/chr.5.***

The correct integration of the *PfCSP* expressing construct into the GIMO locus was confirmed by showing the removal of the h*dhfr::*y*fcu* SM cassette in the cloned chimeric parasite line ***PbANKA-PfCSP(r)***$_{PbCSP}$ (2257 cl2). The Southern blot

was hybridized with a mixture of two probes: one recognizing h*dhfr* and a control probe recognizing chr. 5. As an additional control (ctrl), parasite line 2117cl1 was used with the *hdhfr::yfcu* SM integrated into chr. 3 **(Figure 3.2 D).**

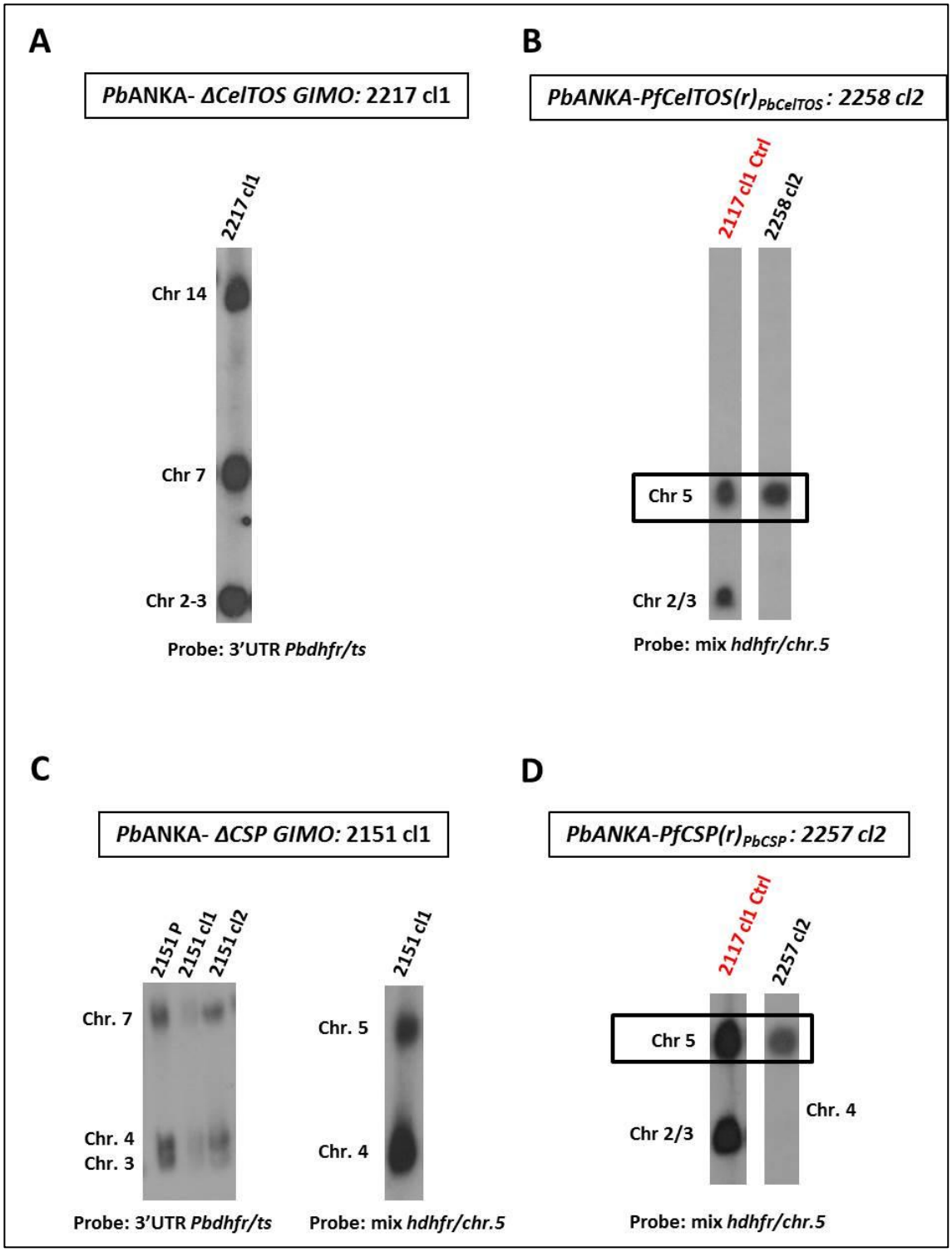

Figure 3.2 Genotype analysis of Replacement Gene [RG] chimeric parasites and their intermediate GIMO mother-line knock out chimeric parasites using Southern analysis of chromosomes (chrs) separated by pulsed-field gel electrophoresis (PFGE) to confirm integration of the DNA construct in the correct chromosome in the chimeric *P. berghei* parasite.

Two different probes were used to recognize the absence or the presence of the selectable marker or the transgene in the chimeric parasites. The first probe mixture consist of a mixture of two probes: one recognizing h*dhfr* in the SM and a control probe recognizing chr-5. While the second probe mixture recognizing the 3'UTR *Pbdhfr/ts* of the SM of the integrated construct which also hybridizes to the endogenous *Pbdhfr/ts* on chr-7.

A. Pb*ANKA- *ΔCelTOS GIMO:* 2217 cl1.** Southern analysis of PFGE-separated chrs to confirm integration of the DNA construct into the target *P. berghei CelTOS (PBANKA_143230)* gene locus in Chr-14 in the cloned parasites selected in step 1 of the transfection protocol to generate generation a Replacement Gene [RG] chimeric parasite. The chrs are hybridized using a probe recognizing the 3'UTR *Pbdhfr/ts* of the SM of the integrated construct which hybridized Chr-3 because of the presence of the GFP-Luc cassette with 3'UTR *Pbdhfr/ts (see* **3.2A),* hybridized Chr-14 which confirms the corrected integration of the SM cassette into the right locus and replacing *PbCelTOS* gene with the SM and also hybridizes to the endogenous *Pbdhfr/ts* on Chr. 7.

B. *PbANKA-PfCelTOS(r)*$_{PbCelTOS}$ *: 2258 cl2.* The correct integration of the *PfCelTOS* expression construct into the GIMO locus was confirmed by showing the removal of the h*dhfr::*y*fcu* SM cassette in the cloned chimeric parasite line (2258cl2). The southern blot is hybridized with a mixture of two probes: one recognizing h*dhfr* and a control probe recognizing chr-5. As an additional control (ctrl), parasite line 2117cl1 is used with the h*dhfr::*y*fcu* SM integrated into chr-3.

C. *Pb*ANKA- *ΔCSP GIMO:* 2151 cl1. The correct integration of the *SM* in the right locus in Chr-4 and replacing the endogenous *PbCSP* gene (PBANKA_040320) was confirmed by using the 3'UTR *Pbdhfr/ts* probe which hybridized Chr-3 because of the presence of the GFP-Luc cassette with 3'UTR *Pbdhfr/ts (see* **3.2C***),* hybridized Chr-4 which confirms the corrected integration of the SM cassette into the right locus and replacing *PbCSP* gene with the SM and also hybridizes to the endogenous *Pbdhfr/ts* on Chr. 7. The correct integration of the SM; also confirmed by using a mixture of two probes ***hdhfr/chr.5.***

D. *PbANKA-PfCSP(r)*$_{PbCSP}$ *: 2257 cl2.* the correct integration of the *PfCSP* expression construct into the GIMO locus was confirm by showing the removal of the h*dhfr::*y*fcu* SM cassette in the cloned chimeric parasite line (2257 cl2). The southern blot is hybridized with a mixture of two probes: one recognizing h*dhfr* and a control probe recognizing chr-5. As an additional control (ctrl), parasite line 2117cl1 is used with the h*dhfr::*y*fcu* SM integrated into chr-3 *(see* **3.2D***)*.

3.2.3.2 Diagnostic integration (confirmation) PCR

Different primers were designed to check the right 5' and 3' integration, the right band sizes for the transfected *P. falciparum* gene expression cassette, and the absence of *P. berghei* gene homologue and *hdhfr::yfcu* selectable marker RG parasite lines; *PbANKA-PfCelTOS(r)*$_{PbCelTOS}$ (2258 cl2) and *PbANKA-PfCSP(r)*$_{PbCSP}$ *(2257 cl2)*. Positive control PCR reactions were used to test the validity of the used primers and to confirm the absence of the knocked out *P. berghei* genes (*PbCelTOS* and *PbCSP*) and selectable marker from the RG chimeric parasites were also checked. Diagnostic PCR analysis confirmed the correct integration of the *P. falciparum* GIMO Insertion construct in the chimeric parasite and shown the absence of the homologous *P. berghei* gene and hdhfr::yfcu marker (**Figure 3.3**). Expected PCR bands' sizes are listed in the tables beneath the gels, while, the used primers' sequences are shown in **Table 2.3**.

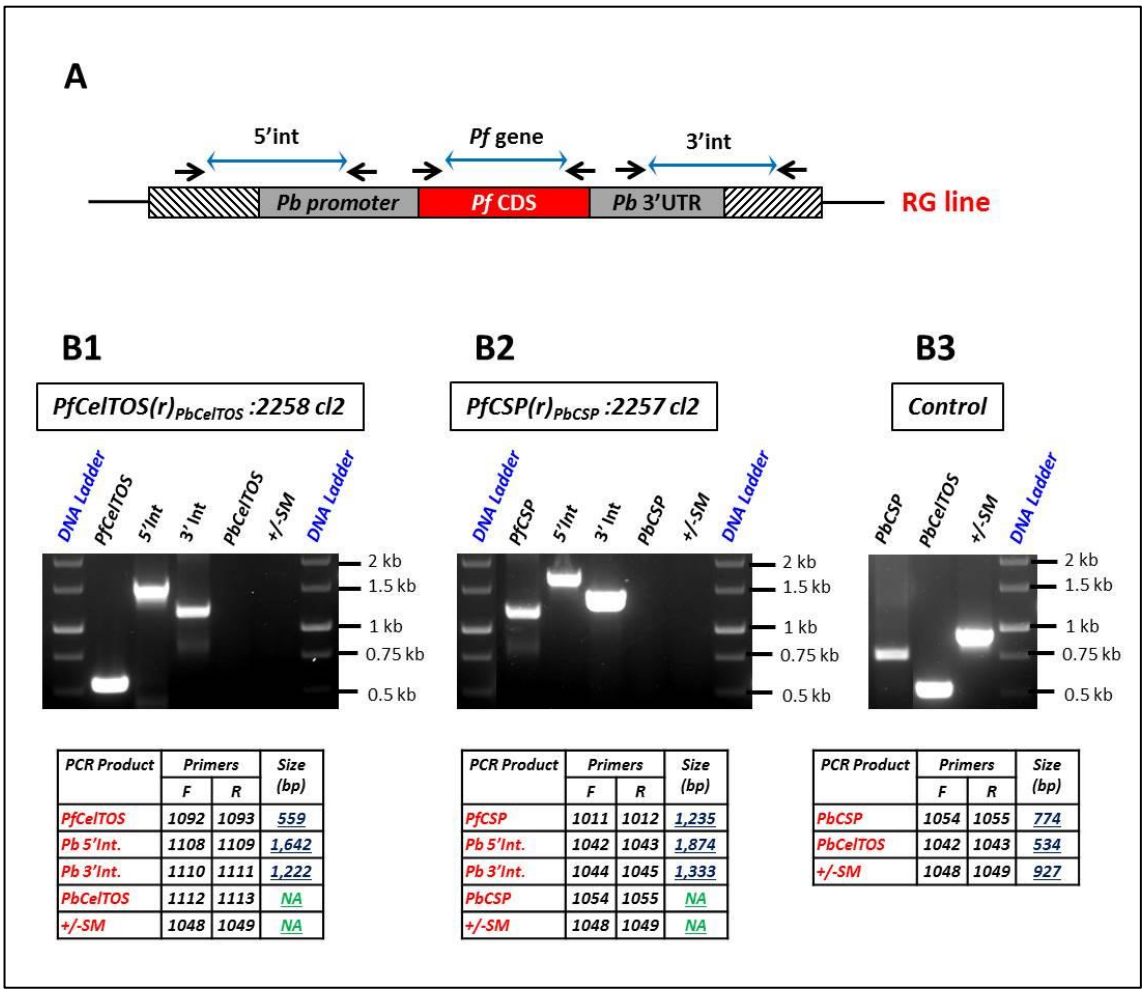

PCR Product	Primers		Size (bp)
	F	R	
PfCelTOS	1092	1093	559
Pb 5'Int.	1108	1109	1,642
Pb 3'Int.	1110	1111	1,222
PbCelTOS	1112	1113	NA
+/-SM	1048	1049	NA

PCR Product	Primers		Size (bp)
	F	R	
PfCSP	1011	1012	1,235
Pb 5'Int.	1042	1043	1,874
Pb 3'Int.	1044	1045	1,333
PbCSP	1054	1055	NA
+/-SM	1048	1049	NA

PCR Product	Primers		Size (bp)
	F	R	
PbCSP	1054	1055	774
PbCelTOS	1042	1043	534
+/-SM	1048	1049	927

Figure 3.3 Genotype analysis; Diagnostic PCR.

A. Schematic representation of the *P. berghei* locus that contains the *P. falciparum* CDS replacing its endogenous *P. berghei* orthologue in the RG transgenic *P. berghei* parasites. In the RG transgenic parasite the *P. falciparum* gene coding sequence is expressed under control of the transcriptional regulatory sequences of its *P. berghei* orthologue (Pb5' promoter and Pb3'UTR). Black arrows: location of PCR primers used for diagnostic PCR-analysis **(see B).** Primers sequences used are shown in **Table 2.3**, while the expected PCR product sizes and the primer numbers are listed in the table below the Agarose gel images in **B.**

B. In the diagnostic (confirmation) PCR; different primers have been designed to check the right 5' & 3' integration, the right band sizes for the transfected *P. falciparum* gene expression cassette, and also the absence of *P. berghei* gene homologue and *hdhfr::yfcu* selectable marker from the successfully transfected replacement gene [RG] Chimeric parasite lines. **(B1)** *PbANKA-Pf*CelTOS(r)$_{PbCelTOS}$; 2258 cl2. **(B2)** *PbANKA-Pf*CSP(r)$_{PbCSP}$; 2257 cl2. (**B3)** Positive control PCR reactions to test the validity of the used primers to confirm the absence of the knocked out *P. berghei* genes (*Pb*CelTOS and *Pb*CSP) and selectable marker from the chimeric parasites. The number of the used primers and expected PCR band sizes are listed in the tables below the PCR image. Diagnostic PCR analysis confirmed the correct integration of the *P. falciparum* GIMO Insertion construct in the chimeric parasite and shown the absence of the homologous *P. berghei gene* and hdhfr::yfcu marker. Primers sequences are shown in **Table 2.3**.

3.2.4 Phenotype analysis of the Replacement gene [RG] chimeric expressing PfCelTOS or PfCSP by Immunofluorescence assay test (IFAT)

Immunofluorescence staining was performed as described in section **2.5.1.** Immunofluorescence staining showed *PfCelTOS* antigen expression in sporozoites of *PbANKA-PfCelTOS(r)*$_{PbCelTOS}$ (2258 cl2) chimeric parasite. Chimeric salivary-gland sporozoites were stained with sera from mice vaccinated against *PfCelTOS* and *PbCelTOS* antigens. Bound IgG was detected with goat anti-mouse IgG-Alexa Fluor 488, green and nuclear DNA stained with 2% Hoechst-33342. As a control, wild-type (WT) *P. berghei* sporozoites were stained with the same sera. Merged images of the different channels are shown for both chimeric and WT *P. berghei* stained images (**Figure 3.4A)**.

Similarly, immunofluorescence staining showed PfCSP antigen expression in sporozoites of *PbANKA-PfCSP(r)*$_{PbCSP}$ (2257 cl2) chimeric parasite. Chimeric salivary-glands porozoites were stained with anti-PfCSP (2A10) [222, 271] or anti-PbCSP (3D11) [272] monoclonal antibodies (MR4). Bound IgG was detected with goat anti-mouse IgG-Alexa Fluor 488, green and nuclear DNA stained with 2% Hoechst-33342, blue. As a control, WT *P. berghei* sporozoites were stained with the same antibodies. Merged images of the different channels are shown for both chimeric PbANKA-PfCS(r)$_{PbCSP}$ (2257 cl2) and WT *P. berghei* stained images **(Figure 3.4B)**.

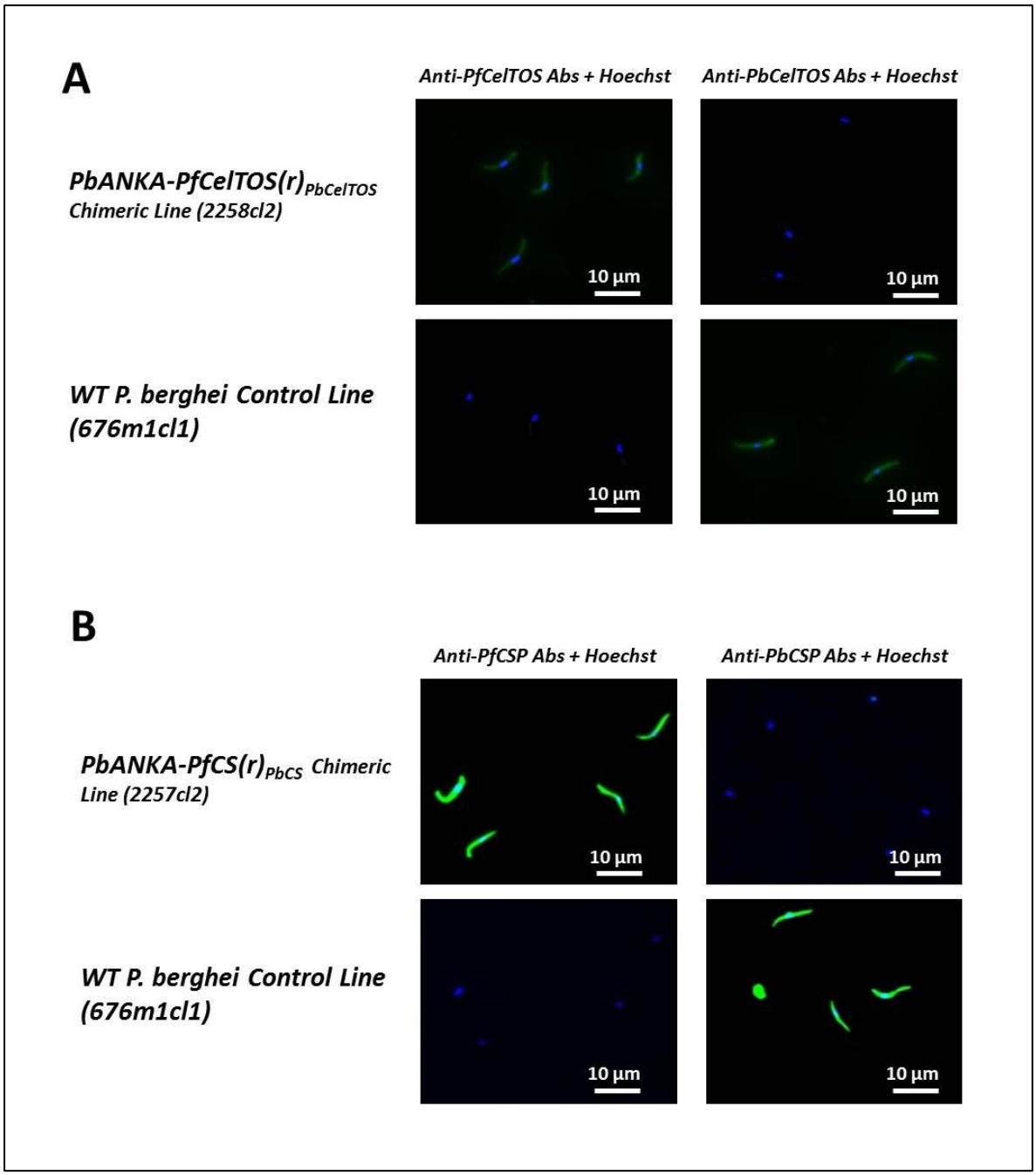

Figure 3.4 Immunofluorescence analysis demonstrating *P. falciparum* antigen expression in sporozoites of the replacement gene [RG] chimeric *P. berghei* parasites. A. Immunofluorescence analysis demonstrating *PfCelTOS* antigen expression in sporozoites of chimeric *Pb* parasite. Chimeric salivary-gland sporozoites were stained with sera from mice vaccinated against *PfCelTOS* and *PbCelTOS* antigens, (Alexa Fluor 488, green) and Hoechst-33342 (blue; nuclear staining). As a control, wild-type (WT) *P. berghei* sporozoites were stained with the same sera. Merged images of the different channels are shown for both chimeric and WT *P. berghei* stained images.

B. Immunofluorescence analysis demonstrating *PfCSP* antigen expression in sporozoites of chimeric *Pb* parasite. Chimeric salivary-gland porozoites were stained with anti-*PfCSP (210A) and anti-PbCSP (3D11)* monoclonal antibodies (Alexa Fluor 488, green) and Hoechst-33342 (blue; nuclear staining). As a control, wild type (WT) *P. berghei* sporozoites were stained with the same antibodies. Merged images of the different channels are shown for both chimeric *PbANKA-PfCS(r)*$_{PbCS}$ (2257 cl2) and WT *P. berghei* stained images.

3.2.5 Fitness of chimeric parasites

Fitness studies indicated similar infectivity, growth rates, and production of oocysts and sporozoites for both RG chimeric parasites expressing *PfCelTOS* and *PfCSP* (2258cl2 and 2257cl2) compared to those of the WT *P. berghei* line. Also, the blood stage growth and prepatent time to reach 1% parasitaemia in naïve mice for both RG chimeric parasites were identical to the WT *P. berghei* line (**Figure 3.5)**.

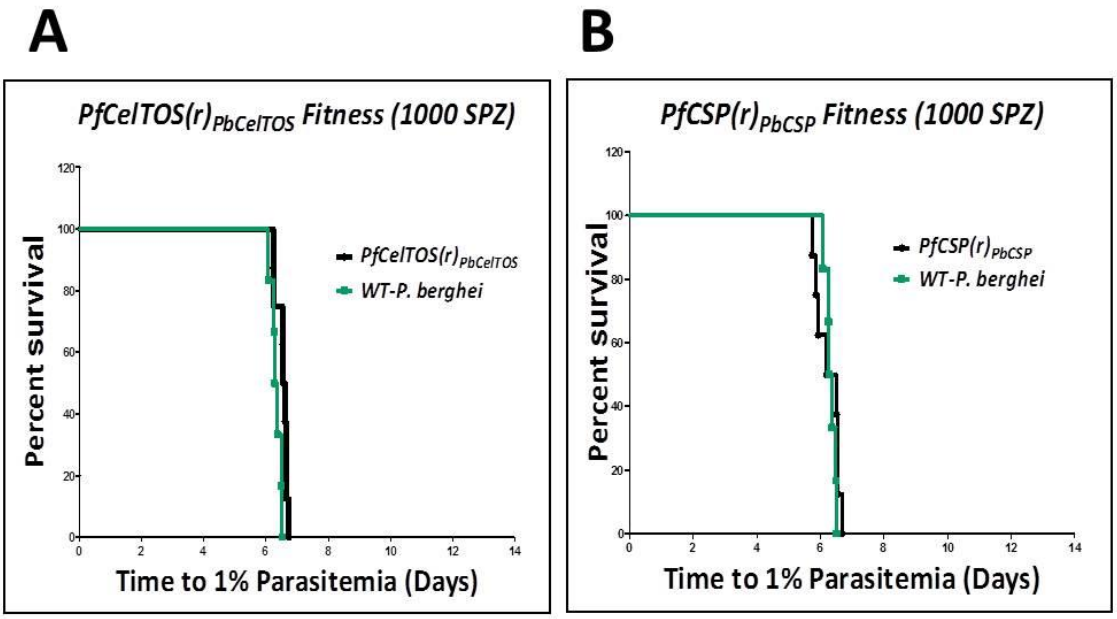

Figure 3.5 Fitness assessment of the replacement Gene [RG] chimeric parasites compared to the wilt-type *P. berghei* parasite. The blood stage growth and prepatent time to reach 1% parasitaemia for both Replacement Gene [RG] chimeric parasites expressing (A) *PfCelTOS* and (B) *PfCSP* (2258cl2 and 2257cl2) were identical to the wild-type *P. berghei* line**.**

3.2.6 Assessment of pre-challenge immunogenicity following heterologous prime-boost ChAd63-MVA PfCelTOS and PfCSP viral vector vaccination.

Two different BALB/c mice (n=8 per group) were vaccinated intramuscularly (i.m.) with $1x10^8$ infectious units (ifu) ChAd63-*PfCelTOS* followed eight weeks later by $1x10^7$ plaque forming units (pfu) MVA-*PfCelTOS*. One week post MVA-boost vaccination the mice were bled and ICS performed to ensure equivalent levels of immunogenicity between challenge groups. There were no statistically significant differences in the immunogenicity between the two mice groups for any cytokine response using Mann Whitney test for both $CD8^+$ T cells cytokines responses, expressed as the percentage of $CD8^+$ cells producing IFNγ, IL-2, TNFα, the cell surface localisation of the degranulation marker CD107a, and $CD4^+$ T cells cytokines responses, expressed as the percentage of $CD8^+$ cells producting IFNγ, IL-2, TNFα or the cell surface localisation of the degranulation marker CD107a (**Figure 3.6)**. To test vaccine efficacy/protective immunity each one of the two mice groups was challenged later with 1,000 chimeric sporozoites 10-14 days post the MVA boost vaccination either with the RG chimeric parasite *PfCelTOS(r)$_{PbCelTOS}$ (2258 cl2), or* the additional gene AG chimeric parasite *PfCelTOS$_{Pbuis4}$ (2231 cl1)*.

Similarly, two different BALB/c mice groups (n=8 per group) were vaccinated intramuscularly (i.m.) with $1x10^8$ infectious units (ifu) ChAd63-*PfCSP* followed eight weeks later by $1x10^7$ plaque forming units (pfu) MVA- *PfCSP* and the cellular immunogenicity / cytokines responses were also assessed by ICS. There were no statistically significant differences in immunogenicity between the two mice groups for any cytokine response using a Mann Whitney test (**Figure 3.7)**. Each one of the two mice groups was challenged later with 1,000 chimeric sporozoites 10-14 days post the MVA boost vaccination either with the replacement gene [RG] chimeric parasite *PfCSP(r)$_{PbCSP}$ (2257 cl2), or* the additional gene [AG] chimeric parasite *PfCSP$_{Pbuis4}$ (2243 cl3)*.

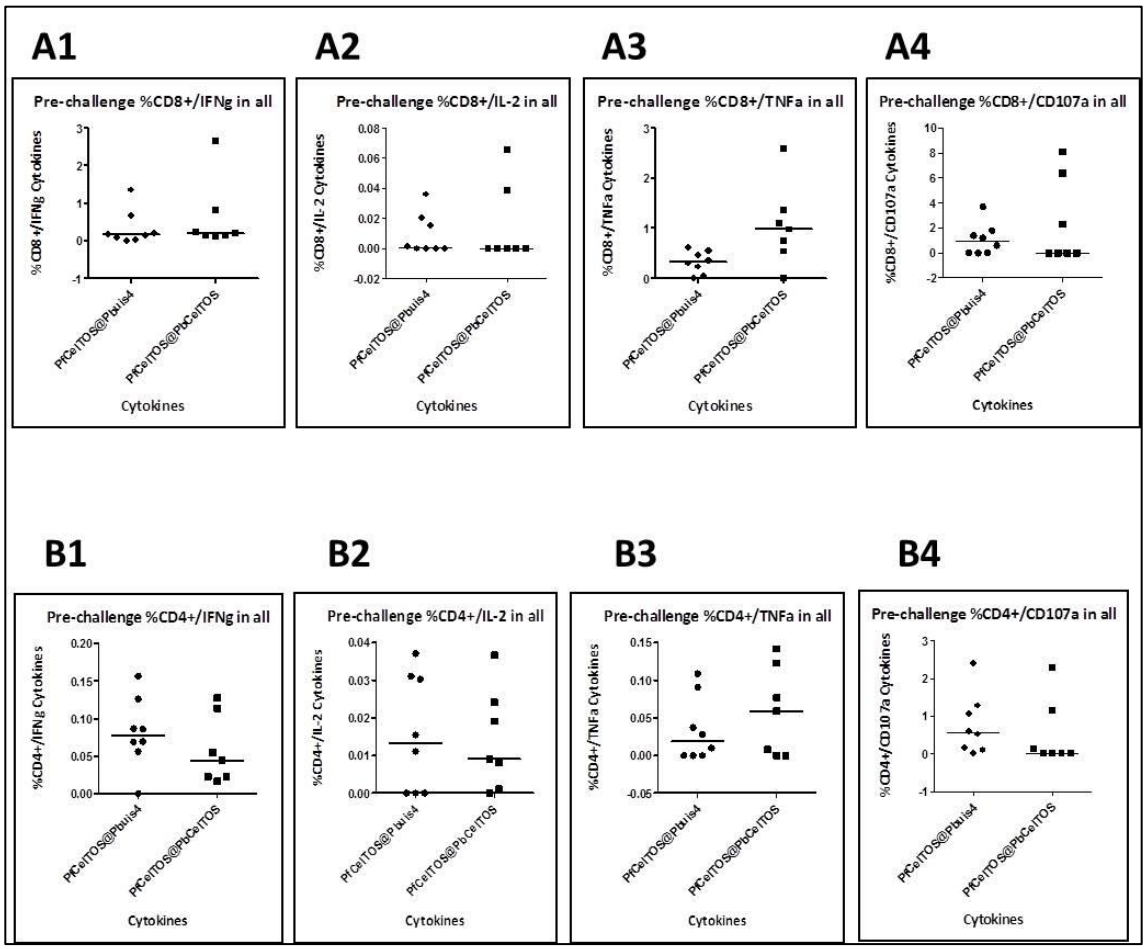

Figure 3.6 Pre-challenge immunogenicity presented as the cytokine responses in the blood following the heterologous prime-boost ChAd63-MVA *P. falciparum* CelTOS viral vector vaccination in two different BALB/c mice groups. Two mice groups (n=8 per group) were vaccinated intramuscularly (i.m.) with $1x10^{8}$ infectious units (ifu) ChAd63-PfCelTOS followed eight weeks later by $1x10^{7}$ plaque forming units (pfu) MVA-PfCelTOS. One week post MVA-boost vaccination the mice were bled, the PBMC were collected, stimulated with *PfCelTOS* overlapping peptide for 6 hours and intracellular staining (ICS) was performed as described earlier in Material and Method sections **2.8.7 and 2.8.8.** There were no statistically significant differences in the immunogenicity / cytokine responses between the two mice groups at any level (Mann Whitney test was used). These mice were challenged with 1,000 chimeric sporozoites 10-14 days post the MVA boost vaccination either with the replacement gene [RG] chimeric parasite ***PfCelTOS(r)*** $_{PbCelTOS}$ ***: 2258 cl2, or*** the additional gene [AG] chimeric parasite ***PfCelTOS*** $_{Pbuis4}$ ***: 2231 cl1.***

(**A**) $CD8^{+}$ cytokines responses measured in the blood one week post-MVA boost, expressed as the percentage of $CD8^{+}$ cells. (**B**) $CD4^{+}$ cytokine responses measured in the blood one week post-boost, expressed as the percentage of $CD4^{+}$ cells. Median with interquartile range values is shown.

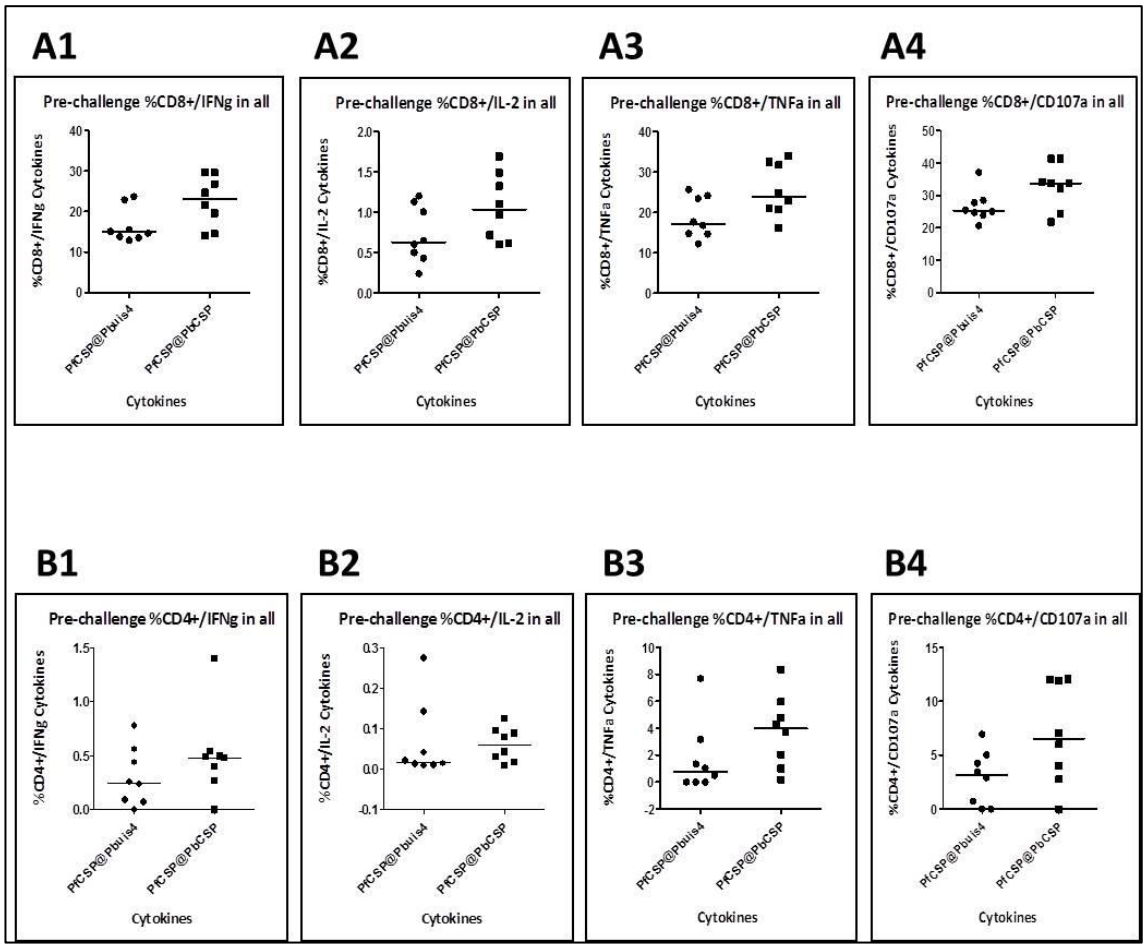

Figure 3.7 Pre-challenge immunogenicity presented as the cytokines responses in the blood following the heterologous prime-boost ChAd63-MVA *P. falciparum* CSP viral vector vaccination in two different BALB/c mice groups. Two mice groups (n=8 per group) were vaccinated intramuscularly (i.m.) with $1x10^{8}$ infectious units (ifu) ChAd63-*PfCSP* followed eight weeks later by $1x10^{7}$ plaque forming units (pfu) MVA-*PfCSP*. One week post MVA-boost vaccination the mice were bled, the PBMC were collected, stimulated with *PfCSP* overlapping peptide for 6 hours and intracellular staining (ICS) was performed as described earlier in Material and Method sections **2.8.7 and 2.8.8.** There were no statistically significant differences in the immunogenicity / cytokines responses between the two mice groups at any level (Mann Whitney test was used). These mice were challenged with 1,000 chimeric sporozoites 10-14 days post the MVA boost vaccination either with the replacement gene [RG] chimeric parasite ***PfCSP(r)*** $_{PbCSP}$ ***: 2257 cl2, or*** the additional gene [AG] chimeric parasite ***PfCSP*** $_{Pbuis4}$ ***: 2243 cl3.***

(**A**) $CD8^{+}$ cytokines responses measured in the blood one week post-MVA boost, expressed as the percentage of $CD8^{+}$ cells. (**B**) $CD4^{+}$ cytokine responses measured in the blood one week post-boost, expressed as the percentage of $CD4^{+}$ cells. Median with interquartile range values is shown.

3.2.7 Comparison of vaccine efficacy as determined in the challenge model after challenge with RG and AG chimeric parasites

After vaccinating mice according to the prime-boost regimen using ChAd63-MVA viral vectors, both the vaccinated and the control naïve mice groups were challenged with 1000 transgenic *P. berghei* sporozoites expressing the equivalent *P. falciparum* antigens. The chimeric parasite development and vaccine efficacy were assessed by determining parasite loads in the liver using an *in vivo* imaging system to quantify luciferase signal intensity levels emanating from the chimeric parasites or by traditional blood-film calculation of infected RBC parasiteamia.

3.2.7.1 Parasite liver loads after challenge as determined by in vivo imaging

At 44 hours after the challenge parasite loads in the liver were measured using an *in vivo* imaging system (IVIS 200). In mice infected with *PfCelTOS(r)*$_{PbCelTOS}$ *(2258 cl2),* no significant difference between the naïve and vaccinated group (p=0.5737, Mann Whitney test) was observed, which could indicate the inability of the *PfCelTOS* vaccine to induce significant efficacy during the liver-stage **(Figure 3.8 A)**. However, in mice infected with *PfCSP(r)*$_{PbCSP}$ *(2257 cl2)* a significant difference between the naïve and vaccinated group (p=0.0019, Mann Whitney test) was observed 44 hours post-infection, indicating the ability of the *PfCSP* vaccine to reduce parasite load in the liver **(Figure 3.8 B)**.

Head to head comparisons were performed between the two groups of naïve or vaccinated mice challenged with the RG or AG chimeric strains. There were no significant differences between luminescence levels in naïve (p=0.0939, Mann Whitney test) or vaccinated mice *for PfCelTOS* (p=0.2072, Mann Whitney test) **(Figure 3.8 C)**. Similar results were seen with PfCSP naïve and vaccinated groups, where no significant difference were observed between luminescence levels in naïve (p=0.0939, Mann Whitney test) or vaccinated mice between the challenge parasites (p=0.3357, Mann Whitney test) **(Figure 3.8 D)**.

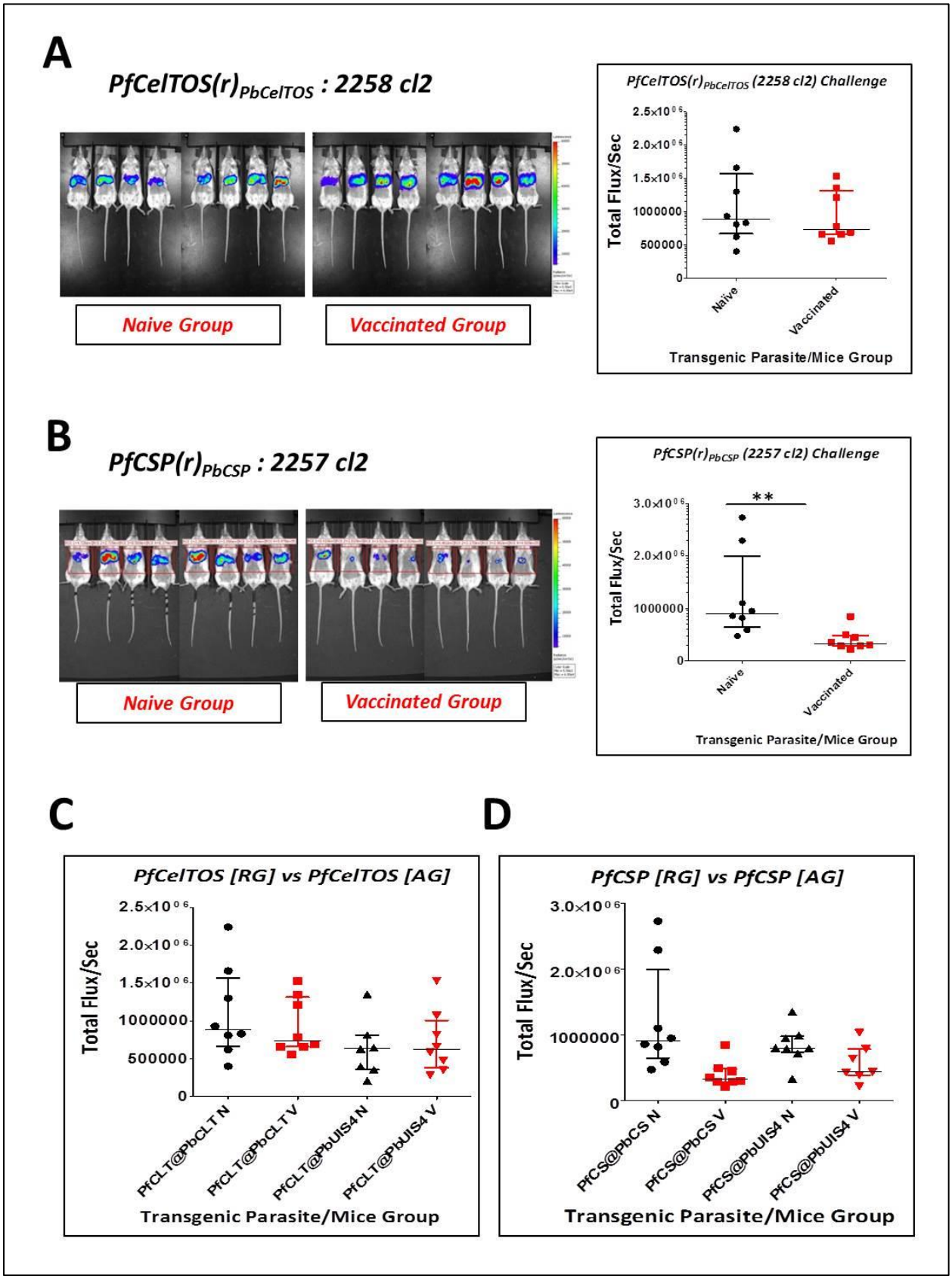
A
PfCelTOS(r)PbCelTOS : 2258 cl2
Naive Group
Vaccinated Group
PfCelTOS(r)PbCelTOS (2258 cl2) Challenge
Total Flux/Sec
2.5x10^06
2.0x10^06
1.5x10^06
1000000
500000
0
Naïve
Vaccinated
Transgenic Parasite/Mice Group
B
PfCSP(r)PbCSP : 2257 cl2
Naive Group
Vaccinated Group
PfCSP(r)PbCSP (2257 cl2) Challenge
**
3.0x10^06
2.0x10^06
1000000
0
Naïve
Vaccinated
Transgenic Parasite/Mice Group
C
PfCelTOS [RG] vs PfCelTOS [AG]
Total Flux/Sec
2.5x10^06
2.0x10^06
1.5x10^06
1000000
500000
0
PfCLT@PbCLT N
PfCLT@PbCLT V
PfCLT@PbUIS4 N
PfCLT@PbUIS4 V
Transgenic Parasite/Mice Group
D
PfCSP [RG] vs PfCSP [AG]
Total Flux/Sec
3.0x10^06
2.0x10^06
1000000
0
PfCS@PbCS N
PfCS@PbCS V
PfCS@PbUIS4 N
PfCS@PbUIS4 V
Transgenic Parasite/Mice Group

Figure 3.8 *In vivo* imaging. Liver loads in naïve and immunized mice that are challenged with transgenic chimeric sporozoites are quantified by measuring luminescence levels at 44 hours after infection using the in **using the IVIS 200 system as described earlier in the Material and Method section 2.5.5** (i.e.: reduction in liver load corresponds to protective immunity).

A. Luciferase activity and the liver load of *PfCelTOS(r)*$_{PbCelTOS}$ *(2258 cl2)* 44 hours after infection . There is no significant difference between the naïve and vaccinated group (p=0.5737, Mann Whitney test).

B. Luciferase activity and the liver load of *PfCSP(r)*$_{PbCSP}$ *(2257 cl2)* 44 hours after infection . There is a significant difference between the naïve and vaccinated group (p=0.0019, Mann Whitney test).

C. Head to head comparison between the two versions of the *PfCelTOS* expressing chimeric parasites; Additional [AG] vs Replacement Gene [RG] to monitor the difference in their liver infectivity in case of using them as challenge models. There were no significant difference between the measured luminescence levels between the two naïve groups (p=0.0939, Mann Whitney test) nor the two vaccinated groups (p=0.2072, Mann Whitney test) when they were challenged with either the Additional Gene [AG] (2231 cl1) or Replacement Gene [RG] (2258 cl2) *PfCelTOS* expressing chimeric parasites. Median with interquartile range values are shown.

D. Head to head comparison between the two versions of the *PfCSP* expressing chimeric parasites; Additional [AG] vs Replacement Gene [RG] to monitor the difference in their liver infectivity in case of using them as challenge models. There were no significant difference between the measured luminescence levels between the two naïve groups (p=0.4418, Mann Whitney test) nor the two vaccinated groups (p=0.3357, Mann Whitney test) when they were challenged with either the Additional Gene [AG] (2243 cl3) or Replacement Gene [RG] (2257 cl2) *PfCSP* expressing chimeric parasites. Median with interquartile range values are shown.

3.2.7.2 Assessment of protective efficacy by determination of the prepatent time to 1% parasitaemia after challenge.

Protections in these challenges were also assessed using the conventional Giemsa stained blood films to calculate the prepatent time to 1% parasitaemia. Vaccination of BALB/c mice with PfCelTOS did not lead to sterile protection or a delay in time to 1% parasitaemia after challenge with either the *Pf*CeTOS RG or AG chimeric parasites **(Figure 3.9 A and C).** In contrast, BALB/c mice immunization with *Pf*CSP resulted in 25% sterile protection after challenge with both *Pf*CSP RG and AG chimeric parasites, with both groups showing a significant delay in time to 1% parasitaemia ($p<0.0001$, Log-rank Mantel-Cox test) **(Figure 3.9 B and D).** In both the *PfCelTOS* and *PfCSP* experiments no differences in vaccine efficacy were found between mice challenged with AG or RG chimeric parasites **(Figure 3.9 E).** In both RG chimeric parasite challenges, the time to 1% parasitaemia is significantly correlated with the liver load as determined by *in vivo* imaging. The correlation between *in vivo* imaging results and the time to reach 1% parasitaemia were tested using Spearman's rank correlation on nonparametric. The time to 1% parasitaemia of all challenged mice (vaccinated and naïve) with $PfCelTOS(r)_{PbCelTOS}$ (2258 cl2) was negatively correlated with the luciferase expression measured by *in vivo* imaging (Spearman $r=-0.7325$, $p=0.0013$). Also the time to 1% parasitaemia of all challenged mice (vaccinated and naïve) with $PfCSP(r)_{PbCSP}$ *(2257 cl2)* was negatively correlated with the luciferase expression measured by *in vivo* imaging (Spearman $r=-0.8755$, $p<0.0001$) **(Figure 3.10).**

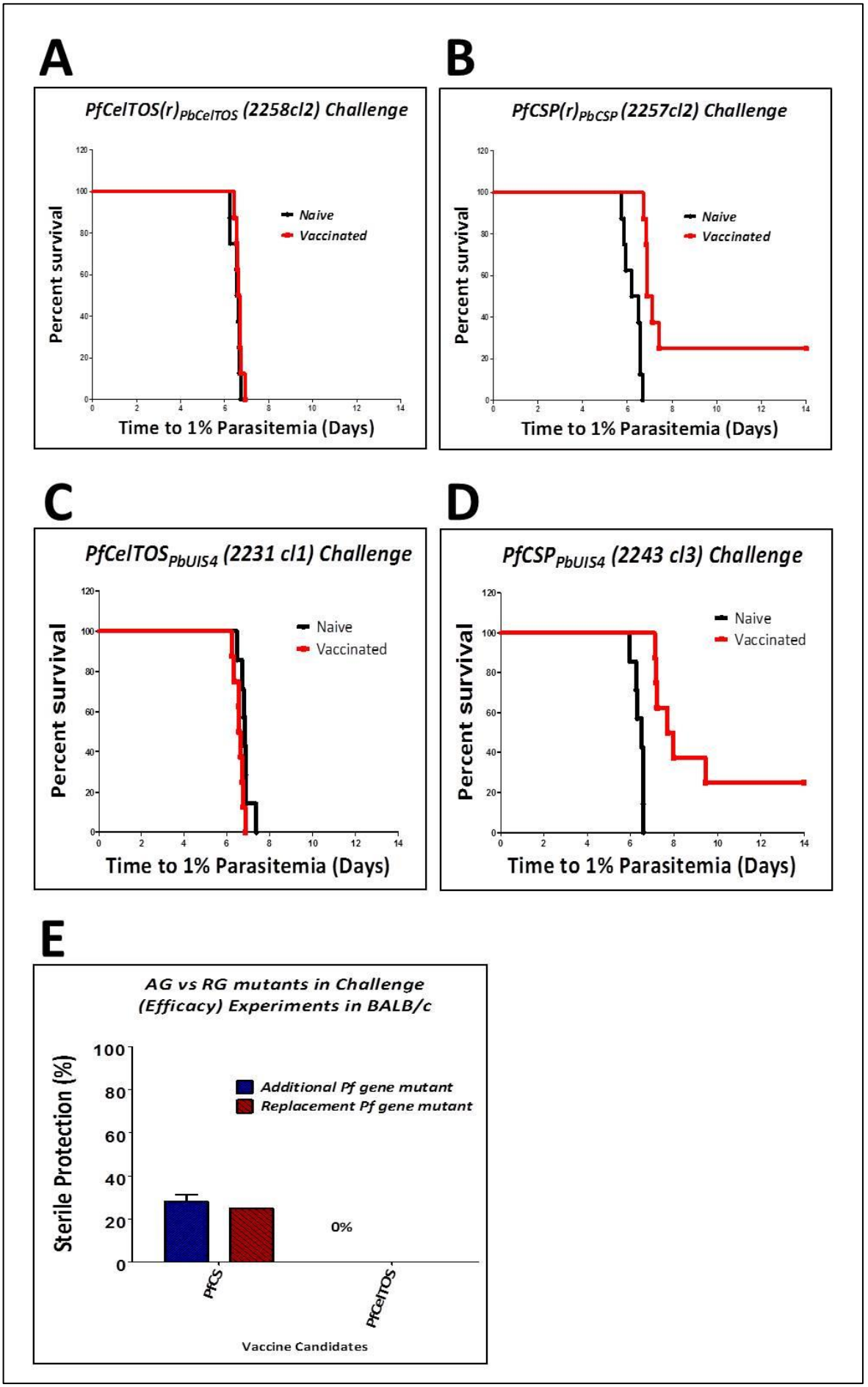
A
PfCelTOS(r)PbCelTOS (2258cl2) Challenge
Percent survival
Time to 1% Parasitemia (Days)
Naive
Vaccinated
B
PfCSP(r)PbCSP (2257cl2) Challenge
Percent survival
Time to 1% Parasitemia (Days)
Naive
Vaccinated
C
PfCelTOSPbUIS4 (2231 cl1) Challenge
Percent survival
Time to 1% Parasitemia (Days)
Naive
Vaccinated
D
PfCSPPbUIS4 (2243 cl3) Challenge
Percent survival
Time to 1% Parasitemia (Days)
Naive
Vaccinated
E
AG vs RG mutants in Challenge (Efficacy) Experiments in BALB/c
Sterile Protection (%)
Additional Pf gene mutant
Replacement Pf gene mutant
0%
PfCS
PfCelTOS
Vaccine Candidates

Figure 3.9

A, B. Protective efficacy after ChAd63-MVA prime boost vaccination in BALB/c mice (as described in the prime-boost vaccination strategy earlier) with the *P. falciparum* candidate and challenge each group with its corresponding Replacement Gene [RG] *P. berghei* chimeric sporozoites expressing the cognate *P. falciparum* antigen *(PfCelTOS or PfCSP)*. Mice were challenged 10-14 days after the MVA-boost vaccination. Mice were monitored daily from day five post challenge to enable calculation of the time to 1% parasitemia. Mice that were slide negative till day 14 post-challenge were considered sterilely protected. The Log-rank (Mantel-Cox) Test was used to assess differences between the survival curves: The previous figures show the time to reach 1% parasitemia only for the groups showed sterile protection or significant delay on the time to reach 1% parasitemia. (A) PfCelTOS vaccination was unable to provide any sterile protection or delay to reach 1% parasitaemia in the challenge with the Replacement Gene [RG] chimeric parasite *Pf*CelTOS(r)$_{PbCelTOS}$, p=0.2194, (B) Vaccination with *PfCSP* protected 2/8 mice (25%) and also caused a delay to reach 1% parasitaemia in the challenge with the Replacement Gene [RG] chimeric parasite *Pf*CSP(r)$_{Pb\text{CSP}}$, p<0.0001.

C.D. Protective efficacy after ChAd63-MVA prime boost vaccination in BALB/c mice (as described in the prime-boost vaccination strategy earlier) with the *P. falciparum* candidate and challenge each group with its corresponding Additional Gene [AG] *P. berghei chimeric* sporozoites expressing the cognate *P. falciparum* antigen *(PfCelTOS or PfCSP).* Mice were challenged 10-14 days after the MVA-boost vaccination. Mice were monitored daily from day five post challenge to enable calculation of the time to 1% parasitemia. Mice that were slide negative till day 14 post-challenge were considered sterilely protected. The Log-rank (Mantel-Cox) Test was used to assess differences between the survival curves: The previous figures show the time to reach 1% parasitemia only for the groups showed sterile protection or significant delay on the time to reach 1% parasitemia. (C) PfCelTOS vaccination was unable to provide any sterile protection or delay to reach 1% parasitaemia in the challenge with the Additional Gene [AG] chimeric parasite *Pf*CelTOS$_{Pbuis4}$, (2231cl1) (D) Vaccination with *PfCSP* protected 2/8 mice (25%) and also caused a delay to reach 1% parasitaemia in the challenge with the Additional Gene [AG] chimeric parasite *Pf*CSP$_{Pb\text{uis4}}$, p<0.0001. These two additional parasites will be discussed in detail in **Chapter-4.**

E. No significant difference in protection (Mann Whitney test) between challenge with additional gene [AG] or replacement gene [RG] chimeric parasites as challenge model in two *P. falciparum* vaccine candidates; *PfCelTOS* and *PfCSP.*

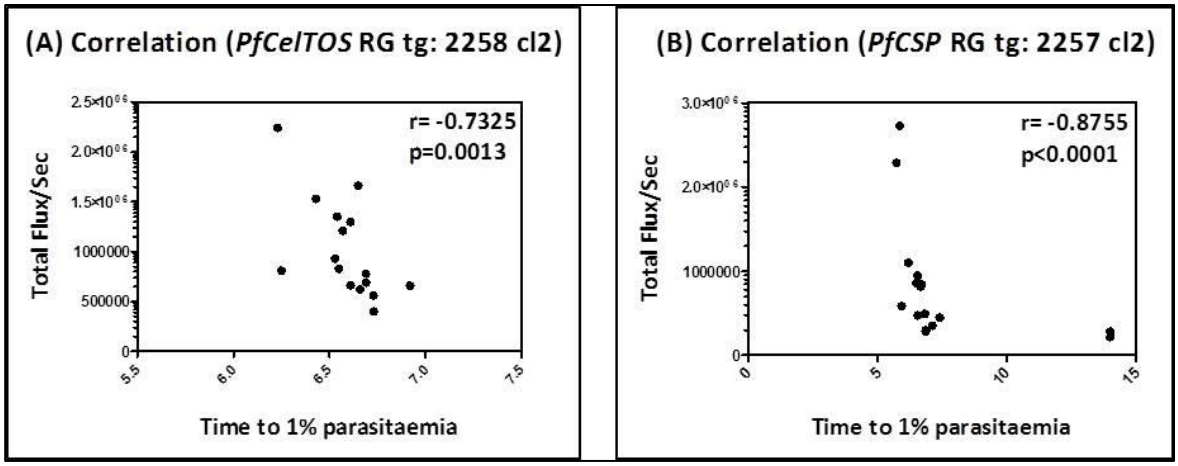

Figure 3.10 The time to 1% parasitaemia correlates with the bioluminescence of the Replacement Gene (RG) transgenic liver-stage parasites.

At 44 hours post chimeric sporozoite challenge in the original experiment, mice were imaged *in vivo* using the IVIS 200 for luciferase expression.

(A) ***PfCelTOS(r)*** $_{PbCelTOS}$ ***(2258 cl2):*** correlation between time to 1% parasitaemia and IVIS imaging data from both vaccinated and naïve control mice (n=16). Spearman r=-0.7325, p=0.0013.

(B) ***PfCSP(r)*** $_{PbCSP}$ ***(2257 cl2):*** correlation between time to 1% parasitaemia and IVIS imaging data from both vaccinated and naïve control mice (n=16). Spearman r=-0.8755, p<0.0001.

3.3 Discussion

To enable the assessment of vaccine efficacy in a pre-clinical model, chimeric *P. berghei* parasite expressing *P. falciparum* antigens were generated. Humanized rodent parasites have been used previously to assess the efficacy of candidate vaccines against the *P. vivax* TRAP protein [236], the *P. falciparum* and *P. vivax* CS proteins [237, 238] , the *P. falciparum* and *P. vivax* Ps25 proteins [239, 240] and the *P. falciparum* MSP1 gene [241, 242]. In addition, humanized *Pb* parasites expressing *P. falciparum* cyclic GMP-dependent protein kinase (PKG) and *P. falciparum* hexose transporter 1 have been generated, permitting *in vivo* screening of inhibitors interfering with PKG and antimalarial sugar analogs respectively [243, 244]. For this work we wished to determine the most appropriate chimeric parasite technology to take forward for assesement of a number of new *P. falciparum* antigens. As several of these new antigens do not have homologs in rodent malaria, it was important to determine whether there was a difference in terms of efficacy when challenging mice with chimeric parasites that express an antigen encoded by a gene that is introduced as an additional copy (AG chimeric parasites) or by a gene that replaced the *P. berghei* gene ortholog (RG chimeric parasites).

The work in this chapter describes the generation of RG and AG chimeric parasites for two major *P. falciparum* antigens which have *P. berghei* orthologs; one expressing the leading malaria vaccine candidate for *P. falciparum* circumsporozoite protein (CSP) which is currently in phase III clinical trials [273] and the second expresses *PfCelTOS* antigen which showed some cross-species protection in murine models in previous studies [195, 274]. Those two mutants (RG vs. AG chimeric parasites) were compared head to head and used to determine whether there was a difference in vaccine efficacy when immunized mice were challenged by either the replacement [RG] or the additional copy [AG] chimeric parasites.

All mutants were generated to express *P. falciparum* transgenes and the GFP::Luciferase fusion protein to determine liver load after challenge by *in vivo* imaging. In addition, expression of GFP-Luciferase throughout the life cycle simplifies/enhances monitoring parasite development in other phases of the life cycle **(Figure 2.5).** Genotype and phenotype analysis confirmed the correct integration and expression of the transgenes in the chimeric parasites. Fitness studies indicated similar infectivity, growth rates, and production of oocysts and sporozoites for both RG chimeric parasites expressing *PfCelTOS and PfCSP (2258cl2 and 2257cl2)* compared to those of the wild-type *P. berghei* line. AG parasites are described in **Chapter-4.**

The RG and AG parasites were used in studies to challenge mice immunized by their equivalent *P. falciparum* antigen. The vaccine efficacy was monitored by two different methods which showed comparable results. First, by determination of vaccine efficacy by measuring liver loads using *in vivo* imaging. Secondly, by measuring the prepatent period after challenge and sterile efficacy by analysis of blood stage parasitemia using conventional Giemsa stained blood-film which is a cheap and relatively easy method. This employs linear regression modeling on blood-stage parasitaemia gathered over three consecutive days to quantify pre-erythrocytic stage vaccine efficacy [275].

When using chimeric *P. berghei* parasites in challenge studies it is important that the expression (and localisation) of the *P. falciparum* antigen in *P. berghei* mimics its expression in *P. falciparum*. In the RG experiments the *P. falciparum* gene coding sequence is under control of the transcriptional regulatory sequences of the *P. berghei* orthologue. Many published studies on *P. berghei* and *P. falciparum* gene function and expression have indicated that it is highly probable that the clear orthologue in both species will have comparable timing and level of expression. However, where no clear ortholog or *P. falciparum* exists in *P. berghei* the expression in sporozoites and liver stages is more difficult to replicate both in terms of timing and level of expression. For the AG mutants

in this study we have chosen to express all candidate proteins under control of the *P. berghei* promoter regulating UIS4 expression. It has been shown that the PbUIS4 promoter is active in both sporozoites and liver stages [276]. It is therefore possible that transgenic *P. berghei* AG line will not express the *P. falciparum* antigen for the duration or at the level that it would be in *P. falciparum*.

In our challenge experiments we found no significant differences in vaccine efficacy after challenge with RG or AG parasites when vaccine efficacy was determined by comparing the parasite liver load using the *in vivo* imaging system (IVIS) or when using the conventional Giemsa stained blood-films to calculate the prepatent time post-challenge to reach 1% parasitaemia.

Unexpectedly, immunization of BALB/c mice with *PfCelTOS* did not result in sterile protection or a delay in time to 1% parasitaemia after challenge with either the replacement or the additional *Pf*CelTOS chimeric parasites despite previous reports of cross-species protection in murine models [195, 274]. In contrast BALB/c mice immunization with *Pf*CSP resulted in 25% sterile protection post-challenge with both *Pf*CSP RG and AG chimeric parasites, with a significant delay in time to 1% parasitaemia. In the case of these Pf candidate antigens there were no statistical difference between the AG or RG approach.

As we did not find differences between AG and RG chimeric parasites, we have decided for future experiments to perform screening of *P. falciparum* vaccine candidates using the AG approach, where all antigens are expressed under the same promoter (UIS4 promoter). This permits a standardized comparison of antigens, in particular for those *P. falciparum* antigens with no orthologs/homologs in *P. berghei* but has the disadvantage that the levels of expression of the antigen may well not correspond to those in the native *P. falciparum* parasite. However, this was considered to be the preferable approach so as to allow all antigens to be assessed.

Chapter 4

The use of a transgenic rodent malaria challenge model for assessment and rank ordering of ten pre-erythrocytic malaria vaccines.

4 The use of a transgenic rodent malaria challenge model for assessment and rank ordering of ten pre-erythrocytic malaria vaccines.

4.1 Introduction

Various genomic and proteomic methods have uncovered new antigens expressed at various stages of the parasite's life-cycle. The genome sequence analysis of *P. falciparum* clone 3D7 revealed a 23-megabase nuclear genome size, which consists of 14 chromosomes and encodes about 5,300 genes [25] expressed throughout the Plasmodium life-cycle; however, only a minority of these have been assessed as sub-unit vaccines, this is partly due to the difficulty in screening human targeted vaccines pre-clinically.

P. falciparum accounts for the majority of the malaria burden in humans [277], but it does not naturally infect small animal models. Therefore rodent malaria strains are routinely used for proof-of-concept studies, although it is still unclear how well results in mice predict the response in humans and several newly identified *P. falciparum* antigen candidates do not have homologues in murine malaria species. Unlike blood-stage vaccines where functional antibody responses can be tested *in vitro* using the growth inhibition assay [278], no such assay currently exists for the liver-stage of malaria due primarily to the difficulties in culturing human hepatocytes and the low rates of *P. falciparum* infection in these cells [279].

So a new screening platform is necessary, which could be used to discover better target antigens for sub-unit based vaccines than the currently known malaria vaccine candidates. The two leading malaria subunit vaccine approaches RTS,S/AS01 and ChAd63-MVA ME-TRAP, are both subunit vaccines targeting the pre-erythrocytic stage of the parasite life-cycle. The pre-erythrocytic stage is considered an excellent target for a malaria vaccine given that it precedes development of clinical symptoms.

In this chapter, we performed a relatively large screen for ten pre-erythrocytic *P. falciparum* malaria vaccine candidates using the newly developed transgenic parasite challenge model *in vivo*. Chosen antigens were expressed in both ChAd63 and MVA, with delivery in a prime-boost regimen which has showed an exceptional ability to induce a $CD8^+$ T cell immune response [280-282]. This regimen with viral vectors was chosen because the liver-stage of malaria infection is thought to be mainly targeted by cell-mediated immunity, as the parasite resides within the hepatocyte and the immune system can only interact with antigenic targets transported to the surface of the infected cell where they can be recognised by T cells as fragments in the groove of MHC molecules. $CD8^+$ T cells, which are MHC class-I restricted are the most efficient effector cells, especially for targeting infected liver cells which have limited MHC class II expression.

As transgenic rodent malaria parasites (in particular *P. berghei*) expressing *P. falciparum* (or *P. vivax*) proteins have previously been used to study *Plasmodium* immunology and assess malaria vaccines in mice [78, 217, 237, 238, 240, 241, 283, 284], and since there was no significant difference observed between using transgenic parasites expressing *P. falciparum* genes as additional or replacement copies (chapter 3), we created ten transgenic *P. berghei* parasites that express eight new candidate *P. falciparum* antigens and another two expressing *P. falciparum* CSP or TRAP. These 'chimeric' *P. berghei* parasites express the coding sequence of the *P. falciparum* vaccine candidate gene under the control of *P. berghei* upregulated in sporozoites 4 (UIS4) gene regulatory elements, with insertion at the neutral *230p* locus in chromosome-3 [245, 249, 285]. The UIS4 gene is specifically expressed at the *Plasmodium* sporozoite and liver-stages [276, 286] and, as expected, analysis of a chimeric line expressing mCherry demonstrated strong and specific transgene expression in both sporozoite and liver-stages. We assessed a number of previously tested antigens, *P. falciparum* (Pf) liver-stage antigen 1 (LSA1) [287], PfLSA3 [204, 206,

207], cell traversal protein for ookinetes and sporozoites (PfCelTOS) [195, 274], PfUIS3 and PfFalstatin [211], as well as more recently identified candidates liver-stage associated protein 1 (PfLSAP1), PfLSAP2 [214] and PfETRAMP5 [215]. Using the additional gene [AG] approach to generate the transgenic parasites has allowed the generation of chimeric parasites for all the novel eight candidates although only three of them have homologs in *P. berghei (CelTOS, UIS3 and Falstatin).* We set out to rank order these antigens based on protection studies in mice, aiming to then select the most promising candidates for further clinical development.

4.2 Results

4.2.1 Design and generation of the candidate vaccines

Candidate antigens were chosen based on several criteria: evidence of being well expressed at the liver-stage, of being targets of a T cell-mediated response in natural infection or during irradiated sporozoite immunization, or if a degree of protection had been reported with vaccine constructs using a rodent homologue or in non-human primates. Vectored vaccines were developed using the available 3D7 *P. falciparum* sequence with the tissue plasminogen activator (tPA) leader sequence [288] added upstream, as in the clinical ME-TRAP vectors, to aid in secretion, expression and thereby immunogenicity [289-291]. This sequence was not added for *PfLSA3*, *PfLSAP1* and *PfUIS3* as these antigens contain two transmembrane domains and so are likely to be anchored in the membrane, based on their predicted structures. *PfLSA1* had repetitive regions deleted to leave only two copies of the 43 degenerative seventeen amino acid repeats (one of the most and one of the least representative), whilst repetitive regions in PfLSA3 were deleted to leave only one copy. All sequences were modified for mammalian codon optimization prior to cloning into the ChAd63 and MVA vectors. As stated earlier, a former DPhil student Rhea J. Longley with the help of the Viral Vector Core Facility at the Jenner Institute had earlier

generated the eight novel *P. falciparum* viral vectored vaccines used in this chapter, while *PfCSP* and *PfTRAP* viral vector vaccines were generated by Dr. Sue Morris, Dr. Matthew Cottingham and Nick Edwards [266]. Rhea J. Longley provided assistance with the transgenic challenges performed in BALB/c mice in this chapter and some of these same results have been presented in her thesis (University of Oxford, 2013).

4.2.2 Transgenic parasite design and generation

Transfection in *Plasmodium* was limited by the availability of only two selectable markers and therefore the GIMO method for rodent malaria parasites transfection was used to generate ten transgenic *P. berghei* parasites that express eight new candidate *P. falciparum* antigens and another two expressing *P. falciparum* CSP or TRAP under the control of *Pbuis4* gene regulatory elements (5'UTR promoter and 3'UTR) in addition to the GFP::Luciferase fused transgenes expressed under the control of *Pb*eef1α promoter **(Figure 4.2)**. Transfection of the mother line was done by integrating DNA-constructs that target the modified 230p locus, followed by negative selection of transformed parasites with 5-Fluorocytosine (5-FC) **(Figure 4.2)** (See section **2.3.1** for more detail**)**. The GFP-Luciferase cassette was included in all the transgenic parasites to allow monitoring the mutants in all the different life stages**.**

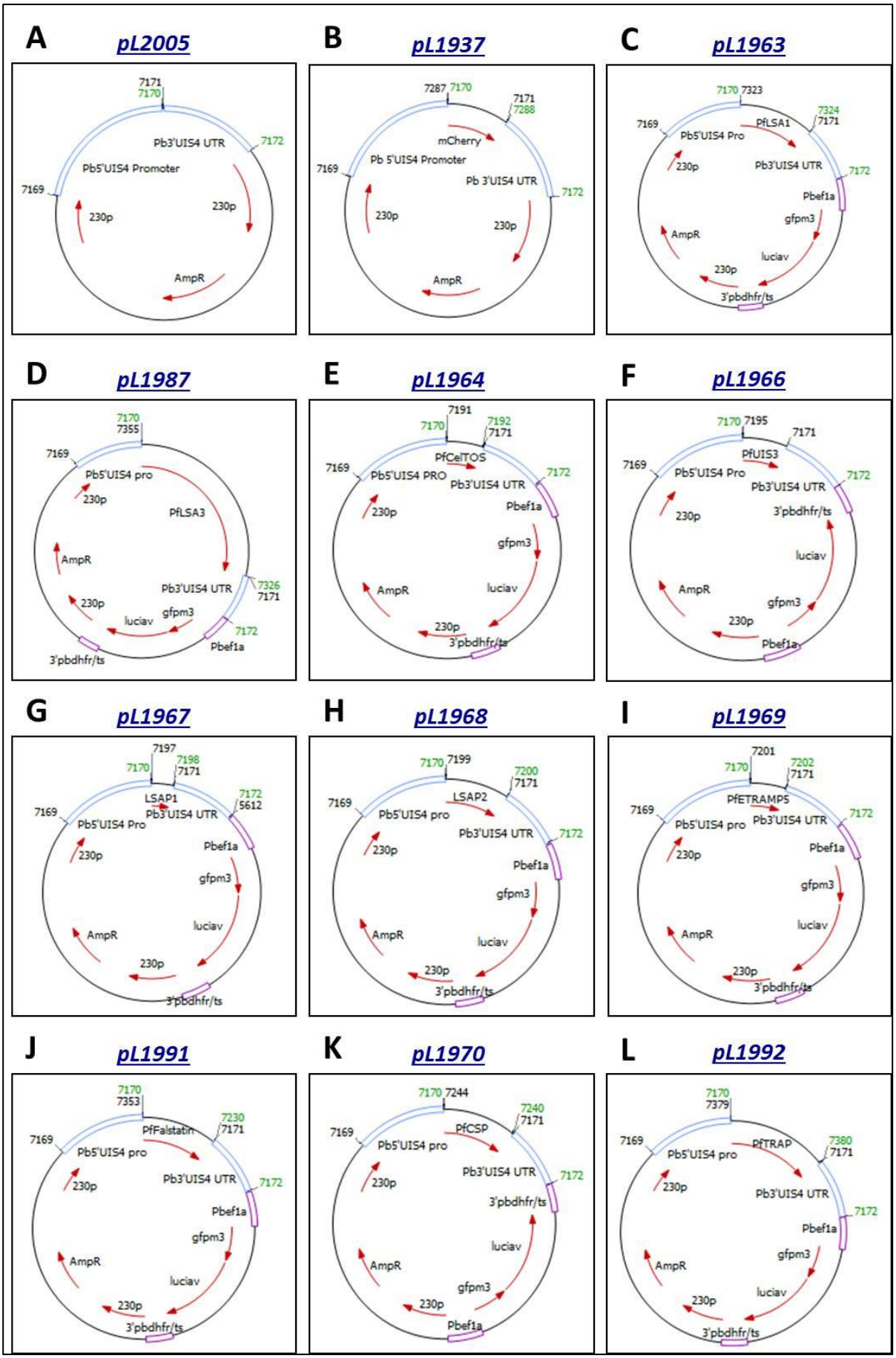
A
pL2005
7171
7170
Pb3'UIS4 UTR
7172
Pb5'UIS4 Promoter
7169
230p
230p
AmpR
B
pL1937
7287 7170
7171
7288
mCherry
7169
Pb 5'UIS4 Promoter
Pb 3'UIS4 UTR
7172
230p
230p
AmpR
C
pL1963
7170 7323
7324
7171
7169
Pb5'UIS4 Pro
PfLSA1
230p
Pb3'UIS4 UTR
7172
Pbef1a
gfpm3
AmpR
luciav
230p
3'pbdhfr/ts
D
pL1987
7170
7355
7169
Pb5'UIS4 pro
230p
PfLSA3
AmpR
Pb3'UIS4 UTR
7326
7171
230p
luciav
gfpm3
7172
Pbef1a
3'pbdhfr/ts
E
pL1964
7191
7170
7192
7171
PfCelTOS
7169
Pb5'UIS4 PRO
Pb3'UIS4 UTR
7172
230p
Pbef1a
gfpm3
AmpR
luciav
230p
3'pbdhfr/ts
F
pL1966
7170 7195
7171
PfUIS3
7169
Pb5'UIS4 Pro
Pb3'UIS4 UTR
7172
230p
3'pbdhfr/ts
luciav
AmpR
gfpm3
230p
Pbef1a
G
pL1967
7197
7170
7198
7171
LSAP1
7172
5612
7169
Pb5'UIS4 Pro
Pb3'UIS4 UTR
230p
Pbef1a
gfpm3
AmpR
luciav
230p
3'pbdhfr/ts
H
pL1968
7170 7199
7200
7171
7169
LSAP2
Pb5'UIS4 pro
Pb3'UIS4 UTR
7172
230p
Pbef1a
gfpm3
AmpR
luciav
230p
3'pbdhfr/ts
I
pL1969
7201
7170
7202
7171
PfETRAMP5
7169
Pb5'UIS4 pro
Pb3'UIS4 UTR
7172
230p
Pbef1a
gfpm3
AmpR
luciav
230p
3'pbdhfr/ts
J
pL1991
7170
7353
PfFalstatin
7230
7171
7169
Pb5'UIS4 pro
230p
Pb3'UIS4 UTR
7172
Pbef1a
gfpm3
AmpR
luciav
230p
3'pbdhfr/ts
K
pL1970
7170 7244
7240
7171
7169
PfCSP
Pb5'UIS4 pro
Pb3'UIS4 UTR
7172
230p
3'pbdhfr/ts
luciav
AmpR
gfpm3
230p
Pbef1a
L
pL1992
7170
7379
7169
Pb5'UIS4 pro
PfTRAP
7380
7171
230p
Pb3'UIS4 UTR
7172
Pbef1a
gfpm3
AmpR
luciav
230p
3'pbdhfr/ts

Figure 4.1 Schematic representation of the plasmid maps used for generating the Additional Gene [AG] chimeric *P. berghei* parasites expressing mCherry or single *P. falciparum* antigens under *Pbuis4* promoter.

Schematic representation of the plasmid maps containing the constructs used for generating the transgenic *P. berghei* parasites expressing mCherry or *P. falciparum* vaccine candidate antigen (as an additional copy) expressed under the control of *Pbuis4* promoter in addition to GFP::Luciferase fused transgenes expressed under the control of *Pb*eef1α promoter. All these constructs contain the *Pb5'* and *3'230p* TRs that targets *Pb230p* neutral locus in chr-3. Each plasmid map shows the DNA fragments annotations and the primers numbers used for generating the DNA construct. Primers sequences and the expected PCR product sizes are shown in **Table 2.2.**

A. Empty basic plasmid containing *Pb5'uis4* promoter and *Pb3'uis4* UTR flanked by the Pb5' and 3'230p targeting regions **(pL2005)**, **B**. mCherry$_{Pbuis4}$ **(pL1937), C.** PfLSA-1$_{Pbuis4}$+GFP::Luc$_{Pbeef1a}$ **(pL1963), D.** PfLSA-3$_{Pbuis4}$+GFP::Luc$_{Pbeef1a}$ **(pL1987), E.** PfCelTOS$_{Pbuis4}$+GFP::Luc$_{Pbeef1a}$ **(pL1964), F.** PfUIS3$_{Pbuis4}$+GFP::Luc$_{Pbeef1a}$ **(pL1966), G.** PfLSAP-1$_{Pbuis4}$+GFP::Luc$_{Pbeef1a}$ **(pL1967), H.** PfLSAP-2$_{Pbuis4}$+GFP::Luc$_{Pbeef1a}$ **(pL1968), I.** PfETRAMP5$_{Pbuis4}$+GFP::Luc$_{Pbeef1a}$ **(pL1969), J.** PfFalstatin$_{Pbuis4}$+GFP::Luc$_{Pbeef1a}$ **(pL1991), K.** PfCSP$_{Pbuis4}$+GFP::Luc$_{Pbeef1a}$ **(pL1970), L.** PfTRAP$_{Pbuis4}$+GFP::Luc$_{Pbeef1a}$ **(pL1992).**

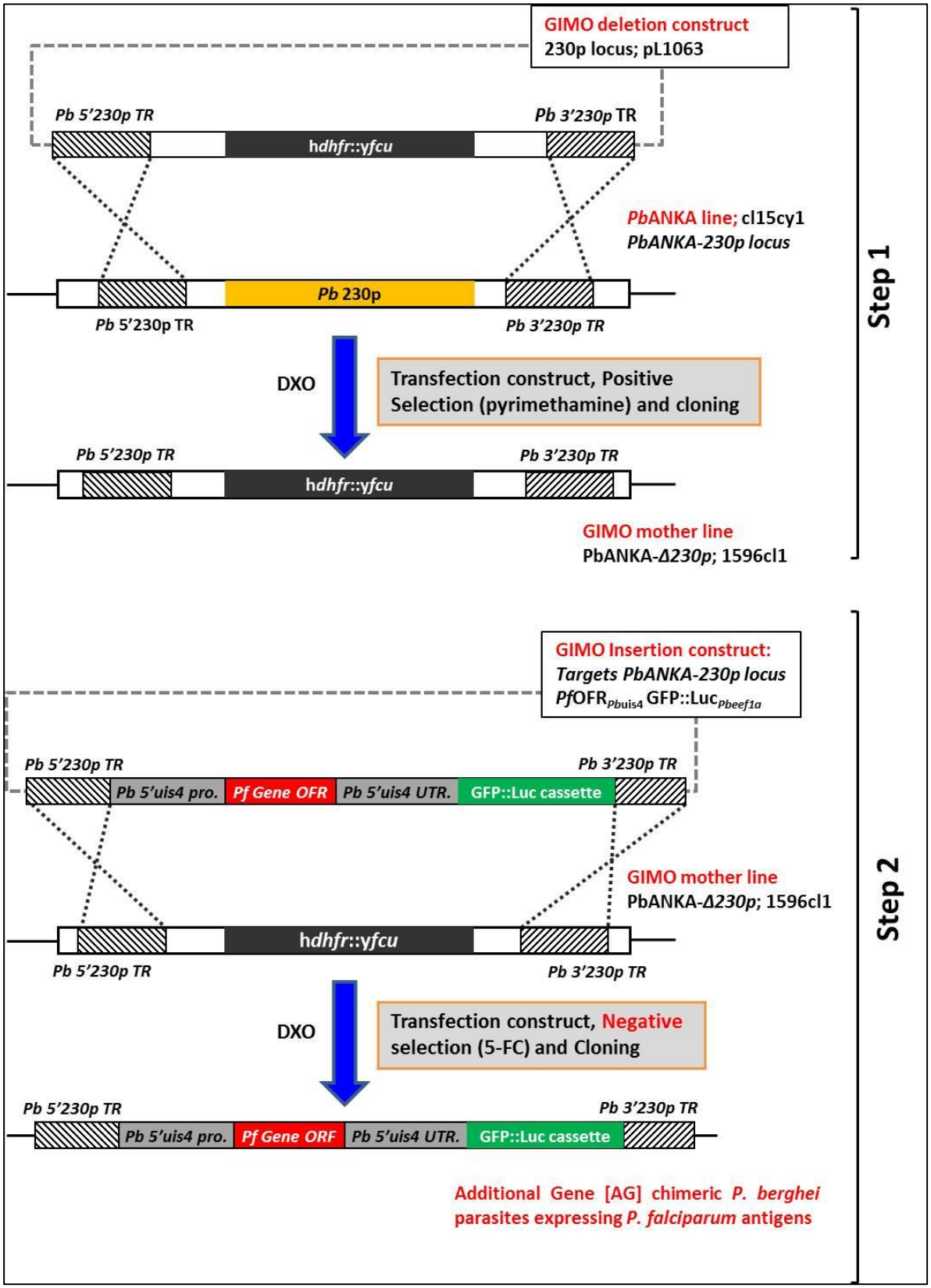
GIMO deletion construct
230p locus; pL1063
Pb 5'230p TR
Pb 3'230p TR
hdhfr::yfcu
PbANKA line; cl15cy1
PbANKA-230p locus
Pb 230p
Pb 5'230p TR
Pb 3'230p TR
DXO
Transfection construct, Positive Selection (pyrimethamine) and cloning
Pb 5'230p TR
Pb 3'230p TR
hdhfr::yfcu
GIMO mother line
PbANKA-Δ230p; 1596cl1
Step 1
GIMO Insertion construct:
Targets PbANKA-230p locus
PfOFR Pbuis4 GFP::Luc Pbeef1a
Pb 5'230p TR
Pb 3'230p TR
Pb 5'uis4 pro.
Pf Gene OFR
Pb 5'uis4 UTR.
GFP::Luc cassette
GIMO mother line
PbANKA-Δ230p; 1596cl1
hdhfr::yfcu
Pb 5'230p TR
Pb 3'230p TR
DXO
Transfection construct, Negative selection (5-FC) and Cloning
Pb 5'230p TR
Pb 3'230p TR
Pb 5'uis4 pro.
Pf Gene ORF
Pb 5'uis4 UTR.
GFP::Luc cassette
Additional Gene [AG] chimeric P. berghei parasites expressing P. falciparum antigens
Step 2

Figure 4.2 Generation of Additional Gene [AG] chimeric *P. berghei* parasites expressing *P. falciparum* antigens
Step 1: Schematic representation of the constructs used to introduce the positive-negative selectable maker cassette into the *P. berghei ANKA* neutral loci (230p locus; pL1063) to generate the GIMO mother-lines which were selected by positive selection using pyrimethamine.
Step 2: Schematic representation showing the introduction of the constructs that contain the '*P. falciparum* antigen expression cassette' into the neutral locus (*230p*) of the *P. berghei* $GIMO_{PbANKA}$ mother line by GIMO-transfection using negative selection (5-FC). These basic constructs contain the coding sequence (CDS) of the *P. falciparum* gene flanked by the *Pb5'uis4 UTR* (containing the *Pbuis4* promoter region) and the *Pb3'uis4 UTR* (containing the *Pbuis4* transcription terminator sequence), a GFP and luciferase fusion reporter (GFP::Luc) cassette and the *230p* targeting sequences. The construct targets the *230p* gene locus at regions (hatched boxes) by double cross-over homologous recombination (DXO), resulting in replacement of the h*dhfr*/*yfcu* selectable marker cassette that is present in the GIMO parasites with the *P. falciparum* antigen expression cassette.

4.2.3 *Pbuis4* promoter characterization using mCherry expressing reporter line

To enable a fair assessment and rank the potential of the new sporozoites/liver-stage antigens in a transgenic *P. berghei* system, I decided to have all antigens expressed under the same *P. berghei* promoter which has a strong sporozoite/liver-stage specific expression. To test the intensity and timing of *Pbuis4* promoter expression a reporter line was generated expressing mCherry transgene under the control of *Pbuis4* promoter (**Figure 4.3 A**).

The reporter line 2204 ($mCherry_{Pbuis4}$) transgenic parasites had normal blood- and mosquito-stage development, but no fluorescence was detected in the blood stages, ookinetes, oocyst and midgut-derived sporozoites. In contrast, the control reporter line 1645 parasites expressing mCherry under the control of the constitutive *Pbeef1α* promoter ($mCherry_{Pbeef1\alpha}$) were fluorescent in all stages demonstrating stage-specific expression of the UIS4 promoter.

Mosquito infections with the $mCherry_{Pbuis4}$ reporter line were also assessed; while no fluorescence was detected in day-9, -13 and -17 oocysts, sporozoites

inside the salivary glands (day-17 and -23) displayed a strong red signal. In contrast, the control reporter line (*mCherry*$_{Pbeef1a}$) oocysts and salivary glands were positive at all time-points (**Figure 4.3 B**). Individual salivary gland sporozoites of the *mCherry*$_{Pbuis4}$ reporter line were also fluorescent, while individual sporozoites of *mCherry*$_{Pbeef1a}$ control line were not bright enough to be detected, suggesting that the *Pbuis4* promoter was stronger. To assess liver-stage expression, hepatocyte cell lines were infected with *mCherry*$_{Pbuis4}$ reporter line sporozoites (**Figure 4.4 A**). We observed a considerable reduction in fluorescence at 5hrs post infection (p.i.). However, from 15hrs p.i onwards the mCherry signal rapidly increased, with expression increasing further after 24 hours and peak fluorescence was observed at 48 hpi, with a slight decrease by 56 hpi, but still higher than all the pre-peak signal intensities (at ~80% of the 48hpi peak). At 65 hpi the signal had largely decreased to slightly above background levels **(Figure 4.4 B).** The data demonstrate that Pbuis4 is a strong and specific promoter with expression limited to sporozoite and liver-stages.

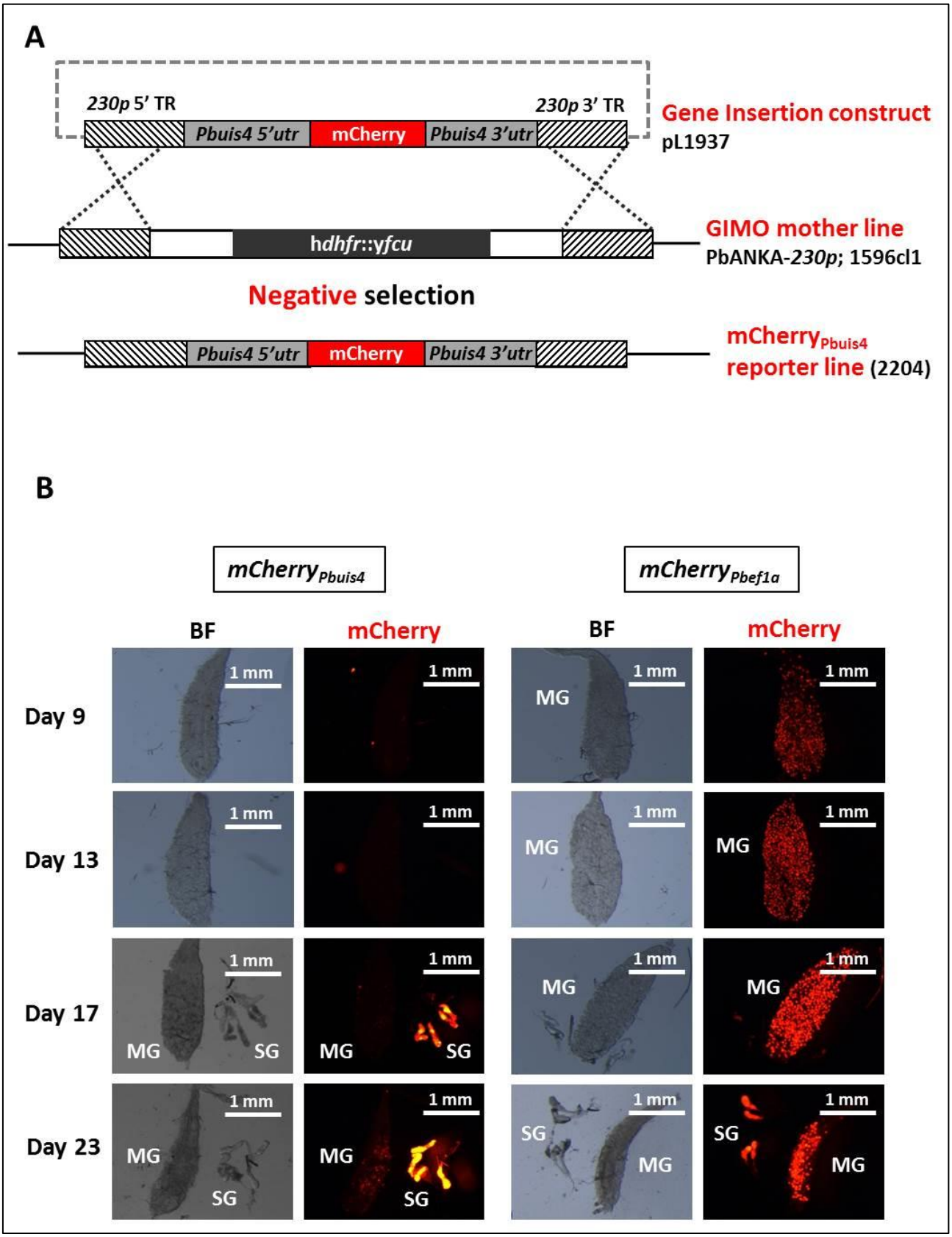
A
230p 5' TR
Pbuis4 5'utr
mCherry
Pbuis4 3'utr
230p 3' TR
Gene Insertion construct
pL1937
hdhfr::yfcu
GIMO mother line
PbANKA-230p; 1596cl1
Negative selection
Pbuis4 5'utr
mCherry
Pbuis4 3'utr
mCherry Pbuis4
reporter line (2204)
B
mCherry Pbuis4
mCherry Pbef1a
BF
mCherry
BF
mCherry
Day 9
Day 13
Day 17
Day 23
1 mm
MG
SG

Figure 4.3 Generation and analysis of a transgenic *mCherry*$_{Pbuis4}$ reporter line expressing mCherry under the control of the *Pbuis4* promoter in mosquito stages

A. Schematic representation showing the introduction of the mCherry-expression cassette into the neutral (*230p*) locus of the *P. berghei* GIMO$_{PbANKA}$ mother line by GIMO-transfection. Construct pL1937 contains the *5'uis4*-mCherry-*3'uis4* cassette and *230p* targeting sequences. This construct is integrated into the modified *P. berghei 230p* locus that contains the h*dhfr::*y*fcu* selectable marker cassette (hatched box) by double cross-over homologous recombination at the target regions (grey boxes). Negative selection with 5-FC selects for the transgenic parasite line (line 2204) that has the mCherry-expression cassette introduced into the *230p* locus and the h*dhfr::*y*fcu* selectable marker cassette removed.

B. mCherry expression in mosquito stages of the transgenic parasite lines, *mCherry*$_{Pbuis4}$ and *mCherry*$_{Pbeef1}$; in oocysts (day-9, -13 and -17) in mosquito midguts (MG) and sporozoites (day-17 and -23) in salivary glands (SG). In *mCherry*$_{Pbuis4}$ parasites mCherry-expression is strongly detected only in SG sporozoites. In *mCherry*$_{Pbeef1}$ parasites mCherry is expressed both in oocysts and sporozoites. Bright field (BF).

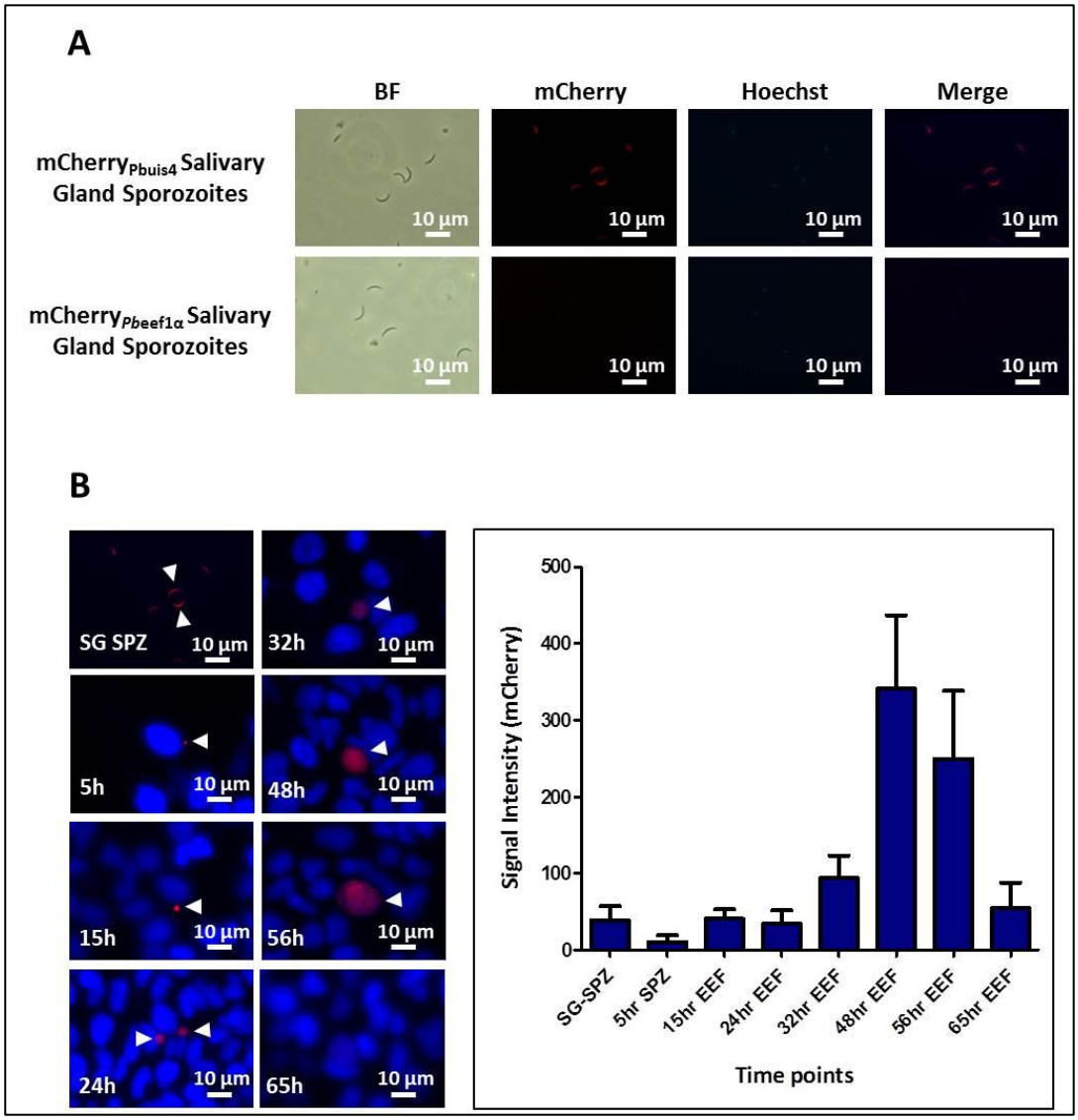

Figure 4.4 Characterisation and analysis of *Pbuis4* promoter in salivary gland sporozoites and liver stages using transgenic *mCherry*$_{Pbuis4}$ reporter line.

A. Salivary gland sporozoites of the transgenic parasite mutant reporter line mCherry$_{Pbuis4}$ compared to the control parasites mCherry$_{Pbeef1\alpha}$. Individual sporozoites of mCherry$_{Pbuis4}$ are much higher mCherry positive compared to mCherry$_{Pbeef1a}$ sporozoites, indicating that *Pb*uis4 is strongly expressed in salivary gland sporozoites

B. mCherry expression in *mCherry*$_{Pbuis4}$ (2204) sporozoites and liver stages. Left panel: Representative images of mCherry-fluorescence in salivary gland sporozoite (SG SPZ) and infected hepatocytes (Huh7-cells) at different hours post infection; hepatocyte nuclei DNA stained with Hoechst (blue). Right panel: Quantification of mCherry fluorescence intensity of the different points of development inside hepatocytes. Pictures were taken of 30-40 sporozoites or liver stages (exo-erythrocytic forms, EEF) using a Leica DM-IRBE Flu fluorescence microscope and fluorescent intensity was determined by gating on parasite area (i.e. mCherry positive area) and measuring maximum intensity of mCherry signal, using the ImageJ software.

4.2.4 Genotype analysis of the Additional Gene chimeric parasites

To confirm the correct integration of the DNA construct in the chimeric *P. berghei* parasite Southern analysis was performed using a mixed probe of Chromosome-5/hDHFR that recognized both hDHFR in the selectable marker and chromosome-5 in the control mutant line (2117 cl1), but only could recognize chromosome-5 in the successfully transfected transgenic parasites, since the *P. falciparum* expression cassette integrated into *P. berghei* 230p locus on chromosome 3 and replaced the selectable marker (hDHFR). Southern analysis of all generated chimeric parasites showed correct integration of the *P. falciparum* expression DNA construct into the target *P. berghei 230p* gene locus in Chr-3 (**Figure 4.5 B**).

Different primers were designed to check correct 5' and 3' integration, and the absence of hdhfr::yfcu selectable marker in the transgenic parasites. Diagnostic PCR analysis confirmed the correct integration of the *P. falciparum* GIMO insertion construct in all the chimeric parasites and showed the absence of the hdhfr::yfcu marker (**Figure 4.5 C**).

A

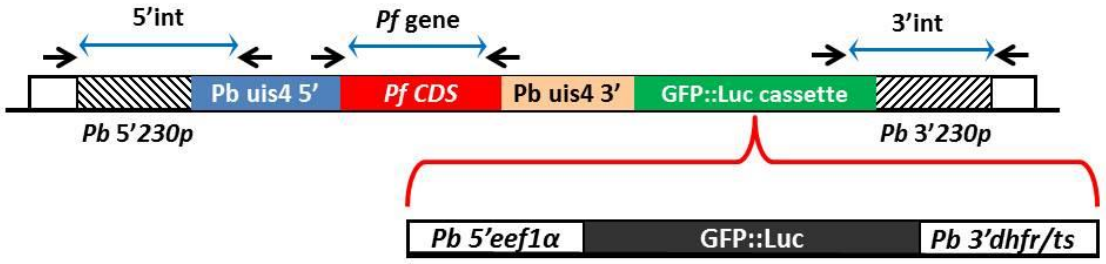

No.	Chimeric parasite name	Line #	No.	Chimeric parasite name	Line #
1	mCherry$_{Pbuis4}$	2204	7	PfLSAP-2$_{Pbuis4}$	2239 cl1
2	PfLSA-1$_{Pbuis4}$	2230 cl1	8	PfETRAMP5$_{Pbuis4}$	2241 cl1
3	PfLSA-3$_{Pbuis4}$	2263 cl2	9	PfFalstatin$_{Pbuis4}$	2280 cl2
4	PfCelTOS$_{Pbuis4}$	2231 cl1	10	PfCSP$_{Pbuis4}$	2243 cl3
5	PfUIS3$_{Pbuis4}$	2236 cl1	11	PfTRAP$_{Pbuis4}$	2281 cl1
6	PfLSAP-1$_{Pbuis4}$	2237 cl1			

B

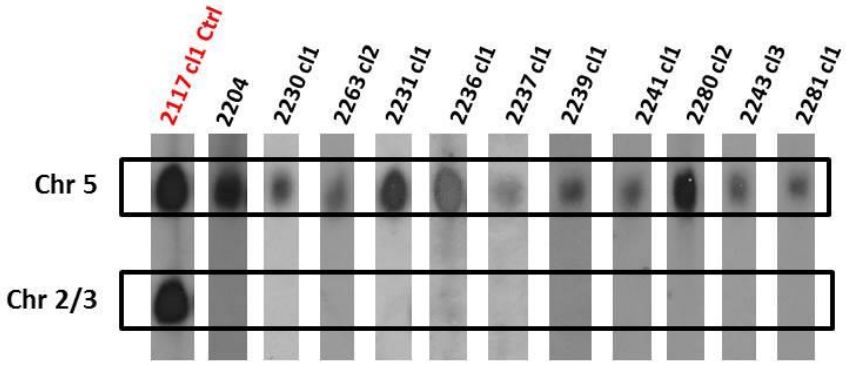

C

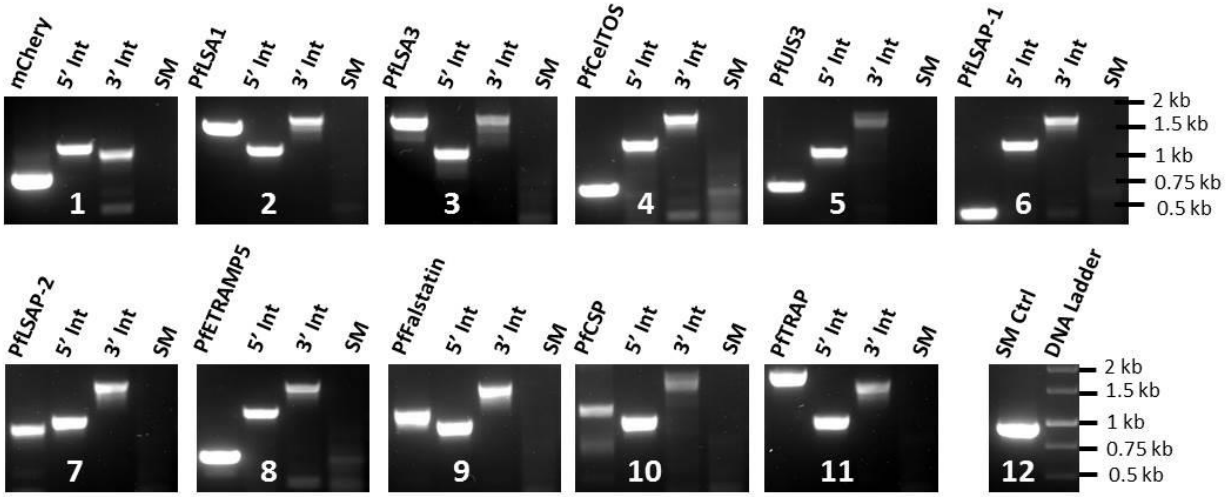

No.	Template (gDNA)	Line #	Pf gene		5'Integration		3'Integration		SM	
			F primer	R primer	F primer	R primer	F primer	R primer	F primer	R primer
			PCR Product (bp)		PCR Product (bp)		PCR Product (bp)		PCR Product (bp)	
1	$mCherry_{Pbuis4}$	2204	1084	1085	1080	1081	1082	1083	1048	1049
			714 bp		1,100 bp		1,602 bp		NA	
2	$PfLSA\text{-}1_{Pbuis4}$	2230 cl1	1086	1087	1080	1081	1051	1083	1048	1049
			1,386 bp		1,100 bp		1,602 bp		NA	
3	$PfLSA\text{-}3_{Pbuis4}$	2263 cl2	1090	1091	1080	1081	1051	1083	1048	1049
			1,472 bp		1,100 bp		1,602 bp		NA	
4	$PfCelTOS_{Pbuis4}$	2231 cl1	1092	1093	1080	1081	1051	1083	1048	1049
			560 bp		1,100 bp		1,602 bp		NA	
5	$PfUIS3_{Pbuis4}$	2236 cl1	1096	1097	1080	1081	1052	1083	1048	1049
			691 bp		1,100 bp		1,637 bp		NA	
6	$PfLSAP\text{-}1_{Pbuis4}$	2237 cl1	1098	1099	1080	1081	1051	1083	1048	1049
			347 bp		1,100 bp		1,602 bp		NA	
7	$PfLSAP\text{-}2_{Pbuis4}$	2239 cl1	1100	1101	1080	1081	1051	1083	1048	1049
			1,023 bp		1,100 bp		1,602 bp		NA	
8	$PfETRAMP5_{Pbuis4}$	2241 cl1	1102	1103	1080	1081	1051	1083	1048	1049
			546 bp		1,100 bp		1,602 bp		NA	
9	$PfFalstatin_{Pbuis4}$	2280 cl2	1104	1105	1080	1081	1051	1083	1048	1049
			1,246 bp		1,100 bp		1,602 bp		NA	
10	$PfCSP_{Pbuis4}$	2243 cl3	1011	1012	1080	1081	1052	1083	1048	1049
			1,235 bp		1,100 bp		1,637 bp		NA	
11	$PfTRAP_{Pbuis4}$	2281 cl1	1106	1107	1080	1081	1051	1083	1048	1049
			1,727 bp		1,100 bp		1,602 bp		NA	
12	SM Ctrl	2117 cl1	NA		NA		NA		1048	1049
									927 bp	

Figure 4.5 Confirmation of correct genotype for the Additional Gene [AG] chimeric *P. berghei* parasite clones expressing *P. falciparum* antigens

A. Schematic representation of the constructs used to generate the transgenic *P. berghei* parasites expressing *P. falciparum* vaccine candidate antigen (as an additional copy) under the control of a strong and specific sporozoite/liver-stage promoter (*Pbuis4*) with GFP::Luciferase fused transgenes expressed under the control of a constitutive promoter which is active for the whole parasite life cycle (*Pb*eef1α). Black arrows: location of PCR primers used for diagnostic PCR-analysis (see **C**). Primers sequences used are shown in **Table 2.3.,** while the expected PCR product sizes and the primer numbers are listed in the table below the Agarose gel images in **C**.

B. Southern analysis of chromosomes (Chr) of chimeric parasite lines separated by pulsed-field gel electrophoresis to confirm integration of the DNA construct in the GIMO locus (*230p* on Chr-3); shown as the removal of the h*dhfr::*y*fcu* SM cassette in cloned chimeric parasites. The Southern blot is hybridized with a mixture of two probes: one recognizing h*dhfr* and a control probe recognizing Chr-5. As an additional control (Ctrl), parasite line 2117cl1 is used, as it retains h*dhfr::*y*fcu* SM in the *230p* locus on Chr-3.

C. Diagnostic PCR analysis of chimeric parasite lines confirming correct integration of the *P. falciparum* antigen expression cassettes. Correct integration in all lines is shown by the absence of the h*dhfr*::y*fcu* selectable marker (SM), the presence of the *P. falciparum* gene CDS and the correct integration of the construct into the genome both at the 5' and 3'regions (5'int and 3'int). Primers sequences used are shown in **Table 2.3.,** while the expected PCR product sizes and the primer numbers are listed in the table below the Agarose gel images. The primers locations are shown in **A** (black arrows).

4.2.5 Phenotype analysis of the additional gene chimeric parasites expressing *P. falciparum* genes by Immunofluorescence assay test (IFAT)

Immunofluorescence staining showed *P. falciparum* antigen expression in sporozoites of the generated chimeric parasites. Chimeric salivary-gland sporozoites were stained with anti-PfCSP (2A10) [222, 271], anti-PbCSP (3D11) [272] monoclonal antibodies (MR4), or sera from mice vaccinated against the corresponding *P. falciparum* antigens. Bound IgG was detected with goat anti-mouse IgG-Alexa Fluor 488, green and nuclear DNA stained with 2% Hoechst-33342. As a control, wild-type (WT) *P. berghei* sporozoites were stained with the same sera. Merged images of the different channels are shown for both chimeric and WT *P. berghei* stained images (**Figure 4.6)**.

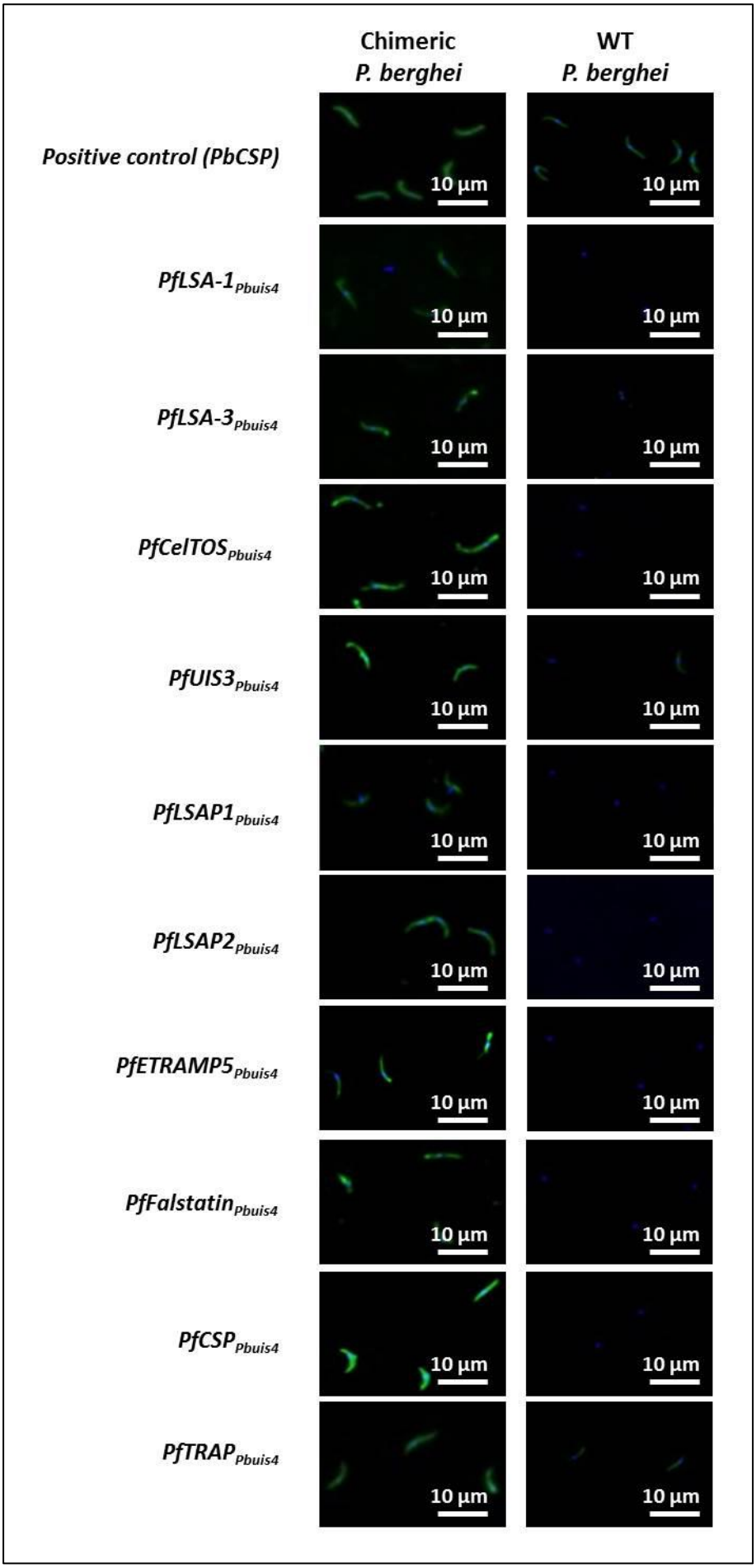
Chimeric
P. berghei
WT
P. berghei
Positive control (PbCSP)
PfLSA-1Pbuis4
PfLSA-3Pbuis4
PfCelTOSPbuis4
PfUIS3Pbuis4
PfLSAP1Pbuis4
PfLSAP2Pbuis4
PfETRAMP5Pbuis4
PfFalstatinPbuis4
PfCSPPbuis4
PfTRAPPbuis4
10 µm

Figure 4.6 Immunofluorescence analysis demonstrating *P. falciparum* antigen expression in sporozoites of chimeric *P. berghei* parasites. Chimeric salivary-gland sporozoites were stained with sera from vaccinated mice or with monoclonal antibodies where available (PbCSP 3D11 and PfCSP 210A) (Alexa Fluor 488, green) and Hoechst-33342 (blue; nuclear staining). As a control, wild-type (WT) *P. berghei* sporozoites were stained with the same antibodies or sera. Merged images of the different channels are shown for both chimeric and WT *P. berghei* stained images.

4.2.6 Transgenic parasite fitness

Parasite fitness studies indicated similar infectivity, growth rates, gametocyte production and production of oocysts and sporozoites for the chimeric parasites expressing *the P. falciparum* genes compared to those of the WT *P. berghei* line. The blood stage growth and prepatent time to reach 1% parasitaemia in naïve mice for chimeric parasites were identical to the WT *P. berghei* line, except for the *Pf*LSA3 expressing transgenic parasite which showed 75% infectivity at 1,000 sporozoite challenge dose, but by increasing the sporozoite challenge dose to 2000 sporozoites per mouse all naïve controls were infected. The chimeric parasite development and efficacy were assessed by determining parasites load in the liver using an *in vivo* imaging system to quantify luciferase, monitoring the luciferase signal levels emanating from the chimeric parasites, or by traditional blood-film calculation of RBC parasitaemias.

4.2.7 Protective efficacy of the candidate vaccines in BALB/c mice

We next assessed the protective efficacy of these *P. falciparum* vaccines in mice, through the use of the chimeric *P. berghei* sporozoites expressing the cognate *P. falciparum* antigen. We chose to screen the efficacy of our vaccines in BALB/c mice, as good immunogenicity to all antigens was observed in this strain while responses were weaker and less consistent in C57BL/6 mice (Rhea Longley, D.Phil Thesis).

Following a standard eight-week interval intramuscular vaccination regimen, mice were challenged eight days post MVA boost with 1000 chimeric sporozoites injected intravenously (i.v.). The identical vaccination-challenge experiments were also performed for the antigens PfCSP and PfTRAP, to provide comparators for the new antigens undergoing assessment.

Vaccination with PfTRAP did not induce sterile protection with this chimeric parasite model, whilst vaccination with PfCSP protected 3/8 mice (37.5%) **(Table 4.1).** In comparison, vaccination with PfLSA1 or PfLSAP2 was able to protect 7/8 mice (87.5%), a statistically significant level of sterile protection compared to their respective naïve controls ($p<0.0001$, Log-Rank (Mantel-Cox) Test). PfUIS3 induced sterile protection in 1/8 mice (12.5%), and a significant delay in the time to 1% parasitaemia compared to naïve controls (1.42 days, $p=0.004$, Log-Rank (Mantel-Cox) Test), overall $p=0.0001$, which was comparable to the level of protection induced by PfCSP vaccination (median delay of 1.47 days, $p=0.0008$, Log-Rank (Mantel-Cox) Test). Both PfFalstatin and PfLSA3 were also able to provide a significant, albeit minor, delay in the time to 1% parasitaemia (PfFalstatin: median 0.59 days, $p=0.007$. PfLSA3: median 0.35 days, $p=0.03$. Log-Rank (Mantel-Cox) Test), with PfLSA3 providing sterile protection for 1/8 mice (12.5%) (overall, $p=0.01$). PfCelTOS vaccination did not provide sterile protection from chimeric parasite challenge, and in fact a negative effect of the vaccine was seen in the delay in time to 1% parasitaemia (median -0.25 days, $p=0.03$, Log-Rank (Mantel-Cox) Test). These experiments were all repeated with the same trends and levels of statistically significant protection observed. Kaplan-Meier survival curves are shown in **(Figure 4.7).**

Table 4.1 Sterile protection and median delay induced by ChAd63-MVA *P. falciparum* vaccines in BALB/c mice.

Vaccine	Gene ID[1]	Protection (%)[2]	Median delay[3]
PfLSA1	PF3D7_1036400	87.5****	2.13
PfLSA3[4]	PF3D7_0220000	12.5*	0.35*
PfCelTOS	PF3D7_1216600	0	-0.25*
PfUIS3	PF3D7_1302200	12.5***	1.42**
PfLSAP1	PF3D7_1201300	0	0.05
PfLSAP2	PF3D7_0202100	87.5****	1.09
PfETRAMP5	PF3D7_0532100	0	0.12
PfFalstatin	PF3D7_0911900	0	0.59**
PfCSP	PF3D7_0304600	37.5****	1.47***
PfTRAP	PF3D7_1335900	0	-0.06

[1] PlasmoDB Gene ID. [2] Percentage of mice that showed sterile protection from vaccination after challenge with 1000 chimeric sporozoites i.v., n=8. [3] The median delay (days) in time to 1% parasitaemia, calculated by: (time to 1% of vaccinees) – (average time to 1% of naïve controls). The difference in survival was generated using Kaplan-Meier survival curves with statistical significance assessed using the Log-Rank (Mantel-Cox) Test, * $p<0.05$-0.01 ** $p<0.01$-0.001 *** $p<0.001$ **** $p<0.0001$. For the median delay, statistical significance was assessed after the removal of uninfected mice (sterile protection). [4] For PfLSA3 challenge, the chimeric sporozoite dose was increased to 2000 sporozoites per mouse in order to infect all naïve controls.

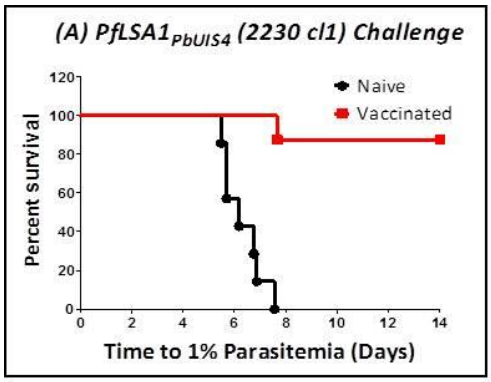
(A) PfLSA1PbUIS4 (2230 cl1) Challenge
Naive
Vaccinated
Percent survival
Time to 1% Parasitemia (Days)

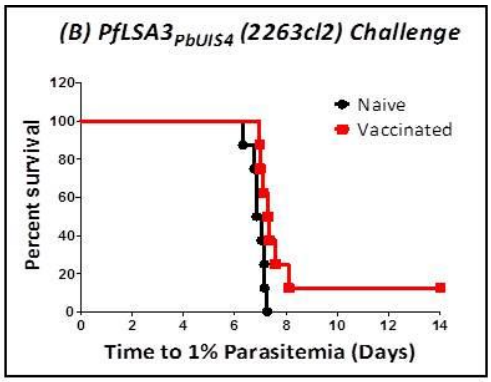
(B) PfLSA3PbUIS4 (2263cl2) Challenge
Naive
Vaccinated
Percent survival
Time to 1% Parasitemia (Days)

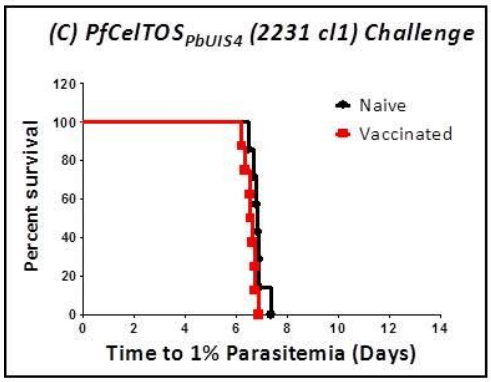
(C) PfCelTOSPbUIS4 (2231 cl1) Challenge
Naive
Vaccinated
Percent survival
Time to 1% Parasitemia (Days)

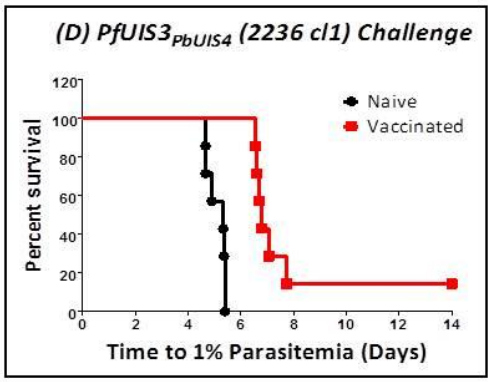
(D) PfUIS3PbUIS4 (2236 cl1) Challenge
Naive
Vaccinated
Percent survival
Time to 1% Parasitemia (Days)

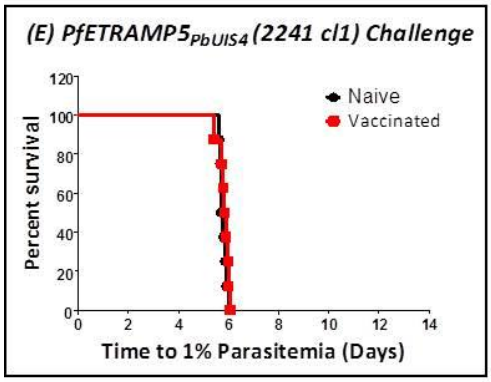
(E) PfETRAMP5PbUIS4 (2241 cl1) Challenge
Naive
Vaccinated
Percent survival
Time to 1% Parasitemia (Days)

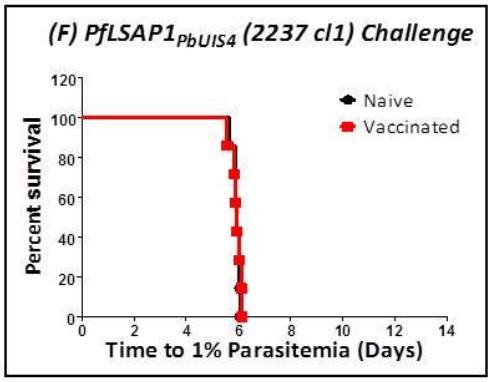
(F) PfLSAP1PbUIS4 (2237 cl1) Challenge
Naive
Vaccinated
Percent survival
Time to 1% Parasitemia (Days)

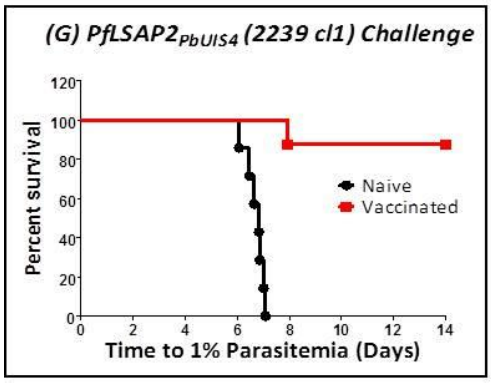
(G) PfLSAP2PbUIS4 (2239 cl1) Challenge
Naive
Vaccinated
Percent survival
Time to 1% Parasitemia (Days)

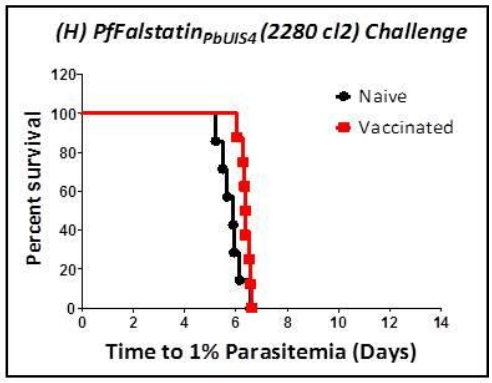
(H) PfFalstatinPbUIS4 (2280 cl2) Challenge
Naive
Vaccinated
Percent survival
Time to 1% Parasitemia (Days)

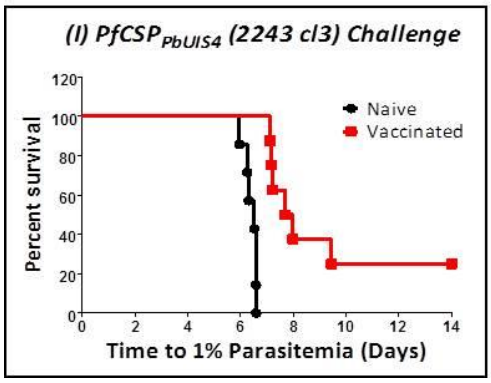
(I) PfCSPPbUIS4 (2243 cl3) Challenge
Naive
Vaccinated
Percent survival
Time to 1% Parasitemia (Days)

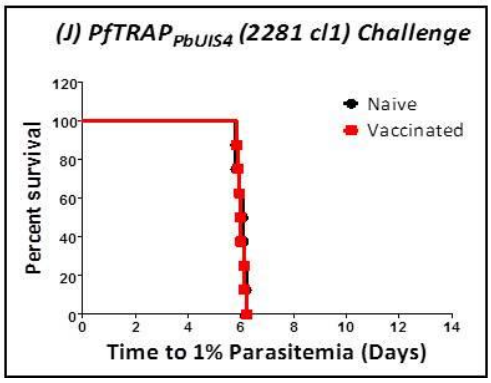
(J) PfTRAPPbUIS4 (2281 cl1) Challenge
Naive
Vaccinated
Percent survival
Time to 1% Parasitemia (Days)

Figure 4.7 Efficacy of the ChAd63-MVA *P. falciparum* vaccines in BALB/c inbred mice. BALB/c mice (n=8 vaccinated and 8 naive) were challenged with 1000 chimeric sporozoites i.v. as previously described. The Kaplan-Meier curve illustrates the time to 1% parasitaemia, whilst statistical significance between the survival curves was assessed using the Log-Rank (Mantel-Cox) Test, (**A**) PfLSA1 p<0.0001, (**B**) PfLSA3 p=0.01, (**C**) PfCelTOS p=0.03, (**D**) PfUIS3 p=0.0001, (**E**) PfETRAMP5 p=0.3 (**F**) PfLSAP1 p=0.2, (**G**) PfLSAP2 p<0.0001, (**H**) PfFalstatin p=0.007, (**I**) PfCSP p=0.03, and (**J**) PfTRAP p=0.3. For the PfLSA3 challenge, the chimeric sporozoite dose was increased to 2000 sporozoites per mouse in order to infect all naïve controls.

4.2.8 Mechanism of protective efficacy in BALB/c inbred mice

P. falciparum antigen expression is under the control of the UIS4 promoter in the chimeric parasite, leading to expression both on sporozoites and during the liver stage **(Figure 4.3)** [276], so protection could be mediated via inhibition of sporozoite invasion and/or killing of infected hepatocytes. Because PfLSA1, PfLSAP2, PfUIS3 and PfFalstatin all induced both a humoral and cellular response in BALB/c mice, we depleted mice $CD8^+$ and $CD4^+$ T cells prior to challenge to determine the relative contribution of each population to protection.

Protection afforded by vaccination with PfUIS3 was shown to be dependent on the presence of $CD8^+$ T cells, since no protection was observed when the $CD8^+$ subset was depleted compared to naïve mice, but there was a significant difference compared to the IgG control group (p<0.0001, Log-Rank (Mantel-Cox) Test) **(Figure 4.8 A).** $CD8^+$ T cell depletion reduced the median delay in time to 1% parasitaemia from 7.37 days in the IgG control group to 5.57 days (p<0.001, Log-Rank (Mantel-Cox) Test). $CD4^+$ T cells were shown to contribute only partly towards protection, as whilst there was reduced protection compared to the IgG control group (p=0.004, Log-Rank (Mantel-Cox) Test), the $CD4^+$ depleted group still provided some protection compared to naïve mice (median of 6.45 days compared to 5.47 days, p<0.0001, Log-Rank (Mantel-Cox) Test).

For PfLSA1 vaccination, the contribution of $CD8^+$ T cells was not as clear **(Figure 4.8 B).** $CD8^+$ depletion reduced protection from 4/7 (57.1%) in the IgG control group to 1/8 (12.5%), but this difference did not reach statistical significance (p=0.07, Log-Rank (Mantel-Cox) Test). Only 2/8 (25%) mice were protected after $CD4^+$ depletion, however again this was not significant compared to the IgG control group (p=0.3, Log-Rank (Mantel-Cox) Test). There was a significant difference between $CD4^+$ depleted mice and the naïve control group (p=0.0003, Log-Rank (Mantel-Cox) Test), suggesting a subset other than $CD4^+$ T cells was mediating protection, most likely $CD8^+$ T cells.

For PfLSAP2 vaccination, protection was dependent on the presence of $CD8^+$ T cells **(Figure 4.8 C).** $CD8^+$ depletion reduced protection from 6/8 (75%) in the IgG control group to 1/8 (12.5%) (p=0.03, Log-Rank (Mantel-Cox) Test) and there was no statistically significant difference between the $CD8^+$ depleted group and naïve mice. $CD4^+$ T cells did not appear to play a protective role following vaccination with PfLSAP2, since no significant difference compared to the IgG control group was observed, with 5/8 (62.5%) mice remaining sterilely protected. Furthermore, there was a statistically significant difference between the $CD4^+$ depleted group and naïve mice (p=0.01, Log-Rank (Mantel-Cox) Test).

For PfFalstatin vaccination, $CD8^+$ and $CD4^+$ depleted groups showed no statistically significant delay to reach 1% parasitaemia compared to the naïve or IgG control group (Log-Rank (Mantel-Cox) Test) **(Figure 4.8 D)**. This would suggest that both $CD8^+$ and $CD4^+$ T cells play a role in the delay to reach 1% parasitaemia.

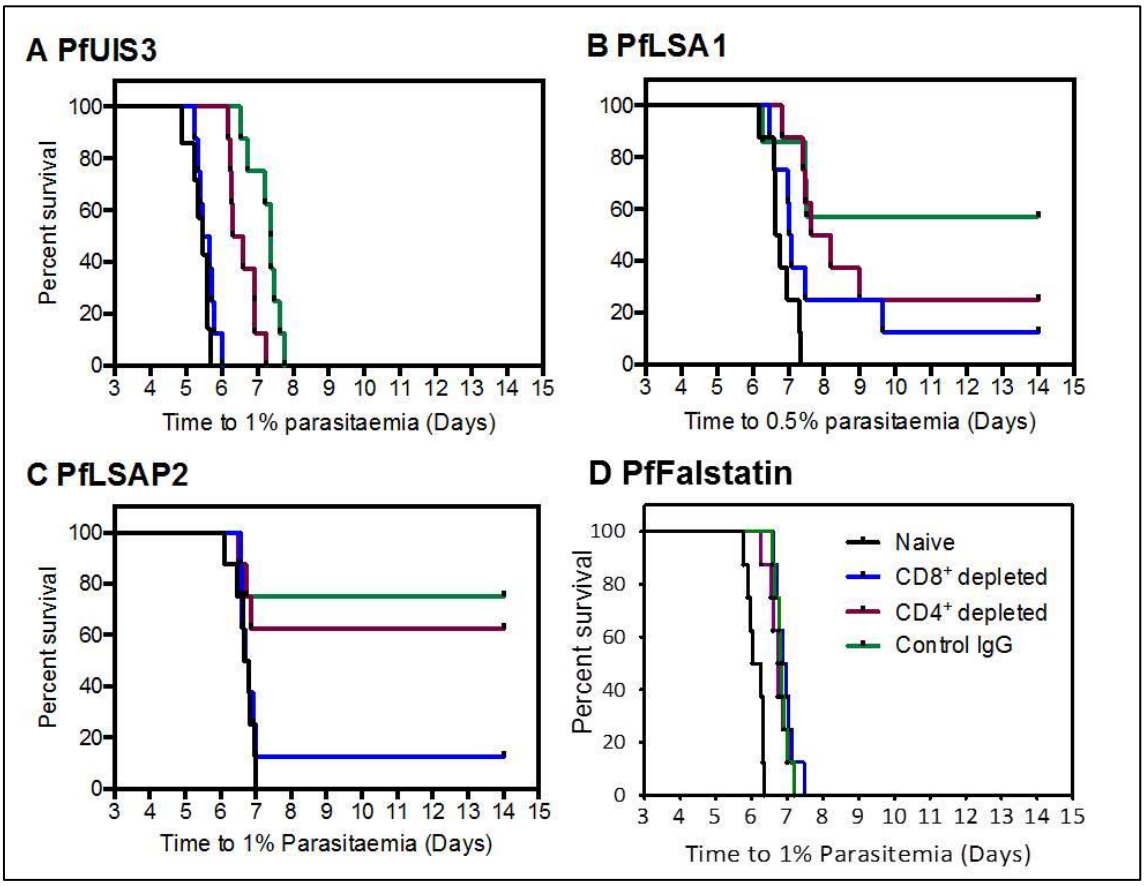

Figure 4.8 Mechanism of protective efficacy of ChAd63-MVA PfUIS3, PfLSA1 and PfLSAP2 vaccination in BALB/c mice.

Mice (n=7-8 per group) were injected with the appropriate monoclonal antibody to deplete $CD4^+$ or $CD8^+$ T cells and challenged with 1000 chimeric parasites i.v. ten days after ChAd63-MVA vaccination as previously described. Kaplan-Meier curves illustrate the time to 0.5 or 1% parasitaemia in vaccinated and control mice. (**A**) The Log-Rank (Mantel-Cox) Test was used to determine statistical significance between groups of PfUIS3 vaccinated mice. $CD8^+$ depleted vs naïve, NS. $CD8^+$ depleted vs control IgG, $p<0.0001$. $CD4^+$ depleted vs naïve, $p<0.0001$. $CD4^+$ depleted vs control IgG, $p=0.004$. In this experiment the MVA dose was reduced to $5x10^6$ pfu to allow all experiments to be performed using the same vaccine batch. (**B**) The Log-Rank (Mantel-Cox) Test was used to determine statistical significance between groups of PfLSA1 vaccinated mice. $CD8^+$ depleted vs naïve, NS. $CD8^+$ depleted vs control IgG, NS. $CD4^+$ depleted vs naïve, $p=0.0003$. $CD4^+$ depleted vs control IgG, NS. (**C**) The Log-Rank (Mantel-Cox) Test was used to determine statistical significance between groups of PfLSAP2 vaccinated mice. $CD8^+$ depleted vs naïve, NS. $CD8^+$ depleted vs control IgG, $p=0.03$. $CD4^+$ depleted vs naïve, $p=0.01$. $CD4^+$ depleted vs control IgG, NS. (**D**) The Log-Rank (Mantel-Cox) Test was used to determine statistical significance between groups of PfFalstatin vaccinated mice. $CD8^+$ depleted vs naïve, NS. $CD8^+$ depleted vs control IgG, NS. $CD4^+$ depleted vs naïve, NS. $CD4^+$ depleted vs control IgG, NS.

4.2.9 In vivo imaging for quantification of chimeric parasite load during the liver-stage using live animal imaging

In the challenge experiments, *in vivo* imaging of mice was also performed using the IVIS 200 imaging system to measure the parasite load 44 hours post-infection. Mann Whitney test were used to assess the statistical significance in luciferase expression level (parasite liver load) between naïve and vaccinated mice**.** Results are presented as the total flux measured per second. Both median and individual data points are shown (**Figure 4.9**)**.** PfLSA1 (p=0.0022), PfUIS3 (p=0.0021), and PfCSP (p=0.0011) were the only vaccines that showed statistically significant decreases in the parasite liver loads in vaccinated mice. While the other vaccines including PfLSAP-2 (p=0.6849) showed no significant difference between the vaccinated and the naïve groups. The luciferase activity of the PfLSA3 transgenic parasite was not tested because of initial infectivity problem at the time of performing this experiment with 1000 sporozoites.

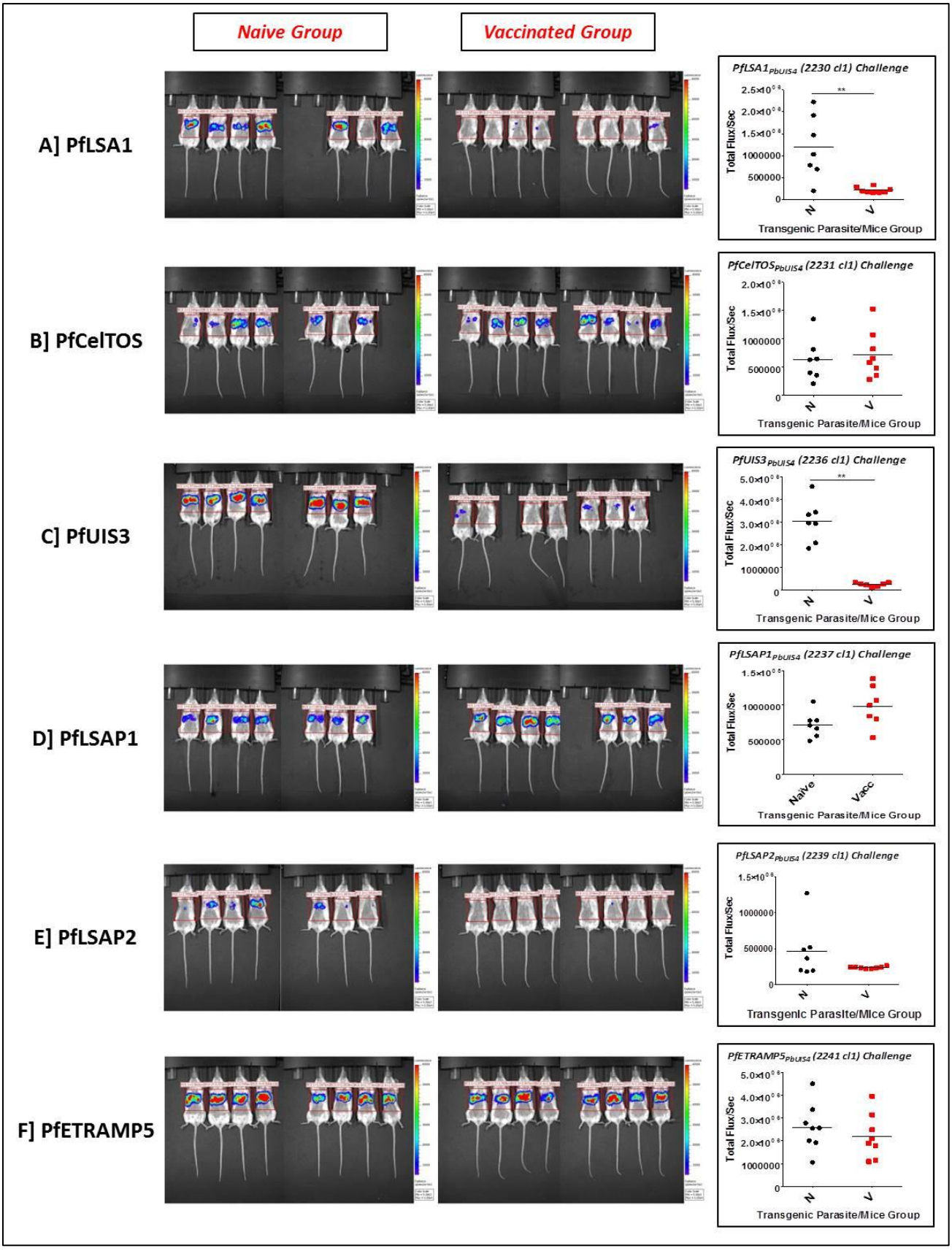
Naive Group
Vaccinated Group
A] PfLSA1
B] PfCelTOS
C] PfUIS3
D] PfLSAP1
E] PfLSAP2
F] PfETRAMP5
PfLSA1PbUIS4 (2230 cl1) Challenge
PfCelTOSPbUIS4 (2231 cl1) Challenge
PfUIS3PbUIS4 (2236 cl1) Challenge
PfLSAP1PbUIS4 (2237 cl1) Challenge
PfLSAP2PbUIS4 (2239 cl1) Challenge
PfETRAMP5PbUIS4 (2241 cl1) Challenge
Total Flux/Sec
N
V
Naive
Vacc
Transgenic Parasite/Mice Group

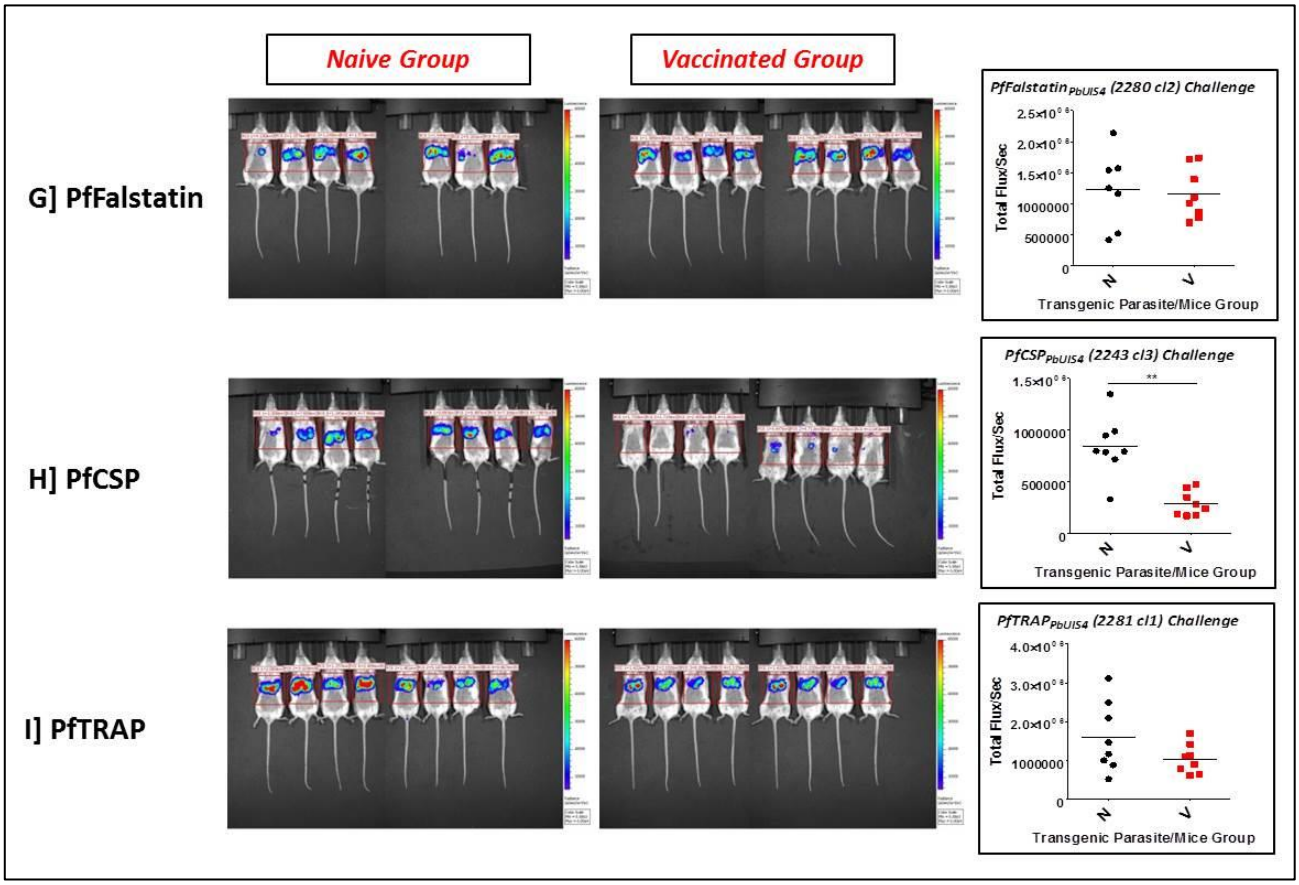

Figure 4.9 *In vivo* imaging. Liver loads in naïve and immunized mice that were challenged with transgenic chimeric sporozoites were quantified by measuring luminescence levels at 44 hours after infection using the IVIS 200 system as described earlier in the Material and Method section **2.5.5** (i.e.: reduction in liver load corresponds to protective immunity). Mann Whitney test was used to assess the statistical significance in the luciferase expression level (parasite liver load) between the naïve and vaccinated mice groups**.** Results are presented as the total flux measured per second. Both median and individual data points are shown.

(A) PfLSA1: significant difference was seen (p=0.0022), **(B) PfCelTOS:** no significant difference was seen (p=0.6943), **(C) PfUIS3:** significant difference was seen (p=0.0021), **(D) PfLSAP1:** no significant difference was seen (p=0.0530), (**E) PfLSAP2** : no significant difference was seen (p=0.6849), **(F) PfETRAMP5 :** no significant difference was seen (p=0.3823), **(G) PfFalstatin**: no significant difference was seen (p=0.8665), **(H) PfCSP :** significant difference was seen (p=0.0011), **(I) PfTRAP :** no significant difference was seen (p=0.2345). **PfLSA3**: is missing in this figure since the transgenic parasite had some infectivity issues at the time of performing this experiment using 1,000 sporozoites as a challenge dose.

4.2.10 Protective efficacy of the candidate vaccines in CD-1 outbred mice

I assessed the ability of *P. falciparum* vaccine candidates in CD-1 outbred mice following the standard prime-boost, eight-week interval ChAd63-MVA vaccination regime. PfLSA1 vaccination protected 7/8 (87.5%) CD-1 mice from chimeric sporozoite challenge, resulting in a significant level of survival compared to naïve controls ($p<0.0001$, Log-Rank (Mantel-Cox) Test). PfLSAP2 protected 7/10 (70%) CD-1 mice challenged with chimeric sporozoites, a significant level of protection compared to naïve controls ($p=0.0009$, Log-Rank (Mantel-Cox) Test. PfUIS3 vaccination was unable to significantly protect CD-1 mice against challenge, despite an initial trend (median of 6.77 days compared to 5.67 days in naïve controls).

As PfCSP and PfTRAP acted as our comparator vaccines, we also assessed their efficacy in CD-1 mice, in order to bypass the tight MHC restriction and immunodominance observed in inbred strains of mice. Following the standard ChAd63-MVA regimen, PfCSP was able to protect 3/9 (33.3%) CD-1 mice and induced a delay in time to 1% parasitaemia by a median 0.48 days (overall $p=0.001$, Log-Rank (Mantel-Cox) Test) (Table 2), similar to the induced efficacy in BALB/c mice. PfTRAP was able to protect 3/10 (30%) CD-1 mice but did not cause a delay in the time to 1% parasitaemia in those for which sterile protection was not induced ($p=0.02$, Log-Rank (Mantel-Cox) Test) **(Figure 4.10)**. PfTRAP provided protection against chimeric sporozoite challenge in CD-1 mice; this was despite the lack of any sterile protection observed in BALB/c mice. Therefore we subsequently assessed efficacy of the remaining antigens (those modestly protective or non-protective in BALB/c) in CD-1 mice to ensure no potential candidates were missed. For PfFalstatin and PfLSA3, which both had provided a small degree of protection in BALB/c mice, a degree of protection was maintained with PfFalstatin in CD-1 mice, with 1/10 (10%) sterilely protected and the rest exhibiting a significant delay in the time to 1% parasitaemia (median delay of 0.97 days, $p<0.0001$, Log-Rank (Mantel-Cox)

Test). For PfLSA3, this effect was not maintained as no protection was observed in CD-1 mice. Of those vaccines that did not induce protection in BALB/c mice, PfCelTOS, PfLSAP1 and PfETRAMP5, none subsequently induced a statistically significant level of protection in CD-1 mice (Table 4.2).

Table 4.2 Sterile protection and median delay induced by ChAd63-MVA *P. falciparum* vaccines in CD-1 mice.

Vaccine	**Protection (%)[1]**	**Median delay[2]**
PfLSA1	87.5****	2
PfLSA3[3]	0	0.22
PfCelTOS	0	0.28
PfUIS3	0	1.1
PfLSAP1	30	0
PfLSAP2	70***	0.29
PfETRAMP5	10	0
PfFalstatin	10****	0.97****
PfCSP	33.3**	0.48*
PfTRAP	30*	0.03

[1] Percentage of mice that received sterile protection from vaccination after challenge with 1000 chimeric sporozoites i.v., n=8-10. [2] The median delay (days) in time to 1% parasitaemia, calculated by: (time to 1% of vaccinee) – (average time to 1% of naïve controls). The difference in survival was generated using Kaplan-Meier survival curves with statistical significance assessed using the Log-Rank (Mantel-Cox) Test, * $p<0.05$-0.01 ** $p<0.01$-0.001 *** $p<0.001$ **** $p<0.0001$. For the median delay, statistical significance was assessed after the removal of uninfected mice (sterile protection). [3] For PfLSA3 challenge, the chimeric sporozoite dose was increased to 2000 sporozoites per mouse in order to infect all naïve controls.

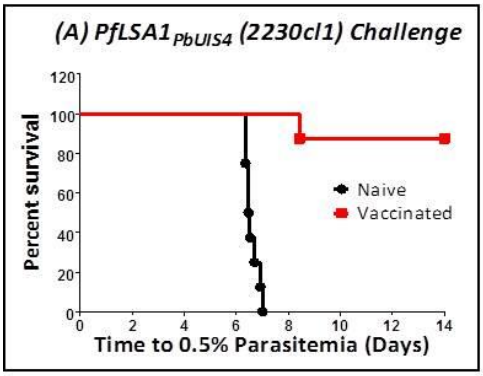
(A) PfLSA1 PbUIS4 (2230cl1) Challenge
Percent survival
Time to 0.5% Parasitemia (Days)
Naive
Vaccinated

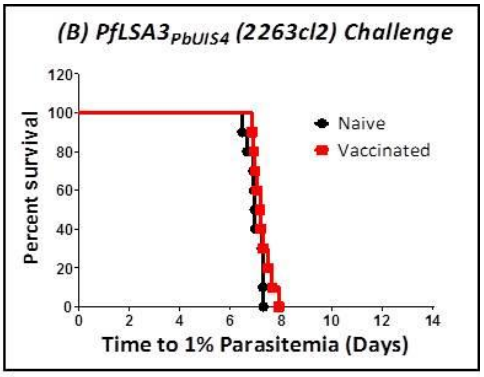
(B) PfLSA3 PbUIS4 (2263cl2) Challenge
Percent survival
Time to 1% Parasitemia (Days)
Naive
Vaccinated

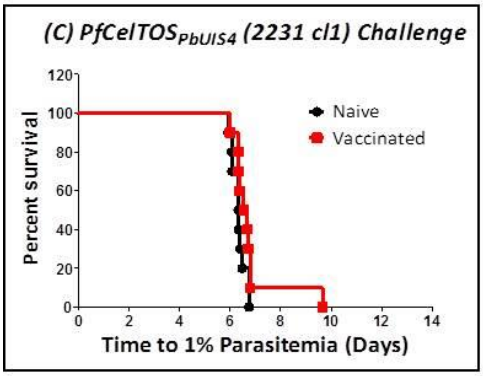
(C) PfCelTOS PbUIS4 (2231 cl1) Challenge
Percent survival
Time to 1% Parasitemia (Days)
Naive
Vaccinated

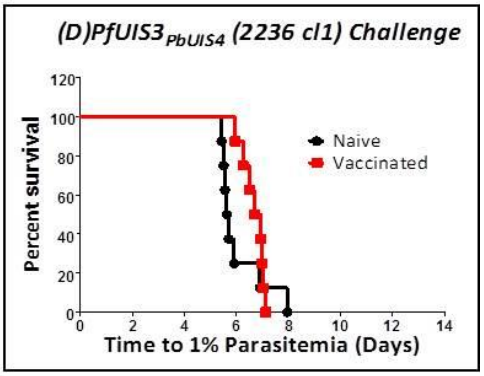
(D)PfUIS3 PbUIS4 (2236 cl1) Challenge
Percent survival
Time to 1% Parasitemia (Days)
Naive
Vaccinated

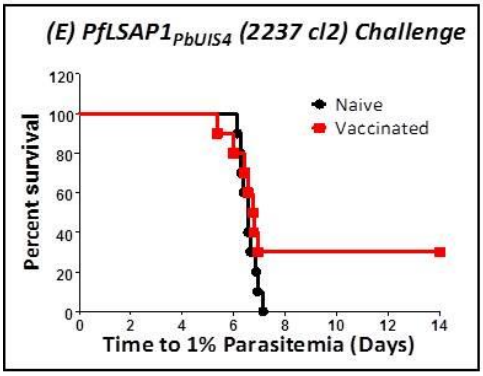
(E) PfLSAP1 PbUIS4 (2237 cl2) Challenge
Percent survival
Time to 1% Parasitemia (Days)
Naive
Vaccinated

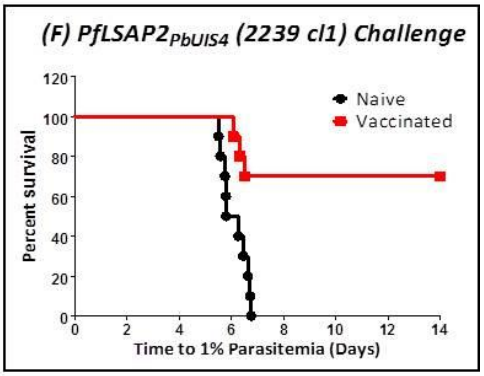
(F) PfLSAP2 PbUIS4 (2239 cl1) Challenge
Percent survival
Time to 1% Parasitemia (Days)
Naive
Vaccinated

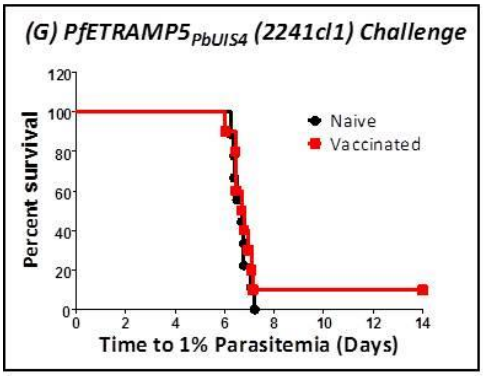
(G) PfETRAMP5 PbUIS4 (2241cl1) Challenge
Percent survival
Time to 1% Parasitemia (Days)
Naive
Vaccinated

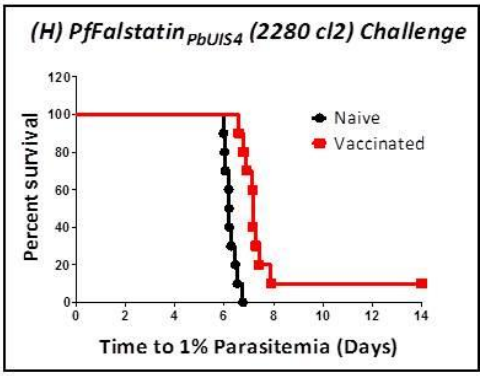
(H) PfFalstatin PbUIS4 (2280 cl2) Challenge
Percent survival
Time to 1% Parasitemia (Days)
Naive
Vaccinated

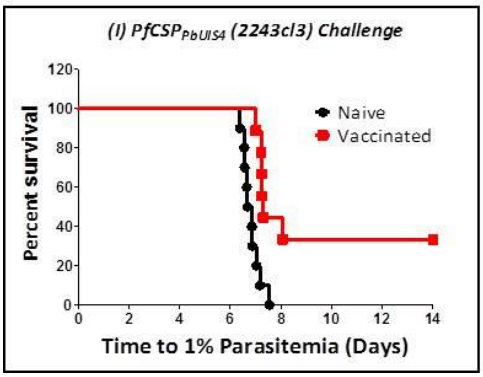
(I) PfCSP PbUIS4 (2243cl3) Challenge
Percent survival
Time to 1% Parasitemia (Days)
Naive
Vaccinated

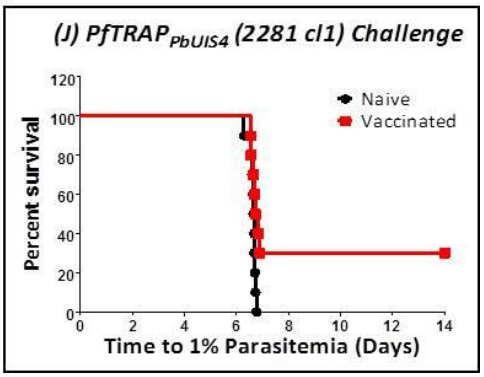
(J) PfTRAP PbUIS4 (2281 cl1) Challenge
Percent survival
Time to 1% Parasitemia (Days)
Naive
Vaccinated

Figure 4.10 Efficacy of the ChAd63-MVA *P. falciparum* vaccines in CD-1 outbred mice. CD-1 mice (n=8-10 vaccinated and 8-10 naive) were challenged with 1000 chimeric sporozoites i.v. The Kaplan-Meier curves illustrate the time to 0.5% or 1% parasitaemia, whilst statistical significance between the survival curves was assessed using the Log-Rank (Mantel-Cox) Test: **(A) PfLSA1** p<0.0001, **(B) PfLSA3** p=0.1506, **(C) PfCelTOS** p=0.0971, **(D) PfUIS3** p=0.2518, **(E) PfLSAP1** p=0.1564, **(F) PfLSAP2** p=0.0.0009, **(G) PfETRAMP5** p=0.4548, **(H) PfFalstatin** p<0.0001, **(I) PfCSP** p=0.0011, and **(J) PfTRAP** p=0.0227. For the PfLSA3 challenge, the chimeric sporozoite dose was increased to 2000 sporozoites per mouse in order to infect all naïve controls.

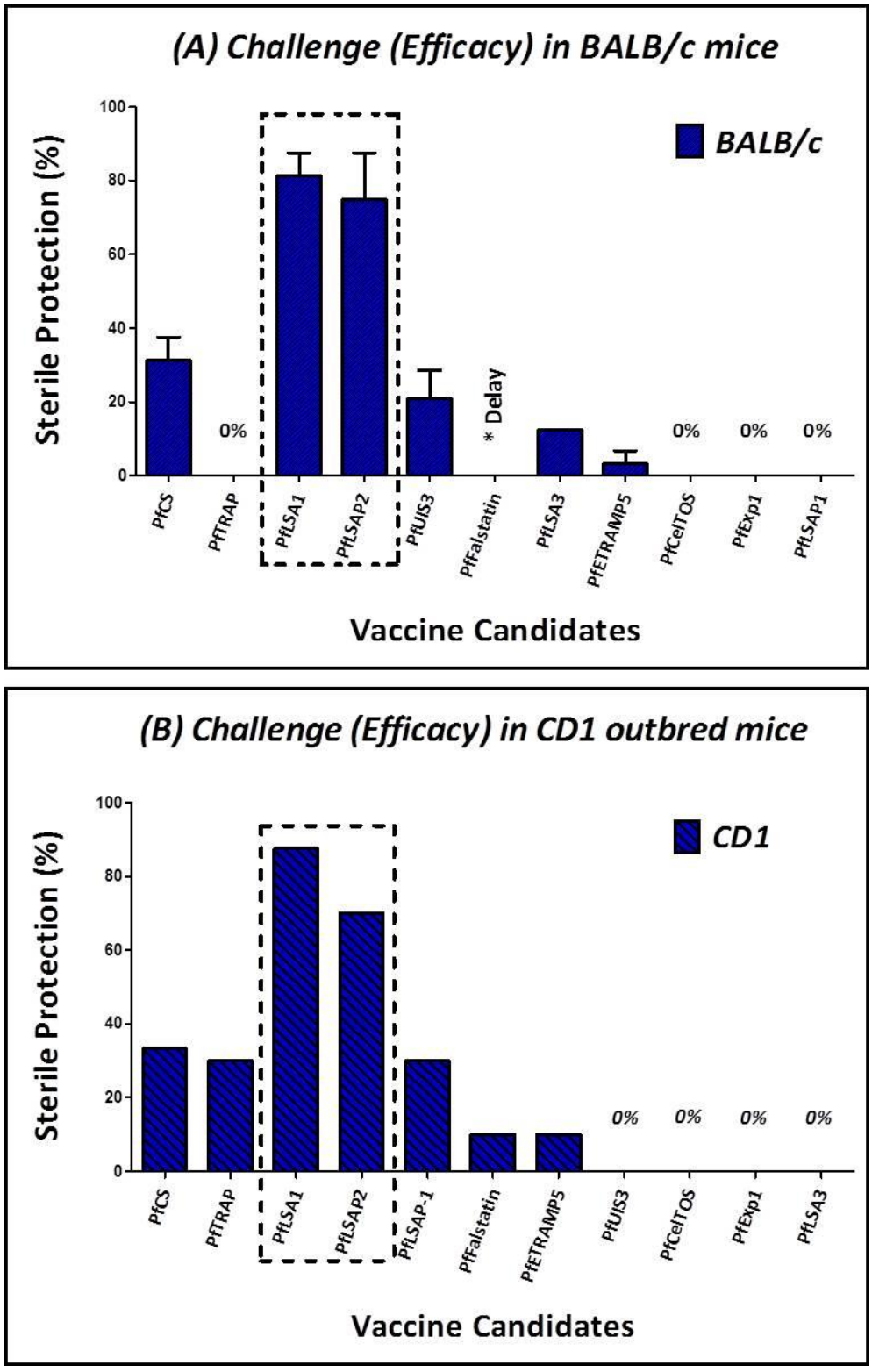

Figure 4.11 The protective efficacy Rank/order of the eight novel *P. falciparum* viral vector vaccine candidates compared to the current two leading malaria vaccines PfCSP and PfTRAP using the transgenic parasite challenging model. Strong protective immunity against PfLSA1 and PfLSAP2 in both (A) inbred BALB/c, and (B) outbred CD1 mice.

4.3 Discussion

Current pre-erythrocytic sub-unit vaccines undergoing clinical assessment are based on a very small repertoire of antigens, namely PfCSP and PfTRAP. Our results demonstrate that alternative antigen candidates may be better targets for a liver-stage malaria vaccine. We found that viral vectored vaccines expressing either PfLSA1 or PfLSAP2 substantially and significantly outperformed both PfCSP and PfTRAP when expressed in the same vaccination platform. Both PfLSA1 and PfLSAP2 sterilely protected 87.5% of BALB/c mice, compared to 37.5% efficacy for PfCSP and 0% efficacy for PfTRAP. Vaccination with PfLSA1 or PfLSAP2 also provided greater than 70% protection in outbred mice, more than that induced by PfCSP (33%) or PfTRAP (30%). Vaccination with PfUIS3, PfFalstatin and PfLSA3 in BALB/c mice provided some degree of protection, manifest largely as a delay in the time to parasitaemia, consistent with previous work with using murine *Plasmodium* challenges [206, 211]. Protection was also induced at a low level for PfFalstatin in outbred mice. Surprisingly, no protection was observed after vaccination with PfCelTOS despite previous reports of cross-species protection in murine models [195, 274].

This study again highlights the capacity of viral vectored vaccines to induce strong cellular immunogenicity. Immune responses were predominantly from $CD8^+$ T cells secreting IFNγ, TNFα or with upregulated expression of the cytotoxicity marker CD107a. Whilst correlates of protection were difficult to determine when the large majority of mice were protected, the depletion experiments highlighted a strong dependence on $CD8^+$ T cells for protection when vaccinating with either PfLSA1 or PfUIS3, and complete dependence following PfLSAP2 vaccination. PfLSA1, PfUIS3 and PfLSAP2 are all likely located in the parasitophorous vacuole membrane (PVM) [214, 292, 293], and therefore are likely good targets for a cell-mediated immune response because antigens that reach the PVM or host cell cytoplasm may be better presented at the

hepatocyte surface on MHC class I molecules [294]. Recent work using a model antigen expressed in *P. berghei* sporozoites found that exported antigen(s) improved the elimination of infected liver cells by antigen-specific $CD8^+$ T cells [295]. Our findings indicate that the antigenic target is of high importance, as hypothesized, and suggest that both PfLSA1 and PfLSAP2 are potentially better candidates than PfCSP or PfTRAP for a pre-erythrocytic vaccine.

Whilst none of the immunological measures applied could explain the difference in protection between PfUIS3, PfLSAP2 and PfLSA1, the significant delay to reach 1% parasitaemia with PfFalstatin, or why particular antigens were protective and others were not, the functional roles of these proteins give some clues. Little is known about PfLSAP2 [214, 296]; this study is the first report of this antigen as a target in a malaria vaccine and hence the current findings warrant further assessment of the functional role of this antigen. PfLSA1, however, was one of the first liver-stage antigens identified [202], is known to be well conserved amongst *P. falciparum* isolates [297, 298] and essential for late liver-stage development [299]. PfLSA1 is thought to be involved in the transition from the liver-stage to the blood-stage, as it is expressed abundantly in the PV as flocculent material surrounding merozoites. Cellular responses to PfLSA1 have been associated with protection in studies of naturally acquired immunity and in volunteers vaccinated with irradiated sporozoites [95, 96, 203, 300-304], yet a clinical trial of recombinant protein PfLSA1 provided no protection against sporozoite challenge [287], most likely due to the absence of induced $CD8^+$ T cells. PfUIS3, also known as PfETRAMP13 [305], is likely essential for liver-stage growth and development, based on studies with PbUIS3 deficient parasites [212], potentially through importation of fatty acids to the PVM [293, 306, 307].

Both PfLSA1 and PfLSAP2 have no known murine homologue, and hence the classical method of pre-clinical testing using rodent homologues of *P. falciparum* antigens as vaccine candidates would not have been able to identify these as

protective, highlighting the value of this chimeric parasite system. There are, however, a number of limitations with this model. First, despite the use of chimeric parasites it is still a murine model and encounters issues of small numbers of MHC restricted epitopes and marked immunodominance, which is less prominent in outbred human populations. Outbred mice can be used to more accurately reflect what may be seen in a human study and importantly, efficacy with PfLSA1 and PfLSAP2 was here maintained in CD-1 mice. This is also likely why PfTRAP was unable to provide any protection in BALB/c mice, but provided sterile protection in 30% of CD-1 mice. Second, the *P. falciparum* antigen is under control of the *P. berghei* UIS4 promoter. Whilst this places all antigens on an even level, in terms of expression, it will be important to also compare efficacy when expression levels are matched as far as possible to those observed with the native *P. falciparum* parasite. However, this approach is not readily applicable to the most protective antigens identified, which have no *P. berghei* homologue. As a proof of concept study, multiple vaccines were developed that induced greater levels of efficacy than PfCSP or PfTRAP, and hence further antigens warrant assessment in the same system. To further evaluate the model we have used, efficacy could be assessed in the recently described humanized mouse system [308-310] or using *in vitro* assays [66, 111, 311, 312]. However, both methods are technically challenging, whilst the production of chimeric rodent malaria parasites has recently become more routine. A better validation would be the demonstration of greater efficacy from PfLSA1 and PfLSAP2 than PfCSP or PfTRAP in a human trial.

This work provides appropriate support for the progression of ChAd63-MVA PfLSA1 to clinical assessment. PfLSA1 provided 87.5% sterile protection in outbred mice (greater than any other sub-unit vaccine has achieved pre-clinically), protection was $CD8^+$ T cell dependent and the level of $CD8^+$ T cells required was of a moderate magnitude that should be achievable in humans with viral vectors, based on previous studies [313, 314]. Furthermore, anti-

PfLSA1 cytokine responses have been associated with protection in field studies [95, 96, 203, 302-304]. PfLSPA2 also warrants clinical assessment, however further pre-clinical work to uncover its functional role is also required. If the protective effect of ChAd63-MVA PfLSA1 or PfLSAP2 is confirmed in efficacy trials of non-immune adults, this would pave the way for a new generation of malaria vaccines incorporating multiple protective antigens that may be identified with this attractive new pre-clinical screening method.

The utility of this *P. falciparum* expressing *P. berghei* transgenic parasite challenging model to rank/order new *P. falciparum* antigens is highlighted by the results presented in **Figure 4.11** where 2 new antigens (*Pf*LSA1 and *Pf*LSAP2) have shown high levels of efficacy in mice which is greater than efficacy achieved with the leading vaccine candidates *Pf*TRAP and *Pf*CSP. Results indicate the feasibility of this approach to find more protective vaccine candidates than the current leading vaccines, since both *Pf*LSA1 and *Pf*LSAP2 have shown better efficacy than *Pf*TRAP and *Pf*CSP in both inbred and outbred mice. In summary, transgenic parasites can successfully be used to screen *P. falciparum* liver-stage vaccines. The transgenic *P. berghei* ANKA expressing *P. falciparum* antigen system appears to be a very powerful experimental model for screening *P. falciparum* malaria vaccines *in vivo.*

Chapter 5

Double Chimeric Parasites: design, generation, characterization and their use as challenge models to assess malaria vaccine combinations.

5 Double Chimeric Parasites: design, generation, characterization and their use as challenge models to assess malaria vaccine combinations.

5.1 Introduction

Despite ongoing efforts to develop a single antigen subunit vaccine against malaria, many speculate that the first highly efficacious subunit vaccine against these protozoan parasites will need to incorporate multiple antigens, targeting a single and/or multiple stages of parasite development. The attempts to combine multiple antigens using subunit vaccines have demonstrated varying levels of success compared to the single antigen vaccines, in studies performed in different *Plasmodium* species, like *P. knowlesi* [315] and *P. yoelii* [211, 316]. The rationale for the manufacture of multi-antigen vaccine regimens is because of the Plasmodium complex life cycle and the massive diversity in most antigens in parasite populations in addition to the fact that single antigen vaccinations may not induce the broad immune responses necessary to protect heterogeneous populations of people and also cover the natural polymorphisms of the vaccine antigen. Therefore, incorporating two or more antigens in the vaccination regimen could elicit a broader immune response increasing vaccine efficacy. However, it has been reported that vaccinating with vaccines comprise of multiple-antigens vaccines can have an antagonistic effect and may reduce protective efficacy, due to antigenic interference [317, 318].

The previous chapters have demonstrated the benefit of using transgenic rodent malaria parasites that express *P. falciparum* proteins to assess and rank the protective efficacy of novel *P. falciparum* vaccines in murine models. In these studies we challenged immunized mice with transgenic parasites that express the corresponding (single) *P. falciparum* antigen. For studies on vaccines consisting of multiple antigens, it would be therefore advantageous if transgenic parasites could be generated that express multiple *P. falciparum* vaccine-candidate antigens. A current limitation in the generation of transgenic parasites that contain multiple additional *P. falciparum* genes (AG transgenic

parasite) is the identification of suitable neutral insertion loci in *P. berghei* genome, which can be used to introduce transgenes.

Most transgenic *P. berghei* containing additional genes that encode fluorescent or luminescent reporter proteins, have been generated by introducing the genes into the silent *p230p* locus or in the *c*- or d-*small unit ribosomal* gene locus [249]. Introducing genes in the ribosomal c- or d-unit gene locus may affect oocyst and sporozoite development and is therefore preferred less than the *p230p* locus for studies that require optimal sporozoite production. In *P. yoelii* a neutral locus for introducing additional genes , the *Pys1* gene (PY05712) has been described [250] having first been identified by Kaiser et al. [63]. The *s1* gene has an orthologue in *P. berghei; Pbs1* (PBANKA_120680) located on chromosome 12. In this study we have generated and analysed a *P. berghei* mutant that lacks expression of *Pbs1* (mutant 2149cl1) and show that this locus is also a neutral locus in *P. berghei*. This new *P. berghei* 'neutral' locus was subsequently used to introduce additional *P. falciparum* genes (as additional copies) by using a novel construct (pL2023) that targets and stably integrates into the *s1* locus by double cross-over recombination. This additional locus enabled us to generate double transgenic parasites expressing two *P. falciparum* antigens; the first *P. falciparum* gene is introduced in the *p230p* locus and the second gene into the *s1* locus.

Using the results from the initial assessment of *P. falciparum* candidate antigens, for their immunogenicity and protective efficacy (Chapter-4) we generated two double transgenic parasites. One expresses the two most promising novel vaccine candidates, *Pf*LSA1 and *Pf*LSAP2 and, as a control, one that expresses the two current leading vaccine candidate antigens, *Pf*CSP and *Pf*TRAP.

Consequently, the four *P. falciparum* vaccine candidates (*Pf*CSP, *Pf*TRAP, *Pf*LSA1 and *Pf*LSAP2) were used to immunize mice, either alone or in different

combinations using the ChAd63-MVA prime-boost regimen, and the protective efficacy of these different combinations was assessed by challenging immunized mice with the corresponding double *P. berghei* transgenic malaria parasite.

5.2 Results

5.2.1 Generation, fitness and genotype analysis of PbΔs1 (knock-out) GIMO mother-line

A specific PbANKA-s1 targeting deletion construct (pL1928) was generated and transfected into the standard reporter *Pb* ANKA parasite line *Pb*GFP-Luc$_{con}$ (676m1cl1) which expresses a fusion protein of GFP (mutant3) and firefly luciferase (LUC-IAV) under the constitutive *eef1a* promoter and is SM free [249] using the standard transfection protocol (Section **2.3)** [248]. The selectable marker expression cassette was stably integrated into the S1 locus in chromosome-12 by double cross-over recombination to generate *PbΔs1 (knock-out)* GIMO mother-line (2149 cl1). Genotype analysis of the clonal *PbΔs1* population confirmed the deletion of *Pbs1 OFR* by Southern analysis of separated chromosomes and diagnostic PCR. The genotype analysis results showed the correct 5' and 3' integration of the hdhfr::yfcu SM expression cassette and the lack of the *Pbs1* ORF and its replacement with the selectable marker **(Figure 5.1).** *PbΔs1* GIMO mother-line was passed through the whole life cycle successfully and showed identical fitness to the wild-type parasite. There were also no differences in the prepatent period for *PbΔs1* GIMO mother-line as compared with *Pb* WT (**Figure 5.2**).

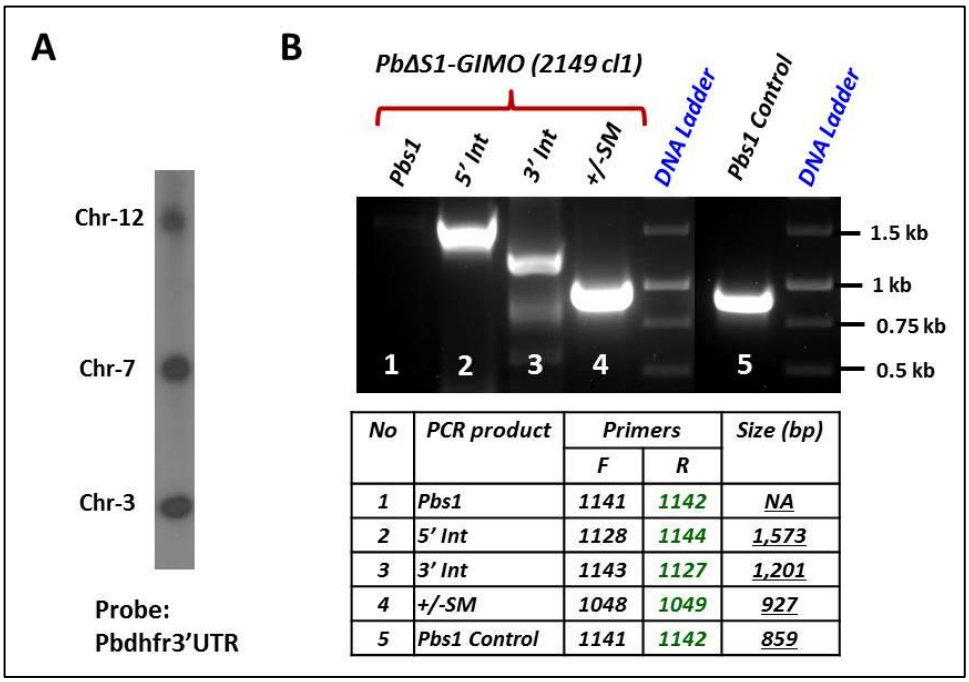

No	PCR product	Primers		Size (bp)
		F	R	
1	Pbs1	1141	1142	NA
2	5' Int	1128	1144	1,573
3	3' Int	1143	1127	1,201
4	+/-SM	1048	1049	927
5	Pbs1 Control	1141	1142	859

Figure 5.1 Genotype analysis of *PbΔS1-GIMO (2149 cl1)*

A. Southern analysis of chromosomes (chr) separated by pulsed-field gel electrophoresis (PFGE) to confirm integration of the GIMO deletion construct into the Pbs1 locus in chromosome 12 in PbΔS1-GIMO line.

The blot was hybridized with a 3'UTR *Pbdhfr/ts* probe, recognizing the 3'UTR *Pbdhfr/ts* of the SM of the integrated construct in *Pbs1* locus in chr-12, the 3'UTR *Pbdhfr/ts* of the GFP-Luciferase cassette on chr-3, and the endogenous *Pbdhfr/ts* on chr-7.

B. Diagnostic PCR. Different primers have been designed to check the right 5' and 3' integration of the GIMO deletion construct in *Pbs1* locus in chr-12, the presence of the hdhfr::yfcu selectable marker, and the absence of *Pbs1 gene.* As a positive control for the primers used to amplify the *Pbs1* gene, we used WT DNA (Pbs1 Control). Primers' sequences used for PCR are shown in **Table 2.3**, while the expected PCR products' sizes are shown in the table below the agarose gel image.

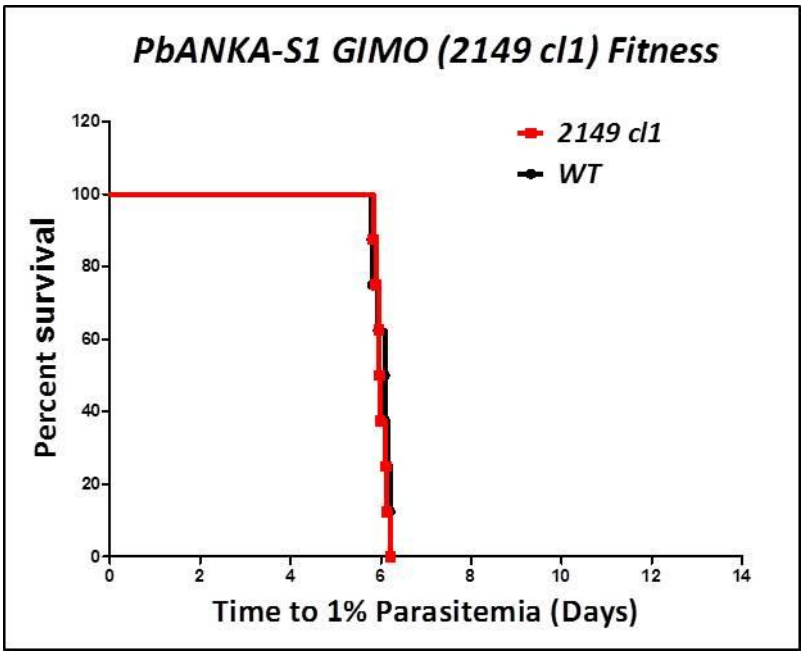

Figure 5.2 Fitness assessment of sporozoites of PbΔS1-GIMO (2149 cl1).
Prepatent period in mice after injection of 1000 sporozoites of *Pb*ΔS1-GIMO line compared to the wild-type *P. berghei* parasite. The blood stage growth and prepatent time to reach 1% parasitaemia for the GIMO mother-line was identical to the wild-type *P. berghei* line**.**

5.2.2 Generation of two double transgenic parasites expressing two different *P. falciparum* genes.

Discovering the new *P. berghei* 'neutral' *Pbs1* locus (PBANKA_120680) in chromosome-12 opened a new possibility of generating double transgenic parasites expressing two *P. falciparum* antigens; with the first antigen expressed in the *Pb230p* neutral locus in chr-3 and the second antigen expressed in the Pbs1 neutral locus in chr-12. Two standard DNA constructs were designed to target the Pbs1 locus in chromosome-12; the first construct is a specific PbANKA-s1 targeting deletion construct (pL1928) to replace the *Pbs1* ORF with the h*dhfr::*y*fcu* SM cassette, while the second construct is a gene insertion construct **(pL2023)** used to rapidly introduce a transgene cassette into the neutral *Pbs1* locus and replacing the SM cassette by GIMO transfection.

The efficacy assessment of the ten *P. falciparum* viral vector vaccines using the newly developed transgenic parasites challenge model in chapter-4 resulted in

the discovery of two novel vaccine candidates (PfLSA1 and PfLSAP2) with better protective efficacy that than the current two leading malaria vaccines antigens (PfCSP and PfTRAP). Therefore the new technology of generating double transgenic parasites expressing two different *P. falciparum* proteins was implemented to enable *in vivo* assessment of protective efficacy of the two candidate vaccine combination.

Two different double additional genes (DAGs) chimeric parasites were generated following the standard GIMO transfection method [245, 248]. The first DAGs chimeric parasite expresses the PfLSA1 and PfLSAP-2 under the control of Pbuis4 promoter (2403 cl1). The single AG chimeric parasite **PfLSA1$_{Pbuis4}$ (2230cl1)** with PfLSA1 gene expression cassette in *Pb230p* locus on chr-3 was used as a background to include the second *P. falciparum* gene expression cassette; **PfLSAP2$_{PbUIS4}$** in *Pbs1* neutral locus on chr-12. This was performed in two independent transfections using pL1928 (the PbANKA-s1 targeting deletion construct) and then **pL2044 (PfLSAP2$_{PbUIS4_S1}$** the gene insertions construct) **(Figure 5.3).** The second DAGs chimeric parasite expresses the two current leading malaria vaccine candidates PfCSP and PfTRAP under the control of *Pbuis4* promoter (2369 cl4). The single AG chimeric parasite **PfTRAP$_{Pbuis4}$ (2281cl1)** with PfTRAP gene expression cassette in *Pb230p* locus on chr-3 was used as a background to include the second *P. falciparum* gene expression cassette; **PfCSP$_{PbUIS4}$** in *Pbs1* neutral locus on chr-12. This was performed in two independent transfections using pL1928 (PbANKA-s1 targeting deletion construct) and then **pL2030; PfCSP$_{PbUIS4_S1}$** (the gene insertion construct) **(Figure 5.3).**

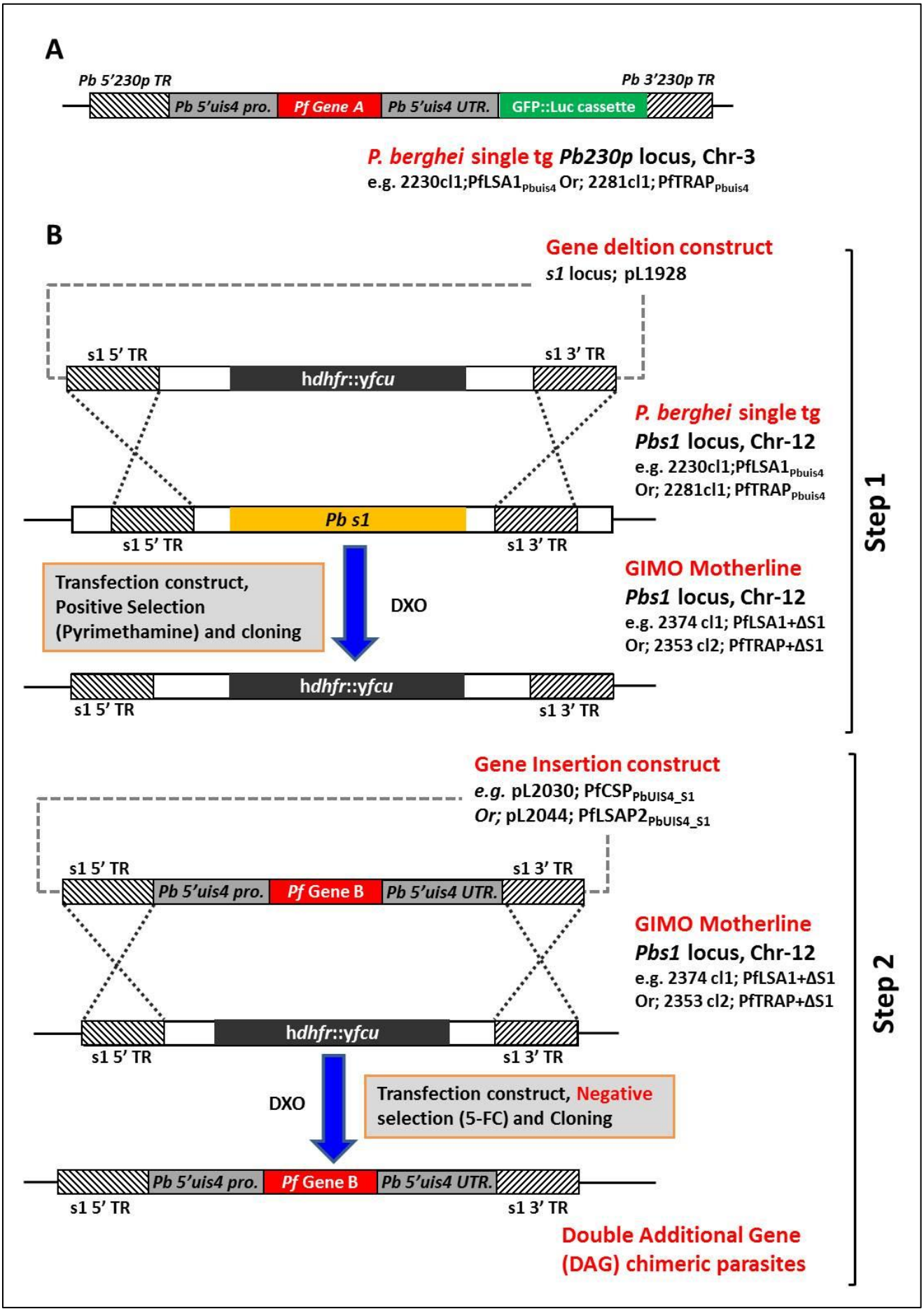
A
Pb 5'230p TR
Pb 5'uis4 pro.
Pf Gene A
Pb 5'uis4 UTR.
GFP::Luc cassette
Pb 3'230p TR
P. berghei single tg Pb230p locus, Chr-3
e.g. 2230cl1;PfLSA1Pbuis4 Or; 2281cl1; PfTRAPPbuis4
B
Gene deltion construct
s1 locus; pL1928
s1 5' TR
hdhfr::yfcu
s1 3' TR
P. berghei single tg
Pbs1 locus, Chr-12
e.g. 2230cl1;PfLSA1Pbuis4
Or; 2281cl1; PfTRAPPbuis4
Pb s1
s1 5' TR
s1 3' TR
Transfection construct,
Positive Selection
(Pyrimethamine) and cloning
DXO
GIMO Motherline
Pbs1 locus, Chr-12
e.g. 2374 cl1; PfLSA1+ΔS1
Or; 2353 cl2; PfTRAP+ΔS1
hdhfr::yfcu
s1 5' TR
s1 3' TR
Step 1
Gene Insertion construct
e.g. pL2030; PfCSPPbUIS4_S1
Or; pL2044; PfLSAP2PbUIS4_S1
s1 5' TR
Pb 5'uis4 pro.
Pf Gene B
Pb 5'uis4 UTR.
s1 3' TR
GIMO Motherline
Pbs1 locus, Chr-12
e.g. 2374 cl1; PfLSA1+ΔS1
Or; 2353 cl2; PfTRAP+ΔS1
hdhfr::yfcu
s1 5' TR
s1 3' TR
DXO
Transfection construct, Negative
selection (5-FC) and Cloning
Pb 5'uis4 pro.
Pf Gene B
Pb 5'uis4 UTR.
s1 5' TR
s1 3' TR
Double Additional Gene
(DAG) chimeric parasites
Step 2

Figure 5.3 Generation of Double Additional Genes (DAGs) chimeric parasites.
A. Schematic representation of a single additional gene (AG) transgenic parasite line used to generate Double Additional Gene (DAGs) chimeric parasites. It expresses a *P. falciparum* gene under the control of the *Pbuis4* promoter and a fusion protein of GFP and firefly luciferase (LUC-IAV) under the constitutive *Pbeef1a* promoter and is selectable marker (SM) free. The first *P. falciparum* gene expression cassette and the reporter-cassette are integrated into the neutral *230p* locus in chromosome-3.
B. Schematic representation describing the transfections and the generation steps of a Double Additional Gene (DAGs) chimeric parasite where the *Pbs1* neutral locus in chromosome-12 is replaced with the second *P. falciparum* gene expression cassette. 1st step: The **GIMO Deletion construct** (**Construct 1; pL1928**) is used to replace the *Pbs1 OFR* with the positive/negative selectable maker (h*dhfr::*y*fcu*) cassette, resulting in the generation of the GIMO line **(*Pb*ANKA- *Δs1*)** after positive selection with pyrimethamine. **Construct 1** targets the *P. berghei* gene by double cross-over homologous recombination. After genotyping and confirming the correct construct integration, these lines are cloned. 2nd step: The **GIMO insertion construct** is used to replace the selectable maker (SM) in the *PbΔs1* GIMO line with the second *P. falciparum* gene expression cassette, under negative (5-FC) selection, resulting in a Double Additional Gene (DAGs) chimeric parasite containing two *P. falciparum* genes; one in the *Pb230p* neutral locus in chr-3 and the other in the *Pbs1* neutral locus in chr-12**.** **Construct 2** integrates by double cross-over homologous recombination using the same targeting regions (TRs) employed in construct 1, resulting in the introduction of the second *P. falciparum* gene under the control of *Pbuis4* promoter and transcriptional terminator sequences.

5.2.3 Genotype analysis of the Double Additional Gene chimeric parasites

To confirm the correct integration of the DNA construct in the Double Additional Genes (DAGs), chimeric parasites and their intermediate GIMO mother-line (knock out) chimeric parasites, Southern analysis was performed using *Pbdhfr 3'UTR* probe to recognizing the *3'UTR Pbdhfr/ts* of the SM of the integrated GIMO deletion construct in Pbs1 locus in chr-12 in both PbΔS1 GIMO mother lines*; PbANKA-PfLSA1+ΔS1 (2374 cl1) and PbANKA-PfTRAP+ΔS1 (2353 cl2)* **(Figure 5.4 A).** The *Mixed Probe hDHFR/Chr-5,* was then used to confirm the correct integration of the second *P. falciparum* gene into the PbΔs1 GIMO neutral locus in chr-12 and the removal of the *hdhfr::yfcu SM cassette* **(Figure 5.4 B).** In addition, different primers were designed to check the presence of the two *transfected P. falciparum* genes in each double transgenic parasite and the absence of the hdhfr::yfcu selectable marker from the cloned transgenic

parasite lines. Diagnostic PCR analysis confirmed the correct integration of the two *P. falciparum* GIMO Insertion constructs in the two DAGs chimeric parasites (2403cl1) and (2369cl4) and showed the absence of hdhfr::yfcu marker (**Figure 5.5**).

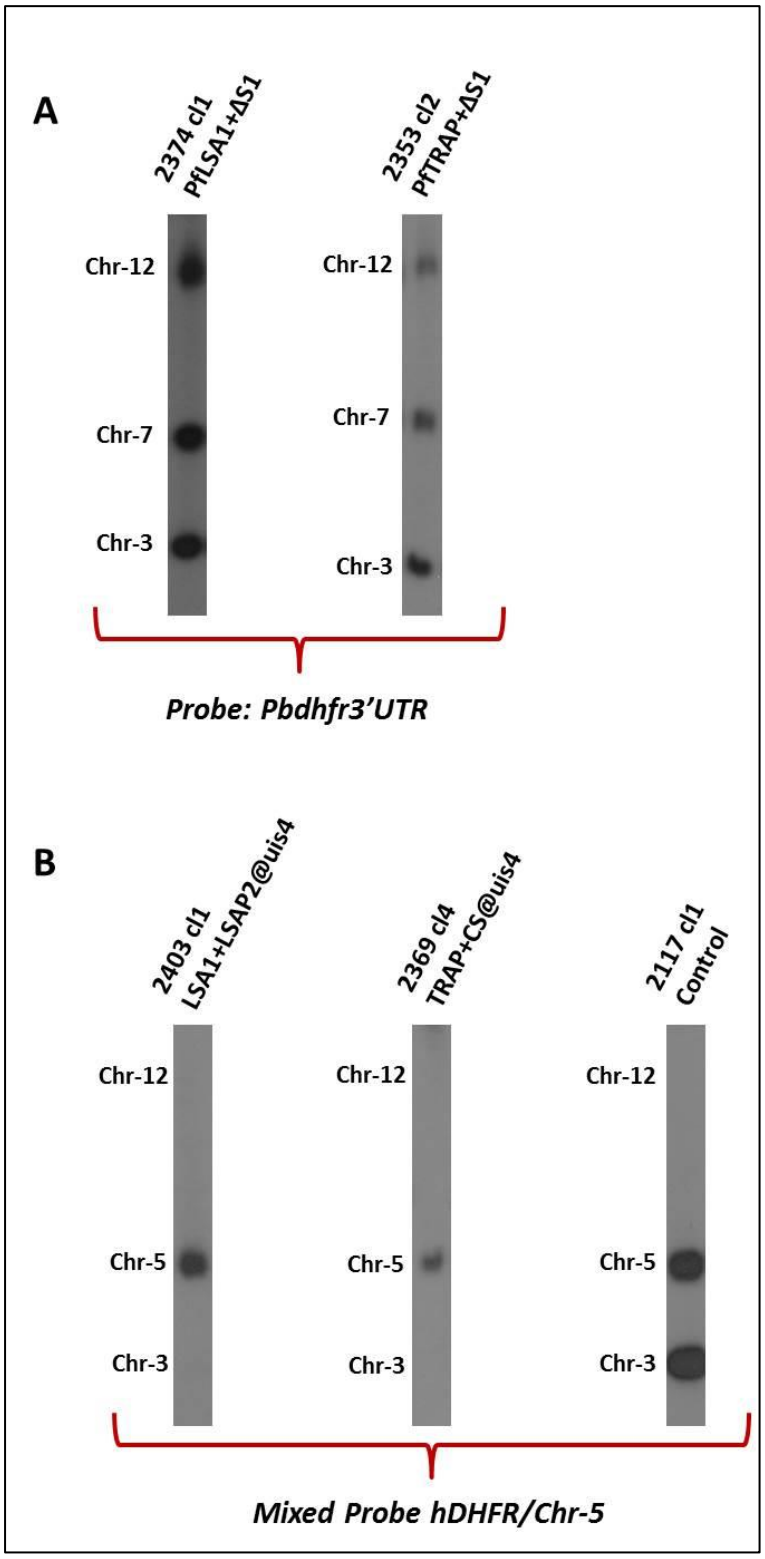

Figure 5.4 Genotype analysis of the Double Additional Genes (DAGs) chimeric parasites and their intermediate GIMO mother-line knock out chimeric parasites using Southern analysis of chromosomes (chrs) separated by pulsed-field gel electrophoresis (PFGE) to confirm the DNA construct integration in the correct chromosome in the chimeric *P. berghei* parasite.

Two different probes were used to recognize the absence or the presence of the selectable marker or the transgene in the chimeric parasites. The first probe consists of a mixture of two probes: one recognizing h*dhfr* in the SM and a control probe recognizing chr-5. The second probe mixture recognizing the 3'UTR *Pbdhfr/ts* of the SM of the integrated construct which also hybridizes to the endogenous *Pbdhfr/ts* on chr-7.

A. PFGE analysis of intermediate GIMO mother-line (knock out) chimeric parasites. The blot was hybridized with a 3'UTR *Pbdhfr/ts* probe, recognizing the 3'UTR *Pbdhfr/ts* of the SM of the integrated construct in *Pbs1* locus in chr-12, the 3'UTR *Pbdhfr/ts* of the GFP-Luciferase cassette on chr-3, and the endogenous *Pbdhfr/ts* on chr-7. PFGE results of both GIMO mother lines (2374cl1 and 2353cl2) used to generate the two double transgenic parasites showed the correct integration of the selectable marker cassette in to the Pbs1 neutral locus on Chr-12.

B. PFGE analysis of the Double Additional Genes (DAGs) chimeric parasites. The correct integration of the second *P. falciparum* expression casette into the *PbΔs1* GIMO neutral locus in chr-12 was confirmed by showing the removal of the h*dhfr::*y*fcu* SM cassette in the cloned double additional genes (DAGs) chimeric parasite lines (2403cl1 and 2369cl4). The southern blot is hybridized with a mixture of two probes: one recognizing h*dhfr* and a control probe recognizing chr-5. As an additional control (ctrl), parasite line 2117cl1 is used with the h*dhfr::*y*fcu* SM integrated into chr-3.

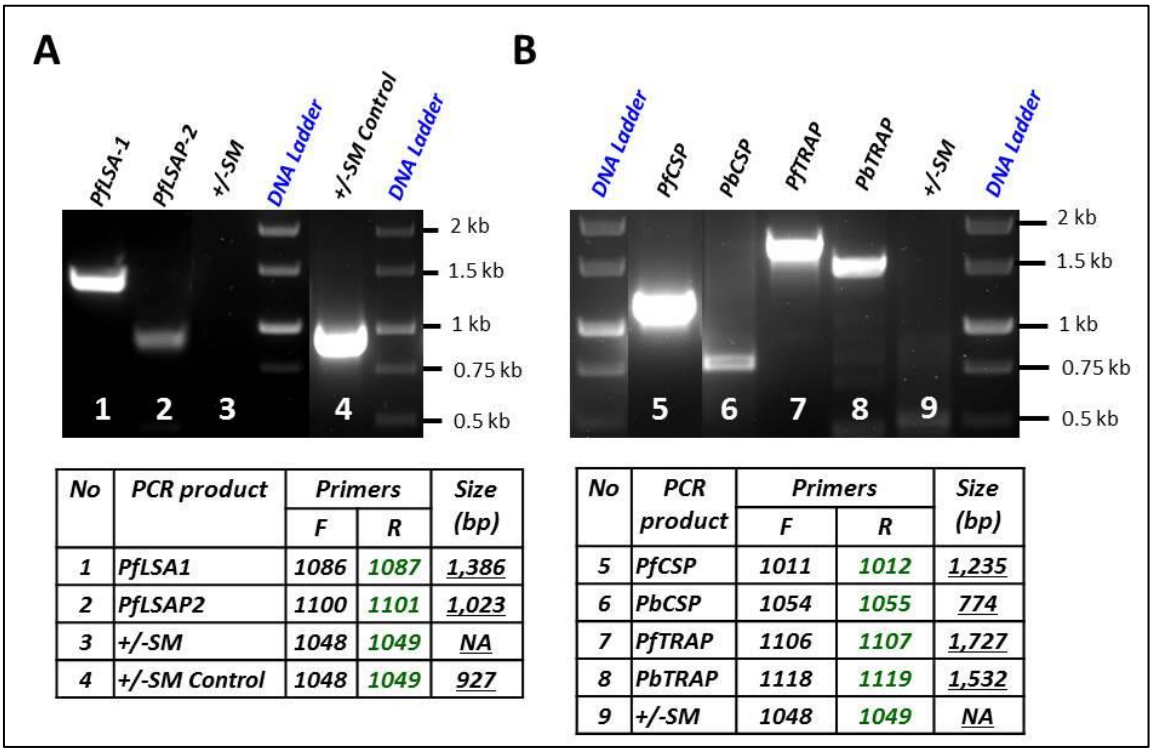

No	PCR product	Primers		Size (bp)
		F	R	
1	PfLSA1	1086	1087	1,386
2	PfLSAP2	1100	1101	1,023
3	+/-SM	1048	1049	NA
4	+/-SM Control	1048	1049	927

No	PCR product	Primers		Size (bp)
		F	R	
5	PfCSP	1011	1012	1,235
6	PbCSP	1054	1055	774
7	PfTRAP	1106	1107	1,727
8	PbTRAP	1118	1119	1,532
9	+/-SM	1048	1049	NA

Figure 5.5 Genotype analysis. Diagnostic PCR of the Double Additional Genes (DAGs) chimeric parasites. Genomic DNA was extracted from the cloned DAGs chimeric parasites and different primers have been designed to check the presence of the *P. falciparum* genes and also the absence of the hdhfr::yfcu selectable marker. As a positive control for the primers used to amplify the hdhfr::yfcu selectable marker we used a control.
A. PfLSA1+LSAP2@Pbuis4 DAGs (2403 cl1),
B. PfCSP+PfTRAP@Pbuis4 DAGs (2369 cl4).
Primers' sequences used for PCR are shown in **Table 2.3**, while the expected PCR products' sizes are shown in the table below the agarose gel image.

5.2.4 Phenotype analysis of the additional gene chimeric parasites expressing *P. falciparum* genes by Immunofluorescence assay test (IFAT).

Immunofluorescence staining showed *P. falciparum* antigen expression in sporozoites of the two generated DAGs chimeric parasite. Chimeric salivary-gland sporozoites were stained with stained with anti-PfCSP (2A10) [222, 271], anti-PbCSP (3D11) [272] monoclonal antibodies (MR4), or sera from mice vaccinated against the corresponding *P. falciparum* antigens. Bound IgG was detected with goat anti-mouse IgG-Alexa Fluor 488, green and nuclear DNA stained with 2% Hoechst-33342. As a control, wild-type (WT) *P. berghei* sporozoites were stained with the same sera. Merged images of the different

channels are shown for both chimeric and WT *P. berghei* stained images (**Figure 5.6)**.

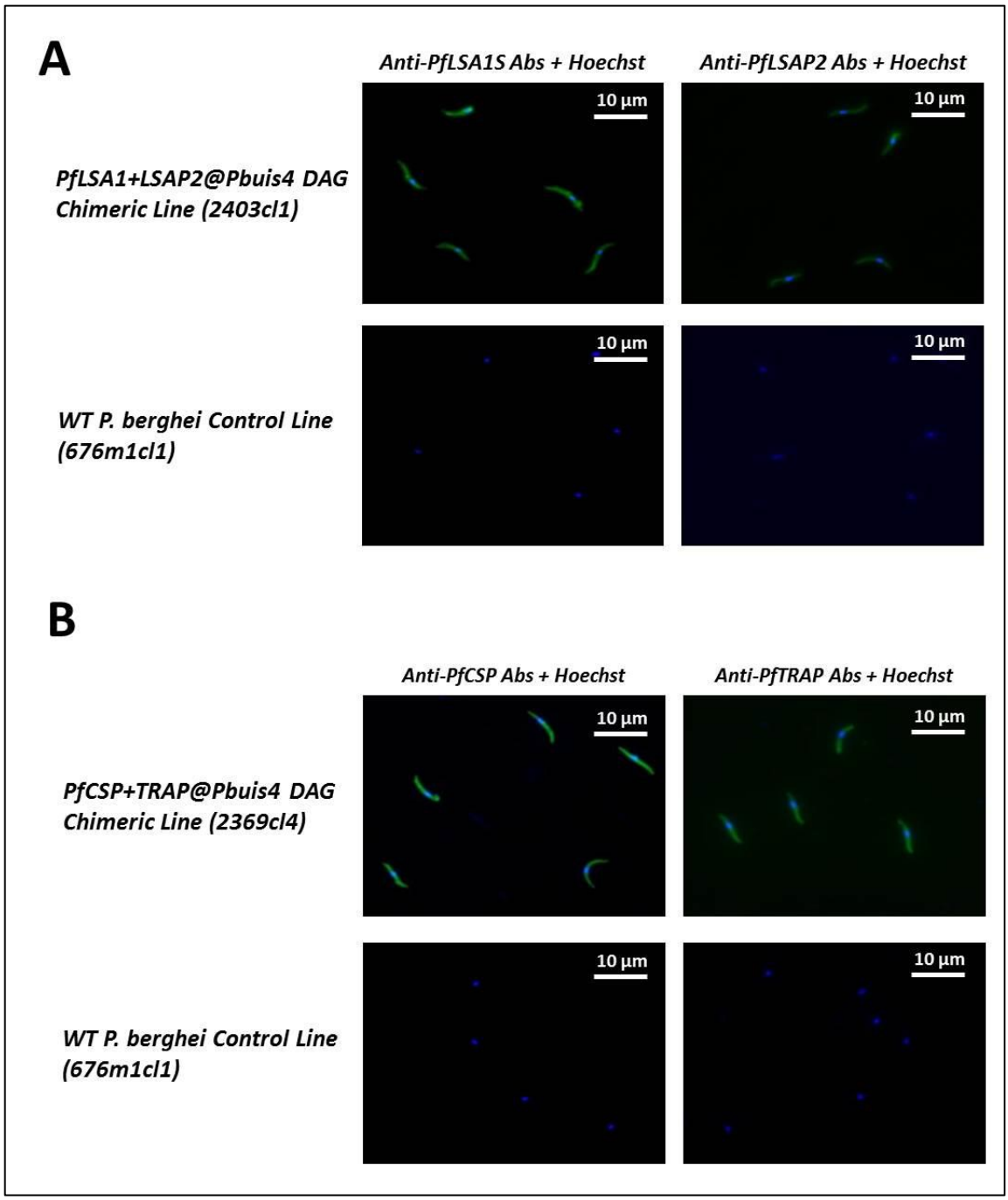

Figure 5.6 Immunofluorescence analysis demonstrating *P. falciparum* antigen expression in sporozoites of chimeric DAGs parasites. Chimeric salivary-gland sporozoites were stained with sera from vaccinated mice or with monoclonal antibodies where available (PbCSP 3D11 and PfCSP 210A), (Alexa Fluor 488, green) and Hoechst-33342 (blue; nuclear staining). As a control, wild-type (WT) *P. berghei* sporozoites were stained with the same antibodies or sera. Merged images of the different channels are shown for both chimeric and WT *P. berghei* stained images.
A. PfLSA1+LSAP2@Pbuis4 DAGs (2403 cl1),
B. PfCSP+PfTRAP@Pbuis4 DAGs (2369 cl4).

5.2.5 In vivo imaging for quantification of chimeric parasite load during the liver-stage.

Five naïve mice were challenged with the Double DAGs chimeric sporozoites to confirm the ability of the DAGs chimeric sporozoites to develop normally to the parasite liver-stage and to assess liver parasite load by luminescence. Both DAGs chimeric parasites (2403 cl1) and (2369 cl4) showed normal development during the liver-stage of infection *in vivo* **(Figure 5.7 A and B).** The emitted signals were quantified at 44 hours post infection using the IVIS 200 system and quantified as total flux/sec **(Figure 5.7 C).**

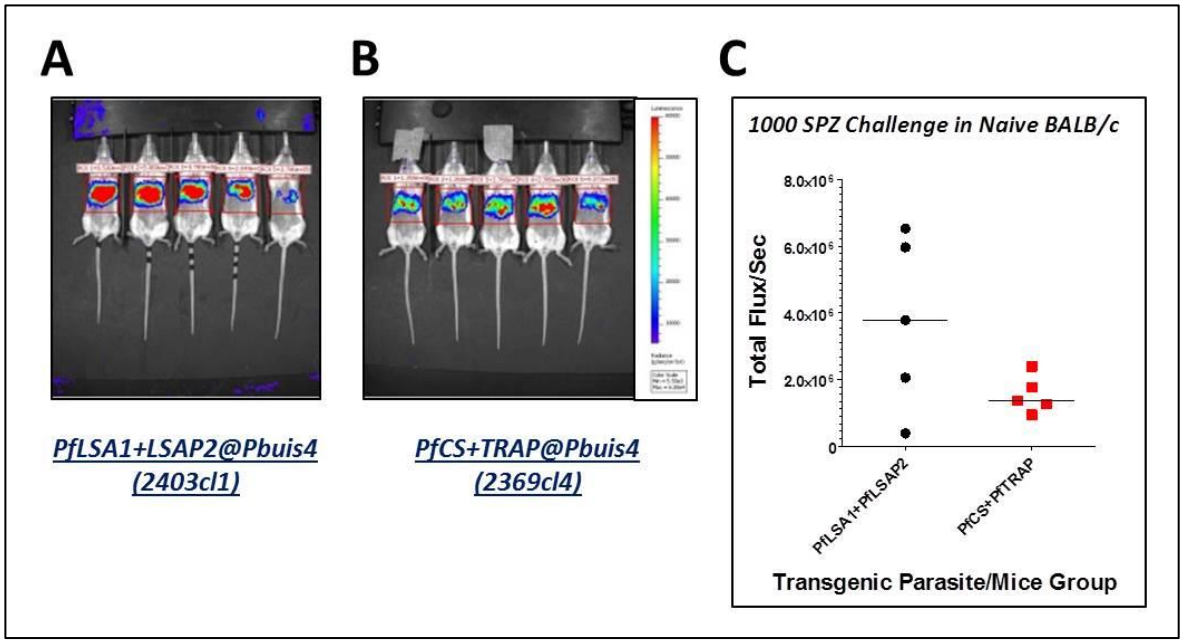

Figure 5.7 Parasite liver loads as determined by i*n vivo* imaging. Parasite liver loads in naïve mice that are challenged with the Double Additional Genes (DAGs) chimeric sporozoites are quantified by measuring luminescence levels at 44 hours after infection using the IVIS 200 system
A. PfLSA1+LSAP2@Pbuis4 DAGs (2403 cl1),
B. PfCSP+PfTRAP@Pbuis4 DAGs (2369 cl4),
C. Quantification of the bioluminescence signals from infected mice measured as total flux/sec.

5.2.6 Combined vaccination strategies

To assess the immunogenicity and protective efficacy associated with combining the PfLSA1 and PfLSAP2 encoding vaccines compared to a combination with the leading antigens PfCSP and TRAP, mice were immunised with the relevant viral vectors. In each DAGs chimeric parasite challenge experiment; five different mice groups were vaccinated, in **Group-1 (G1)** mice were vaccinated with the two vaccines (A+B) mixed together in a total volume of 100 µl split equally between the mouse two legs (50µl/leg), in **Group-2 (G2)** mice were vaccinated with the two vaccines (A+B) administered into different legs (50µl/leg). In **Group-3 (G3)** mice were vaccinated with vaccine-A only (50µl in one leg) and similarly in **Group-4 (G4)** mice were vaccinated with vaccine-B only (50µl in one leg), while **Group-5 (G5)** contained the unvaccinated naïve control. For each vaccine candidate, mice received 10^8 ifu/50µl of ChAd63-Pf vaccine i.m. as a prime followed eight weeks later by 10^7 pfu/50µl of MVA-*Pf* candidate. In case of vaccines combinations in Group-1 and Group-2; each mouse was injected with double the dose of total ChAd63 but the amount of antigen was kept consistent, therefore they received 10^8 ifu of ChAd63-Pf vaccine-A plus 10^8 ifu of ChAd63-Pf vaccine-B in the prime vaccination (2x 10^8 ifu in total), followed by 10^7 pfu of MVA-Pf vaccine-A plus 10^7 pfu of MVA-Pf vaccine-B (2x 10^7 pfu in total) either as a mixture of both vaccines or separately in group-1 and -2, respectively **(Figure 5.8).**

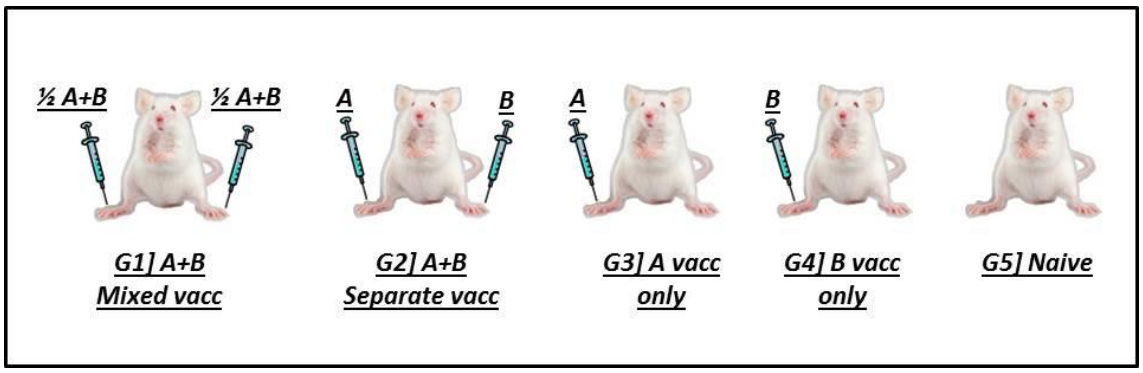

Figure 5.8 Combined vaccination strategies. To assess the immunogenicity and the efficacy of combining the two different *P. falciparum viral vector* vaccine candidates (as example; vaccine A and B), five different mice groups were included in each double transgenic parasite challenge experiment. The five mice groups were prepared as:

(**G1**) Mice vaccinated with the two vaccines (A+B) mixed together with splitting the vaccine dose equally between two hind legs, (**G2**) Mice vaccinated with the two vaccines (A+B) with injecting each vaccine separately in a different leg, (**G3**) Mice vaccinated with vaccine-A only, (**G4**) Mice vaccinated with vaccine-B only, (**G5**) Naïve control.

For each vaccine candidate, mice were vaccinated i.m. with 10^8 ifu of ChAd63-Pf candidate as prime followed eight weeks later by 10^7 pfu of MVA *P. falciparum* candidate as boost vaccinations. In case of combining vaccines in G1 and G2; each mouse was injected with double the dose in total, i.e.: 10^8 ifu of ChAd63-Pf vaccine-A plus 10^8 ifu of ChAd63-Pf vaccine-B in the prime vaccination (2x 10^8 ifu in total), followed by 10^7 pfu of MVA-Pf vaccine-A plus 10^7 pfu of MVA-Pf vaccine-B (2x 10^7 pfu in total).

5.2.7 Assessment of the pre-challenge cellular immunogenicity in blood following the heterologous prime-boost ChAd63-MVA viral vector vaccination

Intracellular staining (ICS) was performed prior to challenge and one week post MVA-boost PBMC were collected and stimulated with overlapping peptide of each one of the two *P. falciparum* antigens. Pre-challenge immunogenicity is presented as the percentage of cytokine$^+$ CD8$^+$ or CD4$^+$ cells. In mice vaccinated with *PfLSA-1* and/or *PfLSAP-2*, the frequency of CD8$^+$ T cells was higher than the frequency of CD4$^+$ T cells. Although there is a trend towards higher frequencies of IFN-γ^+ or TNF-α^+ CD8$^+$ in mice vaccinated with *PfLSA-1* alone, there was no statistically significant difference between the groups. Responses against *PfLSAP-2* were of lower magnitude, but again there was no significant difference between groups.

Similarly, pre-challenge immunogenicity presented as the CD8$^+$ or CD4$^+$ cells cytokines responses in the blood following the heterologous prime-boost ChAd63-MVA *PfCSP* and *PfTRAP* viral vector vaccines' demonstrated no significant difference between the groups (**Figure 5.9 – 5.12**).

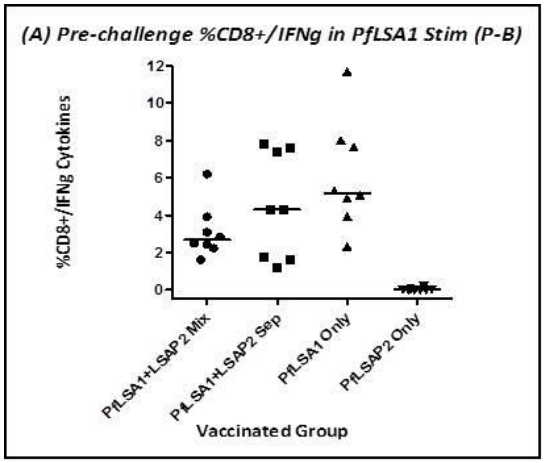
(A) Pre-challenge %CD8+/IFNg in PfLSA1 Stim (P-B)
%CD8+/IFNg Cytokines
0
2
4
6
8
10
12
PfLSA1+LSAP2 Mix
PfLSA1+LSAP2 Sep
PfLSA1 Only
PfLSAP2 Only
Vaccinated Group

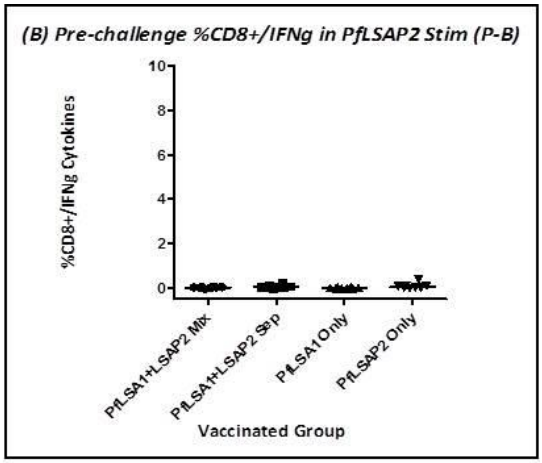
(B) Pre-challenge %CD8+/IFNg in PfLSAP2 Stim (P-B)
%CD8+/IFNg Cytokines
0
2
4
6
8
10
PfLSA1+LSAP2 Mix
PfLSA1+LSAP2 Sep
PfLSA1 Only
PfLSAP2 Only
Vaccinated Group

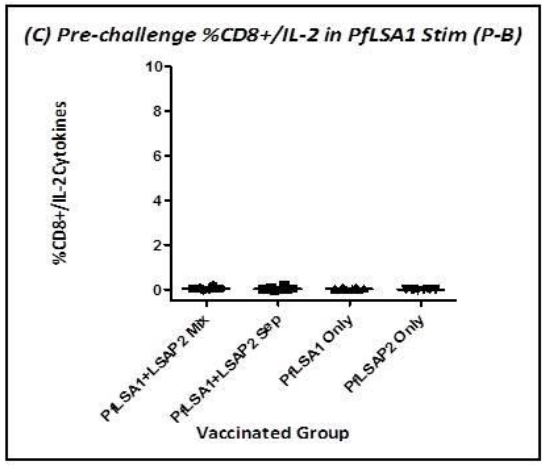
(C) Pre-challenge %CD8+/IL-2 in PfLSA1 Stim (P-B)
%CD8+/IL-2Cytokines
0
2
4
6
8
10
PfLSA1+LSAP2 Mix
PfLSA1+LSAP2 Sep
PfLSA1 Only
PfLSAP2 Only
Vaccinated Group

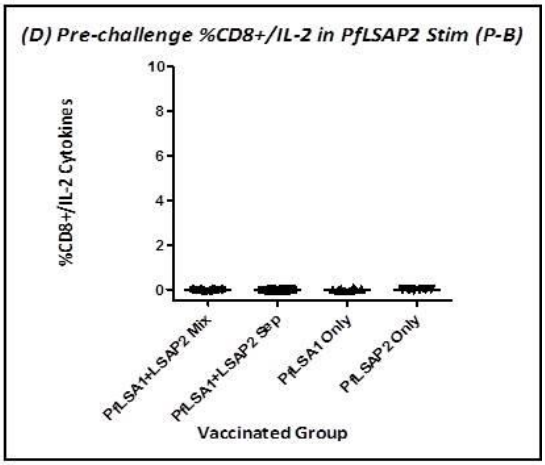
(D) Pre-challenge %CD8+/IL-2 in PfLSAP2 Stim (P-B)
%CD8+/IL-2 Cytokines
0
2
4
6
8
10
PfLSA1+LSAP2 Mix
PfLSA1+LSAP2 Sep
PfLSA1 Only
PfLSAP2 Only
Vaccinated Group

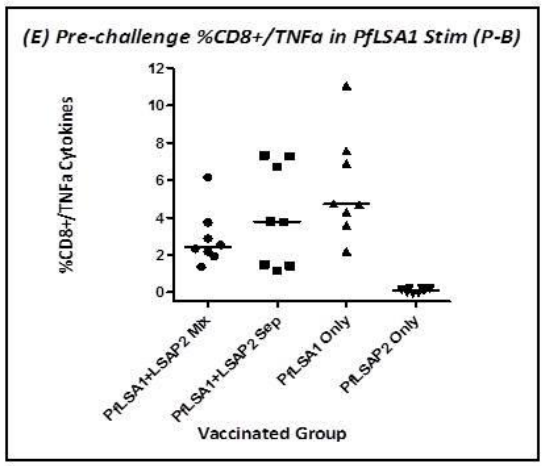
(E) Pre-challenge %CD8+/TNFa in PfLSA1 Stim (P-B)
%CD8+/TNFa Cytokines
0
2
4
6
8
10
12
PfLSA1+LSAP2 Mix
PfLSA1+LSAP2 Sep
PfLSA1 Only
PfLSAP2 Only
Vaccinated Group

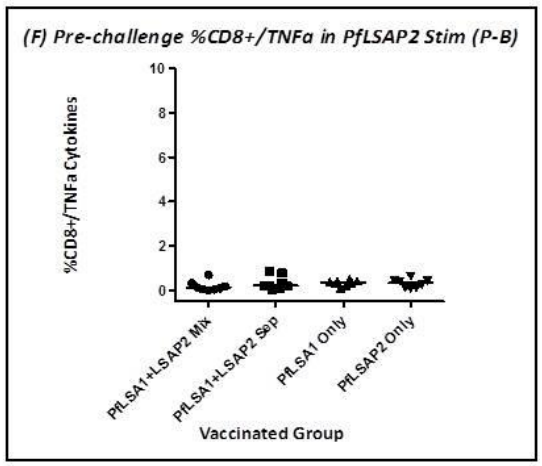
(F) Pre-challenge %CD8+/TNFa in PfLSAP2 Stim (P-B)
%CD8+/TNFa Cytokines
0
2
4
6
8
10
PfLSA1+LSAP2 Mix
PfLSA1+LSAP2 Sep
PfLSA1 Only
PfLSAP2 Only
Vaccinated Group

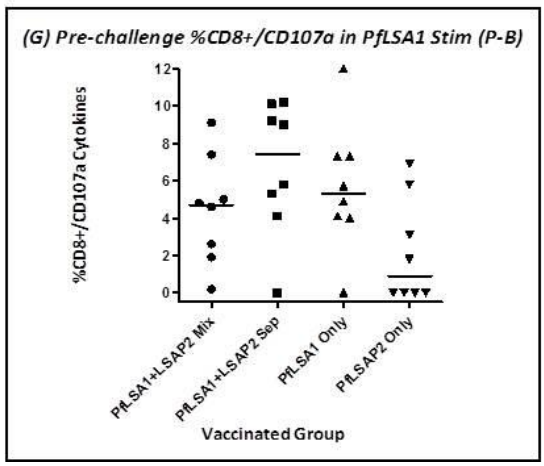
(G) Pre-challenge %CD8+/CD107a in PfLSA1 Stim (P-B)
%CD8+/CD107a Cytokines
0
2
4
6
8
10
12
PfLSA1+LSAP2 Mix
PfLSA1+LSAP2 Sep
PfLSA1 Only
PfLSAP2 Only
Vaccinated Group

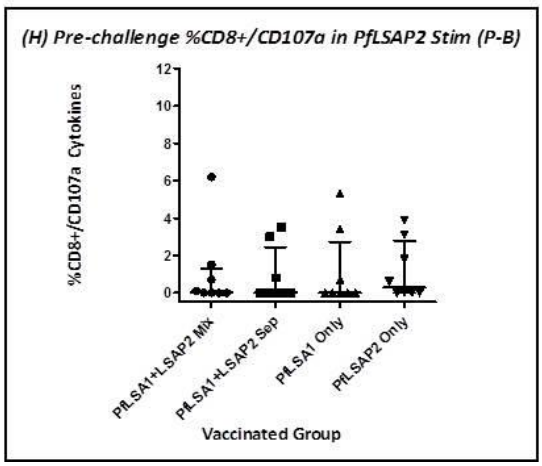
(H) Pre-challenge %CD8+/CD107a in PfLSAP2 Stim (P-B)
%CD8+/CD107a Cytokines
0
2
4
6
8
10
12
PfLSA1+LSAP2 Mix
PfLSA1+LSAP2 Sep
PfLSA1 Only
PfLSAP2 Only
Vaccinated Group

Figure 5.9 Pre-challenge immunogenicity presented as the $CD8^+$ cell cytokine responses in the blood following the heterologous prime-boost ChAd63-MVA *PfLSA1* and *PfLSAP2* viral vector vaccines' combinations.

Four different BALB/c mice groups (n=8) were vaccinated intramuscularly (i.m.) with ChAd63-*PfLSA1,* ChAd63-*PfLSAP2* vaccines or both combined*,* eight weeks later the same corresponding groups were vaccinated intramuscularly (i.m.) with MVA-*PfLSA1,* MVA-*PfLSAP2* vaccines or both combined following the different combination strategies described in **Figure 5.8**. One week post MVA-boost vaccination the mice were bled, the PBMC were collected, stimulated with either *PfLSA1 or PfLSAP-2* protein overlapping peptides for 6 hours and intracellular staining (ICS) was performed as described in Material and Method sections **2.8.7 and 2.8.8.**. $CD8^+$ cytokines responses measured in the blood one week post-MVA boost, expressed as the percentage of $CD8^+$ cells. $CD8^+$ specific cytokine response after PfLSA1 protein overlapping peptides stimulation described in (A) IFNg, (C) IL-2, (E) TNFa, and (G) CD107a. CD8+ specific cytokine response after PfLSAP2 protein overlapping peptides stimulation described in (B) IFNg, (D) IL-2, (F) TNFa, and (H) CD107a. Median with interquartile range values is shown.

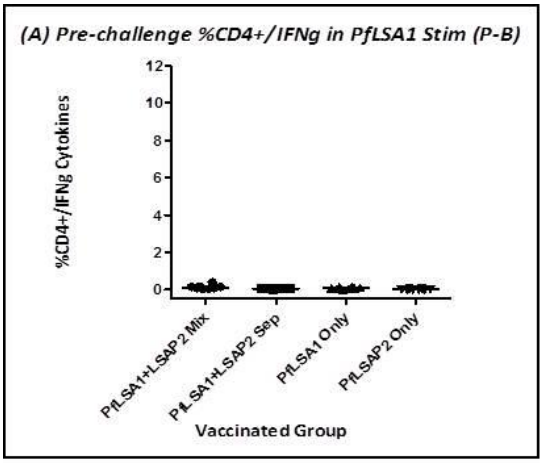
(A) Pre-challenge %CD4+/IFNg in PfLSA1 Stim (P-B)
%CD4+/IFNg Cytokines
12
10
8
6
4
2
0
PfLSA1+LSAP2 Mix
PfLSA1+LSAP2 Sep
PfLSA1 Only
PfLSAP2 Only
Vaccinated Group

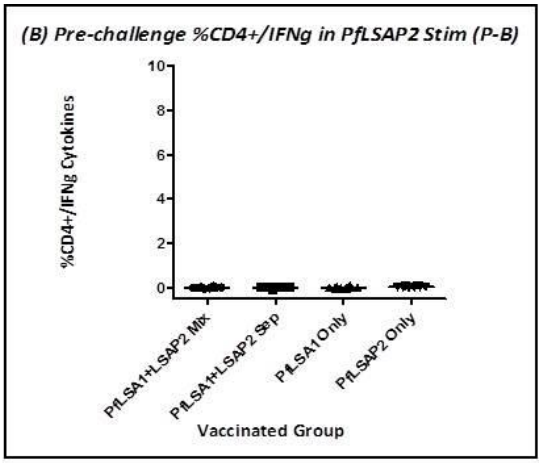
(B) Pre-challenge %CD4+/IFNg in PfLSAP2 Stim (P-B)
%CD4+/IFNg Cytokines
10
8
6
4
2
0
PfLSA1+LSAP2 Mix
PfLSA1+LSAP2 Sep
PfLSA1 Only
PfLSAP2 Only
Vaccinated Group

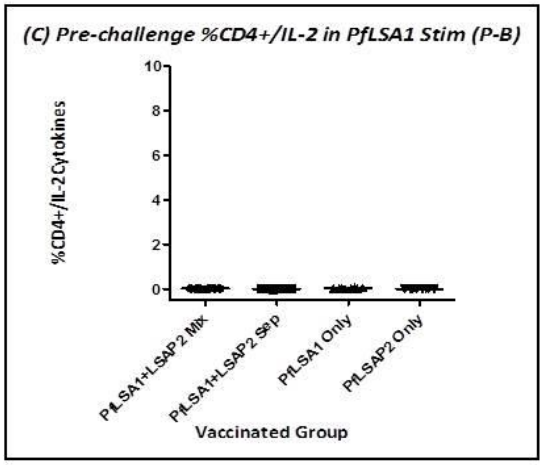
(C) Pre-challenge %CD4+/IL-2 in PfLSA1 Stim (P-B)
%CD4+/IL-2 Cytokines
10
8
6
4
2
0
PfLSA1+LSAP2 Mix
PfLSA1+LSAP2 Sep
PfLSA1 Only
PfLSAP2 Only
Vaccinated Group

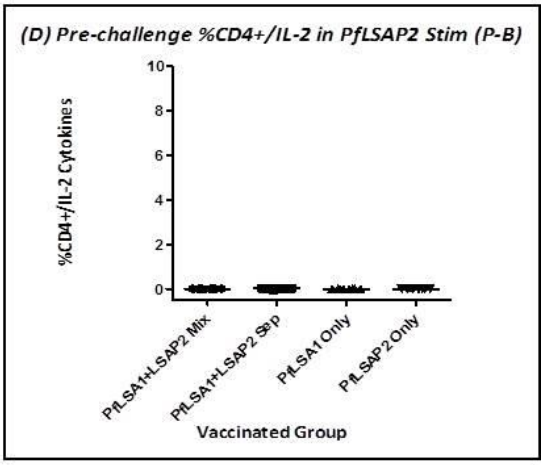
(D) Pre-challenge %CD4+/IL-2 in PfLSAP2 Stim (P-B)
%CD4+/IL-2 Cytokines
10
8
6
4
2
0
PfLSA1+LSAP2 Mix
PfLSA1+LSAP2 Sep
PfLSA1 Only
PfLSAP2 Only
Vaccinated Group

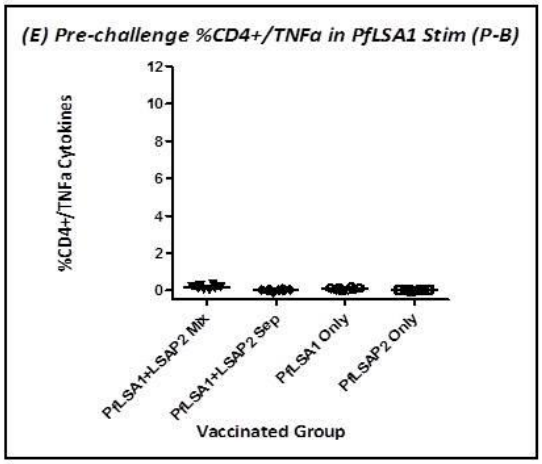
(E) Pre-challenge %CD4+/TNFa in PfLSA1 Stim (P-B)
%CD4+/TNFa Cytokines
12
10
8
6
4
2
0
PfLSA1+LSAP2 Mix
PfLSA1+LSAP2 Sep
PfLSA1 Only
PfLSAP2 Only
Vaccinated Group

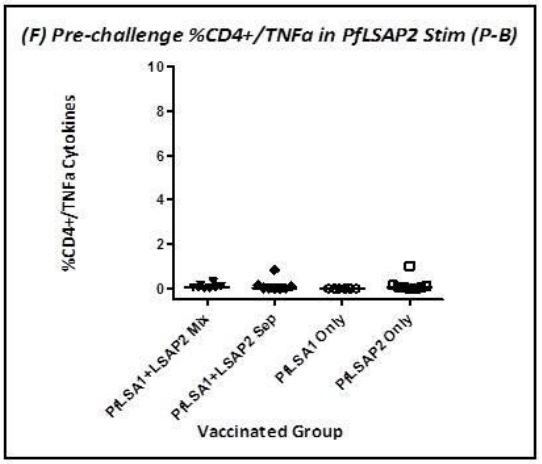
(F) Pre-challenge %CD4+/TNFa in PfLSAP2 Stim (P-B)
%CD4+/TNFa Cytokines
10
8
6
4
2
0
PfLSA1+LSAP2 Mix
PfLSA1+LSAP2 Sep
PfLSA1 Only
PfLSAP2 Only
Vaccinated Group

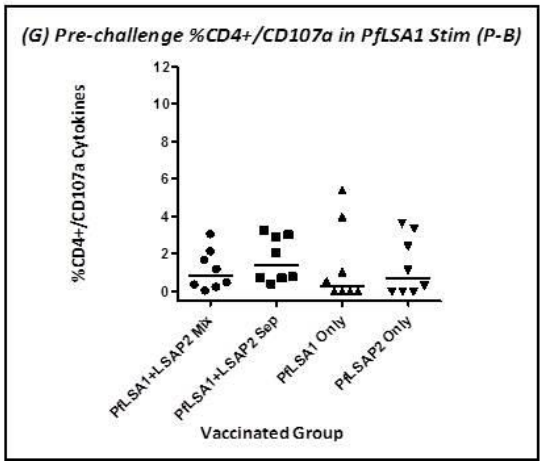
(G) Pre-challenge %CD4+/CD107a in PfLSA1 Stim (P-B)
%CD4+/CD107a Cytokines
12
10
8
6
4
2
0
PfLSA1+LSAP2 Mix
PfLSA1+LSAP2 Sep
PfLSA1 Only
PfLSAP2 Only
Vaccinated Group

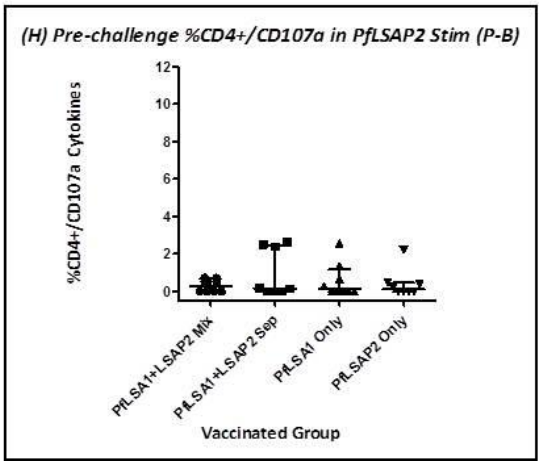
(H) Pre-challenge %CD4+/CD107a in PfLSAP2 Stim (P-B)
%CD4+/CD107a Cytokines
12
10
8
6
4
2
0
PfLSA1+LSAP2 Mix
PfLSA1+LSAP2 Sep
PfLSA1 Only
PfLSAP2 Only
Vaccinated Group

Figure 5.10 Pre-challenge immunogenicity presented as the CD4+ cell cytokine responses in the blood following the heterologous prime-boost ChAd63-MVA *PfLSA1* and *PfLSAP2* viral vector vaccines' combinations.

Four different BALB/c mice groups (n=8) were vaccinated intramuscularly (i.m.) with ChAd63-*PfLSA1,* ChAd63-*PfLSAP2* vaccines *or both combined,* eight weeks later the same corresponding groups were vaccinated intramuscularly (i.m.) with MVA-*PfLSA1,* MVA-*PfLSAP2* vaccines or both combined following the different combinations' strategies described in **Figure 5.8**. One week post MVA-boost vaccination the mice were bled, the PBMC were collected, stimulated with either *PfLSA1 or PfLSAP-2 protein* overlapping peptides for 6 hours and intracellular staining (ICS) was performed as described earlier in Material and Method sections **2.8.7 and 2.8.8.** These mice were challenged with 1,000 chimeric sporozoites 10-14 days post the MVA boost vaccination with *PfLSA1+PfLSAP2@pbuis4 (2403 cl1)* double transgenic parasites and the protective efficacy was assessed. $CD4^+$ cytokines responses measured in the blood one week post-MVA boost, expressed as the percentage of $CD4^+$ cells. $CD4^+$ specific cytokine response after PfLSA1 protein overlapping peptides stimulation described in (A) IFNg, (C) IL-2, (E) TNFa, and (G) CD107a. While $CD4^+$ specific cytokine response after PfLSAP2 protein overlapping peptides stimulation described in (B) IFNg, (D) IL-2, (F) TNFa, and (H) CD107a. Median with interquartile range values is shown.

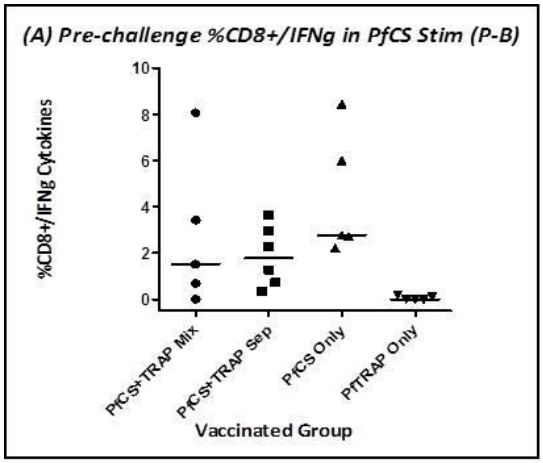
(A) Pre-challenge %CD8+/IFNg in PfCS Stim (P-B)
%CD8+/IFNg Cytokines
PfCS+TRAP Mix
PfCS+TRAP Sep
PfCS Only
PfTRAP Only
Vaccinated Group

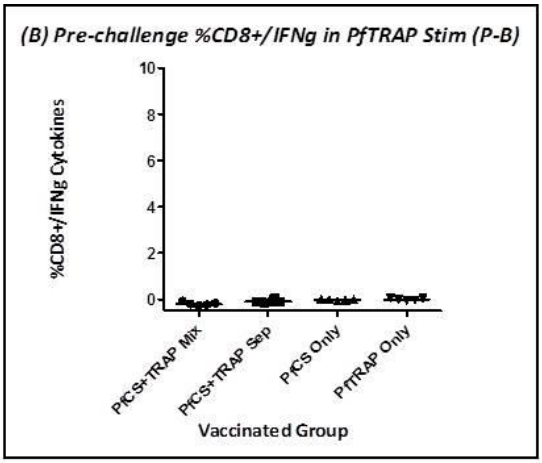
(B) Pre-challenge %CD8+/IFNg in PfTRAP Stim (P-B)
%CD8+/IFNg Cytokines
PfCS+TRAP Mix
PfCS+TRAP Sep
PfCS Only
PfTRAP Only
Vaccinated Group

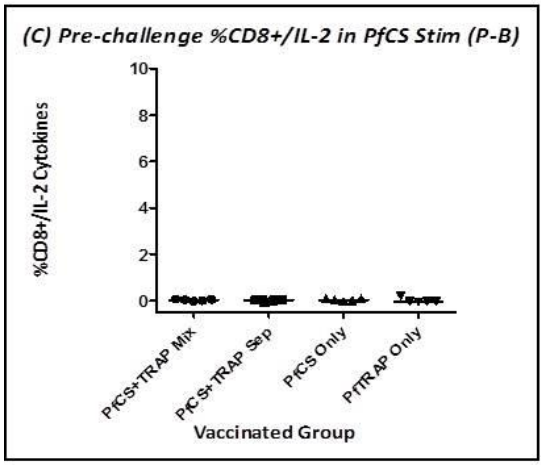
(C) Pre-challenge %CD8+/IL-2 in PfCS Stim (P-B)
%CD8+/IL-2 Cytokines
PfCS+TRAP Mix
PfCS+TRAP Sep
PfCS Only
PfTRAP Only
Vaccinated Group

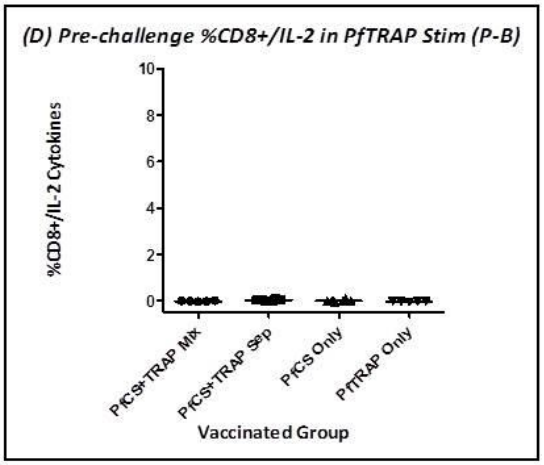
(D) Pre-challenge %CD8+/IL-2 in PfTRAP Stim (P-B)
%CD8+/IL-2 Cytokines
PfCS+TRAP Mix
PfCS+TRAP Sep
PfCS Only
PfTRAP Only
Vaccinated Group

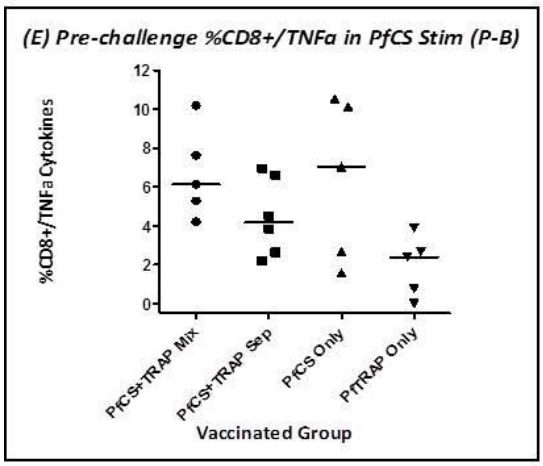
(E) Pre-challenge %CD8+/TNFa in PfCS Stim (P-B)
%CD8+/TNFa Cytokines
PfCS+TRAP Mix
PfCS+TRAP Sep
PfCS Only
PfTRAP Only
Vaccinated Group

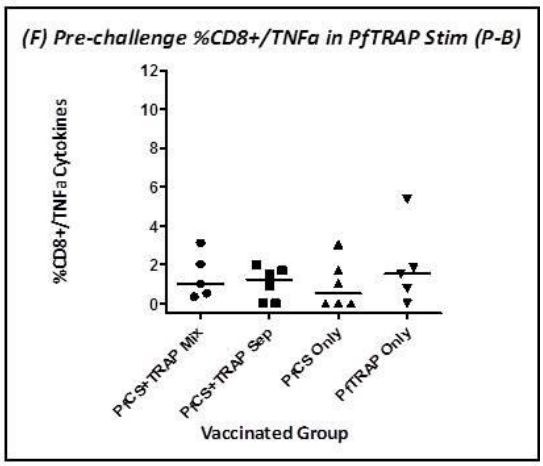
(F) Pre-challenge %CD8+/TNFa in PfTRAP Stim (P-B)
%CD8+/TNFa Cytokines
PfCS+TRAP Mix
PfCS+TRAP Sep
PfCS Only
PfTRAP Only
Vaccinated Group

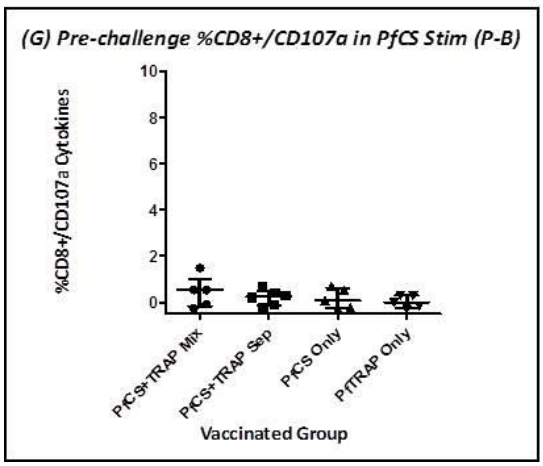
(G) Pre-challenge %CD8+/CD107a in PfCS Stim (P-B)
%CD8+/CD107a Cytokines
PfCS+TRAP Mix
PfCS+TRAP Sep
PfCS Only
PfTRAP Only
Vaccinated Group

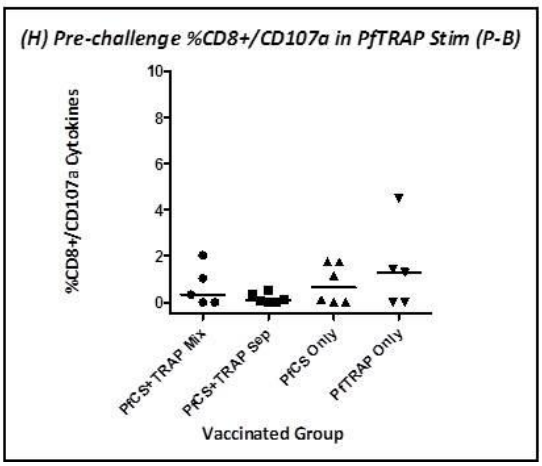
(H) Pre-challenge %CD8+/CD107a in PfTRAP Stim (P-B)
%CD8+/CD107a Cytokines
PfCS+TRAP Mix
PfCS+TRAP Sep
PfCS Only
PfTRAP Only
Vaccinated Group

Figure 5.11 Pre-challenge immunogenicity presented as the CD8+ cells cytokines responses in the blood following the heterologous prime-boost ChAd63-MVA *PfCSP* and *PfTRAP* viral vector vaccines' combinations.

Four different BALB/c mice groups (n=5-6) were vaccinated intramuscularly (i.m.) with ChAd63-*PfCSP,* ChAd63-*PfTRAP* vaccines *or both combined,* eight weeks later the same corresponding groups were vaccinated intramuscularly (i.m.) with MVA-*PfCSP,* MVA-*PfTRAP* vaccines or both combined following the different combinations' strategies described in **Figure 5.8**. One week post MVA-boost vaccination the mice were bled, the PBMC were collected, stimulated with either *PfCSP or PfTRAP protein* overlapping peptides for 6 hours and intracellular staining (ICS) was performed as described earlier in Material and Method sections **2.8.7 and 2.8.8.** These mice were challenged with 1,000 chimeric sporozoites 10-14 days post the MVA boost vaccination with *PfCSP+PfTRAP@pbuis4 (2369 cl4)* double transgenic parasites and the protective efficacy was assessed. $CD8^+$ cytokines responses measured in the blood one week post-MVA boost, expressed as the percentage of $CD8^+$ cells. CD8+ specific cytokine response after PfCSP protein overlapping peptides stimulation described in (A) IFNg, (C) IL-2, (E) TNFa, and (H) CD107a. While $CD8^+$ specific cytokine response after PfTRAP protein overlapping peptides stimulation described in (B) IFNg, (D) IL-2, (F) TNFa, and (G) CD107a. Median with interquartile range values are shown.

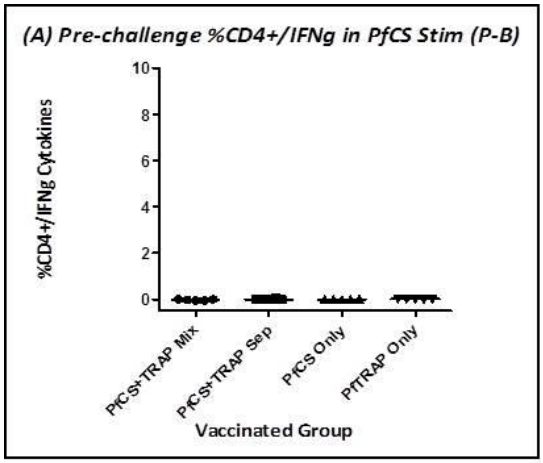
(A) Pre-challenge %CD4+/IFNg in PfCS Stim (P-B)
%CD4+/IFNg Cytokines
10
8
6
4
2
0
PfCS+TRAP Mix
PfCS+TRAP Sep
PfCS Only
PfTRAP Only
Vaccinated Group

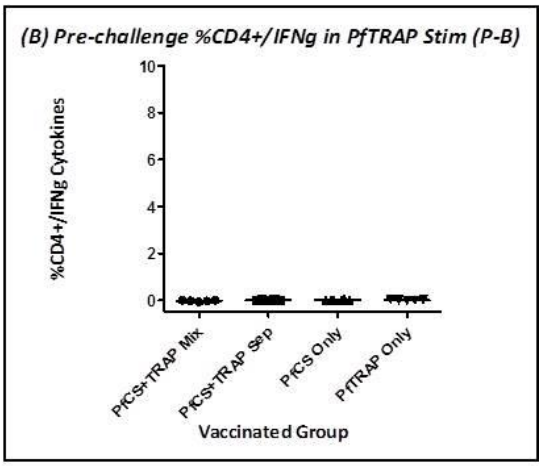
(B) Pre-challenge %CD4+/IFNg in PfTRAP Stim (P-B)
%CD4+/IFNg Cytokines
10
8
6
4
2
0
PfCS+TRAP Mix
PfCS+TRAP Sep
PfCS Only
PfTRAP Only
Vaccinated Group

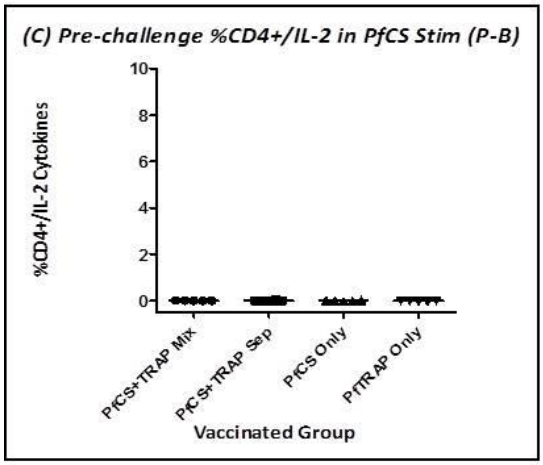
(C) Pre-challenge %CD4+/IL-2 in PfCS Stim (P-B)
%CD4+/IL-2 Cytokines
10
8
6
4
2
0
PfCS+TRAP Mix
PfCS+TRAP Sep
PfCS Only
PfTRAP Only
Vaccinated Group

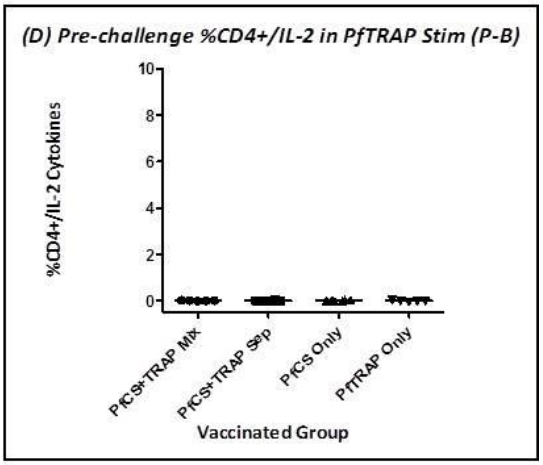
(D) Pre-challenge %CD4+/IL-2 in PfTRAP Stim (P-B)
%CD4+/IL-2 Cytokines
10
8
6
4
2
0
PfCS+TRAP Mix
PfCS+TRAP Sep
PfCS Only
PfTRAP Only
Vaccinated Group

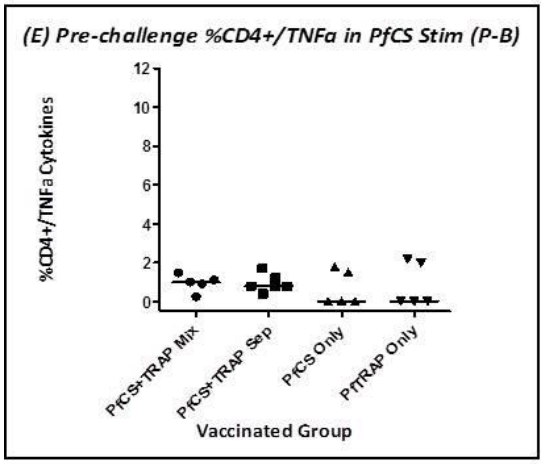
(E) Pre-challenge %CD4+/TNFa in PfCS Stim (P-B)
%CD4+/TNFa Cytokines
12
10
8
6
4
2
0
PfCS+TRAP Mix
PfCS+TRAP Sep
PfCS Only
PfTRAP Only
Vaccinated Group

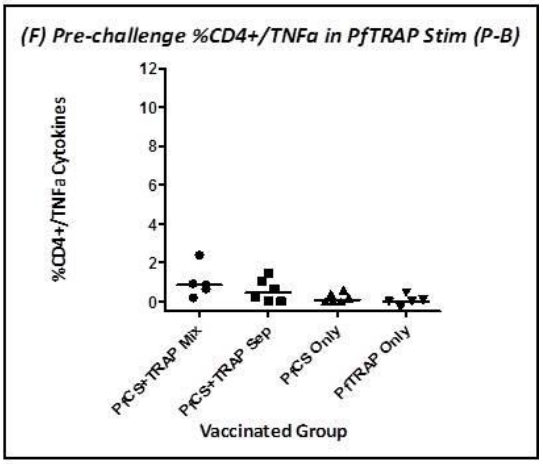
(F) Pre-challenge %CD4+/TNFa in PfTRAP Stim (P-B)
%CD4+/TNFa Cytokines
12
10
8
6
4
2
0
PfCS+TRAP Mix
PfCS+TRAP Sep
PfCS Only
PfTRAP Only
Vaccinated Group

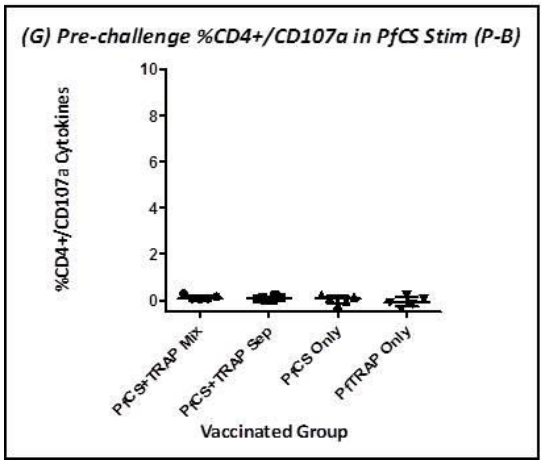
(G) Pre-challenge %CD4+/CD107a in PfCS Stim (P-B)
%CD4+/CD107a Cytokines
10
8
6
4
2
0
PfCS+TRAP Mix
PfCS+TRAP Sep
PfCS Only
PfTRAP Only
Vaccinated Group

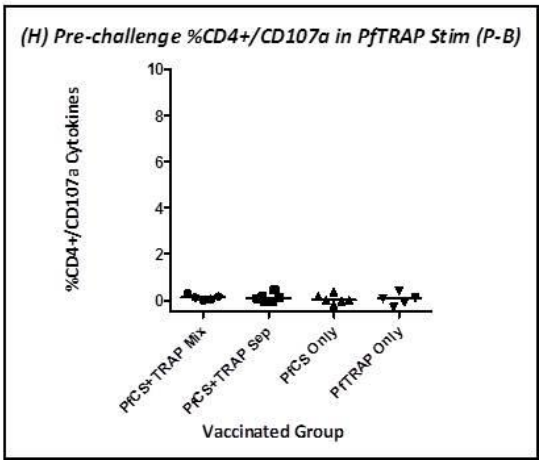
(H) Pre-challenge %CD4+/CD107a in PfTRAP Stim (P-B)
%CD4+/CD107a Cytokines
10
8
6
4
2
0
PfCS+TRAP Mix
PfCS+TRAP Sep
PfCS Only
PfTRAP Only
Vaccinated Group

Figure 5.12 Pre-challenge immunogenicity presented as the CD4+ cells cytokines responses in the blood following the heterologous prime-boost ChAd63-MVA *PfCSP* and *PfTRAP* viral vector vaccines' combinations.

Four different BALB/c mice groups (n=5-6) were vaccinated intramuscularly (i.m.) with ChAd63-*PfCSP,* ChAd63-*PfTRAP* vaccines *or both combined,* eight weeks later the same corresponding groups were vaccinated intramuscularly (i.m.) with MVA-*PfCSP,* MVA-*PfTRAP* vaccines or both combined following the different combinations' strategies described in **Figure 5.8**. One week post MVA-boost vaccination the mice were bled, the PBMC were collected, stimulated with either *PfCSP or PfTRAP protein* overlapping peptides for 6 hours and intracellular staining (ICS) was performed as described earlier in Material and Method sections **2.8.7 and 2.8.8.** These mice were challenged with 1,000 chimeric sporozoites 10-14 days post the MVA boost vaccination with *PfCSP+PfTRAP@pbuis4 (2369 cl4)* double transgenic parasites and the protective efficacy was assessed. $CD4^+$ cytokines responses measured in the blood one week post-MVA boost, expressed as the percentage of $CD4^+$ cells. CD4+ specific cytokine response after PfCSP protein overlapping peptides stimulation described in (A) IFNg, (C) IL-2, (E) TNFa, and (H) CD107a. While CD4+ specific cytokine response after PfTRAP protein overlapping peptides stimulation described in (B) IFNg, (D) IL-2, (F) TNFa, and (G) CD107a. Median with interquartile range values are shown.

5.2.8 Protective efficacy of combined vaccination in BALB/c mice

Vaccinated Balb/c mice were challenge 10-14 days post MVA boost vaccination with 1000 DAGs chimeric sporozoites i.v. and then monitored daily from day five post challenge to calculate time to 1% parasitemia. Mice that were slide negative untill day 14 post-challenge were considered sterilely protected **(Figure 2.13).** The Log-rank (Mantel-Cox) Test was used to assess differences between the survival curves.

The combined vaccination using PfLSA1 and PfLSAP2 vector vaccines induced complete (100%) sterile protection against the DAGs transgenic parasite expressing PfLSA1 and LSAP2 (2403 cl1) when they were injected as mixed or separate vaccines. Single vaccination in group-3 with PfLSA1 only induced 87.5% sterile protection and a significant delay in the time to 1% parasitaemia compared to naïve controls (p=0.008, Log-Rank (Mantel-Cox) Test), while the single vaccination in group-4 with PfLSAP2 induced 75% sterile protection and a significant delay in the time to 1% parasitaemia compared to naïve controls (p=0.005, Log-Rank (Mantel-Cox) Test). All the naïve unvaccinated mice in group-5 became positive after the DAGs chimeric parasite (2403 cl1) sporozoite challenge (**Figure 5.13**). Single vaccination with PfLSA1 or PfLSAP2 alone followed by the DAGs chimeric parasite (2403 cl1) challenge showed similar protection levels to what have been seen earlier against the corresponding single transgenic parasites in Balb/c mice, where vaccination with PfLSA1 or PfLSAP2 was able to protect 7/8 Balb/c mice (87.5%) when they were challenged with $PfLSA1_{Pbuis4}$ (2230 cl1) or $PfLSAP2_{Pbuis4}$ (2237 cl1) **(Chapter 4.2.7).** These results would support the hypothesis that protective efficacy against malaria could be improved by combining the most promising vaccine candidates.

Combining *Pf*CSP and *Pf*TRAP induced 40% sterile protection in the mixed vaccine group-1 against the challenge with the DAGs transgenic parasite expressing PfCSP and TRAP (2369 cl4) and a significant delay in the time to 1%

parasitaemia compared to naïve controls (p=0.0018, Log-Rank (Mantel-Cox) Test) (Figure 5.14). The protective efficacy dropped to 16.7% post-challenge in group-2 when the two vaccines were injected separately in each leg. Single vaccination in group-3 with PfCSP did not confer sterile protection in any animal, but a significant delay in the time to 1% parasitaemia compared to naïve controls was observed (p=0.0018, Log-Rank (Mantel-Cox) Test). Consistent with previous studies single vaccination in group-4 with PfTRAP showed no sterile protection and no significant delay in the time to 1% parasitaemia compared to naïve controls (p= 0.3171, Log-Rank (Mantel-Cox) Test). All the naïve unvaccinated mice in group-5 became positive after the DAGs chimeric parasite (2369 cl9) sporozoite challenge (**Figure 5.14**). Vaccination with PfCSP followed by the DAGs chimeric parasite (2369 cl4) challenge showed no protection, but a significant delay to 1% parasitaemia which differ from what has been seen before on the protection level against the corresponding single transgenic parasite $PfCSP_{Pbuis4}$ (2243 cl3) challenge in Balb/c (37.5%), which could be a result of using fewer mice per group in the DAGs chimeric parasite challenge (n=5 instead of the eight) used previously, or this could be due to chance.

In this challenge model we have identified improved protective efficacy by combining the two novel vaccine candidates *PfLSA1* and *PfLSAP2*, which are more protective than using either of them individually. In addition, combining PfLSA1 and PfLSAP2 viral vaccines induced a better protective efficacy than combining the current most leading malaria vaccines *PfCSP* and *PfTRAP*.

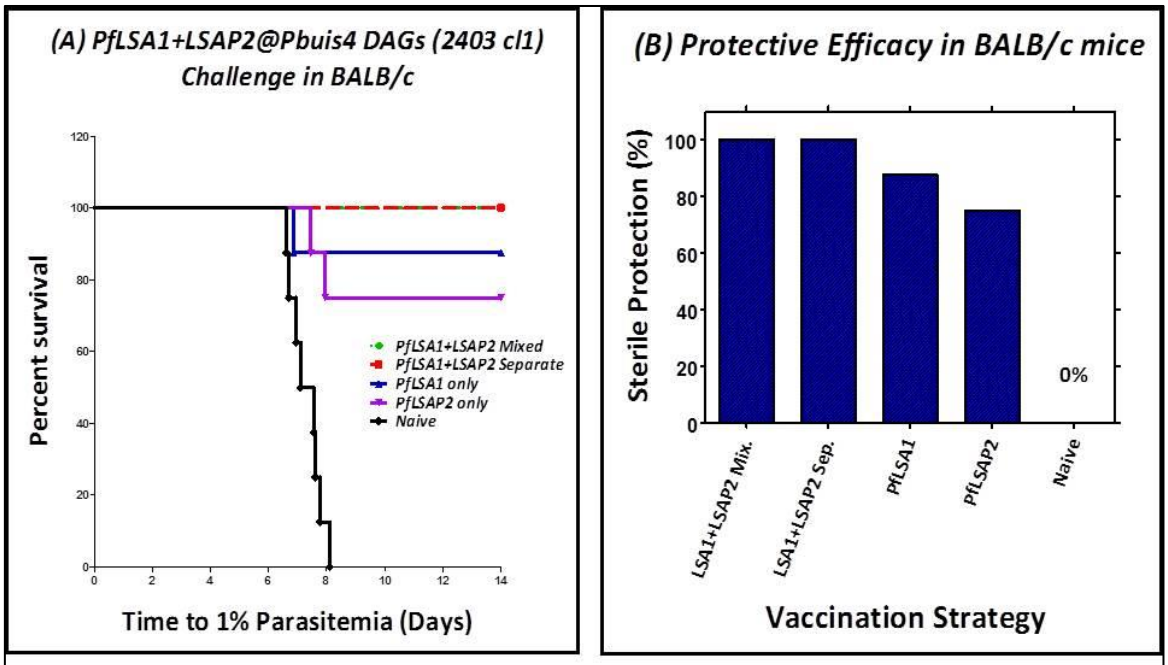

DAGs Chimeric Parasite.	Group No.	Group description	Efficacy	Delay to 1%	P value
PfLSA1+LSAP2@Pbuis4 (2403 cl1)	G1	PfLSA1+LSAP2 Mixed	8/8 (100 %)	-	-
	G2	PfLSA1+LSAP2 Separate	8/8 (100 %)	-	-
	G3	PfLSA1 Only	7/8 (87.5 %)	Yes	0.008 (***)
	G4	PfLSAP2 Only	6/8 (75 %)	Yes	0.005 (***)
	G5	Naive	0/8 (0%)	No	-

Figure 5.13 Post-challenge protective efficacies after PfLSA1and PfLSAP2 ChAd63-MVA prime boost combined vaccination strategy in BALB/c mice. Mice were immunized by the PfLSA1 and PfLSAP2 ChAd63-MVA prime boost combined vaccination strategy as described in the prime-boost combined vaccination strategy in **Figure 5.8.** The five mice groups were challenged 10-14 days after the MVA-boost vaccination. Mice were monitored daily from day five post challenge to enable calculation of the time to 1% parasitemia. Mice that were slide negative till day 14 post-challenge were considered sterilely protected. The Log-rank (Mantel-Cox) Test was used to assess differences between the survival curves.

A. The Kaplan-Meier curve illustrates the time to 1% parasitaemia, whilst statistical significance between the survival curves was assessed using the Log-Rank (Mantel-Cox) Test, as described in the table below the curve; (**G1**) Mice vaccinated with PfLSA1+PfLSAP2 as mixed vaccines with splitting the vaccine dose between the two hind legs, (**G2**) Mice vaccinated with PfLSA1+PfLSAP2 vaccines with injecting each vaccine separately in a different leg, (**G3**) Mice vaccinated with PfLSA1 vaccine only, (**G4**) Mice vaccinated with PfLSAP2 vaccine only, (**G5**) Naïve control.

B. Protective efficacy percentage in the different mice groups induced by the different vaccine combination strategies.

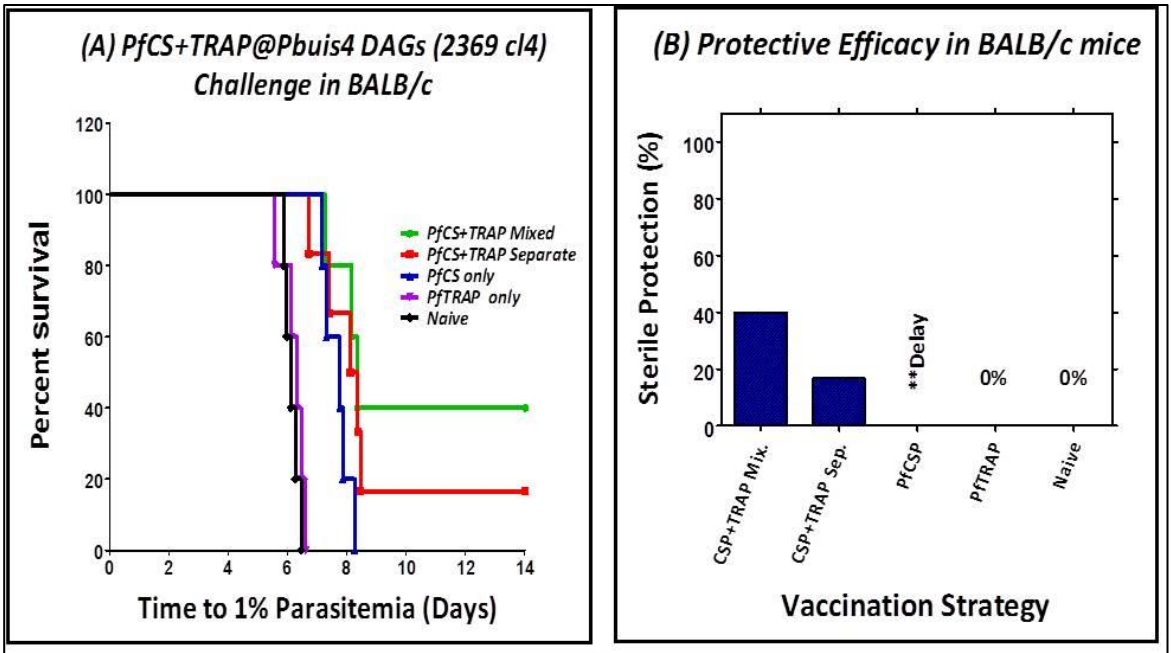

Chimeric Parasite.	Group No.	Group description	Efficacy	Delay to 1%	P value
PffCS+TRAP@Pbuis4 (2369 cl4)	G1	PfCS+TRAP Mixed	2/5 (40 %)	Yes	0.0018 (**)
	G2	PfCS+TRAP Separate	1/6 (16.7 %)	Yes	0.0007 (***)
	G3	PfCS Only	0/5 (0 %)	Yes	0.0018 (**)
	G4	PfTRAP Only	0/5 (0 %)	No	0.3171
	G5	Naive	0/6 (0%)	No	-

Figure 5.14 Post-challenge protective efficacies after PfCSP and PfTRAP ChAd63-MVA prime boost combined vaccination strategy in BALB/c mice. (as described in the prime-boost combined vaccination strategy earlier in **Figure 5.8**) followed by challenging each group with 1000 chimeric sporozoites i.v. as previously described of PfCSP+PfTRAP@Pbuis4 (2369 cl4) double additional genes chimeric sporozoites expressing both PfCSP and PfTRAP. The five mice groups were challenged 10-14 days after the MVA-boost vaccination. Mice were monitored daily from day five post challenge to enable calculation of the time to 1% parasitemia. Mice that were slide negative till day 14 post-challenge were considered sterilely protected. The Log-rank (Mantel-Cox) Test was used to assess differences between the survival curves.

A. The Kaplan-Meier curve illustrates the time to 1% parasitaemia, whilst statistical significance between the survival curves was assessed using the Log-Rank (Mantel-Cox) Test, as described in the table below the curve; (**G1**) Mice vaccinated with PfCSP+PfTRAP as mixed vaccines with splitting the vaccine dose between the two hind legs, (**G2**) Mice vaccinated with PfCSP+PfTRAP vaccines with injecting each vaccine separately in different leg, (**G3**) Mice vaccinated with PfCSP vaccine only, (**G4**) Mice vaccinated with PfTRAP vaccine only, (**G5**) Naïve control.

B. Protective efficacy ratio in the different mice groups induced by the different vaccine combination strategies.

5.3 Discussion

It is widely acknowledged that a multistage or multi-antigen vaccine will likely be necessary to provide high-level efficacy due to the high level of antigenic polymorphism in *Plasmodium* parasites [319], and also because the single antigen vaccinations may not induce broad enough responses able to protect heterogeneous populations of people. Additionally, protection against malaria in humans was demonstrated first through vaccination with irradiated parasites delivered by mosquito bite [24, 28, 320-322]. Irradiated sporozoites are capable of invading hepatocytes but development is arrested, providing a massive repertoire of antigens for the immune system to respond against [32]. Protection by irradiated sporozoites is dependent upon $CD8^+$ T cells targeting the liver-stage [26, 66, 177, 178, 323]. However, over 1000 bites from mosquitoes were required to provide protection in these models, limiting the utility of this approach. Therefore, the theory of incorporating two or more antigens in the vaccination regimen might elicit a broader immunity.

The attempts to combine multiple antigens in subunit vaccines have encountered varying levels of success in other studies. The combined vaccination of monkeys with DNA and poxvirus vectors encoding four *P. knowlesi* antigens, including PkCS, PkTRAP, PkMSP-1, and PkAMA-1 resulted in significantly better control of blood-stage parasitaemia compared to PkCSP vaccination alone [315]. Similarly, the combined administration of PyMSP-1 and PyCSP vectored vaccines elicited higher level of protection than the same vaccines administered alone [316]. In addition, Limbach *et al.* reported that the protection elicited by a combination of *P. yoelii* UIS3 (upregulated in infectious sporozoites 3) and falstatin antigens in the DNA followed by MVA vaccination regimen exceeded the sum of the protection elicited by the single antigen vaccines against the *P. yoelii* sporozoite challenge, indicating a synergistic, or at least super-additive, interaction [211]. The concurrent injection of DNA plasmids

encoding PyHEP17 and PyCSP antigens enhanced levels of protection in various strains of mice as compared to the same single antigen vaccinations against pre-erythrocytic challenge [318]. However it has been difficult to assess combination strategies against the human malaria parasites (*P. falciparum* and *P. vivax*) due to the lack of a suitable pre-clinical challenge models since human malaria doesn't infect small rodent animals.

Discovering a new *P. berghei* 'neutral' locus in chromosome-12; *Pbs1* locus (PBANKA_120680) [250] in additional to the previously known *Pb230p* neutral locus in chr-3 opened up the possibility to easily generate a double transgenic parasite expressing two transgenes from other *Plasmodium* strains even in the absence of endogenous homologues in *P. berghei.* As a proof of concept, a knock-out *PbΔs1* GIMO mother-line (2149 cl1) was generated to assess the effect of deleting *Pbs1 OFR* on the mutated parasite through the whole parasite life cycle. *PbΔs1* GIMO mother-line (2149 cl1) showed no growth defect and was identical to WT parasites throughout the life cycle.

In this chapter we applied the new technology of generating double transgenic parasites to assess the protective efficacy of combining two subunit viral vector vaccines against two different *P. falciparum* antigens. Two different double additional genes (DAGs) chimeric parasites were generated; one expressing the most promising two novel candidates Liver-stage antigen 1 (PfLSA1) and Liver-Stage Associated Protein 2 (PfLSAP2) based on our protective efficacy rank/order results of ten pre-erythrocytic malaria vaccines in Chapter-4. As a control, a DAGs chimeric parasites expresses the current two leading *P. falciparum* malaria vaccine candidates *Pf*CSP and *Pf*TRAP was also generated.

To compare the immunogenicity and protective efficacy associated with different pre-erythrocytic stage malaria antigen combinations using the double additional genes (DAGs) transgenic *P. berghei* challenge model. PfLSA1 and PfLSAP2 were comparatively assessed alone or in combined co-administration

as a mixture or individually using the heterologous ChAd63-MVA prime-boost approach which used to induce strong T cell responses and high-titre Abs against malaria antigens in preclinical studies in mice, rabbits, rhesus macaques [190, 194, 281, 324-327] and human [191]. In parallel, PfCSP and PfTRAP combined vaccination were selected as a control because different vaccine formulation based on these antigens having been extensively explored and having consistently elicited some level of protective efficacy in pre-clinical [328] and clinical studies [166, 267, 329].

Mixed versus separate-sites administration for the combined vaccination were tested in this study because it has been previously shown that multiple malaria Ags administration can lead to antigenic interference as compared to the mixture single-site DNA [317] and viral vector [316] vaccinations. It seems that the immunological interference is not specific to malarial Ags. Larke *et al.* reported that the combination of multiple single-clade HIV-1 vaccines resulted in *in vivo* $CD8^+$ T cell immune interference [330].

This Chapter investigated the protective potential associated with combining the two most promising *P. falciparum* vaccines PfLSA1 and PfLSAP2 and demonstrated 100% sterile protection in vaccinated BALB/c mice. This level of efficacy is the highest level seen using the *in vivo* challenge model either through the single transgenic challenge model experiments in BALB/c or CD-1 outbred mice strains **(Chapter-4)** or injecting each vaccine individually followed by the corresponding DAGs chimeric parasite challenge. Combining PfLSA1 and PfLSAP2 viral vaccines showed substantially higher protective efficacy compared to the current combination of the most leading malaria vaccines *Pf*CSP and *Pf*TRAP, which induced only 40% sterile protection at best when used as a mixed vaccine co-administration or 16.7% sterile protection when the two vaccines were injected into separate legs. Perhaps, these challenge experiments need to be repeated in different mice strains like outbred CD1 mice or with higher

sporozoites number to see how far we could keep the complete 100% sterile protection when PfLSA1 and PfLSAP2 vaccines combined.

Schneider *et al.* showed high sterile protection by combining PbCSP and PbTRAP antigens using DNA/MVA prime-boost vaccination regime by eliciting 60% and 100% sterile protection against 1000 and 200 *P. berghei* sporozoite challenges, respectively [331]. However, in the latter case at the time of boosting MVA was administered intravenously, which is a more protective but not a deployable mode of vaccination for African infants [331]. Since the intravenous injection of MVA viral vectors is clearly not ideal for a clinical setting, the intramuscular route of administration was chosen for the studies described in this thesis.

This work provides the first demonstration that complete protective immunity against malaria challenge can be induced in a rodent animal model using the combination of two viral vector vaccines and only two immunisations. These data have important implications for the development of a multi-stage or multi-component viral vectored malaria vaccine.

Chapter 6

Generation of five novel pre-erythrocytic viral vector vaccines and protective efficacy assessment using the Additional Gene (AG) chimeric parasite challenge model

6 Generation of five novel pre-erythrocytic viral vector vaccines and protective efficacy assessment using the Additional Gene (AG) chimeric parasite challenge model

6.1 Introduction

Malaria infections of mammals are initiated by the transmission of *Plasmodium* salivary gland sporozoites during the mosquito bite. Sporozoites travel from skin at site of injection to the liver, where they infect hepatocytes. Blocking this initial stage of infection is a promising malaria vaccine strategy. The available genomic data in combination of improved sample purification and high mass accuracy mass spectrometry has facilitated a detailed characterization of the proteome of *P. falciparum* sporozoites resulting in the identification of a total of 1991 proteins [229]. Better understanding of the protein composition of sporozoites will enhance the identification of additional proteins that are putative vaccine candidates that can be used to develop vaccines that block the infection before the development of clinical symptoms.

In this chapter we have analysed five new antigens that had been identified in a proteome analysis of the sporozoite surface- and of liver-stages. The proteins were chosen based on their expression pattern (mainly in sporozoite and/or the liver-stages) and are thought to be a main target of cell-mediated immunity. The chosen antigens were expressed in both ChAd63 and MVA viral vectors. These viral vectors were delivery using a prime-boost regimen that have been shown to induce the most potent $CD8^+$ T cell response in previous studies [281, 282, 313].

To show the protective efficacy of these vaccines, the immunized mice were challenged with transgenic *P. berghei* rodent malaria parasites expressing *P. falciparum* antigens. This approach has been used successfully as a challenge model to assess the protective efficacy *in vivo* as described in the previous chapters and in other studies [78, 217, 237, 238, 240, 241, 283, 284]. We

created five different transgenic *P. berghei* parasites that express the new *P. falciparum* antigens as additional copy genes under the control of *Pbuis4* gene regulatory elements. The *P. falciparum* gene expression cassettes were introduced into either the neutral *230p* locus in chr-3 or the neutral *s1* locus in chr-12. These new antigens were then rank ordered in comparison with all the previously tested antigens based on their protective efficacy in different mice strains.

6.1.1 Sporozoite microneme Proteins Essential for Cell Traversal (PfSPECT-1 and PfSPECT-2).

The most studied sporozoites/pre-erythrocytic proteins to date are the circumsporozoite protein (CSP) [332, 333] and the thrombospondin-related anonymous protein (TRAP) [334] both involved in sporozoites traversal of mammalian cells and s invasion of hepatocytes. Two additional proteins have been shown to play essential roles in sporozoite traversal of the dermis, sinusoidal cell layer and Kupffer cells, namely the sporozoite microneme proteins essential for cell traversal, SPECT-1 and SPECT-2 [333, 335, 336]. SPECT-1 and SPECT-2 proteins are stored in the micronemes and translocated to the sporozoite's membrane (surface) during the infection of the vertebrate host **(Figure 6.1).** SPECT-1, and SPECT2 are involved in sporozoite movement and interaction with host cell receptors, and could induce a protective immune response [335-338]. SPECT-1, and SPECT-2 were considered attractive pre-erythrocytic immune targets because of their key role in crossing of the malaria sporozoites across the dermis and the liver sinusoidal wall, prior to invasion of hepatocytes [231, 339].

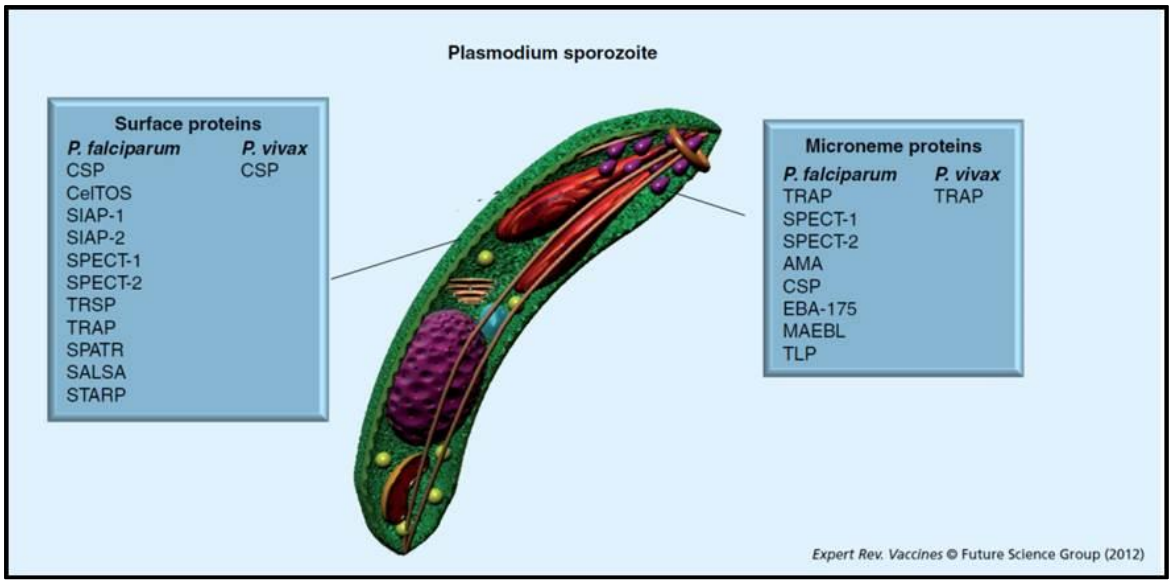

Figure 6.1 Actual state of proteins identified in sporozoite stages in *Plasmodium falciparum* shows the proteins described to date with their respective localization in the parasite (surface and micronemes) (Patarroyo, M.A. et al, 2012).

6.1.2 Hexose Transporter (PfHT)

The Hexose Transporter protein has been identified as a sporozoite surface-exposed protein [229, 244] *P. falciparum* hexose transporter (PfHT) is the key supplier of hexose to *P. falciparum*. PfHT is a facilitative hexose transporter in the Major Facilitator Superfamily of integral membrane proteins that mediates the uptake of glucose and fructose by the parasite [340]. PfHT is a single copy gene in the *P. falciparum* genome with no close paralogues. It is one of the identified surface-exposed proteins in malaria parasite salivary gland Sporozoites which bears 12 predicted transmembrane domains [228, 229] and was first identified as a potential antimalarial drug target [341]. It has an essential function for erythrocytic parasite growth as it was not possible to knockout PfHT unless the gene was complemented by an episomal construct [228]. The Hexose transporter is constitutively expressed through all parasite stages which may reflects its critical role for survival. These previous studies provide support for considering PfHT as a target for a novel vaccine that can inhibit glucose uptake and kill parasites.

6.1.3 Ribosomal Protein-L3 (RP-L3)

Unlike the well-studied CSP antigen that coats the sporozoite, the Ribosomal Protein-L3 (RP-L3) is not highly expressed until later in the liver and RBC stages [342]. Studies showed the anti-RP-L3 response after immunisation with sporozoites was mediated by $CD8^+$ T cells because anti-CD8 but not anti-CD4 antibodies blocked the response. RP-L3 is conserved in *Plasmodium berghei* ANKA (PBANKA_051190), *Plasmodium falciparum* (PF10_0272), and *Plasmodium vivax* (PVX_111330) [230].

6.1.4 Plasmodium 6-Cys family-related protein (PfB9).

PfB9 is one of the '6-cysteine protein family' in the Plasmodium parasite, a family which consists of proteins that possess two or more structurally conserved domains, each of which comprise a core of 6 interspaced cysteine amino acid residues and all contain a signal sequence. Several of these proteins have a critical function in fertilization or in infection of hepatocytes. Reverse genetic analysis of B9 protein shows that it plays an important role in development of the pre-erythrocytic parasite forms and is critical to Plasmodium liver-stage development. RT-PCR and immunofluorescence assays show that B9 is translationally repressed in sporozoites and is expressed after hepatocyte invasion where it localizes to the parasite plasma membrane. Mutants lacking B9 expression in the rodent malaria parasites *P. berghei* and *P. yoelii* and the human parasite *P. falciparum* developmentally arrest in hepatocytes [21].

6.2 Results:

6.2.1 Design and generation of ChAd63 and MVA viral vector vaccines

Vectored vaccines were developed using the available 3D7 *P. falciparum* coding sequence with the tissue plasminogen activator (tPA) leader sequence [288] added upstream, as in the clinical ME-TRAP vectors, to aid in secretion, expression and thereby immunogenicity [289-291]. Vaccine sequences were modified for mammalian codon optimization prior to cloning into the ChAd63 and MVA vectors. Adenovirus vector preparation and transfection was carried out as described in **2.7.2.** The size and the sequence details of the five antigens and their ChAd63 viral vaccines production records are attached in the **Appendix Section.** Recombination of MVA virus and transfection was carried out as described in **2.7.3**. Integration, ID and purity PCR were performed to confirm correct insertion and integration of each *P. falciparum* antigen in the correct locus of its viral vector vaccine (**Figure 6.2, and 6.3**).

6.2.2 Design and generation of *P. berghei* Additional Gene chimeric parasites expressing *P. falciparum* antigens

Five AG chimeric parasites expressing the novel proteins were generated by introduction of the coding sequence of the *P. falciparum* antigens into the silent *230p* locus in chr-3 or s1 locus in chr-12 of the two reference *Pb*ANKA GIMO lines (1596 cl1 or 2149 cl1) following the GIMO transfection method [245] as previously described **(Figure 2.8;** see chapter **2.3.1** for more details**)**. The GFP-Luciferase cassette was included in all the transgenic parasites to allow monitoring the mutants in all the different life stages**.** The *P. falciparum* gene coding sequence was placed under control of the regulatory regions (the promoter and transcriptional terminator sequences) of the *Pbuis4* gene to be specifically expressed at the *Plasmodium* sporozoite and liver-stages [276, 286].

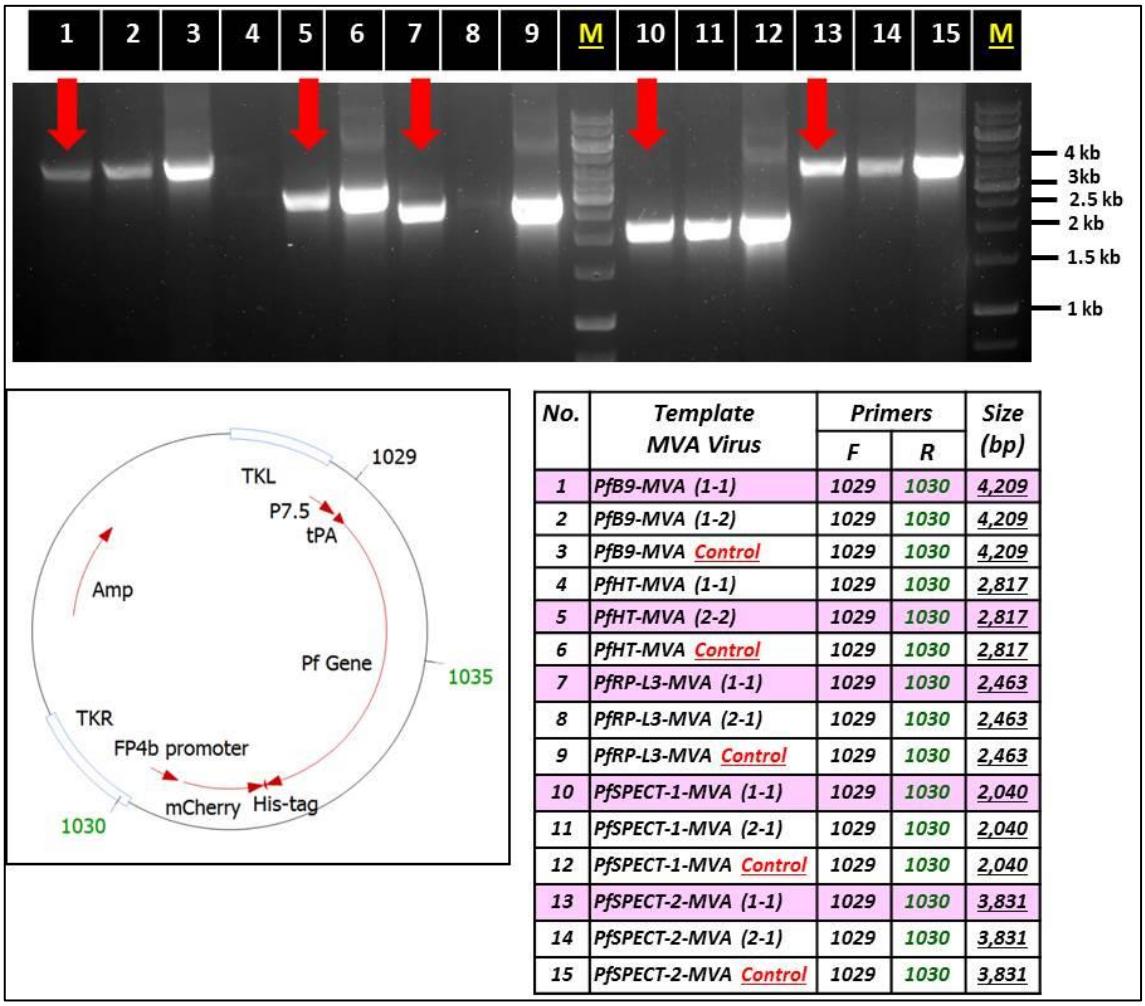

No.	Template MVA Virus	Primers		Size (bp)
		F	R	
1	PfB9-MVA (1-1)	1029	1030	4,209
2	PfB9-MVA (1-2)	1029	1030	4,209
3	PfB9-MVA Control	1029	1030	4,209
4	PfHT-MVA (1-1)	1029	1030	2,817
5	PfHT-MVA (2-2)	1029	1030	2,817
6	PfHT-MVA Control	1029	1030	2,817
7	PfRP-L3-MVA (1-1)	1029	1030	2,463
8	PfRP-L3-MVA (2-1)	1029	1030	2,463
9	PfRP-L3-MVA Control	1029	1030	2,463
10	PfSPECT-1-MVA (1-1)	1029	1030	2,040
11	PfSPECT-1-MVA (2-1)	1029	1030	2,040
12	PfSPECT-1-MVA Control	1029	1030	2,040
13	PfSPECT-2-MVA (1-1)	1029	1030	3,831
14	PfSPECT-2-MVA (2-1)	1029	1030	3,831
15	PfSPECT-2-MVA Control	1029	1030	3,831

Figure 6.2 First round ID and purity PCR for the five MVA recombinant viral vector vaccines (10 plaques).

Different PCR reactions were done to confirm the integration of *P. falciparum* antigen into the MVA viral vector vaccines in comparison to equivalent controls. Positive MVA plaques (highlighted with red) have been tittered, bulkled up and purified.

Expected PCR band sizes are listed in the table beneath each gel, while, primers sequences used and product sizes are shown in **Table 2.4.**

A ***PfHT-MVA*** **B** ***PfRP-L3-MVA*** **C** ***PfSPECT1-MVA***

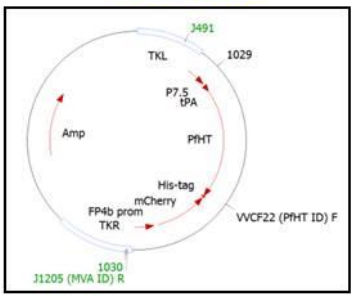

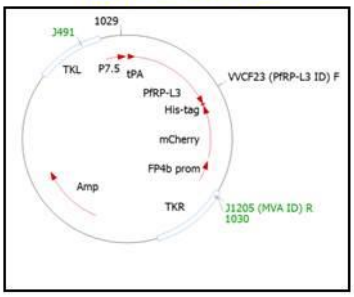

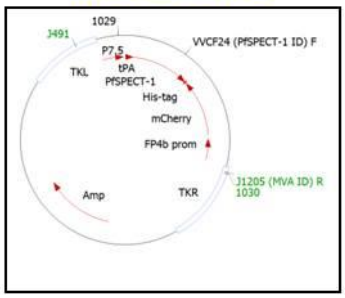

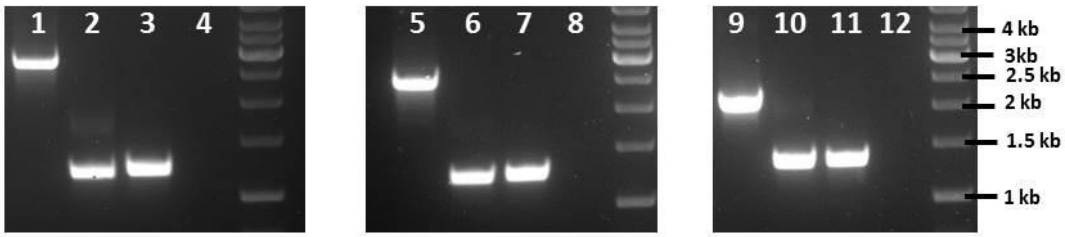

No	Template MVA Virus	Primers		Size (bp)
		F	R	
1	PfHT-MVA (2-2)	1029	1030	2,817
2	PfHT-MVA (2-2)	VVCF22	J1205	1,213
3	PfHT-MVA (2-2)	VVCF22	1030	1,228
4	PfHT-MVA (2-2)	J492F	J491R	NA

No	Template MVA Virus	Primers		Size (bp)
		F	R	
5	PfRP-L3-MVA (1-1)	1029	1030	2,463
6	PfRP-L3-MVA (1-1)	VVCF23	J1205	1,230
7	PfRP-L3-MVA (1-1)	VVCF23	1030	1,245
8	PfRP-L3-MVA (1-1)	J492F	J491R	NA

No	Template MVA Virus	Primers		Size (bp)
		F	R	
9	PfSPECT-1-MVA (1-1)	1029	1030	2,040
10	PfSPECT-1-MVA (1-1)	VVCF24	J1205	1,318
11	PfSPECT-1-MVA (1-1)	VVCF24	1030	1,333
12	PfSPECT-1-MVA (1-1)	J492F	J491R	NA

D ***PfSPECT2-MVA*** **E** ***PfB9-MVA*** **F** ***Parental-MVA virus***

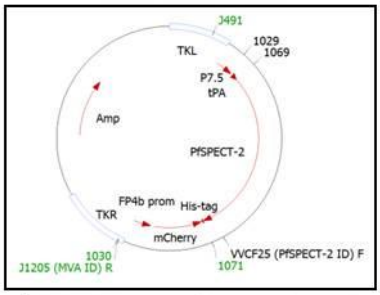

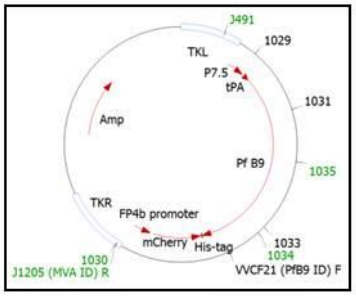

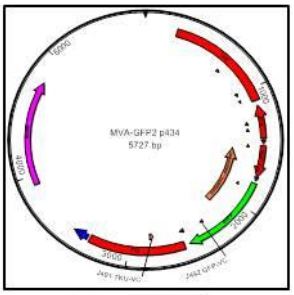

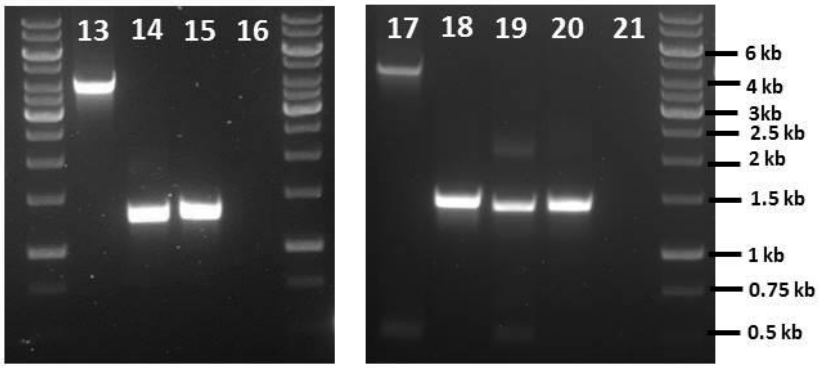

No	Template MVA Virus	Primers		Size (bp)
		F	R	
13	PfSPECT-2-MVA (1-1)	1029	1030	3,831
14	PfSPECT-2-MVA (1-1)	VVCF24	J1205	1,278
15	PfSPECT-2-MVA (1-1)	VVCF24	1030	1,293
16	PfSPECT-2-MVA (1-1)	J492F	J491R	NA

No	Template MVA Virus	Primers		Size (bp)
		F	R	
17	PfB9-MVA (1-1)	1029	1030	4,209
18	PfB9-MVA (1-1)	1029	1035	1,423
19	PfB9-MVA (1-1)	VVCF21	J1205	1,392
20	PfB9-MVA (1-1)	VVCF21	1030	1,407
21	PfB9-MVA (1-1)	J492F	J491R	NA

No	Template MVA Virus	Primers		Size (bp)
		F	R	
22	Parental-MVA virus (#1378 MVA-GFP)	J492F	J491R	499

Figure 6.3 Final ID and purity PCR for the purified MVA recombinant viral vector vaccines.
Different PCR reactions were done to confirm insertion and integration of *P. falciparum* antigen into the correct locus in the viral vector vaccines in comparison to the parental vector or irrelevant viral vector as controls to confirm the MVA vaccines purity.
(A) MVA-PfHT, (B) MVA-PfSPECT-1, (C) MVA-PfSPECT-1, (D) MVA-PfSPECT-2, (E) MVA-PfB9, (F) MVA-Parental virus control.
Expected PCR band sizes are listed in the table beneath each gel, while, primers sequences used and product sizes are shown in **Table 2.4.**

6.2.3 Genotype analysis of the Additional Gene chimeric parasites

To confirm the correct integration of the DNA construct in the chimeric *P. berghei* parasite Southern analysis was performed using a mixed probe of Chromosome-5/hDHFR that recognized both hDHFR selectable marker (SM) and chromosome-5 in the control mutant line (2117 cl1), but could only recognize chromosome-5 in the successfully transfected transgenic parasites, since the *P. falciparum* expression cassette integrated into *P. berghei* 230p locus on chr-3 and replaced the SM. Southern analysis of all generated chimeric parasites showed correct integration of the *P. falciparum* expression DNA construct into the target *P. berghei 230p* gene locus in Chr-3 or *s1* gene locus in Chr-12 (**Figure 6.4**).

Different primers were designed to check correct 5' and 3' integration, and the absence of the SM in the transgenic parasites. Diagnostic PCR analysis confirmed the correct integration of the *P. falciparum* GIMO insertion construct in the chimeric parasites and showed the absence of the SM. **Figure 6.5** shows the results for three of the five AG chimeric parasites expressing *P. falciparum* antigens (i.e.: PfHT, PfRP-L3, and PfPECT-1). These 3 lines showed normal fitness and oocyst/sporozoite production (data not shown) and sporozoites were infective as shown by *in vivo* imaging of liver loads after infection of mice with 1000 sporozites **(Figure 6.6).** Infection of mice with sporozoites of two AG lines did not result in detectable liver infection (PfB9 and PfSPECT-2).

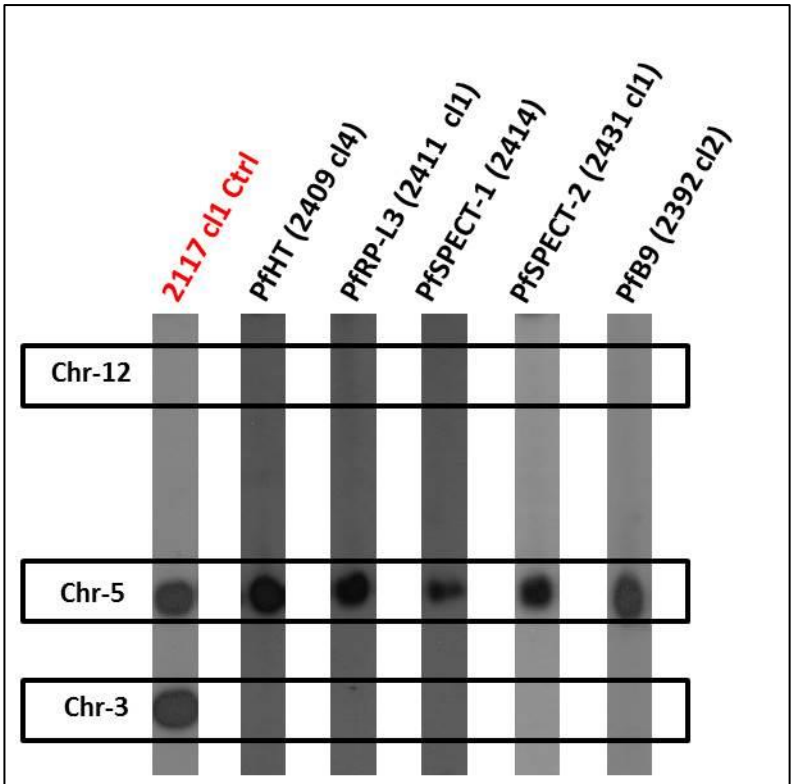

No.	Chimeric parasite name	Line #
1	$PfHT_{Pbuis4}$	2409 cl4
2	$PfRP\text{-}L3_{Pbuis4}$	2411 cl1
3	$PfSPECT\text{-}1_{Pbuis4}$	2414 cl1
4	$PfSPECT\text{-}2_{Pbuis4}$	2431 cl1
5	$PfB9_{Pbuis4}$	2392 cl2

Figure 6.4 Confirmation of correct genotype for the Additional Gene (AG) chimeric *P. berghei* parasite expressing *P. falciparum* antigens.

Southern analysis of chromosomes (Chr) of chimeric parasite lines separated by pulsed-field gel electrophoresis to confirm integration of the *P. faciparum gene* expression cassette in the GIMO locus (*230p* on Chr-3) or (*s1* on Chr-12); shown as the removal of the h*dhfr::*y*fcu* SM cassette in cloned chimeric parasites. The Southern blot is hybridized with a mixture of two probes: one recognizing h*dhfr* and a control probe recognizing Chr-5. As an additional control (Ctrl), parasite line 2117cl1 is used, as it retains h*dhfr::*y*fcu* SM in the *230p* locus on Chr-3.

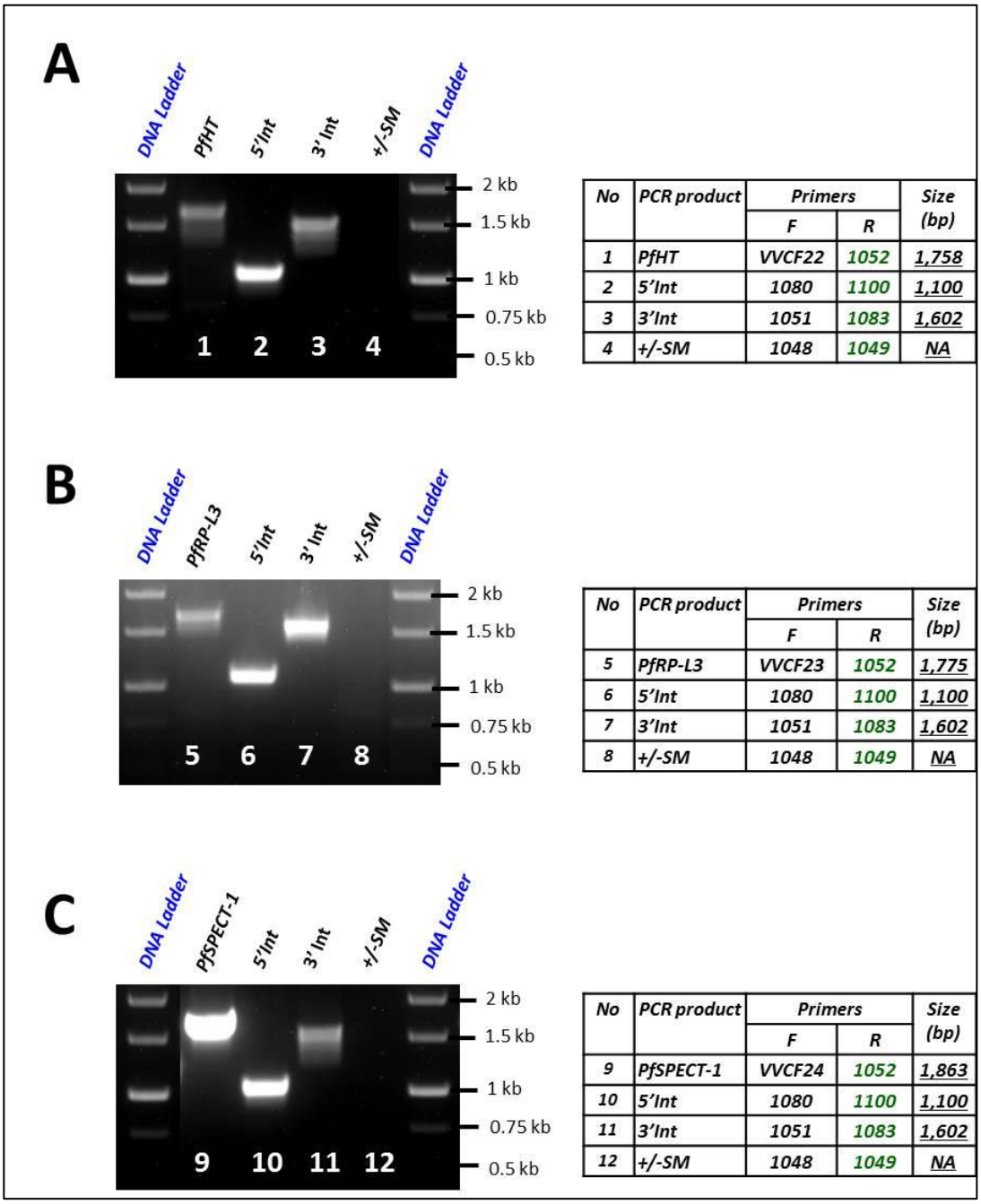

No	PCR product	Primers		Size (bp)
		F	R	
1	PfHT	VVCF22	1052	1,758
2	5'Int	1080	1100	1,100
3	3'Int	1051	1083	1,602
4	+/-SM	1048	1049	NA

No	PCR product	Primers		Size (bp)
		F	R	
5	PfRP-L3	VVCF23	1052	1,775
6	5'Int	1080	1100	1,100
7	3'Int	1051	1083	1,602
8	+/-SM	1048	1049	NA

No	PCR product	Primers		Size (bp)
		F	R	
9	PfSPECT-1	VVCF24	1052	1,863
10	5'Int	1080	1100	1,100
11	3'Int	1051	1083	1,602
12	+/-SM	1048	1049	NA

Figure 6.5 Confirmation of correct genotype for the Additional Gene (AG) chimeric *P. berghei* parasite expressing *P. falciparum* antigens.

Diagnostic PCR analysis of the three chimeric parasite lines that showed identical fitness and infectivity to the WT parasite, confirming correct integration of the *P. falciparum* antigen expression cassettes. Correct integration in all lines is shown by the absence of the h*dhfr*::y*fcu* selectable marker (SM), the presence of the the *P. falciparum* gene CDS and the correct integration of the construct into the genome both at the 5'and 3' regions (5' int and 3' int). **(A) PfHT$_{Pbuis4}$ (2409 cl4), (B) PfRP-L3$_{Pbuis4}$ (2411 cl1), (C) PfSPECT-1$_{Pbuis4}$ (2414 cl1).**

Expected PCR band sizes are listed in the table beside each gel, while, primers sequences used and product sizes are shown in **Table 2.3.**

6.2.4 In vivo imaging for quantification of chimeric parasite load during the liver-stage by imaging

Five naïve mice were infected with the AG chimeric sporozoites to confirm the ability of the DAGs chimeric sporozoites to develop normally to the parasite liver-stage and to assess liver parasite loads by luminescence. The three AG chimeric parasites expressing PfHT (2409 cl4) PfRP-L3 (2411 cl1), and PfSPECT-1 (2414 cl1) showed normal development during the liver-stage of infection *in vivo* **(Figure 6.6).** PfSPECT-2 and PfB9 chimeric parasites (2431 cl1, and 2392 cl2 respectively) were not able to develop a hepatocyte infection *in vivo* or to complete the life cycle. These two parasites were not analysed further. The emitted signals were quantified at 44 hours post infection using the IVIS 200 system and quantified from as total flux/sec.

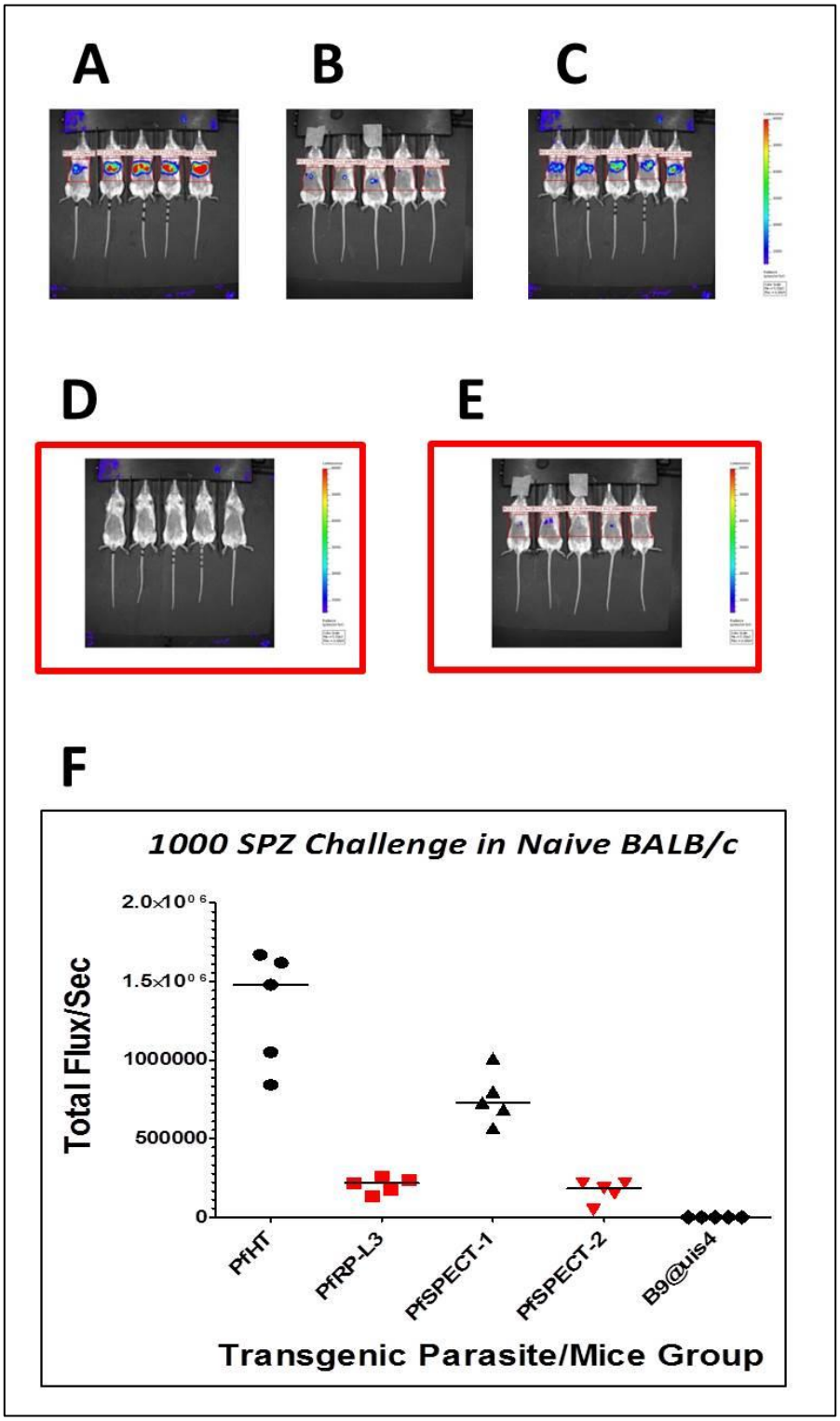

Figure 6.6 *In vivo* imaging. Liver loads in naïve mice that were challenged with transgenic chimeric sporozoites were quantified by measuring luminescence levels at 44 hours after infection using the IVIS 200 system. Results are presented as the total flux measured per second. Both median and individual data points are shown.
A. PfHT$_{Pbuis4}$ (2409 cl4), B. PfRP-L3$_{Pbuis4}$ (2411 cl1), C. PfSPECT-1$_{Pbuis4}$ (2414 cl1), D. PfSPECT-2$_{Pbuis4}$ (2431 cl1), E. PfB9$_{Pbuis4}$ (2392 cl2), F. Quantification of the bioluminescence signal emitted from infected mice measured as total flux/sec.

6.2.5 Phenotype analysis of the additional gene chimeric parasites expressing *P. falciparum* genes by Immunofluorescence assay test (IFAT)

Immunofluorescence staining showed *P. falciparum* antigen expression in sporozoites of the three AG chimeric parasites expressing PfHT (2409 cl4) PfRP-L3 (2411 cl1), and PfSPECT-1 (2414 cl1). Chimeric salivary-gland sporozoites were stained with stained with sera from mice vaccinated against the corresponding *P. falciparum* antigens. Bound IgG was detected with goat anti-mouse IgG-Alexa Fluor 488, green and nuclear DNA stained with 2% Hoechst-33342. As a control, wild-type (WT) *P. berghei* sporozoites were stained with the same sera. Merged images of the different channels are shown for both chimeric and WT *P. berghei* stained images (**Figure 6.7)**.

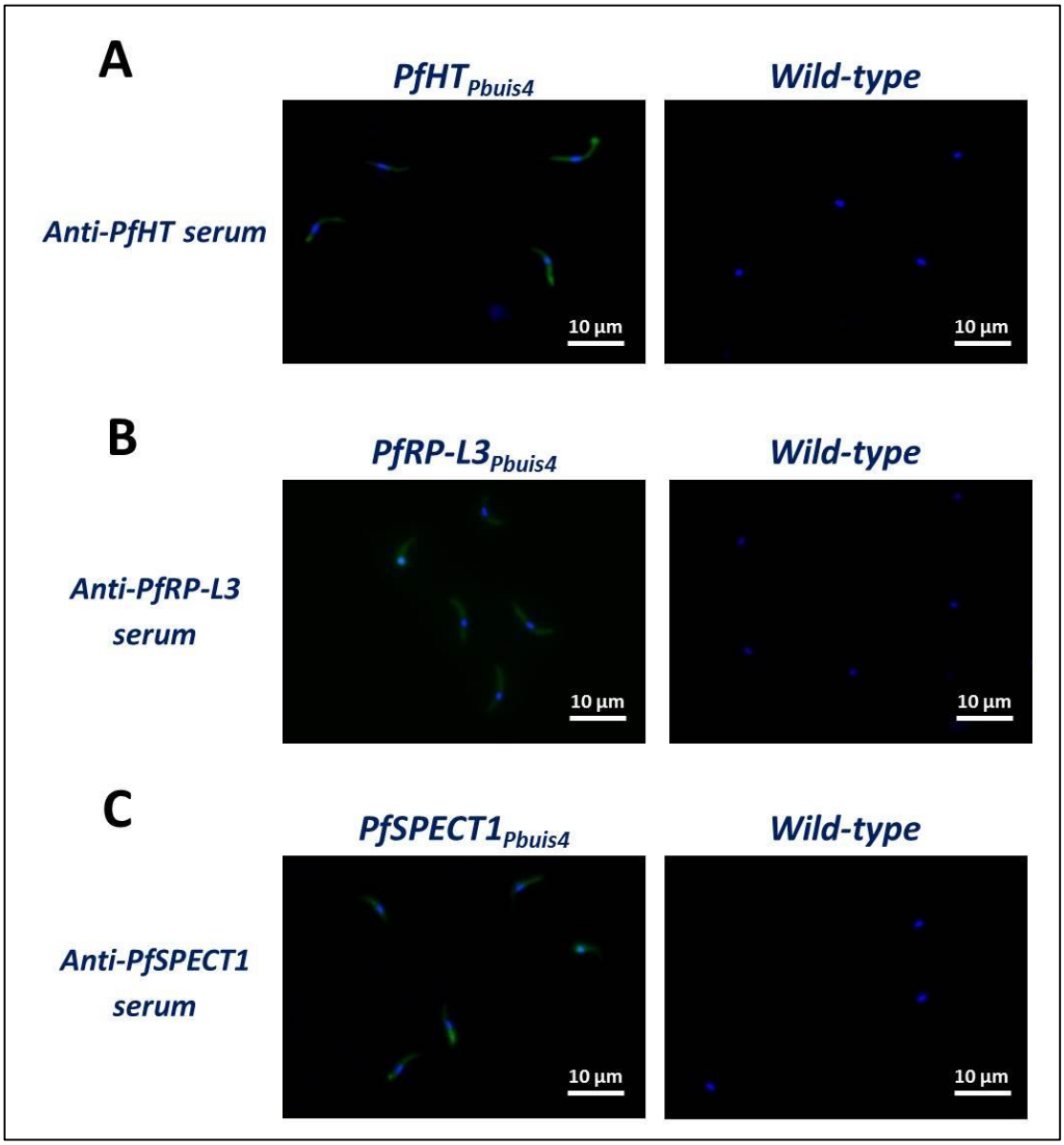

Figure 6.7 Immunofluorescence staining analysis of the AG rodent chimeric parasites.
IFAT staining demonsted *P. falciparum* antigen expression in sporozoites of chimeric *P. berghei* parasites. Chimeric salivary-gland sporozoites were stained with sera from vaccinated mice, secondary antibody (Alexa Fluor 488, green) and Hoechst-33342 (blue; nuclear staining). As a control, wild-type (WT) *P. berghei* sporozoites were stained with the same serum and secondary antibody. Merged images of the different channels are shown for both chimeric parasite and WT *P. berghei* stained images. **(A) $PfHT_{Pbuis4}$ (2409 cl4), (B) $PfRP\text{-}L3_{Pbuis4}$ (2411 cl1), (C) $PfSPECT\text{-}1_{Pbuis4}$ (2414 cl1).**

6.2.6 Immunisation and protective efficacy assessment of three *P. falciparum* vaccines in BALB/c inbred and CD-1 outbred mice *in vivo.*

The standard heterologous ChAd63-MVA prime-boost vaccination strategy was followed with mice vaccinated i.m. with $1x10^8$ ifu ChAd63-Pf antigen followed eight weeks later by $1x10^7$ pfu MVA-Pf antigen (**2.8.2**). Mice were challenged i.v. with 1000 transgenic sporozoites ten days post-MVA boost, along with naive control mice. Mice were monitored daily to enable calculation of the time to 1% parasitaemia with mice that were slide-negative at fourteen days post-challenge considered sterilely protected. The Log-rank (Mantel-Cox) test was used to assess differences between the survival curves. PfHT vaccination did not confer sterile protection in any animal nor was there a significant delay in the time to 1% parasitaemia compared to naïve controls in both BALB/c (p=0.4755) and CD-1 outbred mice (p=0.7663). A similar result was found in PfRP-L3 vaccinated groups, which showed no sterile protection and no significant delay in the time to 1% parasitaemia compared to their naïve controls in both BALB/c (p= 0.4275) and CD-1 outbred mice (P=0.8562). PfSPECT-1 vaccination, however, conferred a high degree of sterile protection and a significant delay to 1% parasitaemia. In BALB/c mice (vaccinated n=8, naive n=8); PfSPECT-1 induced 37.5% sterile protection with a significant delay to 1% parasitaemia (p=0.0008). While in CD-1 outbred mice (vaccinated n=10, naive n=10), PfSPECT-1 induced 70% sterile protection with a significant delay to 1% parasitaemia p=0.0023 **(Figure 6.8).** PfSPECT-1 showed a good rank in the overall rank/order in an overall comparison to all the other single subunit vaccine candidates screened with the

same challenge model *in vivo*. In particular, PfSPECT-1 induced a higher protection level in this challenge model in comparison to our standard current leading *P. falciparum* malaria vaccine PfCSP which showed 31.25% and 33.3% sterile protection in BALB/c and CD-1 mice, respectively **(Figure 6.9).**

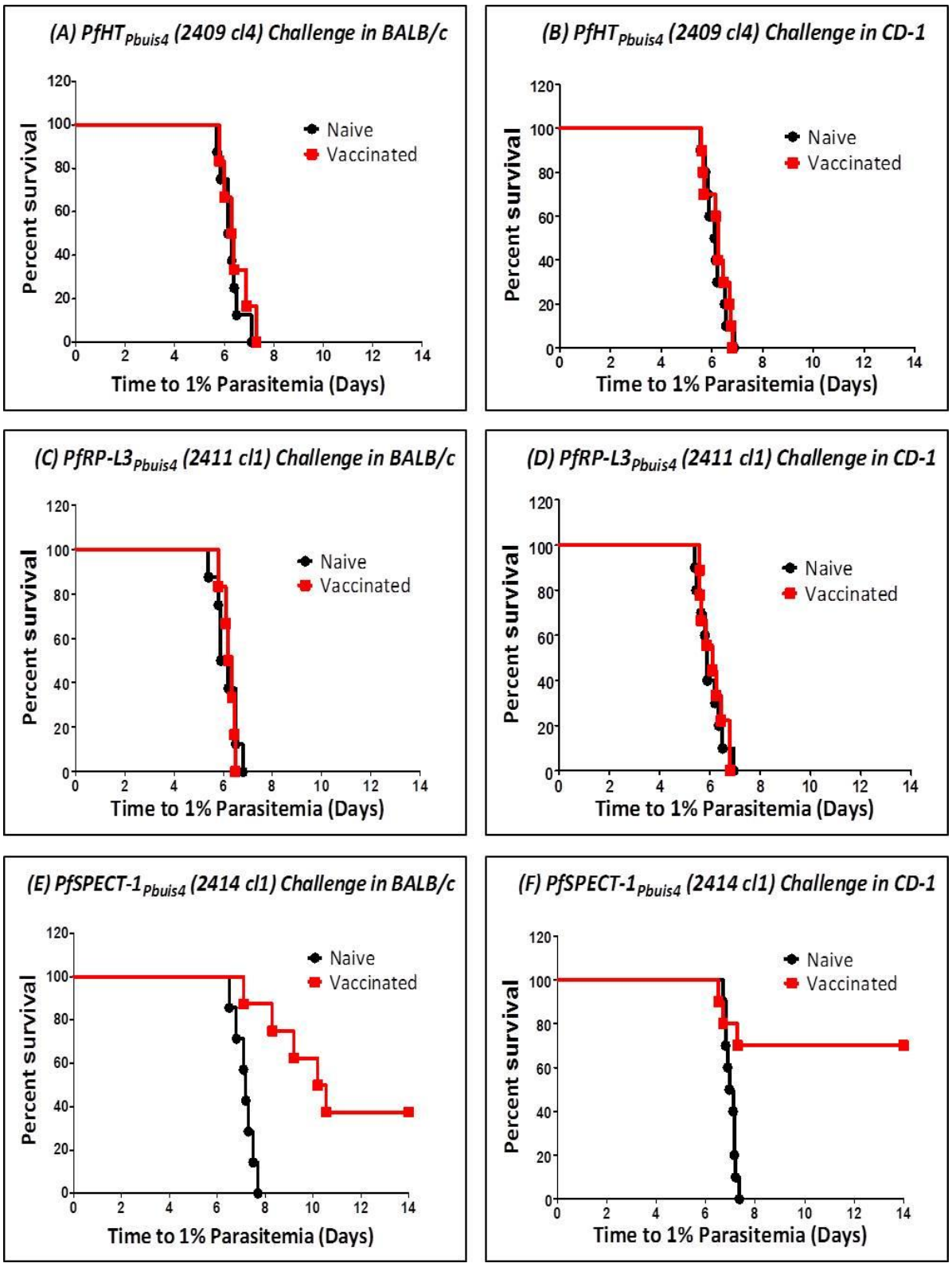

Figure 6.8 Protective efficacy of the ChAd63-MVA *P. falciparum* vaccination in both inbred BALB/c and outbred CD-1 mice.

Mice were vaccinated i.m. with $1x10^8$ ifu ChAd63-Pf vaccine followed eight weeks later by $1x10^7$ pfu MVA- Pf vaccine. Mice were challenged i.v. with 1000 sporozoites of the corresponding AG chimeric parasite ten days post-MVA boost, along with naive control mice. Mice were monitored daily to enable calculation of the time to 1% parasitaemia. Mice that were slide-negative at fourteen days post-challenge were considered sterilely protected. The Kaplan-Meier curve illustrates the time to 1% parasitaemia, whilst statistical significance between the survival curves was assessed using the Log-Rank (Mantel-Cox) Test. Group size of inbred BALB/c mice (n=6-8), where group size of CD-1 outbred mice (n=9-10), where (**A**) PfHT in BALB/c, p=0.4755. (**B**) PfHT in CD-1, p=0.7663. (**C**) PfRP-L3 in BALB/c, p=0.4275. (**D**) PfRP-L3 in CD-1, p=0.8562. (**E**) PfSPECT-1 in BALB/c, p=0.0008. (**F**) PfSPECT-1 in CD-1, p=0.0023.

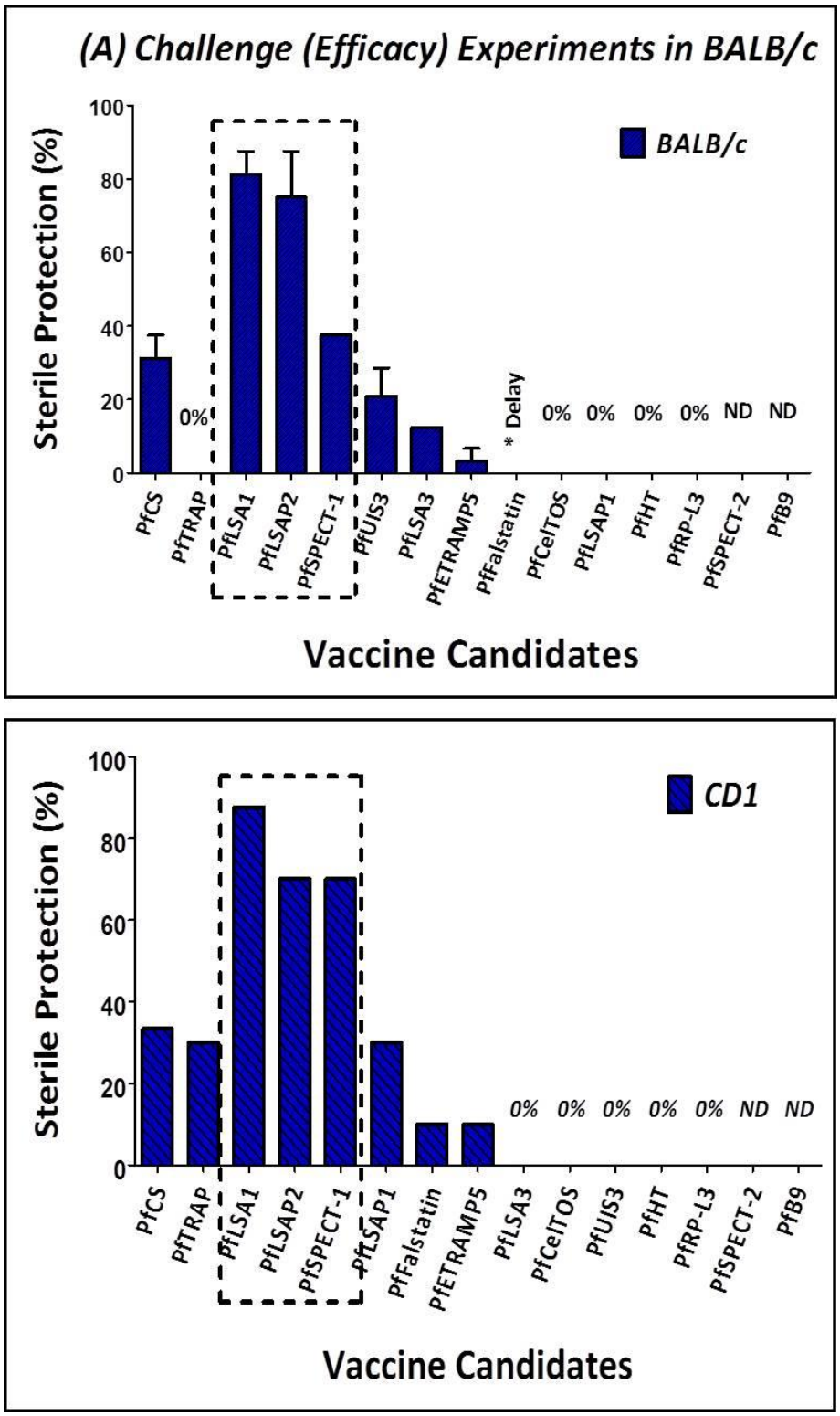

Figure 6.9 Overall rank/order showing the protective efficacy of PfSPECT-1 compared to all the assesse *P. falciparum* vaccine candidate in the same challenge model using chimeric parasites. Screening of 15 novel *P. falciparum* malaria vaccine candidates using the transgenic malaria challenge model identified three novel promising malaria vaccine candidates *(PfLSA1, LSAP-2, and PfSPECT-1)* which could induce high level of sterile protection in both (A) BALB/c inbred, and (B) CD-1 outbred mice strains compared to the current leading *P. falciaprum* malaria vaccines.

6.3 Discussion

The Plasmodium pathogen's life cycle begins when an infected *Anopheles* mosquito injects sporozoites into the skin of the human host during a blood meal. These sporozoites have to cross the dermis to reach blood vessels, travel to the liver via the bloodstream and cross the sinusoidal wall by passing through the Kupffer cells (the macrophages of the liver) to finally invade hepatocytes, in a process mediated by specific interactions between host–cell receptors and parasite proteins [332, 333, 337]. Proteins essential for this bottleneck stage of infection could be promising malaria vaccine candidates.

In this chapter, five new *P. falciparum* antigens were assessed as pre-erythrocytic subunit vaccine targets: HT, RP-L3, SPECT-1, SPECT-2 and B9. These target antigens were attractive candidates due to their relatively high expression in the sporozoite and/or the liver-stage and the key role they play in the pre-erythrocytic stage of infection. Unfortunately, it was not possible to assess the protective efficacy for the newly generated viral vector vaccines candidates PfSPECT-2 and PfB9, because their corresponding AG chimeric sporozoites (2431 cl1) and (2392 cl2) were not infectious: all naive mice remained negative till day-14 post challenge. Two different chimeric parasite clones from PfSPECT-2 and PfB9 were tested but they showed the same fitness problems in terms of sporozoite infectivity. The PfSPECT-2_{Pbuis4} transgenic parasite couldn't develop to the blood stage of infection although it could partially infect the liver, since positive signals were detected *in vivo* by luciferase activity in the liver 44 hours post-infection (**Figure 6.6 D)**. A detectable GFP signal was measured *in vitro* by flow cytometry at 28-30 hours post-infection of Huh-7 hepatocyte (data not shown). One explanation could be that fitness is affected by the size of the inserted *P. falciparum* gene, since fitness problems were only detected with the transgenic parasites which had large inserted transgene such as PfSPECT-2 (2,526 bp) and PfB9 (3,201 bp), both are greater than 2Kb. In addition, only 75% infectivity was seen with PfLSA3 challenged

naïve mice by injecting the standard dose of 1,000 sporozoites i.v., while, 100 % infectivity was only reached with increasing the challenge dose to 2,000 sporozoites i.v. The size of the inserted PfLSA-3 gene is 4,146 bp.

In this chapter, three novel vaccine candidates (HT, RP-L3 and SPECT-1) were assessed for their protective efficacy in the *in vivo* transgenic parasite challenge model. No protection and no significant delay in the time to 1% parasitaemia were observed after vaccination with PfHT or PfRP-L3 in either inbred BALB/c mice or CD-1 outbred mice. PfSPECT-1 vaccination, however, resulted in a good levels of sterile protection in BALB/c mice (37.5%) with a significant delay to 1% parasitaemia p=0.0008. PfSPECT-1 vaccination induced an impressive level of sterile protection CD-1 outbred mice (70%) with a significant delay to 1% parasitaemia p=0.0023**.** In a separate study, performed by a masters student in the lab Ana Rodriguez, serum from mice vaccinated with PfSPECT-1 showed high level of hepatocyte infection blocking; 95% and 93% invasion blocking using 10% serum from BALB/c and CD-1 mice, respectively, and 87% and 74% invasion blocking using 2% serum from BALB/c and CD-1 mice, respectively. Using serum from BALB/c mice vaccinated against PfCSP in the same showed 99% and 81% hepatocyte invasion blocking with 10% and 2% serum, respectively (data not shown). This suggests that protection could be mediated by antibodies, although further characterisation of the immune response and protective mechanism is required to confirm this hypothesis.

In reference to previously assessed antigens, PfSPECT-1 demonstrated a good overall rank/order, with comparable level of protection to the best two promising candidates from the initial screening, PfLSA-1 and PfLSAP-2. Most importantly, protection conferred by vaccination with PfSPECT-1 was consistently higher than protection observed for the the current two leading malaria vaccines, PfCSP and PfTRAP. In particular, PfSPECT-1 induced a higher protection level in this challenge model in comparison to our standard current

leading *P. falciparum* malaria vaccine PfCSP which showed 31.25% and 33.3% sterile protection in BALB/c and CD-1 mice, respectively **(Figure 6.9).**

SPECT-1 and SPECT-2 proteins play essential roles in sporozoite traversal of the dermis, sinusoidal cell layer and Kupffer cells [333, 335, 336]. The 28 kDa SPECT-1 and 95 kDa SPECT-2 proteins are stored in the micronemes and highly expressed on the sporozoite's surface during the liver-stage of infection [229, 343]. Targeted disruption of SPECT genes has been shown to affect sporozoite infectivity *in vivo*, and completely abolish traversal of HeLa cells *in vitro*, suggesting that SPECT molecules are important for the parasite's ability to cross cell barriers, particularly for the progression of the sporozoite from the dermis to the hepatocyte [344]. *In vitro* cell invasion assays have shown that sporozoites containing a deletion of the gene encoding SPECT (*spect*-disrupted parasites) completely lose their ability to pass through Kupffer cells; however, these sporozoites preserve their normal ability to infect hepatocytes, suggesting that passing through cells and the ability to infect are independent phenomena [336, 345]. It has been also suggested that sporozoite passage through Kupffer cells is not obligatory for infection of hepatocytes [231, 335, 336, 344]. SPECT disruption did not affect parasite proliferation in rat red blood cells or interfere with parasite development in the mosquito midgut or salivary glands, but it did have an effect on the parasite's ability to infect the liver [332, 333, 335-338].

Results from Patarroyo et al [231], together with the ones previously described for CSP by Herrera *et. al.* [346], strongly suggests that SPECT-1, SPECT-2 and CSP could be using similar host cell surface receptors to mediate cell traversal processes. The identification of sequences derived from the cell traversal-associated SPECT-1 and SPECT-2 proteins with specific binding activity to HeLa cells, most of which display high affinity for heparin and chondroitin sulfate-containing receptors, which is similar for other sporozoite proteins involved in cell traversal, highlighted the potential of SPECT-1 and SPECT-2 as attractive

targets to be included as antigens in the search of a multi-stage, multi-antigenic, minimal subunit-based, chemically synthesized fully effective vaccine against *P. falciparum* malaria [231].

Components of the cell traversal machinery, such as sporozoite protein essential for cell traversal (SPECT-1 and SPECT2) are attractive candidates to be evaluated as vaccine candidates. The cell traversal activity is important for many steps of sporozoite progression from the skin to the final hepatocyte. Therefer proteins involved in these process attractive targets for cellular immunity and antibody-mediated inhibition strategies. High levels of antibodies against SPECT2 correlate with protection from malaria episodes caused by *P. falciparum* in children [347]. Along with antibodies to the CS protein, which inhibit sporozoite motility in the dermis [348] and presumably elsewhere, antibodies targeting the cell traversal-associated factors would likely further help preventing sporozoites from reaching their final destination in the liver [349].

PfSPECT1 demonstrated a strong protective immunity after vaccination in both BALB/c and CD-1 mice and it is therefore crucial to determine the immunological mechanism underlying this high-level protection by performing detailed characterisation of the immune response induced by vaccination, in addition to T-cell depletion and antibody transfer challenge experiments. A better understanding of the the protective mechanism would help in the combination vaccine studies and future clinical development.

Chapter 7

Discussion and Future Directions

7 Discussions

7.1 Overview

Development of any new vaccine is a difficult task, and the malaria parasite is even more challenging because of its complex life cycle and antigenic complexity. At present, malaria control strategies are based on medications, vector (mosquito) elimination and the prevention of bites. There is no vaccine available that provides an effective long-term protection against *P. falciparum* disease. However, the life cycle provides a number of opportunities to disrupt transmission of the parasite, and to clear infection once it has established itself in humans. A vaccine remains a feasible prevention strategy that could potentially allow complete eradication of malaria, if it could be cheaply and efficiently manufactured and delivered throughout endemic areas. Most researchers agree that a future malaria vaccine will certainly contain a central pre-erythrocytic component as the first line of defense against malaria [154].

The two leading malaria vaccine, RTS,S and ChAd63-MVA ME-TRAP, are both sub-unit vaccines targeting the pre-erythrocytic stage of the parasite's life-cycle. Unfortunately, neither of these vaccines showed the higher level of protective efficacy induced by irradiated sporozoites through mosquito bites [24, 28, 77, 320-322]. However, a sub-unit vaccine has a more practical manufacturing process, a more standard delivery route (intramuscular immunization) and more accessible storage conditions (without the requirement for LN2), leading to the conclusion that a sub-unit vaccine is more feasible for field deployment.

A new screening platform is necessary to enable the discovery of better target antigens than the currently known malaria vaccine candidates. It is highly likely that there are better target antigens among the 5,300 protein-encoding genes that have been identified throughout the *Plasmodium* life-cycle [25]. This is supported by other studies that showed irradiated sporozoite tolerized to the leading vaccines antigen epitopes including CSP are still able to induce protection in mice model [199, 209].

The available genomic data in combination with improved mass spectrometry data has facilitated the best proteome coverage to date for a pre-erythrocytic stage of the human malaria parasite, in total 1991 *P. falciparum* sporozoite proteins [229]. Sporozoite protein studies have substantially helped in identifying many new potential candidates for a pre-erythrocytic vaccine to block the infection before the development of clinical symptoms. However only a minority of these have been assessed to date, and this is partly due to the difficulty in screening human targeted pre-clinically, because *P. falciparum* can't infect small animals and there is no simple way to culture parasites of this stage *in vitro* [279].

Rodent malaria parasites are therefore used as models to identify vaccine targets for protective immune responses against human malaria *in vivo*. Although a high level of orthology and homology exists between the genes of *Plasmodium* species that infect rodents and humans [232, 233], critical differences often exist in the sequence and structure between the encoded proteins. In addition, many *P. falciparum* malaria parasite genes are absent from rodent parasite genomes, making pre-clinical efficacy studies unachievable in murine models.

Research on the biology of malaria parasites has greatly benefited from the application of reverse genetic technologies, which have been applied to allow the genetic modification of rodent malaria parasites and therefore enable the generation of mutants that stably express heterologous proteins and are free of drug-selectable markers in their genome [245]. Generation of transgenic rodent malaria parasites expressing *P. falciparum* can help to circumvent problems arising from structural differences that exist between functional *P. falciparum* and rodent malaria parasite orthologs. In addition, it increases the possibilities of analyzing *P. falciparum*-specific proteins, *in vivo* [270].

In this work, a relatively large screen of thirteen out of initially proposed fifteen *P. falciparum* pre-erythrocytic malaria vaccine candidates was performed using the newly developed *in vivo* transgenic parasites challenge model. Chosen

antigens were expressed in both ChAd63 and MVA, with delivery in a prime-boost regimen which can induce an exceptionally high $CD8^+$ T cells immune response [280-282]. The liver-stage of malaria infection is thought to be mainly targeted by cell-mediated immunity, as the parasite resides within the hepatocyte and the immune system can only interact with antigenic targets transported to the surface of the cell by interacting with $CD8^+$ T cells.

All antigens were ranked/ordered in comparison to the two leading malaria candidates PfCSP and PfTRAP using the same challenge model. Three antigens, PfLSA1, PfLSAP2 and PfSPECT-1, provided better protective efficacy compared to PfCSP and PfTRAP in inbred BALB/c mice. Since different strains of mice are not equally susceptible to malaria infection [350], and to minimize the risk of using an inbred murine model as an indicator for the protective efficacy in humans, CD-1 outbred mice with diverse MHC repertoires were also used, and again PfLSA1, PfLSAP2 and PfSPECT-1 showed better protective efficacy compared to PfCSP and PfTRAP.

Based on results from the initial efficacy screening 'ranking' in Chapter-4, two double transgenic parasites were also constructed, one expressing the most promising two novel candidates combined (*Pf*LSA1 and *Pf*LSAP2) and as a control a double transgenic parasite expressing *Pf*CSP and *Pf*TRAP. It has therefore been possible to assess multi-antigen combination using an *in vivo* model, and to generate better protection than a single-antigen immunization. This work provides the first demonstration that complete protective immunity against malaria can be induced in a rodent animal model using the combination of two viral vector vaccines expressing *Pf*LSA1 and *Pf*LSAP2 after only two immunisations.

7.2 Conclusions and future directions

7.2.1 Transgenic *P. berghei* technology

Studies on rodent malaria parasites have greatly contributed to the knowledge on the developmental biology of malaria parasites. There are four rodent malaria models*; P. berghei P. yoelii, P. chabaudi and P. vinckei. Plasmodium berghei* is the most widely used model for research for many reasons; the availability of technologies for *in vitro* cultivation and large scale production and purification of the different life cycle stages, knowledge of the genome sequence and organization and the relatively easy methodologies for genetic modification of the parasite.

Research on the biology of malaria parasites has greatly benefited from the application of reverse genetic technologies, in particular through the analysis of gene deletion mutants and studies on transgenic parasites that express heterologous or mutated proteins [312]. Transgenic *P. berghei* technology has revolutionized the malaria field. Various knockout transgenic *P. berghei* clones have been instrumental in deciphering parasite protein functions [351], mechanisms of severe malaria pathology [352], or basic parasite biology [93]. Transgenic *P. berghei* models have also been used in vaccine studies where they offer an *in vitro* or *in vivo* assessment of functional immunogenicity. Humanized rodent parasites have been used to assess the efficacy of candidate vaccines against the *P. vivax* TRAP protein [236], the *P. falciparum* and *P. vivax* CS proteins [237, 238] , the *P. falciparum* and *P. vivax* P25 proteins [239, 240] and the *P. falciparum* MSP1 gene [241, 242].

In this work we considered two obstacles which used to be associated with using the traditional *P. berghei* transfection methods. First, transfection in *Plasmodium* was limited by the paucity of drug-selectable markers that hampers subsequent genetic modification of the same mutant. Here the newly developed ‘gene insertion/marker out’ (GIMO) method was used, which uses negative selection to rapidly generate transgenic mutants free of the drug

selectable marker which are ready for subsequent modifications [312]. Additionally, this novel transfection strategy permits the removal of the resistance cassette which could possibly contribute to the transgenic *P. berghei* infectivity profile. It has been shown that merely inserting the *hDHFR* resistance marker downstream of an otherwise unaltered PbCSP gene can negatively affect the transgenic parasite's ability to infect mosquito and vertebrate hosts [353], suggesting that preserving the WT 3'UTR *P. berghei* sequence region may be crucial for successful transcription termination. Second, we wished to determine the most appropriate chimeric parasite technology to take forward for assessment of a number of new *P. falciparum* antigens. As several of these new antigens do not have homologs in rodent malaria, it was important to determine whether there was a difference in terms of efficacy when challenging mice with chimeric parasites that express an antigen encoded by a gene that is introduced as an additional copy (AG chimeric parasites) or by a gene that replaced the *P. berghei* gene ortholog (RG chimeric parasites). For the comparison between AG and RG chimeric parasites **(Chapter-3)** two major *P. falciparum* antigens which have *P. berghei* orthologs were chosen, one expressed the lead malaria vaccine candidate for *P. falciparum* circumsporozoite protein (CSP) [273] and the second expressed *PfCelTOS* antigen which has shown some cross-species protection [195, 274]. Those two mutants (RG vs. AG chimeric parasites) were compared head to head and used to determine whether there was a difference in vaccine efficacy when immunized mice were challenged by either the replacement [RG] or the additional copy [AG] chimeric parasites. As no differences between AG and RG chimeric parasites was observed, all future experiments were performed using the AG approach, where all antigens were expressed under the same promoter (UIS4 promoter). This enabled a standardized comparison of antigens, in particular for those *P. falciparum* antigens with no orthologs/homologs in *P. berghei*.

7.2.2 *P. falciparum* subunit vaccines development technology

The protection mediated by irradiated sporozoite vaccination of mice has been shown to be predominantly dependent on cellular immune responses, through the use of depletion and adoptive as well as passive transfer studies, along with humoral immunity against various sporozoite stage antigens [26, 177, 178, 349]. Some reports also suggest that the direct contact of $CD8^+$ cytotoxic T lymphocytes (CTLs) with the infected hepatocyte is crucial [112] in order for the CTLs to exercise their effector functions. The extensive literature on the subject suggests that the type of protective $CD8^+$ T cell effector functions utilized against the intrahepatic parasites depend not only on the mice strain used, but also vaccination strategy [354] which requires further dissection for the molecular basis behind the $CD8^+$ T cell effector functions during the malaria liver-stage of infection. The liver-stage of malaria infection is thought to be mainly targeted with $CD8^+$ cell-mediated immunity, as the parasite resides within the hepatocyte and the immune system can only interact with antigenic targets transported to the surface of the cell on MHC class I or II molecules to present to $CD8^+$ or $CD4^+$ T cells.

Since our work aims to develop a subunit malaria vaccine against the pre-erythrocytic stage of infection, the chosen antigens were expressed in both ChAd63 and MVA and delivered in a prime-boost regimen which has been shown to induce an exceptionally high CD8+ T cells immune response [280-282] and high antibody titres. The virus itself is also able to act as an adjuvant, not only a delivery system, enhancing the specific response [355]. The *P. falciparum* liver-stage vaccine candidates were cloned into both recombinant chimpanzee adenoviruses (ChAd63) and Modified Vaccinia Ankara viruses (MVA) [190, 194]. Many combinations have existed, but using a ChAd63 prime followed by a MVA boost has shown to be the most potent at producing $CD8^+$ T cells [313] and protective efficacy in the field [356]. Interestingly, both the order and the length of interval have been crucially important in inducing a good response [281];

MVA is not good at priming, but is excellent at boosting, and an extended eight-week interval has shown the best results in our group so far [194].

CD8+ T cells responses are required for an effect at the liver-stage of infection, and hence crucial for a pre-erythrocytic vaccine, while antibodies thought to be primarily needed against the sporozoite are highly effective and also for the blood-stage effect. Whilst viral vectors can induce high levels of antibodies, prime-boost regimens incorporating a protein vaccine have also demonstrated potent antibody production [282]. This may prove vital in combination vaccine, targeting both the liver and blood or sporozoite stages, where both a high level of $CD8^+$ T cells and antibodies will be required to exert the anticipated effect. Experience in our group indicates that chimpanzee adenoviral and MVA vectored vaccines are highly immunogenic and stimulate both arms of the adaptive immune response [194, 357]. We are using the heterologous prime-boost ChAd63-MVA vaccination strategy because it is safe, and to avoid the issue of pre-existing immunity to human adenoviral vectors. The rapid and relatively easy generation of viral vaccines stands in contrast to the time-consuming processes associated with the irradiated sporozoite or many recombinant protein production and purification protocols. The rapid development of effective viral vaccine once appropriate target antigens have been identified, demonstrates the potential contribution of these recombinant vectors in the fight against new and emerging infectious diseases [358-361].

7.2.3 Comparative assessment of novel pre-erythrocytic malaria subunit vaccines using AG transgenic rodent malaria challenge model.

The aim of this project is to construct transgenic parasites expressing the human malaria parasite antigens which are capable of infecting small pre-clinical models. This work has permitted an early and rapid assessment of new *P. falciparum* vaccine candidates, without the requirement of expensive clinical trials and avoiding difficulties in obtaining *P. falciparum* parasite isolates available only in countries where malaria is endemic. In this protective efficacy

ranking/order screening fifteen single AG transgenic *P. berghei* parasites were generated to assess novel *P. falciparum* malaria vaccine protective efficacy in mouse models; LSA1, LSA3, CelTOS, UIS3, LSAP1, LSAP2, ETRAMP5, Falstatin, CSP, TRAP, HT, RP-L3, SPECT-1, SPECT-2 and B9. The infectivity and phenotype analysis of thirteen single AG transgenic parasites were identical to the wild-type *P. berghei* parasites, while two AG transgenic parasites (SPECT-2 and B9) were not fit and didn't infect naïve mice. The thirteen AG transgenic parasites with the normal fitness feature were used to assess efficacy of their corresponding *P. falciparum* viral vector vaccines. Two viral vectored vaccines expressing PfLSA1, PfLSAP2 or PfSPECT-1, showed substantially and significantly higher protective efficacy than both PfCSP and PfTRAP when expressed in the same vaccination platform. Both PfLSA1 and PfLSAP2 sterilely protected 87.5% of BALB/c mice, while PfSPECT-1 sterilely protected 37.5% of BALB/c mice, compared to 37.5% efficacy for PfCSP and 0% efficacy for PfTRAP. Vaccination with PfLSA1 (87.5%), PfLSAP2 (70%) or PfSPECT-1 (70%) also provided significantly higher sterile protection in outbred CD-1 mice, greater than that induced by PfCSP (33%) or PfTRAP (30%). Vaccination with PfUIS3, PfFalstatin, PfLSA3 and PfETRAMP-5 in BALB/c mice provided some degree of protection, manifested largely as a delay in the time to parasitaemia, consistent with previous work with using murine *Plasmodium* challenges [206, 211]. Protection was also induced at a low level for PfLSAP-1, PfFalstatin and PfETRAMP-5 in outbred mice. No protection was seen with the remainder of the candidates. Surprisingly, no protection was observed after vaccination with PfCelTOS despite previous reports of cross-species protection in murine models [195, 274].

The depletion experiments highlighted a strong dependence on $CD8^+$ T cells for protection when vaccinating with PfLSA1, and complete dependence following PfLSAP2 vaccination. PfLSA1 and PfLSAP2 are thought to be located in the parasitophorous vacuole membrane (PVM) [214, 292, 293], and therefore are

likely good targets for a cell-mediated immune response as antigens may be better presented on the hepatocyte surface [294]. $CD8^+$ T cells exert their cytotoxic effector functions through recognition of MHC class I-epitope complexes loaded onto the surface of the infected hepatocytes. Since the parasite's intrahepatic development is confined within the parasitophorous vacuole, it seems that the export of parasite proteins outside the parasitophorous vacuole is tightly regulated [362, 363] and only crucial proteins necessary for parasite's liver stage development may be granted access to the hepatocyte cytosol [364]. Therefore, for a T cell vaccine to be able to confer protection, not only does the target antigen needs to be antigenic, but must also be present, at least as a breakdown product, within hepatocyte's cytoplasm [365].

Recent work using a model antigen expressed in *P. berghei* sporozoites found that exported antigens improved the elimination of infected liver cells by antigen-specific $CD8^+$ T cells [295]. Our findings indicate that the antigenic target is of high importance, and suggest that both PfLSA1 and PfLSAP2 are potentially better candidates than PfCSP or PfTRAP for a pre-erythrocytic vaccine. Both PfLSA1 and PfLSAP2 have no known murine homologue, and hence the classical method of pre-clinical testing using rodent homologues of *P. falciparum* antigens as vaccine candidates would not have been able to identify these as protective, highlighting the value of this transgenic parasite challenge model.

PfSPECT-1 proteins play essential roles in sporozoite traversal of the dermis, sinusoidal cell layer and Kupffer cells [335, 336, 366]. It is stored in the micronemes and highly expressed on the sporozoite's surface during the liver-stage of infection [229, 343]. In this study, PfSPECT1 demonstrated a strong protective immunity after vaccination in both BALB/c and CD-1 mice and it is therefore crucial to determine the immunological mechanism underlying this high-level protection. A better understanding of the protective mechanism would help in the combination vaccine studies and future clinical development.

Although it needs to be confirmed, it is likely that protection mediated by PfSPECT-1 vaccination could be a combination of both cellular and humoral immune response, because the cell traversal protein family is important for many steps of sporozoite progression from the skin to the final hepatocyte and its members are good targets for cellular immunity and antibody-mediated inhibition strategies. A study in our laboratory has found that serum from mice vaccinated with PfSPECT-1 could induce high level of blocking of hepatocyte infection of cell lines which was comparable to the blocking induced by PfCSP**.** This suggests that protection could be mediated by antibodies, although further characterisation of the immune response and protective mechanism is required to confirm this hypothesis. Additionally, Manuel E. Patarroyo et al.'s results [231], together with the ones previously described for CSP by Herrera *et. al.* [346], strongly suggests that SPECT-1, SPECT-2 and CSP could be using similar host cell surface receptors to mediate cell traversal processes. Another study by Crompton, P.D., et al. showed that high levels of antibodies against SPECT2 correlated with protection from malaria episodes caused by *P. falciparum* in children [347]. Along with antibodies to the CS protein, which inhibit sporozoite motility in the dermis [348], antibodies targeting the cell traversal-associated factors would likely prevent sporozoites from reaching their final destination in the liver [349].

7.2.4 Assessment of subunit malaria vaccine combinations

The advantage of the novel GIMO transfection method to recycle the selection marker, along with the discovery of the new neutral *Pbs1* locus in chromosome-12 allowed multiple genetic modifications in the same mutant and the insertion of the second antigen into transgenic *P. berghei* already expressing *P. falciparum* gene in the neutral *Pb230p* locus in chr-3. Moreover, the double-transgenic parasite's infectivity of mice was comparable to the WT parasites. The successful generation of double-transgenic *P. berghei* is not only notable

from the transgenic parasite technology point of view, but also may provide some insights related to the combination of two malaria pre-erythrocytic stage vaccines.

Using the results from the initial assessment of *P. falciparum* candidate antigens (Chapter-4) two double transgenic parasites were generated expressing either PfLSA1 and PfLSAP2 or PfCSP and PfTRAP. DAG transgenic parasite challenge model opened the door to assess the combination of two different antigens in the vaccination regimen. However, it has been reported that vaccinating with multiple-antigen vaccines can have an antagonistic effect and may reduce protective efficacy because of antigenic interference [317, 318]. This was not the case when combining PfLSA1 and PfLSAP2 viral vector vaccines in the standard ChAd63-MVA prime-boost regimen. The combined vaccination with *Pf*LSA1 and *Pf*LSAP2 vector vaccines induced complete (100%) sterile protection against the DAGs transgenic parasite expressing PfLSA1 and LSAP2 (2403 cl1) when they administered as a mixture or separately into different legs when compared to individual antigen immunization, PfLSA1 and PfLSAP2 individual vaccination induced 87.5% and 75% sterile protection respectively. Additionally, combining PfLSA1 and PfLSAP2 showed a significantly higher protection in comparison to the current leading vaccines combination *Pf*CSP and *Pf*TRAP, which induced only 40% sterile protection against the challenge with the DAGs transgenic parasite expressing PfCSP and TRAP (2369 cl4). In human *P. falciparum* malaria, synergistic multi-antigens vaccine regimen is expected to be more efficient than the single vaccine strategy because of the complexity of the *Plasmodium* parasite life cycle and diversity in the antigens in parasite populations, in addition to the fact that single antigen vaccinations may not induce broad immune responses necessary to protect heterogeneous populations of people, and this approach also should cover better the natural polymorphism of the vaccine antigen.

In conclusion, the generation of transgenic *P. berghei* expressing different pre-erythrocytic stage *P. falciparum* antigens provides useful tools for the malaria vaccine community. The use of these transgenic models should expedite the development and optimization the pre-clinical screening of the novel human malaria vaccines combinations given the chance for direct head to head comparison to PfCSP and PfTRAP antigens in the same challenge model *in vivo.*

7.2.5 Efficiency of using *P. berghei* transgenic parasite as a challenge model

Identification of protective antigens and correlates of protection has become a major focus in malaria vaccine research, however it usually difficult to identify statistical correlates in both murine studies and clinical trials, where often only small proportions of volunteers are protected or delayed. This highlights the value of the transgenic *P. berghei* system to screen for efficacy of novel *P. falciparum* malaria vaccines *in vivo* using a cheap pre-clinical model. Additionally, we have demonstrated the feasibility of generating a large number of transgenic parasites utilizing the GIMO technology which provides an extremely useful tool to study all stages of the parasite's lifecycle. The transgenic parasite challenge model illustrates how this technology can be applied to selection of antigens from complex pathogens for vaccine development. This technology was very useful in this study where it helped to identify three key protective liver-stage antigens that are significantly better than the current leading malaria vaccines in clinical trials.

The recycling of selection marker from the generated transgenic parasites permits more genetic modifications, for example DAG transgenic parasite could be used as a background to insert a third *P. falciparum* pre-erythrocytic stage antigen into transgenic *P. berghei* already carrying two *P. falciparum* genes by allelic replacement. This could be a revolutionary strategy to assess the combined vaccination between three different antigens *in vivo.* This idea could

be applied to introduce PfSPECT-1 gene as a replacement copy for the endogenous PbSPECT-1 in the PfLSA1+PfLSAP2 DAG transgenic parasite that could be used to asses combinations of these three promising *P. falciparum* vaccine candidates.

Despite the high value of using this transgenic parasite system for vaccines assessments *in vivo,* there are two limitations with this model. First, despite the use of chimeric parasites it is still a murine model and encounters issues of small numbers of MHC restricted epitopes and marked immunodominance, which is less prominent in outbred human populations. Outbred mice can be used to more accurately reflect what may be seen in a human study and importantly, efficacy with PfLSA1, PfLSAP2 and PfSPECT-1 was here maintained in CD-1 mice and still higher than what have seen with both PfCSP and PfTRAP. Second, the *P. falciparum* antigen is under control of the *Pbuis*4 promoter. Whilst this places all antigens on an even level, in terms of expression, it might be significantly different from the natural level of expression in the wild-type *P. falciparum* parasite. Perhaps the best approach is performing the preliminary screening with AG transgenic parasites since it is a relatively easier and faster method and also allows the expression of any *P. falciparum* transgene in *P. berghei* even if it doesn't have an endogenous homolog in *P. berghei*. This would be useful, especially in case of making a large scale comparison study between many vaccine candidates. However, the generation of RG transgenic *P. berghei* for only the promising candidates might be considered –if possible-. This will help to narrow down the number of the generated RG transgenic parasites if needed.

7.3 Final Remarks

This work in this thesis describes a new and highly successful approach for identifying novel protective *P. falciparum* liver-stage antigens *in vivo* using the transgenic parasite challenge model. We have showed three novel *P. falciparum* antigens, PfLSA1, PfLSAP2 and PSPECT-1 that induced substantially high level of protection better than the two widely used PfCSP and PfTRAP antigens in both inbred and out-bred mice. Whilst PfLSA1 is well known and has long been considered ineffective as a vaccine target based on a failed clinical trial of a protein-adjuvant vaccine; our results appear to refute such previous work and show the value of our new pre-clinical screening system particularly when the focus of the vaccine is induction of effector $CD8^+$ T cells. PfLSAP2 is a new candidate, and our findings strongly suggest this protein has an essential role during liver-stage development. Importantly, neither of these antigens has a rodent malaria homologue and so could not have been identified by studies of rodent malaria antigens, an approach attempted by other groups. PfSPECT-1 is a newly discovered parasite protein which has been shown to play an essential role in sporozoite traversal of the dermis, sinusoidal cell layer and Kupffer cells. SPECT-1 is stored in the micronemes and translocated to the sporozoite's membrane (surface) during the infection of the vertebrate host, and is very involved in sporozoite movement and interaction with host cell receptors. The use of viral vectors circumvents problems associated with irradiated sporozoites or recombinant protein technologies based vaccines, and the need for a chemical adjuvant. ChAd63-MVA prime-boost regimes can elicit protective antibody responses, and also induce T cell responses that may, with further investigation, prove highly effective against both the liver-stage parasite.

This work reported here has clearly and quantitatively demonstrated synergistic effect by combining the two promising vaccine candidates PfLSA1 and PfLSAP2 which lead to complete (100%) sterile protection in vaccinated BALB/c mice. Both PfLSA1 and PfLSAP2 protective mechanisms are based on $CD8^+$ T cells,

while PfSPECT-1 has showed some signs based on several studies [347-349] to be a good antibody stimulator along with inducing $CD8^+$ cellular immune response (further characterisation of the protective mechanism will be done). The two leading pre-erythrocytic stage malaria vaccine candidates in human clinical trials, RTS,S and ChAd63.MVA ME-TRAP rely on the induction of high Ab titres and powerful T cell responses, against PfCSP and PfTRAP proteins respectively. There are some ideas and clinical trials in progress combining these two vaccines to generate better efficacy. Since all the new three promising candidates have shown better protection, it would be a good idea to test the combined vaccination between these three promising candidates.

The most protective regimen demonstrated in this thesis; incorporating ChAd63-MVA of PfLSA1 and ChAd63-MVA of PfLSAP2 vaccines would currently require manufacturing two different recombinant ChAd63 and two MVA viral vectors. Currently such regimen, if proven successful in further pre-clinical and clinical studies, could be too expensive to deploy for wide-scale vaccinations. One way to make ChAd63-MVA PfLSA1 and PfLSAP2 combination vaccine more affordable would be to incorporate both PfLSA1 and PfLSAP2 antigens within the genome of one ChAd63 or MVA viral vector for the use as a single injection at the prime. The Glycine-Proline (GGGPGGG) linker has been employed successfully to fuse two different AMA-1 alleles in tandem and place the construct within the backbone of single recombinant Adenovirus [327]. Further optimization of combination vaccine strategy could be made if the future pre-clinical combinations between the three promising vaccine candidates were successful. Theoretically, it would be possible to incorporate all the three antigens in one ChAd63 or MVA viral vector, where all the three vaccines coding sequences combined would be less than 4 Kb, as the ChAd63 vector can carry up to a 6 Kb DNA insert and MVA tolerates even larger transgene sizes. Further optimization of the vaccine viral vector and the combination strategies could make the regime more protective and feasible for large-scale vaccinations. This

could speed up the process of taking the most promising vaccine approach into the clinical challenge study to further assess the clinical utility of this combination vaccine in the fight against *P. falciparum* malaria.

References

1. Bousema, T. and C. Drakeley, *Epidemiology and infectivity of Plasmodium falciparum and Plasmodium vivax gametocytes in relation to malaria control and elimination.* Clin Microbiol Rev, 2011. **24**(2): p. 377-410.

2. WHO, *World Health Organization: World Malaria Report 2013.* 2013.

3. Flannery, E.L., A.K. Chatterjee, and E.A. Winzeler, *Antimalarial drug discovery - approaches and progress towards new medicines.* Nat Rev Microbiol, 2013. **11**(12): p. 849-62.

4. Lee, S.J., G. Gonzalez-Aseguinolaza, and M.C. Nussenzweig, *Disseminated candidiasis and hepatic malarial infection in mannose-binding-lectin-A-deficient mice.* Mol Cell Biol, 2002. **22**(23): p. 8199-203.

5. Greenwood, B.M., et al., *Malaria.* Lancet, 2005. **365**(9469): p. 1487-98.

6. Sachs, J. and P. Malaney, *The economic and social burden of malaria.* Nature, 2002. **415**(6872): p. 680-5.

7. Hollingdale, M.R., et al., *Biology of malarial liver stages: implications for vaccine design.* Ann Trop Med Parasitol, 1998. **92**(4): p. 411-7.

8. Cerami, C., F. Kwakye-Berko, and V. Nussenzweig, *Binding of malarial circumsporozoite protein to sulfatides [Gal(3-SO4)beta 1-Cer] and cholesterol-3-sulfate and its dependence on disulfide bond formation between cysteines in region II.* Mol Biochem Parasitol, 1992. **54**(1): p. 1-12.

9. Nadkarni, G.D., et al., *Plasma orosomucoid metabolism and susceptibility to malarial infection in rodents.* Indian J Exp Biol, 1990. **28**(11): p. 1078-81.

10. Murray, C.J., et al., *Global malaria mortality between 1980 and 2010: a systematic analysis.* Lancet, 2012. **379**(9814): p. 413-31.

11. Penny, M.A., et al., *What should vaccine developers ask? Simulation of the effectiveness of malaria vaccines.* PLoS One, 2008. **3**(9): p. e3193.

12. Maire, N., et al., *Predictions of the epidemiologic impact of introducing a pre-erythrocytic vaccine into the expanded program on immunization in sub-Saharan Africa.* Am J Trop Med Hyg, 2006. **75**(2 Suppl): p. 111-8.

13. Hanson, K.K., et al., *Torins are potent antimalarials that block replenishment of Plasmodium liver stage parasitophorous vacuole membrane proteins.* Proc Natl Acad Sci U S A, 2013. **110**(30): p. E2838-47.

14. Suhrbier, A., et al., *Survival and antigenic profile of irradiated malarial sporozoites in infected liver cells.* Infect Immun, 1990. **58**(9): p. 2834-9.

15. Krotoski, W.A., et al., *Demonstration of hypnozoites in sporozoite-transmitted Plasmodium vivax infection.* Am J Trop Med Hyg, 1982. **31**(6): p. 1291-3.

16. Hollingdale, M.R., et al., *Inhibition of entry of Plasmodium falciparum and P. vivax sporozoites into cultured cells; an in vitro assay of protective antibodies.* J Immunol, 1984. **132**(2): p. 909-13.

17. Ishino, T., Y. Chinzei, and M. Yuda, *Two proteins with 6-cys motifs are required for malarial parasites to commit to infection of the hepatocyte.* Mol Microbiol, 2005. **58**(5): p. 1264-75.

18. Stanisic, D.I., A.E. Barry, and M.F. Good, *Escaping the immune system: How the malaria parasite makes vaccine development a challenge.* Trends Parasitol, 2013. **29**(12): p. 612-22.

19. Hoffman, S.L., et al., *Irradiated sporozoite vaccine induces cytotoxic T lymphocytes that recognize malaria antigens on the surface of infected hepatocytes.* Immunol Lett, 1990. **25**(1-3): p. 33-8.

20. Sagna, A.B., et al., *Plasmodium falciparum infection during dry season: IgG responses to Anopheles gambiae salivary gSG6-P1 peptide as sensitive biomarker for malaria risk in Northern Senegal.* Malar J, 2013. **12**: p. 301.

21. Annoura, T., et al., *Two Plasmodium 6-Cys family-related proteins have distinct and critical roles in liver-stage development.* FASEB J, 2014. **28**(5): p. 2158-70.

22. Taechalertpaisarn, T., et al., *Biochemical and functional analysis of two Plasmodium falciparum blood-stage 6-cys proteins: P12 and P41.* PLoS One, 2012. **7**(7): p. e41937.

23. Kadota, K., et al., *Essential role of membrane-attack protein in malarial transmission to mosquito host.* Proc Natl Acad Sci U S A, 2004. **101**(46): p. 16310-5.

24. Rieckmann, K.H., et al., *Letter: Sporozoite induced immunity in man against an Ethiopian strain of Plasmodium falciparum.* Trans R Soc Trop Med Hyg, 1974. **68**(3): p. 258-9.

25. Gardner, M.J., et al., *Genome sequence of the human malaria parasite Plasmodium falciparum.* Nature, 2002. **419**(6906): p. 498-511.

26. Weiss, W.R., et al., *CD8+ T cells (cytotoxic/suppressors) are required for protection in mice immunized with malaria sporozoites.* Proc Natl Acad Sci U S A, 1988. **85**(2): p. 573-6.

27. Speer, C.A. and P.H. Silverman, *Recent advances in applied malaria immunology.* Z Parasitenkd, 1979. **60**(1): p. 3-17.

28. Rieckmann, K.H., et al., *Use of attenuated sporozoites in the immunization of human volunteers against falciparum malaria.* Bull World Health Organ, 1979. **57 Suppl 1**: p. 261-5.

29. Clark, I.A., *Does endotoxin cause both the disease and parasite death in acute malaria and babesiosis?* Lancet, 1978. **2**(8080): p. 75-7.

30. Kwiatkowski, D., *Tumour necrosis factor, fever and fatality in falciparum malaria.* Immunol Lett, 1990. **25**(1-3): p. 213-6.

31. Gimenez, F., et al., *Tumor necrosis factor alpha in the pathogenesis of cerebral malaria.* Cell Mol Life Sci, 2003. **60**(8): p. 1623-35.

32. Mellouk, S., et al., *Protection against malaria induced by irradiated sporozoites.* Lancet, 1990. **335**(8691): p. 721.

33. Wijayalath, W., et al., *Strain-specific protective effect of the immunity induced by live malarial sporozoites under chloroquine cover.* PLoS One, 2012. **7**(9): p. e45861.

34. Coban, C., et al., *Toll-like receptor 9 mediates innate immune activation by the malaria pigment hemozoin.* J Exp Med, 2005. **201**(1): p. 19-25.

35. Parroche, P., et al., *Malaria hemozoin is immunologically inert but radically enhances innate responses by presenting malaria DNA to Toll-like receptor 9.* Proc Natl Acad Sci U S A, 2007. **104**(6): p. 1919-24.

36. Togbe, D., et al., *Murine cerebral malaria development is independent of toll-like receptor signaling.* Am J Pathol, 2007. **170**(5): p. 1640-8.

37. Muller, O., et al., *Malaria in sub-Saharan Africa.* Lancet, 2009. **373**(9658): p. 122.

38. Noor, A.M., et al., *The use of insecticide treated nets by age: implications for universal coverage in Africa.* BMC Public Health, 2009. **9**: p. 369.

39. Kajfasz, P., *Malaria prevention.* Int Marit Health, 2009. **60**(1-2): p. 67-70.

40. Lengeler, C., *Insecticide-treated bed nets and curtains for preventing malaria.* Cochrane Database Syst Rev, 2004(2): p. CD000363.

41. Pluess, B., et al., *Indoor residual spraying for preventing malaria.* Cochrane Database Syst Rev, 2010(4): p. CD006657.

42. Najera, J.A., M. Gonzalez-Silva, and P.L. Alonso, *Some lessons for the future from the Global Malaria Eradication Programme (1955-1969).* PLoS Med, 2011. **8**(1): p. e1000412.

43. Baird, J.K., *Resurgent malaria at the millennium: control strategies in crisis.* Drugs, 2000. **59**(4): p. 719-43.

44. Brooke, B.D., et al., *Bioassay and biochemical analyses of insecticide resistance in southern African Anopheles funestus (Diptera: Culicidae).* Bull Entomol Res, 2001. **91**(4): p. 265-72.

45. Curtis, C., et al., *Scaling-up coverage with insecticide-treated nets against malaria in Africa: who should pay?* Lancet Infect Dis, 2003. **3**(5): p. 304-7.

46. Hargreaves, K., et al., *Anopheles funestus resistant to pyrethroid insecticides in South Africa.* Med Vet Entomol, 2000. **14**(2): p. 181-9.

47. Ranson, H., et al., *Pyrethroid resistance in African anopheline mosquitoes: what are the implications for malaria control?* Trends Parasitol, 2011. **27**(2): p. 91-8.

48. Goodman, C.A., P.G. Coleman, and A.J. Mills, *Cost-effectiveness of malaria control in sub-Saharan Africa.* Lancet, 1999. **354**(9176): p. 378-85.

49. Yeung, S., et al., *Antimalarial drug resistance, artemisinin-based combination therapy, and the contribution of modeling to elucidating policy choices.* Am J Trop Med Hyg, 2004. **71**(2 Suppl): p. 179-86.

50. Bardaji, A., et al., *Intermittent preventive treatment of malaria in pregnant women and infants: making best use of the available evidence.* Expert Opin Pharmacother, 2012. **13**(12): p. 1719-36.

51. Meremikwu, M.M., et al., *Intermittent preventive treatment for malaria in children living in areas with seasonal transmission.* Cochrane Database Syst Rev, 2012. **2**: p. CD003756.

52. Roberts, D.R. and R.G. Andre, *Insecticide resistance issues in vector-borne disease control.* Am J Trop Med Hyg, 1994. **50**(6 Suppl): p. 21-34.

53. Ndiath, M.O., et al., *How the malaria vector Anopheles gambiae adapts to the use of insecticide-treated nets by African populations.* PLoS One, 2014. **9**(6): p. e97700.

54. Krogstad, D.J., et al., *Efflux of chloroquine from Plasmodium falciparum: mechanism of chloroquine resistance.* Science, 1987. **238**(4831): p. 1283-5.

55. Ashley, E.A., et al., *Spread of artemisinin resistance in Plasmodium falciparum malaria.* N Engl J Med, 2014. **371**(5): p. 411-23.

56. Eastman, R.T. and D.A. Fidock, *Artemisinin-based combination therapies: a vital tool in efforts to eliminate malaria.* Nat Rev Microbiol, 2009. **7**(12): p. 864-74.

57. Plotkin, S.A., *[New vaccination strategies].* Bull Acad Natl Med, 2008. **192**(3): p. 511-8; discussion 518-9.

58. Fenner, F., *A successful eradication campaign. Global eradication of smallpox.* Rev Infect Dis, 1982. **4**(5): p. 916-30.

59. Strassburg, M.A., *The global eradication of smallpox.* Am J Infect Control, 1982. **10**(2): p. 53-9.

60. Greenwood, B.M. and G.A. Targett, *Malaria vaccines and the new malaria agenda.* Clinical microbiology and infection : the official publication of the European Society of Clinical Microbiology and Infectious Diseases, 2011. **17**(11): p. 1600-7.

61. Janse, C.J., et al., *A genotype and phenotype database of genetically modified malaria-parasites.* Trends Parasitol, 2011. **27**(1): p. 31-9.

62. Amino, R., R. Menard, and F. Frischknecht, *In vivo imaging of malaria parasites--recent advances and future directions.* Curr Opin Microbiol, 2005. **8**(4): p. 407-14.

63. Kaiser, K., et al., *Differential transcriptome profiling identifies Plasmodium genes encoding pre-erythrocytic stage-specific proteins.* Mol Microbiol, 2004. **51**(5): p. 1221-32.

64. Clyde, D.F., *Immunity to falciparum and vivax malaria induced by irradiated sporozoites: a review of the University of Maryland studies, 1971-75.* Bull World Health Organ, 1990. **68 Suppl**: p. 9-12.

65. Wang, R., et al., *Protection against malaria by Plasmodium yoelii sporozoite surface protein 2 linear peptide induction of CD4+ T cell- and IFN-gamma-dependent elimination of infected hepatocytes.* J Immunol, 1996. **157**(9): p. 4061-7.

66. Hoffman, S.L., et al., *Sporozoite vaccine induces genetically restricted T cell elimination of malaria from hepatocytes.* Science, 1989. **244**(4908): p. 1078-81.

67. Baird, J.K., *Age-dependent characteristics of protection v. susceptibility to Plasmodium falciparum.* Ann Trop Med Parasitol, 1998. **92**(4): p. 367-90.

68. Almeida, A.P., et al., *Long-lasting humoral and cellular immune responses elicited by immunization with recombinant chimeras of the Plasmodium vivax circumsporozoite protein.* Vaccine, 2014. **32**(19): p. 2181-7.

69. Rodriguez, A., et al., *Evaluation of a prime-boost vaccine schedule with distinct adenovirus vectors against malaria in rhesus monkeys.* Vaccine, 2009. **27**(44): p. 6226-33.

70. Felgner, P.L., et al., *Pre-erythrocytic antibody profiles induced by controlled human malaria infections in healthy volunteers under chloroquine prophylaxis.* Sci Rep, 2013. **3**: p. 3549.

71. Bruce-Chwatt, L.J., *A LONGITUDINAL SURVEY OF NATURAL MALARIA INFECTION IN A GROUP OF WEST AFRICAN ADULTS.* West Afr Med J, 1963. **12**: p. 199-217.

72. Ma, J., et al., *Dynamics of the major histocompatibility complex class I processing and presentation pathway in the course of malaria parasite development in human hepatocytes: implications for vaccine development.* PLoS One, 2013. **8**(9): p. e75321.

73. Kaiser, J., *Infectious diseases. Unconventional vaccine shows promise against malaria.* Science, 2013. **341**(6146): p. 605.

74. Kimura, K., et al., *CD8+ T cells specific for a malaria cytoplasmic antigen form clusters around infected hepatocytes and are protective at the liver stage of infection.* Infect Immun, 2013. **81**(10): p. 3825-34.

75. Nganou-Makamdop, K. and R.W. Sauerwein, *Liver or blood-stage arrest during malaria sporozoite immunization: the later the better?* Trends Parasitol, 2013. **29**(6): p. 304-10.

76. McCoy, M.E., et al., *Mechanisms of protective immune responses induced by the Plasmodium falciparum circumsporozoite protein-based, self-assembling protein nanoparticle vaccine.* Malar J, 2013. **12**: p. 136.

77. Seder, R.A., et al., *Protection against malaria by intravenous immunization with a nonreplicating sporozoite vaccine.* Science, 2013. **341**(6152): p. 1359-65.

78. Porter, M.D., et al., *Transgenic parasites stably expressing full-length Plasmodium falciparum circumsporozoite protein as a model for vaccine down-selection in mice using sterile protection as an endpoint.* Clin Vaccine Immunol, 2013. **20**(6): p. 803-10.

79. Powell, T.J., et al., *Plasmodium falciparum synthetic LbL microparticle vaccine elicits protective neutralizing antibody and parasite-specific cellular immune responses.* Vaccine, 2013. **31**(15): p. 1898-904.

80. Chuang, I., et al., *DNA prime/Adenovirus boost malaria vaccine encoding P. falciparum CSP and AMA1 induces sterile protection associated with cell-mediated immunity.* PLoS One, 2013. **8**(2): p. e55571.

81. Ndungu, F.M., et al., *A statistical interaction between circumsporozoite protein-specific T cell and antibody responses and risk of clinical malaria episodes following vaccination with RTS,S/AS01E.* PLoS One, 2012. **7**(12): p. e52870.

82. Obeid, M., et al., *Skin-draining lymph node priming is sufficient to induce sterile immunity against pre-erythrocytic malaria.* EMBO Mol Med, 2013. **5**(2): p. 250-63.

83. Kennedy, M., et al., *A rapid and scalable density gradient purification method for Plasmodium sporozoites.* Malar J, 2012. **11**: p. 421.

84. Przysiecki, C., et al., *Sporozoite neutralizing antibodies elicited in mice and rhesus macaques immunized with a Plasmodium falciparum repeat peptide conjugated to meningococcal outer membrane protein complex.* Front Cell Infect Microbiol, 2012. **2**: p. 146.

85. Bijker, E.M., et al., *Protection against malaria after immunization by chloroquine prophylaxis and sporozoites is mediated by preerythrocytic immunity.* Proc Natl Acad Sci U S A, 2013. **110**(19): p. 7862-7.

86. Richie, T.L., et al., *Clinical trial in healthy malaria-naive adults to evaluate the safety, tolerability, immunogenicity and efficacy of MuStDO5, a five-gene, sporozoite/hepatic stage Plasmodium falciparum DNA vaccine combined with escalating dose human GM-CSF DNA.* Hum Vaccin Immunother, 2012. **8**(11): p. 1564-84.

87. Coutant, F., et al., *A nonintegrative lentiviral vector-based vaccine provides long-term sterile protection against malaria.* PLoS One, 2012. **7**(11): p. e48644.

88. Ploemen, I.H., et al., *Plasmodium liver load following parenteral sporozoite administration in rodents.* Vaccine, 2013. **31**(34): p. 3410-6.

89. Renia, L., et al., *Vaccination using normal live sporozoites under drug treatment.* Methods Mol Biol, 2013. **923**: p. 567-76.

90. Vaughan, A.M. and S.H. Kappe, *Vaccination using radiation- or genetically attenuated live sporozoites.* Methods Mol Biol, 2013. **923**: p. 549-66.

91. Remarque, E.J., et al., *Humoral immune responses to a single allele PfAMA1 vaccine in healthy malaria-naive adults.* PLoS One, 2012. **7**(6): p. e38898.

92. Bairwa, M., et al., *Malaria vaccine: a bright prospect for elimination of malaria.* Hum Vaccin Immunother, 2012. **8**(6): p. 819-22.

93. Portugal, S., et al., *Host-mediated regulation of superinfection in malaria.* Nat Med, 2011. **17**(6): p. 732-7.

94. Vaughan, A.M. and S.H. Kappe, *Malaria vaccine development: persistent challenges.* Curr Opin Immunol, 2012. **24**(3): p. 324-31.

95. John, C.C., et al., *Cytokine responses to Plasmodium falciparum liver-stage antigen 1 vary in rainy and dry seasons in highland Kenya.* Infect Immun, 2000. **68**(9): p. 5198-204.

96. Migot-Nabias, F., et al., *Immune response to Plasmodium falciparum liver stage antigen-1: geographical variations within Central Africa and their relationship*

with protection from clinical malaria. Trans R Soc Trop Med Hyg, 2000. **94**(5): p. 557-62.

97. Todryk, S.M., et al., *Correlation of memory T cell responses against TRAP with protection from clinical malaria, and CD4 CD25 high T cells with susceptibility in Kenyans.* PLoS One, 2008. **3**(4): p. e2027.

98. Reece, W.H., et al., *A CD4(+) T-cell immune response to a conserved epitope in the circumsporozoite protein correlates with protection from natural Plasmodium falciparum infection and disease.* Nat Med, 2004. **10**(4): p. 406-10.

99. Fell, A.H., J. Currier, and M.F. Good, *Inhibition of Plasmodium falciparum growth in vitro by CD4+ and CD8+ T cells from non-exposed donors.* Parasite Immunol, 1994. **16**(11): p. 579-86.

100. Pombo, D.J., et al., *Immunity to malaria after administration of ultra-low doses of red cells infected with Plasmodium falciparum.* Lancet, 2002. **360**(9333): p. 610-7.

101. Taylor-Robinson, A.W., et al., *The role of TH1 and TH2 cells in a rodent malaria infection.* Science, 1993. **260**(5116): p. 1931-4.

102. Amante, F.H. and M.F. Good, *Prolonged Th1-like response generated by a Plasmodium yoelii-specific T cell clone allows complete clearance of infection in reconstituted mice.* Parasite Immunol, 1997. **19**(3): p. 111-26.

103. Lau, L.S., et al., *Blood-stage Plasmodium berghei infection generates a potent, specific CD8+ T-cell response despite residence largely in cells lacking MHC I processing machinery.* J Infect Dis, 2011. **204**(12): p. 1989-96.

104. Biswas, S., et al., *Recombinant viral-vectored vaccines expressing Plasmodium chabaudi AS apical membrane antigen 1: mechanisms of vaccine-induced blood-stage protection.* J Immunol, 2012. **188**(10): p. 5041-53.

105. Butler, N.S., et al., *Therapeutic blockade of PD-L1 and LAG-3 rapidly clears established blood-stage Plasmodium infection.* Nat Immunol, 2012. **13**(2): p. 188-95.

106. van der Heyde, H.C., et al., *The resolution of acute malaria in a definitive model of B cell deficiency, the JHD mouse.* J Immunol, 1994. **152**(9): p. 4557-62.

107. Riley, E.M., et al., *Naturally acquired cellular and humoral immune responses to the major merozoite surface antigen (PfMSP1) of Plasmodium falciparum are associated with reduced malaria morbidity.* Parasite Immunol, 1992. **14**(3): p. 321-37.

108. Carvalho, L.H., C.J. Fontes, and A.U. Krettli, *Cellular responses to Plasmodium falciparum major surface antigens and their relationship to human activities*

associated with malaria transmission. Am J Trop Med Hyg, 1999. **60**(4): p. 674-9.

109. Epstein, J.E., et al., *Live attenuated malaria vaccine designed to protect through hepatic CD8(+) T cell immunity.* Science, 2011. **334**(6055): p. 475-80.

110. Rodrigues, M., R.S. Nussenzweig, and F. Zavala, *The relative contribution of antibodies, CD4+ and CD8+ T cells to sporozoite-induced protection against malaria.* Immunology, 1993. **80**(1): p. 1-5.

111. Renia, L., et al., *In vitro activity of CD4+ and CD8+ T lymphocytes from mice immunized with a synthetic malaria peptide.* Proc Natl Acad Sci U S A, 1991. **88**(18): p. 7963-7.

112. Trimnell, A., et al., *Genetically attenuated parasite vaccines induce contact-dependent CD8+ T cell killing of Plasmodium yoelii liver stage-infected hepatocytes.* J Immunol, 2009. **183**(9): p. 5870-8.

113. Balam, S., et al., *CSP--a model for in vivo presentation of Plasmodium berghei sporozoite antigens by hepatocytes.* PloS one, 2012. **7**(12): p. e51875.

114. Leiriao, P., M.M. Mota, and A. Rodriguez, *Apoptotic Plasmodium-infected hepatocytes provide antigens to liver dendritic cells.* J Infect Dis, 2005. **191**(10): p. 1576-81.

115. Chakravarty, S., et al., *CD8+ T lymphocytes protective against malaria liver stages are primed in skin-draining lymph nodes.* Nat Med, 2007. **13**(9): p. 1035-41.

116. Cohen, S., G.I. Mc, and S. Carrington, *Gamma-globulin and acquired immunity to human malaria.* Nature, 1961. **192**: p. 733-7.

117. Sabchareon, A., et al., *Parasitologic and clinical human response to immunoglobulin administration in falciparum malaria.* Am J Trop Med Hyg, 1991. **45**(3): p. 297-308.

118. John, C.C., et al., *Correlation of high levels of antibodies to multiple pre-erythrocytic Plasmodium falciparum antigens and protection from infection.* Am J Trop Med Hyg, 2005. **73**(1): p. 222-8.

119. John, C.C., et al., *Antibodies to pre-erythrocytic Plasmodium falciparum antigens and risk of clinical malaria in Kenyan children.* J Infect Dis, 2008. **197**(4): p. 519-26.

120. Bouharoun-Tayoun, H., et al., *Antibodies that protect humans against Plasmodium falciparum blood stages do not on their own inhibit parasite growth and invasion in vitro, but act in cooperation with monocytes.* J Exp Med, 1990. **172**(6): p. 1633-41.

121. Aucan, C., et al., *High immunoglobulin G2 (IgG2) and low IgG4 levels are associated with human resistance to Plasmodium falciparum malaria.* Infect Immun, 2000. **68**(3): p. 1252-8.

122. Tebo, A.E., P.G. Kremsner, and A.J. Luty, *Plasmodium falciparum: a major role for IgG3 in antibody-dependent monocyte-mediated cellular inhibition of parasite growth in vitro.* Exp Parasitol, 2001. **98**(1): p. 20-8.

123. Bouharoun-Tayoun, H., et al., *Mechanisms underlying the monocyte-mediated antibody-dependent killing of Plasmodium falciparum asexual blood stages.* J Exp Med, 1995. **182**(2): p. 409-18.

124. Giribaldi, G., et al., *Growth of Plasmodium falciparum induces stage-dependent haemichrome formation, oxidative aggregation of band 3, membrane deposition of complement and antibodies, and phagocytosis of parasitized erythrocytes.* Br J Haematol, 2001. **113**(2): p. 492-9.

125. Polley, S.D., et al., *Human antibodies to recombinant protein constructs of Plasmodium falciparum Apical Membrane Antigen 1 (AMA1) and their associations with protection from malaria.* Vaccine, 2004. **23**(5): p. 718-28.

126. Leech, J.H., et al., *Identification of a strain-specific malarial antigen exposed on the surface of Plasmodium falciparum-infected erythrocytes.* J Exp Med, 1984. **159**(6): p. 1567-75.

127. Marsh, K. and R.J. Howard, *Antigens induced on erythrocytes by P. falciparum: expression of diverse and conserved determinants.* Science, 1986. **231**(4734): p. 150-3.

128. Biggs, B.A., et al., *Antigenic variation in Plasmodium falciparum.* Proc Natl Acad Sci U S A, 1991. **88**(20): p. 9171-4.

129. Chan, J.A., et al., *Targets of antibodies against Plasmodium falciparum-infected erythrocytes in malaria immunity.* J Clin Invest, 2012.

130. Langreth, S.G. and E. Peterson, *Pathogenicity, stability, and immunogenicity of a knobless clone of Plasmodium falciparum in Colombian owl monkeys.* Infect Immun, 1985. **47**(3): p. 760-6.

131. Horrocks, P., et al., *Variable var transition rates underlie antigenic variation in malaria.* Proc Natl Acad Sci U S A, 2004. **101**(30): p. 11129-34.

132. Lavstsen, T., et al., *Plasmodium falciparum erythrocyte membrane protein 1 domain cassettes 8 and 13 are associated with severe malaria in children.* Proc Natl Acad Sci U S A, 2012. **109**(26): p. E1791-800.

133. Claessens, A., et al., *A subset of group A-like var genes encodes the malaria parasite ligands for binding to human brain endothelial cells.* Proc Natl Acad Sci U S A, 2012. **109**(26): p. E1772-81.

134. Smith, J.D., et al., *Switches in expression of Plasmodium falciparum var genes correlate with changes in antigenic and cytoadherent phenotypes of infected erythrocytes.* Cell, 1995. **82**(1): p. 101-10.

135. Jensen, A.T., et al., *Plasmodium falciparum associated with severe childhood malaria preferentially expresses PfEMP1 encoded by group A var genes.* J Exp Med, 2004. **199**(9): p. 1179-90.

136. Vigan-Womas, I., et al., *An in vivo and in vitro model of Plasmodium falciparum rosetting and autoagglutination mediated by varO, a group A var gene encoding a frequent serotype.* Infect Immun, 2008. **76**(12): p. 5565-80.

137. Vigan-Womas, I., et al., *Allelic diversity of the Plasmodium falciparum erythrocyte membrane protein 1 entails variant-specific red cell surface epitopes.* PLoS One, 2011. **6**(1): p. e16544.

138. Ghumra, A., et al., *Immunisation with recombinant PfEMP1 domains elicits functional rosette-inhibiting and phagocytosis-inducing antibodies to Plasmodium falciparum.* PLoS One, 2011. **6**(1): p. e16414.

139. Rowe, J.A., et al., *P. falciparum rosetting mediated by a parasite-variant erythrocyte membrane protein and complement-receptor 1.* Nature, 1997. **388**(6639): p. 292-5.

140. Ndungu, F.M., et al., *CD4 T cells from malaria-nonexposed individuals respond to the CD36-Binding Domain of Plasmodium falciparum erythrocyte membrane protein-1 via an MHC class II-TCR-independent pathway.* J Immunol, 2006. **176**(9): p. 5504-12.

141. Urban, B.C., et al., *Plasmodium falciparum-infected erythrocytes modulate the maturation of dendritic cells.* Nature, 1999. **400**(6739): p. 73-7.

142. Mo, M., et al., *The C-terminal segment of the cysteine-rich interdomain of Plasmodium falciparum erythrocyte membrane protein 1 determines CD36 binding and elicits antibodies that inhibit adhesion of parasite-infected erythrocytes.* Infect Immun, 2008. **76**(5): p. 1837-47.

143. Salanti, A., et al., *Evidence for the involvement of VAR2CSA in pregnancy-associated malaria.* J Exp Med, 2004. **200**(9): p. 1197-203.

144. Turner, G.D., et al., *An immunohistochemical study of the pathology of fatal malaria. Evidence for widespread endothelial activation and a potential role for intercellular adhesion molecule-1 in cerebral sequestration.* Am J Pathol, 1994. **145**(5): p. 1057-69.

145. Newbold, C., et al., *Receptor-specific adhesion and clinical disease in Plasmodium falciparum.* Am J Trop Med Hyg, 1997. **57**(4): p. 389-98.

146. Bouharoun-Tayoun, H. and P. Druilhe, *Plasmodium falciparum malaria: evidence for an isotype imbalance which may be responsible for delayed acquisition of protective immunity.* Infect Immun, 1992. **60**(4): p. 1473-81.

147. Guevara Patino, J.A., et al., *Antibodies that inhibit malaria merozoite surface protein-1 processing and erythrocyte invasion are blocked by naturally acquired human antibodies.* J Exp Med, 1997. **186**(10): p. 1689-99.

148. Uthaipibull, C., et al., *Inhibitory and blocking monoclonal antibody epitopes on merozoite surface protein 1 of the malaria parasite Plasmodium falciparum.* J Mol Biol, 2001. **307**(5): p. 1381-94.

149. Genton, B., et al., *A recombinant blood-stage malaria vaccine reduces Plasmodium falciparum density and exerts selective pressure on parasite populations in a phase 1-2b trial in Papua New Guinea.* J Infect Dis, 2002. **185**(6): p. 820-7.

150. Sheehy, S.H., et al., *ChAd63-MVA-vectored blood-stage malaria vaccines targeting MSP1 and AMA1: assessment of efficacy against mosquito bite challenge in humans.* Mol Ther, 2012. **20**(12): p. 2355-68.

151. White, M.T., et al., *The relationship between RTS,S vaccine-induced antibodies, CD4(+) T cell responses and protection against Plasmodium falciparum infection.* PLoS One, 2013. **8**(4): p. e61395.

152. Craig, A.G., et al., *The role of animal models for research on severe malaria.* PLoS pathogens, 2012. **8**(2): p. e1002401.

153. *A research agenda for malaria eradication: vaccines.* PLoS medicine, 2011. **8**(1): p. e1000398.

154. Friesen, J., S. Borrmann, and K. Matuschewski, *Induction of antimalaria immunity by pyrimethamine prophylaxis during exposure to sporozoites is curtailed by parasite resistance.* Antimicrobial agents and chemotherapy, 2011. **55**(6): p. 2760-7.

155. Ellis, R.D., et al., *Blood stage vaccines for Plasmodium falciparum: current status and the way forward.* Human vaccines, 2010. **6**(8): p. 627-34.

156. Goodman, A.L. and S.J. Draper, *Blood-stage malaria vaccines - recent progress and future challenges.* Ann Trop Med Parasitol, 2010. **104**(3): p. 189-211.

157. Miotto, O., et al., *Multiple populations of artemisinin-resistant Plasmodium falciparum in Cambodia.* Nat Genet, 2013. **45**(6): p. 648-55.

158. Na-Bangchang, K., et al., *Identification of resistance of Plasmodium falciparum to artesunate-mefloquine combination in an area along the Thai-Myanmar border: integration of clinico-parasitological response, systemic drug exposure, and in vitro parasite sensitivity.* Malar J, 2013. **12**: p. 263.

159. Mita, T. and K. Tanabe, *Evolution of Plasmodium falciparum drug resistance: implications for the development and containment of artemisinin resistance.* Jpn J Infect Dis, 2012. **65**(6): p. 465-75.

160. Noor, A.M., et al., *Insecticide-treated net coverage in Africa: mapping progress in 2000-07.* Lancet, 2009. **373**(9657): p. 58-67.

161. Klenerman, P. and A. Hill, *T cells and viral persistence: lessons from diverse infections.* Nat Immunol, 2005. **6**(9): p. 873-9.

162. Hoffman, S.L., et al., *Development of a metabolically active, non-replicating sporozoite vaccine to prevent Plasmodium falciparum malaria.* Hum Vaccin, 2010. **6**(1): p. 97-106.

163. Cohen, J., et al., *From the circumsporozoite protein to the RTS, S/AS candidate vaccine.* Hum Vaccin, 2010. **6**(1): p. 90-6.

164. Ballou, W.R., *The development of the RTS,S malaria vaccine candidate: challenges and lessons.* Parasite Immunol, 2009. **31**(9): p. 492-500.

165. Rts, S.C.T.P., et al., *A phase 3 trial of RTS,S/AS01 malaria vaccine in African infants.* N Engl J Med, 2012. **367**(24): p. 2284-95.

166. Agnandji, S.T., et al., *First results of phase 3 trial of RTS,S/AS01 malaria vaccine in African children.* N Engl J Med, 2011. **365**(20): p. 1863-75.

167. *Efficacy and Safety of the RTS,S/AS01 Malaria Vaccine during 18 Months after Vaccination: A Phase 3 Randomized, Controlled Trial in Children and Young Infants at 11 African Sites.* PLoS Med, 2014. **11**(7): p. e1001685.

168. Olotu, A.I., G. Fegan, and P. Bejon, *Further analysis of correlates of protection from a phase 2a trial of the falciparum malaria vaccines RTS,S/AS01B and RTS,S/AS02A in malaria-naive adults.* J Infect Dis, 2010. **201**(6): p. 970-1.

169. Limbach, K.J. and T.L. Richie, *Viral vectors in malaria vaccine development.* Parasite Immunol, 2009. **31**(9): p. 501-19.

170. Crompton, P.D., S.K. Pierce, and L.H. Miller, *Advances and challenges in malaria vaccine development.* J Clin Invest, 2010. **120**(12): p. 4168-78.

171. Draper, S.J. and J.L. Heeney, *Viruses as vaccine vectors for infectious diseases and cancer.* Nat Rev Microbiol, 2010. **8**(1): p. 62-73.

172. Alcock, R., et al., *Long-term thermostabilization of live poxviral and adenoviral vaccine vectors at supraphysiological temperatures in carbohydrate glass.* Sci Transl Med, 2010. **2**(19): p. 19ra12.

173. Nussenzweig, R.S. and A.U. Krettli, *Breakthroughs towards a malaria vaccine.* Hist Cienc Saude Manguinhos, 2011. **18**(2): p. 559-64.

174. Mendes, E.A., et al., *Recombinant vaccines against T. gondii: comparison between homologous and heterologous vaccination protocols using two viral vectors expressing SAG1.* PLoS One, 2013. **8**(5): p. e63201.

175. Ratto-Kim, S., et al., *Heterologous prime-boost regimens using rAd35 and rMVA vectors elicit stronger cellular immune responses to HIV proteins than homologous regimens.* PLoS One, 2012. **7**(9): p. e45840.

176. Sheehy, S.H., et al., *Phase Ia clinical evaluation of the safety and immunogenicity of the Plasmodium falciparum blood-stage antigen AMA1 in ChAd63 and MVA vaccine vectors.* PLoS One, 2012. **7**(2): p. e31208.

177. Schofield, L., et al., *Gamma interferon, CD8+ T cells and antibodies required for immunity to malaria sporozoites.* Nature, 1987. **330**(6149): p. 664-6.

178. Weiss, W.R. and C.G. Jiang, *Protective CD8+ T lymphocytes in primates immunized with malaria sporozoites.* PLoS One, 2012. **7**(2): p. e31247.

179. Tse, S.W., A.J. Radtke, and F. Zavala, *Induction and maintenance of protective CD8+ T cells against malaria liver stages: implications for vaccine development.* Memorias do Instituto Oswaldo Cruz, 2011. **106 Suppl 1**: p. 172-8.

180. Hafalla, J.C., et al., *Identification of targets of CD8(+) T cell responses to malaria liver stages by genome-wide epitope profiling.* PLoS pathogens, 2013. **9**(5): p. e1003303.

181. Kaushansky, A., et al., *Development of a quantitative flow cytometry-based assay to assess infection by Plasmodium falciparum sporozoites.* Mol Biochem Parasitol, 2012. **183**(1): p. 100-3.

182. Trieu, A., et al., *Sterile protective immunity to malaria is associated with a panel of novel P. falciparum antigens.* Mol Cell Proteomics, 2011. **10**(9): p. M111 007948.

183. Roestenberg, M., et al., *Long-term protection against malaria after experimental sporozoite inoculation: an open-label follow-up study.* Lancet, 2011. **377**(9779): p. 1770-6.

184. Jordan-Villegas, A., et al., *Immune responses and protection of Aotus monkeys immunized with irradiated Plasmodium vivax sporozoites.* Am J Trop Med Hyg, 2011. **84**(2 Suppl): p. 43-50.

185. Voza, T., C. Kebaier, and J.P. Vanderberg, *Intradermal immunization of mice with radiation-attenuated sporozoites of Plasmodium yoelii induces effective protective immunity.* Malar J, 2010. **9**: p. 362.

186. Cong, H., et al., *Human immunome, bioinformatic analyses using HLA supermotifs and the parasite genome, binding assays, studies of human T cell responses, and immunization of HLA-A*1101 transgenic mice including novel adjuvants provide a foundation for HLA-A03 restricted CD8+T cell epitope based, adjuvanted vaccine protective against Toxoplasma gondii.* Immunome Res, 2010. **6**: p. 12.

187. Tewari, K., et al., *Poly(I:C) is an effective adjuvant for antibody and multi-functional CD4+ T cell responses to Plasmodium falciparum circumsporozoite protein (CSP) and alphaDEC-CSP in non human primates.* Vaccine, 2010. **28**(45): p. 7256-66.

188. Mahajan, B., et al., *Multiple antigen peptide vaccines against Plasmodium falciparum malaria.* Infect Immun, 2010. **78**(11): p. 4613-24.

189. Douradinha, B. and D.L. Doolan, *Harnessing immune responses against Plasmodium for rational vaccine design.* Trends Parasitol, 2011. **27**(6): p. 274-83.

190. Draper, S.J., et al., *Enhancing blood-stage malaria subunit vaccine immunogenicity in rhesus macaques by combining adenovirus, poxvirus, and protein-in-adjuvant vaccines.* J Immunol, 2010. **185**(12): p. 7583-95.

191. Sheehy, S.H., et al., *Phase Ia clinical evaluation of the Plasmodium falciparum blood-stage antigen MSP1 in ChAd63 and MVA vaccine vectors.* Mol Ther, 2011. **19**(12): p. 2269-76.

192. Capone, S., et al., *Immune responses against a liver-stage malaria antigen induced by simian adenoviral vector AdCh63 and MVA prime-boost immunisation in non-human primates.* Vaccine, 2010. **29**(2): p. 256-65.

193. Reyes-Sandoval, A., et al., *Single-dose immunogenicity and protective efficacy of simian adenoviral vectors against Plasmodium berghei.* Eur J Immunol, 2008. **38**(3): p. 732-41.

194. Reyes-Sandoval, A., et al., *Prime-boost immunization with adenoviral and modified vaccinia virus Ankara vectors enhances the durability and polyfunctionality of protective malaria CD8+ T-cell responses.* Infect Immun, 2010. **78**(1): p. 145-53.

195. Bergmann-Leitner, E.S., et al., *Immunization with pre-erythrocytic antigen CelTOS from Plasmodium falciparum elicits cross-species protection against heterologous challenge with Plasmodium berghei.* PLoS One, 2010. **5**(8): p. e12294.

196. Schmidt, N.W., et al., *Extreme CD8 T cell requirements for anti-malarial liver-stage immunity following immunization with radiation attenuated sporozoites.* PLoS Pathog, 2010. **6**(7): p. e1000998.

197. Ruiz, A., et al., *Development of Eimeria ninakohlyakimovae in vitro in primary and permanent cell lines.* Vet Parasitol, 2010. **173**(1-2): p. 2-10.

198. Gruner, A.C., et al., *Sterile protection against malaria is independent of immune responses to the circumsporozoite protein.* PLoS One, 2007. **2**(12): p. e1371.

199. Kumar, K.A., et al., *The circumsporozoite protein is an immunodominant protective antigen in irradiated sporozoites.* Nature, 2006. **444**(7121): p. 937-40.

200. Mauduit, M., et al., *Minimal role for the circumsporozoite protein in the induction of sterile immunity by vaccination with live rodent malaria sporozoites.* Infect Immun, 2010. **78**(5): p. 2182-8.

201. Doolan, D.L., et al., *Degenerate cytotoxic T cell epitopes from P. falciparum restricted by multiple HLA-A and HLA-B supertype alleles.* Immunity, 1997. **7**(1): p. 97-112.

202. Guerin-Marchand, C., et al., *A liver-stage-specific antigen of Plasmodium falciparum characterized by gene cloning.* Nature, 1987. **329**(6135): p. 164-7.

203. Hill, A.V., et al., *Molecular analysis of the association of HLA-B53 and resistance to severe malaria.* Nature, 1992. **360**(6403): p. 434-9.

204. Daubersies, P., et al., *Protection against Plasmodium falciparum malaria in chimpanzees by immunization with the conserved pre-erythrocytic liver-stage antigen 3.* Nat Med, 2000. **6**(11): p. 1258-63.

205. Aidoo, M., et al., *Cytotoxic T-lymphocyte epitopes for HLA-B53 and other HLA types in the malaria vaccine candidate liver-stage antigen 3.* Infection and immunity, 2000. **68**(1): p. 227-32.

206. Sauzet, J.P., et al., *DNA immunization by Plasmodium falciparum liver-stage antigen 3 induces protection against Plasmodium yoelii sporozoite challenge.* Infection and immunity, 2001. **69**(2): p. 1202-6.

207. Perlaza, B.L., et al., *Protection against Plasmodium falciparum challenge induced in Aotus monkeys by liver-stage antigen-3-derived long synthetic peptides.* European journal of immunology, 2008. **38**(9): p. 2610-5.

208. Prieur, E. and P. Druilhe, *The malaria candidate vaccine liver stage antigen-3 is highly conserved in Plasmodium falciparum isolates from diverse geographical areas.* Malaria journal, 2009. **8**.

209. Doolan, D.L., et al., *Identification of Plasmodium falciparum antigens by antigenic analysis of genomic and proteomic data.* Proc Natl Acad Sci U S A, 2003. **100**(17): p. 9952-7.

210. Kariu, T., et al., *CelTOS, a novel malarial protein that mediates transmission to mosquito and vertebrate hosts.* Molecular Microbiology, 2006. **59**(5): p. 1369-1379.

211. Limbach, K., et al., *Identification of two new protective pre-erythrocytic malaria vaccine antigen candidates.* Malaria journal, 2011. **10**: p. 65.

212. Mueller, A.K., et al., *Genetically modified Plasmodium parasites as a protective experimental malaria vaccine.* Nature, 2005. **433**(7022): p. 164-167.

213. Hoffman, B.U. and R. Chattopadhyay, *Plasmodium falciparum: Effect of radiation on levels of gene transcripts in sporozoites.* Experimental parasitology, 2008. **118**(2): p. 247-252.

214. Siau, A., et al., *Temperature shift and host cell contact up-regulate sporozoite expression of Plasmodium falciparum genes involved in hepatocyte infection.* PLoS Pathog, 2008. **4**(8): p. e1000121.

215. Vignali, M., et al., *Interaction of an atypical Plasmodium falciparum ETRAMP with human apolipoproteins.* Malaria journal, 2008. **7**.

216. Andre, F.E., et al., *Vaccination greatly reduces disease, disability, death and inequity worldwide.* Bulletin of the World Health Organization, 2008. **86**(2): p. 140-6.

217. Tewari, R., et al., *Function of region I and II adhesive motifs of Plasmodium falciparum circumsporozoite protein in sporozoite motility and infectivity.* The Journal of biological chemistry, 2002. **277**(49): p. 47613-8.

218. Wang, Q., H. Fujioka, and V. Nussenzweig, *Exit of Plasmodium sporozoites from oocysts is an active process that involves the circumsporozoite protein.* PLoS pathogens, 2005. **1**(1): p. 72-79.

219. Rathore, D., et al., *Binding and invasion of liver cells by Plasmodium falciparum sporozoites - Essential involvement of the amino terminus of circumsporozoite protein.* Journal of Biological Chemistry, 2002. **277**(9): p. 7092-7098.

220. Gwadz, R.W., et al., *Preliminary studies on vaccination of rhesus monkeys with irradiated sporozoites of Plasmodium knowlesi and characterization of surface antigens of these parasites.* Bulletin of the World Health Organization, 1979. **57 Suppl 1**: p. 165-73.

221. Nardin, E.H., et al., *Circumsporozoite proteins of human malaria parasites Plasmodium falciparum and Plasmodium vivax.* The Journal of experimental medicine, 1982. **156**(1): p. 20-30.

222. Zavala, F., et al., *Rationale for development of a synthetic vaccine against Plasmodium falciparum malaria.* Science, 1985. **228**(4706): p. 1436-40.

223. Robson, K.J., et al., *A highly conserved amino-acid sequence in thrombospondin, properdin and in proteins from sporozoites and blood stages of a human malaria parasite.* Nature, 1988. **335**(6185): p. 79-82.

224. Rogers, W.O., et al., *Characterization of the Gene Encoding Sporozoite Surface Protein-2, a Protective Plasmodium-Yoelii Sporozoite Antigen.* Molecular and biochemical parasitology, 1992. **53**(1-2): p. 45-51.

225. Ghosh, A.K., et al., *Malaria Parasite Invasion of the Mosquito Salivary Gland Requires Interaction between the Plasmodium TRAP and the Anopheles Saglin Proteins.* PLoS pathogens, 2009. **5**(1).

226. Sultan, A.A., et al., *TRAP is necessary for gliding motility and infectivity of plasmodium sporozoites.* Cell, 1997. **90**(3): p. 511-522.

227. Gilbert, S.C., et al., *A protein particle vaccine containing multiple malaria epitopes.* Nature Biotechnology, 1997. **15**(11): p. 1280-1284.

228. Slavic, K., et al., *Life cycle studies of the hexose transporter of Plasmodium species and genetic validation of their essentiality.* Molecular microbiology, 2010. **75**(6): p. 1402-13.

229. Lindner, S.E., et al., *Total and putative surface proteomics of malaria parasite salivary gland sporozoites.* Molecular & cellular proteomics : MCP, 2013. **12**(5): p. 1127-43.

230. Murphy, S.C., et al., *A T-cell response to a liver-stage Plasmodium antigen is not boosted by repeated sporozoite immunizations.* Proceedings of the National Academy of Sciences of the United States of America, 2013. **110**(15): p. 6055-60.

231. Patarroyo, M.E., M.P. Alba, and H. Curtidor, *Biological and structural characteristics of the binding peptides from the sporozoite proteins essential for cell traversal (SPECT)-1 and -2.* Peptides, 2011. **32**(1): p. 154-60.

232. Carlton, J.M., et al., *Genome sequence and comparative analysis of the model rodent malaria parasite Plasmodium yoelii yoelii.* Nature, 2002. **419**(6906): p. 512-9.

233. Kooij, T.W., C.J. Janse, and A.P. Waters, *Plasmodium post-genomics: better the bug you know?* Nat Rev Microbiol, 2006. **4**(5): p. 344-57.

234. Butler, N.S., N.W. Schmidt, and J.T. Harty, *Differential effector pathways regulate memory CD8 T cell immunity against Plasmodium berghei versus P. yoelii sporozoites.* J Immunol, 2010. **184**(5): p. 2528-38.

235. Butler, N.S., et al., *Superior antimalarial immunity after vaccination with late liver stage-arresting genetically attenuated parasites.* Cell Host Microbe, 2011. **9**(6): p. 451-62.

236. Bauza, K., et al., *Efficacy of a Plasmodium vivax malaria vaccine using ChAd63 and modified vaccinia Ankara expressing thrombospondin-related anonymous protein as assessed with transgenic Plasmodium berghei parasites.* Infect Immun, 2014. **82**(3): p. 1277-86.

237. Espinosa, D.A., et al., *Development of a chimeric Plasmodium berghei strain expressing the repeat region of the P. vivax circumsporozoite protein for in vivo evaluation of vaccine efficacy.* Infect Immun, 2013. **81**(8): p. 2882-7.

238. Persson, C., et al., *Cutting edge: a new tool to evaluate human pre-erythrocytic malaria vaccines: rodent parasites bearing a hybrid Plasmodium falciparum circumsporozoite protein.* J Immunol, 2002. **169**(12): p. 6681-5.

239. Goodman, A.L., et al., *A viral vectored prime-boost immunization regime targeting the malaria Pfs25 antigen induces transmission-blocking activity.* PLoS One, 2011. **6**(12): p. e29428.

240. Ramjanee, S., et al., *The use of transgenic Plasmodium berghei expressing the Plasmodium vivax antigen P25 to determine the transmission-blocking activity of sera from malaria vaccine trials.* Vaccine, 2007. **25**(5): p. 886-94.

241. Cao, Y., D. Zhang, and W. Pan, *Construction of transgenic Plasmodium berghei as a model for evaluation of blood-stage vaccine candidate of Plasmodium falciparum chimeric protein 2.9.* PLoS One, 2009. **4**(9): p. e6894.

242. de Koning-Ward, T.F., et al., *A new rodent model to assess blood stage immunity to the Plasmodium falciparum antigen merozoite surface protein 119 reveals a protective role for invasion inhibitory antibodies.* J Exp Med, 2003. **198**(6): p. 869-75.

243. Tewari, R., et al., *Development of a Transgenic Plasmodium berghei Line (Pbpfpkg) Expressing the P. falciparum cGMP-Dependent Protein Kinase, a Novel Antimalarial Drug Target.* PLoS One, 2014. **9**(5): p. e96923.

244. Blume, M., et al., *A constitutive pan-hexose permease for the Plasmodium life cycle and transgenic models for screening of antimalarial sugar analogs.* FASEB J, 2011. **25**(4): p. 1218-29.

245. Lin, J.W., et al., *A novel 'gene insertion/marker out' (GIMO) method for transgene expression and gene complementation in rodent malaria parasites.* PLoS One, 2011. **6**(12): p. e29289.

246. Pfander, C., et al., *A scalable pipeline for highly effective genetic modification of a malaria parasite.* Nat Methods, 2011. **8**(12): p. 1078-82.

247. Ploemen, I., et al., *Evaluation of immunity against malaria using luciferase-expressing Plasmodium berghei parasites.* Malar J, 2011. **10**: p. 350.

248. Janse, C.J., J. Ramesar, and A.P. Waters, *High-efficiency transfection and drug selection of genetically transformed blood stages of the rodent malaria parasite Plasmodium berghei.* Nature protocols, 2006. **1**(1): p. 346-56.

249. Janse, C.J., et al., *High efficiency transfection of Plasmodium berghei facilitates novel selection procedures.* Mol Biochem Parasitol, 2006. **145**(1): p. 60-70.

250. Jacobs-Lorena, V.Y., et al., *A dispensable Plasmodium locus for stable transgene expression.* Mol Biochem Parasitol, 2010. **171**(1): p. 40-4.

251. Narum, D.L., et al., *Codon optimization of gene fragments encoding Plasmodium falciparum merzoite proteins enhances DNA vaccine protein expression and immunogenicity in mice.* Infect Immun, 2001. **69**(12): p. 7250-3.

252. Yadava, A. and C.F. Ockenhouse, *Effect of codon optimization on expression levels of a functionally folded malaria vaccine candidate in prokaryotic and eukaryotic expression systems.* Infect Immun, 2003. **71**(9): p. 4961-9.

253. Menard, R. and C. Janse, *Gene targeting in malaria parasites.* Methods, 1997. **13**(2): p. 148-57.

254. Spaccapelo, R., et al., *Plasmepsin 4-deficient Plasmodium berghei are virulence attenuated and induce protective immunity against experimental malaria.* Am J Pathol, 2010. **176**(1): p. 205-17.

255. Janse, C.J., B. Franke-Fayard, and A.P. Waters, *Selection by flow-sorting of genetically transformed, GFP-expressing blood stages of the rodent malaria parasite, Plasmodium berghei.* Nat Protoc, 2006. **1**(2): p. 614-23.

256. Lin, J.W., et al., *Screening inhibitors of P. berghei blood stages using bioluminescent reporter parasites.* Methods Mol Biol, 2013. **923**: p. 507-22.

257. Janse, C.J. and A.P. Waters, *Plasmodium berghei: the application of cultivation and purification techniques to molecular studies of malaria parasites.* Parasitol Today, 1995. **11**(4): p. 138-43.

258. Janse, C.J., et al., *In vitro formation of ookinetes and functional maturity of Plasmodium berghei gametocytes.* Parasitology, 1985. **91 (Pt 1)**: p. 19-29.

259. van Dijk, M.R., et al., *A central role for P48/45 in malaria parasite male gamete fertility.* Cell, 2001. **104**(1): p. 153-64.

260. Ramakrishnan, C., et al., *Laboratory maintenance of rodent malaria parasites.* Methods Mol Biol, 2013. **923**: p. 51-72.

261. Annoura, T., et al., *Quantitative analysis of Plasmodium berghei liver stages by bioluminescence imaging.* Methods Mol Biol, 2013. **923**: p. 429-43.

262. Annoura, T., et al., *Assessing the adequacy of attenuation of genetically modified malaria parasite vaccine candidates.* Vaccine, 2012. **30**(16): p. 2662-70.

263. Bruna-Romero, O., et al., *Detection of malaria liver-stages in mice infected through the bite of a single Anopheles mosquito using a highly sensitive real-time PCR.* Int J Parasitol, 2001. **31**(13): p. 1499-502.

264. Ploemen, I.H., et al., *Visualisation and quantitative analysis of the rodent malaria liver stage by real time imaging.* PloS one, 2009. **4**(11): p. e7881.

265. Bejon, P., et al., *Calculation of liver-to-blood inocula, parasite growth rates, and preerythrocytic vaccine efficacy, from serial quantitative polymerase chain reaction studies of volunteers challenged with malaria sporozoites.* J Infect Dis, 2005. **191**(4): p. 619-26.

266. Cottingham, M.G., et al., *Preventing spontaneous genetic rearrangements in the transgene cassettes of adenovirus vectors.* Biotechnol Bioeng, 2012. **109**(3): p. 719-28.

267. McConkey, S.J., et al., *Enhanced T-cell immunogenicity of plasmid DNA vaccines boosted by recombinant modified vaccinia virus Ankara in humans.* Nat Med, 2003. **9**(6): p. 729-35.

268. Kim, Y., et al., *Immune epitope database analysis resource.* Nucleic Acids Res, 2012. **40**(Web Server issue): p. W525-30.

269. Rammensee, H., et al., *SYFPEITHI: database for MHC ligands and peptide motifs.* Immunogenetics, 1999. **50**(3-4): p. 213-9.

270. Cockburn, I.A., et al., *In vivo imaging of CD8+ T cell-mediated elimination of malaria liver stages.* Proc Natl Acad Sci U S A, 2013. **110**(22): p. 9090-5.

271. Zavala, F., et al., *Circumsporozoite proteins of malaria parasites contain a single immunodominant region with two or more identical epitopes.* J Exp Med, 1983. **157**(6): p. 1947-57.

272. Yoshida, N., et al., *Hybridoma produces protective antibodies directed against the sporozoite stage of malaria parasite.* Science, 1980. **207**(4426): p. 71-3.

273. Kester, K.E., et al., *Randomized, double-blind, phase 2a trial of falciparum malaria vaccines RTS,S/AS01B and RTS,S/AS02A in malaria-naive adults: safety, efficacy, and immunologic associates of protection.* J Infect Dis, 2009. **200**(3): p. 337-46.

274. Bergmann-Leitner, E.S., et al., *Self-adjuvanting bacterial vectors expressing pre-erythrocytic antigens induce sterile protection against malaria.* Front Immunol, 2013. **4**: p. 176.

275. Reyes-Sandoval, A., et al., *CD8+ T effector memory cells protect against liver-stage malaria.* J Immunol, 2011. **187**(3): p. 1347-57.

276. Mueller, A.K., et al., *Plasmodium liver stage developmental arrest by depletion of a protein at the parasite-host interface.* Proc Natl Acad Sci U S A, 2005. **102**(8): p. 3022-7.

277. *World Malaria Report*, 2012, World Health Organization: Geneva, Switzerland.

278. Duncan, C.J., A.V. Hill, and R.D. Ellis, *Can growth inhibition assays (GIA) predict blood-stage malaria vaccine efficacy?* Hum Vaccin Immunother, 2012. **8**(6): p. 706-14.

279. Mazier, D., et al., *Complete development of hepatic stages of Plasmodium falciparum in vitro.* Science, 1985. **227**(4685): p. 440-2.

280. Ewer, K.J., et al., *Protective CD8(+) T-cell immunity to human malaria induced by chimpanzee adenovirus-MVA immunisation.* Nature communications, 2013. **4**: p. 2836.

281. Draper, S.J., et al., *Effective induction of high-titer antibodies by viral vector vaccines.* Nat Med, 2008. **14**(8): p. 819-21.

282. de Cassan, S.C., et al., *The requirement for potent adjuvants to enhance the immunogenicity and protective efficacy of protein vaccines can be overcome by prior immunization with a recombinant adenovirus.* Journal of immunology, 2011. **187**(5): p. 2602-16.

283. Cockburn, I., *Chimeric parasites as tools to study Plasmodium immunology and assess malaria vaccines.* Methods Mol Biol, 2013. **923**: p. 465-79.

284. Mlambo, G., J. Maciel, and N. Kumar, *Murine model for assessment of Plasmodium falciparum transmission-blocking vaccine using transgenic Plasmodium berghei parasites expressing the target antigen Pfs25.* Infect Immun, 2008. **76**(5): p. 2018-24.

285. van Dijk, M.R., et al., *Three members of the 6-cys protein family of Plasmodium play a role in gamete fertility.* PLoS Pathog, 2010. **6**(4): p. e1000853.

286. Silvie, O., et al., *Post-transcriptional silencing of UIS4 in Plasmodium berghei sporozoites is important for host switch.* Mol Microbiol, 2014. **91**(6): p. 1200-13.

287. Cummings, J.F., et al., *Recombinant Liver Stage Antigen-1 (LSA-1) formulated with AS01 or AS02 is safe, elicits high titer antibody and induces IFN-gamma/IL-2 CD4+ T cells but does not protect against experimental Plasmodium falciparum infection.* Vaccine, 2010. **28**(31): p. 5135-44.

288. Ny, T., F. Elgh, and B. Lund, *The structure of the human tissue-type plasminogen activator gene: correlation of intron and exon structures to functional and structural domains.* Proc Natl Acad Sci U S A, 1984. **81**(17): p. 5355-9.

289. Becker, S.I., et al., *Protection of mice against Plasmodium yoelii sporozoite challenge with P. yoelii merozoite surface protein 1 DNA vaccines.* Infect Immun, 1998. **66**(7): p. 3457-61.

290. Li, Z., et al., *Immunogenicity of DNA vaccines expressing tuberculosis proteins fused to tissue plasminogen activator signal sequences.* Infect Immun, 1999. **67**(9): p. 4780-6.

291. Luo, M., et al., *Immunization with plasmid DNA encoding influenza A virus nucleoprotein fused to a tissue plasminogen activator signal sequence elicits strong immune responses and protection against H5N1 challenge in mice.* J Virol Methods, 2008. **154**(1-2): p. 121-7.

292. Hollingdale, M.R., et al., *Non-CS pre-erythrocytic protective antigens.* Immunol Lett, 1990. **25**(1-3): p. 71-6.

293. Mikolajczak, S.A., et al., *L-FABP is a critical host factor for successful malaria liver stage development.* Int J Parasitol, 2007. **37**(5): p. 483-9.

294. Spielmann, T., et al., *Molecular make-up of the Plasmodium parasitophorous vacuolar membrane.* Int J Med Microbiol, 2012. **302**(4-5): p. 179-86.

295. Montagna, G.N., et al., *Antigen Export during Liver Infection of the Malaria Parasite Augments Protective Immunity.* MBio, 2014. **5**(4).

296. Sargeant, T.J., et al., *Lineage-specific expansion of proteins exported to erythrocytes in malaria parasites.* Genome Biol, 2006. **7**(2): p. R12.

297. Fidock, D.A., et al., *Plasmodium falciparum liver stage antigen-1 is well conserved and contains potent B and T cell determinants.* J Immunol, 1994. **153**(1): p. 190-204.

298. Yang, C., et al., *Sequence variations in the non-repetitive regions of the liver stage-specific antigen-1 (LSA-1) of Plasmodium falciparum from field isolates.* Mol Biochem Parasitol, 1995. **71**(2): p. 291-4.

299. Mikolajczak, S.A., et al., *Disruption of the Plasmodium falciparum liver-stage antigen-1 locus causes a differentiation defect in late liver-stage parasites.* Cell Microbiol, 2011. **13**(8): p. 1250-60.

300. Connelly, M., et al., *T-cell immunity to peptide epitopes of liver-stage antigen 1 in an area of Papua New Guinea in which malaria is holoendemic.* Infect Immun, 1997. **65**(12): p. 5082-7.

301. Krzych, U., et al., *T lymphocytes from volunteers immunized with irradiated Plasmodium falciparum sporozoites recognize liver and blood stage malaria antigens.* J Immunol, 1995. **155**(8): p. 4072-7.

302. Kurtis, J.D., et al., *Interleukin-10 responses to liver-stage antigen 1 predict human resistance to Plasmodium falciparum.* Infect Immun, 1999. **67**(7): p. 3424-9.

303. Luty, A.J., et al., *Interferon-gamma responses are associated with resistance to reinfection with Plasmodium falciparum in young African children.* J Infect Dis, 1999. **179**(4): p. 980-8.

304. Luty, A.J., et al., *Parasite antigen-specific interleukin-10 and antibody reponses predict accelerated parasite clearance in Plasmodium falciparum malaria.* Eur Cytokine Netw, 1998. **9**(4): p. 639-46.

305. Spielmann, T., D.J. Fergusen, and H.P. Beck, *etramps, a new Plasmodium falciparum gene family coding for developmentally regulated and highly charged membrane proteins located at the parasite-host cell interface.* Mol Biol Cell, 2003. **14**(4): p. 1529-44.

306. Favretto, F., et al., *Evidence from NMR interaction studies challenges the hypothesis of direct lipid transfer from L-FABP to malaria sporozoite protein UIS3.* Protein Sci, 2013. **22**(2): p. 133-8.

307. Sharma, A., et al., *Crystal structure of soluble domain of malaria sporozoite protein UIS3 in complex with lipid.* J Biol Chem, 2008. **283**(35): p. 24077-88.

308. Morosan, S., et al., *Liver-stage development of Plasmodium falciparum, in a humanized mouse model.* J Infect Dis, 2006. **193**(7): p. 996-1004.

309. Sacci, J.B., Jr., et al., *Plasmodium falciparum infection and exoerythrocytic development in mice with chimeric human livers.* Int J Parasitol, 2006. **36**(3): p. 353-60.

310. Vaughan, A.M., et al., *Complete Plasmodium falciparum liver-stage development in liver-chimeric mice.* J Clin Invest, 2012. **122**(10): p. 3618-28.

311. Renia, L., et al., *Effector functions of circumsporozoite peptide-primed CD4+ T cell clones against Plasmodium yoelii liver stages.* J Immunol, 1993. **150**(4): p. 1471-8.

312. Weiss, W.R., et al., *Cytotoxic T cells recognize a peptide from the circumsporozoite protein on malaria-infected hepatocytes.* J Exp Med, 1990. **171**(3): p. 763-73.

313. Ewer, K.J., et al., *Protective CD8+ T-cell immunity to human malaria induced by chimpanzee adenovirus-MVA immunisation.* Nat Commun, 2013. **4**: p. 2836.

314. O'Hara, G.A., et al., *Clinical assessment of a recombinant simian adenovirus ChAd63: a potent new vaccine vector.* J Infect Dis, 2012. **205**(5): p. 772-81.

315. Weiss, W.R., et al., *Protection of rhesus monkeys by a DNA prime/poxvirus boost malaria vaccine depends on optimal DNA priming and inclusion of blood stage antigens.* PLoS One, 2007. **2**(10): p. e1063.

316. Forbes, E.K., et al., *Combining liver- and blood-stage malaria viral-vectored vaccines: investigating mechanisms of CD8+ T cell interference.* J Immunol, 2011. **187**(7): p. 3738-50.

317. Sedegah, M., et al., *Reduced immunogenicity of DNA vaccine plasmids in mixtures.* Gene Ther, 2004. **11**(5): p. 448-56.

318. Doolan, D.L., et al., *Circumventing genetic restriction of protection against malaria with multigene DNA immunization: CD8+ cell-, interferon gamma-, and nitric oxide-dependent immunity.* J Exp Med, 1996. **183**(4): p. 1739-46.

319. Thera, M.A., et al., *A field trial to assess a blood-stage malaria vaccine.* N Engl J Med, 2011. **365**(11): p. 1004-13.

320. Clyde, D.F., *Immunization of man against falciparum and vivax malaria by use of attenuated sporozoites.* Am J Trop Med Hyg, 1975. **24**(3): p. 397-401.

321. Clyde, D.F., et al., *Immunization of man against sporozite-induced falciparum malaria.* Am J Med Sci, 1973. **266**(3): p. 169-77.

322. Hoffman, S.L., et al., *Protection of humans against malaria by immunization with radiation-attenuated Plasmodium falciparum sporozoites.* J Infect Dis, 2002. **185**(8): p. 1155-64.

323. Seguin, M.C., et al., *Induction of nitric oxide synthase protects against malaria in mice exposed to irradiated Plasmodium berghei infected mosquitoes: involvement of interferon gamma and CD8+ T cells.* J Exp Med, 1994. **180**(1): p. 353-8.

324. Draper, S.J., et al., *Recombinant viral vaccines expressing merozoite surface protein-1 induce antibody- and T cell-mediated multistage protection against malaria.* Cell Host Microbe, 2009. **5**(1): p. 95-105.

325. Goodman, A.L., et al., *New candidate vaccines against blood-stage Plasmodium falciparum malaria: prime-boost immunization regimens incorporating human and simian adenoviral vectors and poxviral vectors expressing an optimized antigen based on merozoite surface protein 1.* Infect Immun, 2010. **78**(11): p. 4601-12.

326. Douglas, A.D., et al., *Tailoring subunit vaccine immunogenicity: maximizing antibody and T cell responses by using combinations of adenovirus, poxvirus and protein-adjuvant vaccines against Plasmodium falciparum MSP1.* Vaccine, 2010. **28**(44): p. 7167-78.

327. Biswas, S., et al., *Transgene optimization, immunogenicity and in vitro efficacy of viral vectored vaccines expressing two alleles of Plasmodium falciparum AMA1.* PLoS One, 2011. **6**(6): p. e20977.

328. Hutchings, C.L., et al., *Combination of protein and viral vaccines induces potent cellular and humoral immune responses and enhanced protection from murine malaria challenge.* Infect Immun, 2007. **75**(12): p. 5819-26.

329. Dunachie, S.J., et al., *A DNA prime-modified vaccinia virus ankara boost vaccine encoding thrombospondin-related adhesion protein but not circumsporozoite protein partially protects healthy malaria-naive adults against Plasmodium falciparum sporozoite challenge.* Infect Immun, 2006. **74**(10): p. 5933-42.

330. Larke, N., et al., *Combined single-clade candidate HIV-1 vaccines induce T cell responses limited by multiple forms of in vivo immune interference.* Eur J Immunol, 2007. **37**(2): p. 566-77.

331. Schneider, J., et al., *Enhanced immunogenicity for CD8+ T cell induction and complete protective efficacy of malaria DNA vaccination by boosting with modified vaccinia virus Ankara.* Nat Med, 1998. **4**(4): p. 397-402.

332. Kappe, S.H.I., C.A. Buscaglia, and V. Nussenzweig, *Plasmodium sporozoite molecular cell biology.* Annual Review of Cell and Developmental Biology, 2004. **20**: p. 29-59.

333. Yuda, M. and T. Ishino, *Liver invasion by malarial parasites - how do malarial parasites break through the host barrier?* Cellular Microbiology, 2004. **6**(12): p. 1119-1125.

334. Akhouri, R.R., et al., *Role of Plasmodium falciparum thrombospondin-related anonymous protein in host-cell interactions.* Malaria Journal, 2008. **7**.

335. Ishino, T., Y. Chinzei, and M. Yuda, *A Plasmodium sporozoite protein with a membrane attack complex domain is required for breaching the liver sinusoidal cell layer prior to hepatocyte infection.* Cellular Microbiology, 2005. **7**(2): p. 199-208.

336. Ishino, T., et al., *Cell-passage activity is required for the malarial parasite to cross the liver sinusoidal cell layer.* Plos Biology, 2004. **2**(1): p. 77-84.

337. Garcia, J.E., A. Puentes, and M.E. Patarroyo, *Developmental biology of sporozoite-host interactions in Plasmodium falciparum malaria: implications for vaccine design.* Clin Microbiol Rev, 2006. **19**(4): p. 686-707.

338. Frevert, U., et al., *Intravital observation of Plasmodium berghei sporozoite infection of the liver.* Plos Biology, 2005. **3**(6): p. 1034-1046.

339. Baum, J., et al., *Host-cell invasion by malaria parasites: insights from Plasmodium and Toxoplasma.* Trends Parasitol, 2008. **24**(12): p. 557-63.

340. Woodrow, C.J., J.I. Penny, and S. Krishna, *Intraerythrocytic Plasmodium falciparum expresses a high affinity facilitative hexose transporter.* J Biol Chem, 1999. **274**(11): p. 7272-7.

341. Joet, T., et al., *Validation of the hexose transporter of Plasmodium falciparum as a novel drug target.* Proc Natl Acad Sci U S A, 2003. **100**(13): p. 7476-9.

342. Sacci, J.B., Jr., et al., *Laser capture microdissection and molecular analysis of Plasmodium yoelii liver-stage parasites.* Mol Biochem Parasitol, 2002. **119**(2): p. 285-9.

343. Santos, J.M., et al., *Apicomplexan cytoskeleton and motors: key regulators in morphogenesis, cell division, transport and motility.* Int J Parasitol, 2009. **39**(2): p. 153-62.

344. Amino, R., et al., *Host cell traversal is important for progression of the malaria parasite through the dermis to the liver.* Cell Host & Microbe, 2008. **3**(2): p. 88-96.

345. Mota, M.M., et al., *Migration of Plasmodium sporozoites through cells before infection.* Science, 2001. **291**(5501): p. 141-144.

346. Herrera, S., et al., *Antigenicity and immunogenicity of multiple antigen peptides (MAP) containing P. vivax CS epitopes in Aotus monkeys.* Parasite Immunol, 1997. **19**(4): p. 161-70.

347. Crompton, P.D., et al., *A prospective analysis of the Ab response to Plasmodium falciparum before and after a malaria season by protein microarray.* Proc Natl Acad Sci U S A, 2010. **107**(15): p. 6958-63.

348. Vanderberg, J.P. and U. Frevert, *Intravital microscopy demonstrating antibody-mediated immobilisation of Plasmodium berghei sporozoites injected into skin by mosquitoes.* Int J Parasitol, 2004. **34**(9): p. 991-6.

349. Tavares, J., et al., *Role of host cell traversal by the malaria sporozoite during liver infection.* J Exp Med, 2013. **210**(5): p. 905-15.

350. Scheller, L.F., R.A. Wirtz, and A.F. Azad, *Susceptibility of different strains of mice to hepatic infection with Plasmodium berghei.* Infect Immun, 1994. **62**(11): p. 4844-7.

351. Wengelnik, K., et al., *The A-domain and the thrombospondin-related motif of Plasmodium falciparum TRAP are implicated in the invasion process of mosquito salivary glands.* EMBO J, 1999. **18**(19): p. 5195-204.

352. Fonager, J., et al., *Reduced CD36-dependent tissue sequestration of Plasmodium-infected erythrocytes is detrimental to malaria parasite growth in vivo.* J Exp Med, 2012. **209**(1): p. 93-107.

353. Aldrich, C., et al., *Roles of the amino terminal region and repeat region of the Plasmodium berghei circumsporozoite protein in parasite infectivity.* PLoS One, 2012. **7**(2): p. e32524.

354. Doolan, D.L. and S.L. Hoffman, *The complexity of protective immunity against liver-stage malaria.* J Immunol, 2000. **165**(3): p. 1453-62.

355. Duffy, P.E., et al., *Pre-erythrocytic malaria vaccines: identifying the targets.* Expert review of vaccines, 2012. **11**(10): p. 1261-80.

356. Spencer, A.J., et al., *Enhanced Vaccine-Induced CD8+ T Cell Responses to Malaria Antigen ME-TRAP by Fusion to MHC Class II Invariant Chain.* PLoS One, 2014. **9**(6): p. e100538.

357. Khan, S.M., et al., *Genetic engineering of attenuated malaria parasites for vaccination.* Curr Opin Biotechnol, 2012. **23**(6): p. 908-16.

358. Qiao, C., et al., *Development of a recombinant fowlpox virus vector-based vaccine of H5N1 subtype avian influenza.* Dev Biol (Basel), 2006. **124**: p. 127-32.

359. Gao, W., et al., *Effects of a SARS-associated coronavirus vaccine in monkeys.* Lancet, 2003. **362**(9399): p. 1895-6.

360. Gao, W., et al., *Protection of mice and poultry from lethal H5N1 avian influenza virus through adenovirus-based immunization.* J Virol, 2006. **80**(4): p. 1959-64.

361. Chen, Z., et al., *Recombinant modified vaccinia virus Ankara expressing the spike glycoprotein of severe acute respiratory syndrome coronavirus induces*

protective neutralizing antibodies primarily targeting the receptor binding region. J Virol, 2005. **79**(5): p. 2678-88.

362. Hiller, N.L., et al., *A host-targeting signal in virulence proteins reveals a secretome in malarial infection.* Science, 2004. **306**(5703): p. 1934-7.

363. Marti, M., et al., *Targeting malaria virulence and remodeling proteins to the host erythrocyte.* Science, 2004. **306**(5703): p. 1930-3.

364. Singh, A.P., et al., *Plasmodium circumsporozoite protein promotes the development of the liver stages of the parasite.* Cell, 2007. **131**(3): p. 492-504.

365. Cockburn, I.A., et al., *Dendritic cells and hepatocytes use distinct pathways to process protective antigen from plasmodium in vivo.* PLoS Pathog, 2011. **7**(3): p. e1001318.

366. Yuda, M. and T. Ishino, *Liver invasion by malarial parasites--how do malarial parasites break through the host barrier?* Cell Microbiol, 2004. **6**(12): p. 1119-25.